University of Strathclyde

Strathclyde Institute of Pharmacy and Biomedical Sciences

Phage-Based Therapy for Nasal and Respiratory Infections

by

Munerah Alfadhel

A thesis presented in fulfilment of the requirements for the degree of Doctor of Philosophy

2013

Copyright Statement

Signed: *Date:*

Abstract

The adoption of therapy based on bacteriophage for the reduction of harboured pathogens is limited by a lack of understanding regarding their formulation as medicines. The product must able to efficiently deliver phage without deterioration and since oral delivery results in the destruction of the lytic activity, a nasal delivery system was investigated.

This thesis first describes the formulation of lyophilised nasal inserts carrying a bacteriophage selective for *S. aureus*, for the eradication of MRSA resident in the nose. Lyophilization of bacteriophages in 1 mL of 1–2% (w/v) hydroxypropyl methylcellulose (HPMC) with or without the addition of 1% (w/v) mannitol yielded nasal inserts composed of a highly porous leaflet-like matrix. The bacteriophage titre fell following lyophilization to 10^8 pfu per insert, then reduced 100- to 1000-fold over 6 to 12 months storage at 4 ^{o}C.

The second part of this thesis presented a new phage bioprocess method which involved co-precipitation of an aqueous mixture of phage and a crystallisable carrier (glutamine or glycine) is described. Inclusion of albumin or trehalose at 5% w/w during co-precipitation provided additional stabilization of the phage.

In the third part of this thesis, a lipid vehicle (Lamellasomes^{TM}) as a carrier in pulmonary delivery for antibiotics and/or bacteriophage was characterised. We

further investigated the potential for co-formulation of antibiotics or bacteriophage by dispersion into LMS and nebulization of aerosolized droplets. Patients with cystic fibrosis (CF) may harbour antibiotic-resistant, mucoid strains of *Pseudomonas aeruginosa* in the lung.

Bacteriophages were carried with the bulk fraction, rather than being selectively carried in larger or smaller aerosols. Dilution of colistin or tobramycin into LMS increased the nebulized drug fraction deposited into stages 2-5. This suggests that the surface activity of the LMS facilitates the generation of smaller aerosol droplets during nebulization.

In conclusion, the work reported in this thesis suggests that bacteriophages can be formulated in a stable preparation and therefore have a potential as an alternative therapeutic agent for treatment of resistant bacterial infection on mucous surfaces.

Publications

- Munerah Alfadhel, Utsana Puapermpoonsiri, Steven J. Ford, Fiona J. McInnes, Christopher F. van der Walle. Lyophilized inserts for nasal administration harboring bacteriophage selective for *Staphylococcus aureus*: in vitro evaluation. International Journal of Pharmaceutics 416 (2011) 280-287.
- E. Alvarez-Gonzalez, M. Alfadhel, P. Mane, S.J. Ford, B.D. Moore, C.F. van der Walle. Bioprocessing of Bacteriophages via Rapid Drying onto Micro-crystals. Biotechnology Progress, 28 (2012) 540-548.
- Alfadhel, M., Walle, C. Formulation and evaluation of a novel bacteriophage delivery system for MRSA nasal colonisation. Abstract for oral presentation at the 3rd PharmSciFair Conference in Prague, Czech Republic (13 – 17 June, 2011).
- Alfadhel, M., Walle, C. Lyophilized inserts for nasal administration harboring bacteriophage selective for *Staphylococcus aureus*. Abstract for poster presentation at Saudi International Conference (SIC), Coventry, UK (23 June, 2011) and at Strathclyde University Research Day (2012).
- Alfadhel, M., Park, G., Walle, C. Improved pulmonary delivery of antibiotics and bacteriophages using lamellasome Abstract for poster presentation at the American Association of Pharmaceutical Scientists (AAPS), Chicago, USA (October, 2012).
- Alfadhel, M., Alvarez-Gonzalez, E., Walle, C. Bioprocessing of Bacteriophages via Rapid Drying onto Micro-crystals. Abstract for poster presentation at the Academy of Pharmaceutical Sciences (APS), Edinburgh, UK (September, 2013).

Acknowledgements

The ability to study for a PhD is the greatest gift which would not have been possible without the grace of God. I am grateful to Him for all the blessings that have led me to this.

I would first like to thank my supervisor Dr. Christopher van der Walle for providing me the opportunity to undertake this PhD project, accompanied by his expertise and guidance. He has unconditionally offered me help and advice throughout my study. I would like to express a special gratitude to him for giving me a positively attitude in life, He is an amazing supervisor with a great sense of humour. Chris, it was a great honour to be your student.

Also, my sincere thanks go to my supervisor Prof. Clive Wilson whom I am indebted to for his invaluable advice despite his academic commitments. His generosity to share his knowledge and his great support has given me the motivation throughout my writing stage. My thanks are also extended to my second supervisor Dr. Christine Dufès.

I acknowledge Margaret Mullin, University of Glasgow, for her assistance with SEM, David Blatchford for his assistance with CLSM and Dr. Steven Ford for his help in KF. Sincere thanks to my colleague Utsana for her training on the bacteriophage technique. I also thank Lamellar Biomedical Ltd and Dr Graham Park for supporting the lamellasome work.

I acknowledge the Saudi Cultural Bureau and Ministry of Health for funding my study.

Thanks to all my friends and colleagues in the office and the lab. My deep thanks to my friend Dr. Eva Alvarez-Gonzalez which has always been there to help me. Thanks Eva, I am grateful to your endless help, care and warm friendship.

I have been blessed with incredibly supportive friends, my soul sister Huda Alakeel and my dear friend Sana, thank you for being there whenever I needed you.

Last but not least, my greatest appreciation goes to my family who have been there for me to achieve my ambition. I am grateful to my mother and father, my sisters and brothers for their unconditional love and carefulness. I owe everlasting gratefulness to my mother and my sister Sadeen for taking care of my baby (Yasser) throughout my study years. My appreciation goes to my husband for believing in me. A big thank you to my beloved kids for their love: Abdullah, Nora and Alya, thanks for always knowing how to cheer me up.

List of Contents

List of Figures

List of Tables

List of Abbreviations

alv	Alveolus
AM	Artificial mucus
ATCC	American Type Culture Collection
ATII	Alveolar type II
BSA	Bovine serum albumin
ca.	Approximately
CF	Cystic fibrosis
cf.	Compare
CFC	Critical flow controller
CFTR	Cystic fibrosis‟s transmembrane conductance regulator
CFU	Colony forming unit
CLSM	Confocal electron microscopy
cm	Centimetre
COPD	Chronic obstruction pulmonary disease
CsCl	Cesium chloride
da	Aerodynamic diameter
DLS	Dynamic light scattering
DLVO	Derjaguin-Landau-Verwey-Overbeek
DNA	Deoxyribose nucleic acid
DSC	Differential scanning calorimetry
DVS	Dynamic vapor sorption
e.g.	For example
FITC	Fluorescein isothiocyanate
FRET	Fluorescence resonance energy transfer
GRAS	Generally regarded as safe
GSD	Geometric standard deviation
h	Hour
H_c	Heat of crystallization

HPMC	Hydroxypropyl methylcellulose
IU	International unit
KCl	Potassium chloride
KF	Karl Fischer
LB	Luria Bertani
LMS	Lamellasome
min	Minute
mJ	Millijoule
mL or mL	Millilitre
MLV	Multilamellar vesicle
mm	Millimetre
mM	Millimole
MMAD	Mass median aerodynamic diameter
MRSA	Methicillin-resistant *Staphylococcus aureus*
MSLI	multi-stage liquid impinger
mTorr	Millitorre
mV	Millivolt
MW	Molecular weight
NaCl	Sodium chloride
NCIMB	National Collectional Industrial, food and Marine Bacteria
nm	Nanometer
^{o}C	Degree Celsius
OD	Outer diameter
Pa·s	Pascal-second
PBS	Phosphate buffer saline
PCMC	Protein-coated microcrystals
PEG	Polyethylene glycol
PFU	Plaque forming unit
Q	Flow rate
RH	Relative humidity
RNA	Ribonucleic acid

rpm	Rotations per minute
SD	Standard deviation
SEM	Scanning electron microscopy
SM	Storage media
TEM	Transmission electron microscopy
T_g	Glass transition
TMDSC	Temperature-modulated DSC
UV	Ultraviolet
v/v	Volume by volume
VRE	Vancomycin resistant *Enterococcus faecium*
w/v	Weight by volume
ZP	Zeta potential
ZS	Zetasizer
µm	Micrometre
ϕ-CMC	Phage-coated microcrystals

Chapter 1: Introduction

1.1. Antibiotics and infection: the emergence of resistance

Infectious diseases of the respiratory tract are common. Many are self-limiting and require only palliative treatment – the common cold and mild flu. Others have intermediate danger in susceptible groups: the young, unfit, nursing mothers and the elderly. A few become life threatening because of the emergence of infections that are refractory to treatment. Currently, the medical community is witnessing an increase in the incidence of difficult infectious diseases that result from an accelerating emergence and spreading of profoundly antibiotic-resistance pathogens such as *Mycobacterium tuberculosis, Enterococcus faecalis, Staphylococcus aureus, Acinetobacter baumannii and Pseudomonas aeruginosa.* Of major concern is the methicillin-resistant *Staphylococcus aureus*,'MRSA', (Coelho *et al.,* 2004) and *Pseudomonas aeruginosa* (Salunkhe *et al.,* 2005). The lack of treatment options for infections caused by multi-resistant bacteria has been exacerbated by slow progress in the discovery of new generations of antibiotics. The risk of pandemics caused by resistant bacteria leads researchers to investigate improved strategies for the delivery and treatment of existing agents.

1.1.1. Staphylococcus aureus

The genus *Staphylococcus* has more than 30 species, with three species that are of clinical importance: *S. epidermidis, S. saprophyticus* and *S. aureus. S. aureus* is a Gram positive spherical bacterium also known as "golden staph" (Saadatin-Elahi *et*

al., 2008) which is a commensal of human and animals (Chambers, 2001). It lives on human skin and in the nasal cavity causing little harm and is spread from person to person through hand contact. Colonisation by *S. aureus* occurs in about 30% of the healthy population and a higher rate of colonisation has been found among hospitalised patients (Nishijima *et al.,* 1993). Patients become colonised mainly from other patients, and by transfer of strains from health care workers (Voss and Doebbeling, 1995). *S. aureus* can cause serious infections such as skin ulcers, wound infections, endocarditis, soft tissue abscesses and bacteraemia (Chambers, 2001). It has been reported from HELICS (the international network for collection, analysis and dissemination of valid data on the risks of nosocomial infections in European hospitals) that from 416 bacteria isolated, *S. aureus* formed 48.6% of the pathogens (Saadatin-Elahi *et al.,* 2008). The mechanism of resistance to penicillin is mediated by production of β-lactamase (penicillinase) enzyme which cleaves the β-lactam ring of the penicillin molecule rendering the antibiotic ineffective.

1.1.1.1. Methicillin Resistant Staphylococcus aureus (MRSA):

In the last two decades, more serious Staphylococcal infections have increased due to the emergence of methicillin resistant *S. aureus* (MRSA) (Ewan, 2004), which signalled the beginning of a major health concern. It became clear that the number of useful antibiotics was decreasing. MRSA is considered the most important cause of antibiotic resistant infections (Karchmer, 2000) and is responsible for a large increase in bacteraemia associated with *S. aureus* with a reported incidence of over 50% in many countries (Gould, 2007). Currently, due to the resistance of *S. aureus* to

six or more antibiotics, the remaining possible treatment is usually based on vancomycin or teicoplanin; unfortunately, many cases of vancomycin resistant *S. aureus* have also recently appeared (Gould, 2007). MRSA was identified approximately twenty years ago as a serious therapeutic and infection control problem (Cookson, 1993). It still remains a health problem and is considered periodically in the literature (Levy 2005, Fung 2012). Although there are a large number of antibiotics available in the market, many of the chemical motifs are structurally related.

1.1.2. Pseudomonas aeruginosa

P. aeruginosa is a Gram-negative, aerobic rod belonging to the bacterial family Pseudomonadaceae. It is a non-fermentative γ-proteobacterium widely distributed in nature. It grows readily on many common media to form large colonies which may secrete distinctive pigments that aid its preliminary identification (Ryan and Ray, 2004). The typical *Pseudomonas* bacterium in nature might be found in a biofilm, attached to some surface or substrate, or in a planktonic form, as a unicellular organism.

P. aeruginosa is an opportunistic pathogen, and is an important cause of nosocomial infections including complicated urinary tract infections, sepsis and ventilator-associated pneumonia. In pulmonary diseases, *P. aeruginosa* infections generally persist despite the use of long-term antibiotic therapy and induce a host inflammatory response by the elaboration of the bacterial products, particularly the exo-polysaccharide alginate. This inflammation leads to degradation of pulmonary extracellular matrix resulting in an impaired ability to destroy lung pathogens as occurs in emphysema (Alexis *et al.*, 2006).

Chronic infection with *P. aeruginosa* is known to be the main cause of respiratory failure and ultimate mortality in cystic fibrosis (CF) patients (Lyczak *et al.*, 2002). Chronic *P. aeruginosa* infection is related to the mucoid phenotype which causes epithelial surface damage and leads to deterioration of pulmonary function. Exposure of non-mucoid *P. aeruginosa* to oxygen radicals from hydrogen peroxide induces mutations in the mucA gene, which is responsible for expression of the alginate

biosynthesis (Mathee *et al.,* 1999). As a result, the resident *P. aeruginosa* strains mutate to a mucoid type that is resistant to phagocytosis by cells of the immune system, and increases tolerance to toxic oxygen radicals and antibiotics. Thus, over time, *P. aeruginosa* strains that undergo mucoid conversion, display a biofilm mode of growth in vivo and indicate overproduction of a linear polysaccharide alginate (Hoiby, 2002). It has been reported that the phenomena of antibiotic resistance and biofilm formation are genetically linked. Additionally, *P. aeruginosa* strain that is resistant to antibiotic and has enhanced ability to form biofilm arise at high frequency both in vitro and in the lungs of CF patients (Drenkard and Ausubel, 2002). Moreover, *P. aeruginosa* possesses several mechanisms of drug resistance: it may cause changes in cell permeability, enzymatic inactivation of drug or present an altered drug target. Thus, a multidrug-resistant phenotype can arise through the emergence of multiple mechanisms of resistance (Masuda *et al.*, 2000).

1.2. The respiratory route

The respiratory system is responsible for providing the body with the necessary oxygen required to produce the energy used for cell maintenance, growth, defence and division. It is also responsible for protecting the body against pathogenic attacks during inhalation. The air must be humidified and warmed prior to entrance into the lungs, where gas exchange across the alveoli removes carbon dioxide dissolved in plasma and regenerates oxy-haemoglobin in the erythrocyte (Martini and Nath, 2009c).

1.2.1. Physiology of the respiratory system

The respiratory system is divided into two major parts: the upper respiratory tract and the lower respiratory tract (Figure 1.1). The upper respiratory tract consists of the nose, nasal cavity, paranasal sinuses and pharynx. The lower respiratory tract consists of the larynx, trachea, bronchi, bronchioles and alveoli.

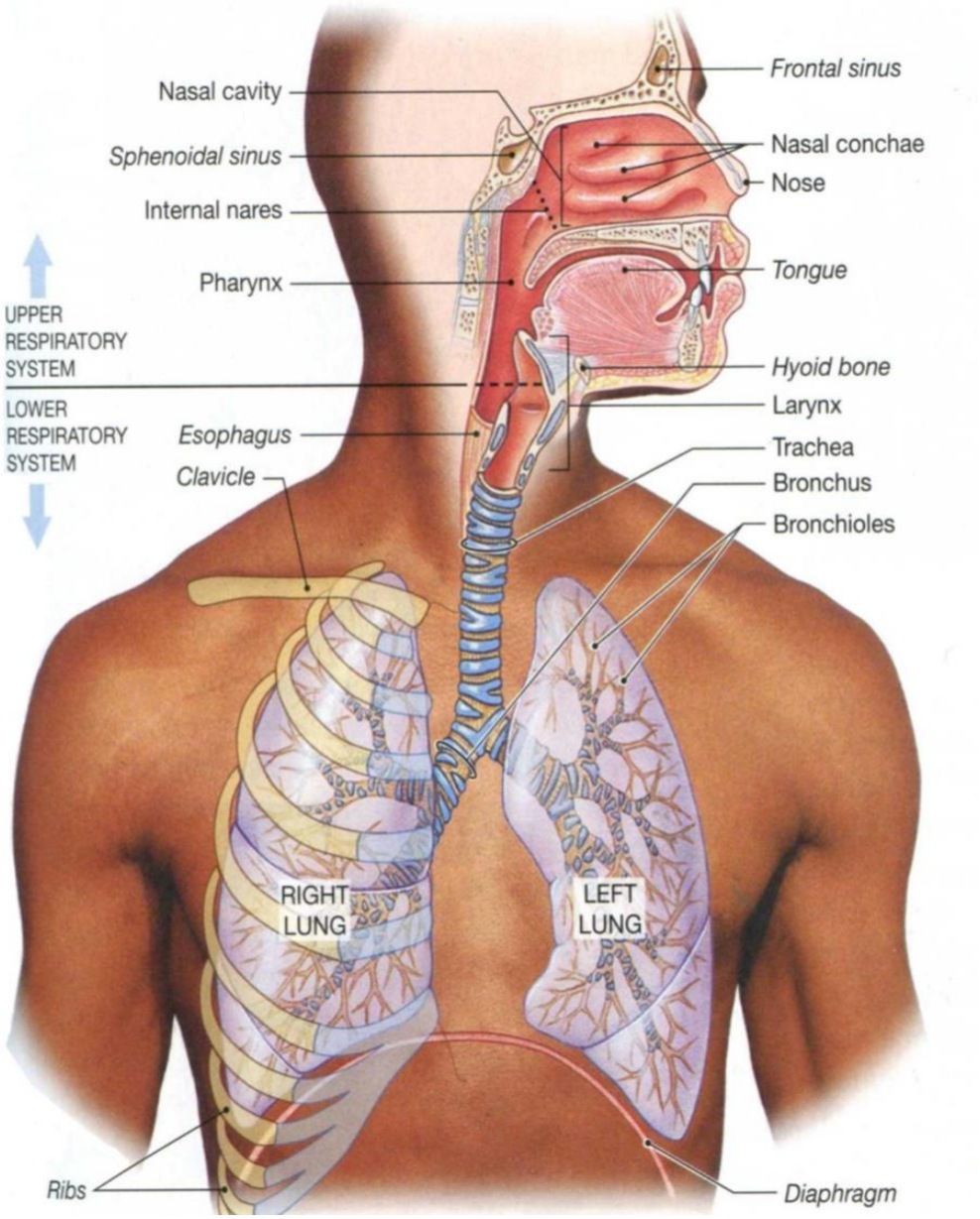

Figure 1.1. Structure of the respiratory system, *adapted from Martini and Nath (2009c).*

1.2.1.1. Upper respiratory tract (The nasal cavity)

The primary entrance of gas occurs through the nose, where air enters through the nostrils into the nasal cavity. The anatomical and the physiological structure of the nasal cavity play an essential role in the successful delivery of drugs via this route. The general architecture and morphology of the human nasal cavity is shown in Figure 1.2.

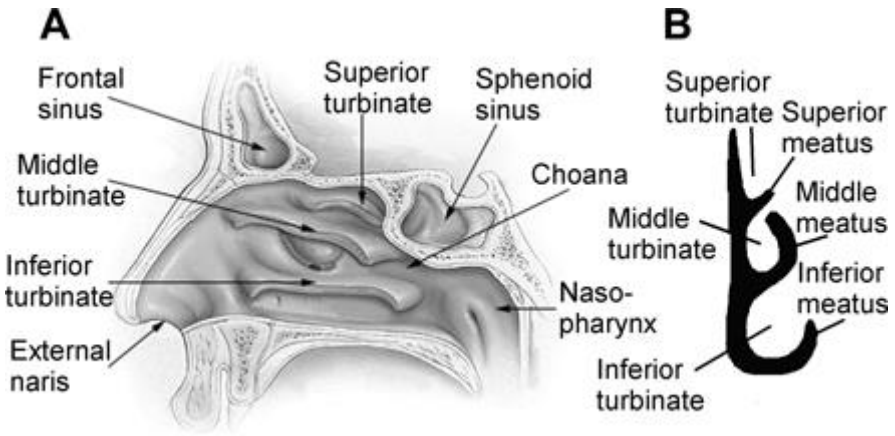

Figure 1.2. Anatomy of the human nasal cavity schematic of a sagittal plane cut (*A*) and sample coronal plane midway through the nasal cavity (*B*) (Liu *et al.*, 2009).

The nasal cavity is divided into two halves by the nasal septum and extended to the nasopharynx posteriorly. The respiratory region, the nasal conchae or turbinates, occupies the major part of nasal cavity. The nasal absorption of drugs occurs mainly in the respiratory region comprising the turbinates and part of the nasal septum because of its large surface area and rich vasculature (Illum, 2002). The airflow in the nose attempts to trap particles on mucus-covered epithelium of the turbinates and

clear debris by mucocilary action. The air flow to the lungs is pulled over the turbinates by expansion of the lungs, the outward movement of the ribcage by the intercostal muscles creating a vacuum in pleural cavity.

1.2.1.2. Lower respiratory tract (Bronchi, bronchial tree and lungs)

The path to right and left lung divides at the first division of the bronchi to smaller bronchioles and eventually to alveolar sacs as shown in Figure 1.3. The division increases resistance to flow and air flow velocity consequently becomes slower allowing small particles to settle (Illum, 2002).

The bronchial tree has a multiple branching starting from the primary bronchi until the formation of the minute respiratory bronchioles. The primary bronchi branch into secondary bronchi, known as lobular bronchi which further divide forming segmental bronchi. Each segmental bronchus provides air to a bronchopulmonary segment of the lung and undergoes multiple branching to form bronchioles. Terminal bronchiole delivers air to one pulmonary lobule. Each lobule contains many respiratory bronchioles which are connected to the alveoli, the site of gas exchange (Martini and Nath, 2009c).

Alveoli are very thin structures lined with two types of pneumocytes. They exist individually and in groups of 15-20 forming an alveolar sac. About 150 million alveoli are present in each lung (Smola *et al.*, 2008) providing a total absorptive surface area of about 70-140 m^2 (Groneberg *et al.*, 2003). They are surrounded by the capillaries that provide blood supply and gas exchange. Alveolar epithelium is one of the structural components of the respiratory membrane in addition to the endothelial

cells lining the alveolus and the fused basal lamina lying between epithelial and endothelial layers. The respiratory membrane is 0.1-0.5µm thick which allows rapid gas exchange between alveolar air and capillary blood (Washington *et al.*, 2001b).

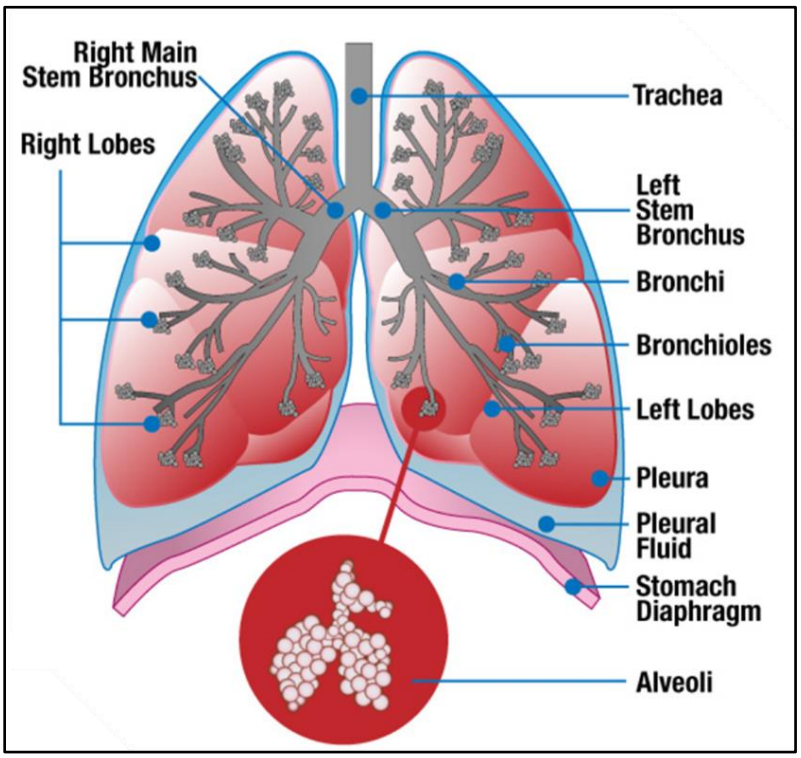

Figure 1.3. Diagram of bronchi, bronchial tree and lungs (*accessed from* http://breathmatter.org. on 27-05-2013).

1.2.2. Structure and function of respiratory mucus

Mucus is a complex biological substance that lines the luminal surface of many organs in the human body including the lungs, gastrointestinal tract, vagina and eyes (Lai *et al.*, 2009). It contains glycoproteins and lipids (0.5–5%), mineral salts (0.5–1%), and free proteins 1% with the remaining 95% being water and electrolytes

(Rathbone and Hadgraft, 1991). Respiratory mucus is composed of a complex and variable mixture of glycoproteins, proteins, lipids, nucleic acids and electrolytes. Approximately 1.5-2 litres of mucus are secreted daily by goblet cells and serous glands within the nasal cavity (Lansley and Martin, 2000).

The function of mucus varies between different organs. In the respiratory tract, mucus lubricates the lungs and protects the epithelia. It serves as a physical barrier against environmental foreign particles, toxins and pathogens and is propelled along the airways to the mouth, where it is swallowed. In the eye, the mucus preserves corneal clarity and resists drying. In the large intestine, the function again is a surface lubricant.

The main component of respiratory secretion is water. Mucin is a glycoprotein of high molecular weight which is secreted by epithelial goblet cells and submucosal glands. Mucin is a linear molecule consisting of several monomeric subunits linked by disulphide-bonds. It is also characterized by high carbohydrate content. The oligosaccharide side chains of mucin are attached to the protein core via O-glycosidic linkages (Figure 1.4). Mucin is responsible for the extent of the viscoelastic nature of mucus secretions. The rate of mucociliary clearance is dependent on the physical properties of respiratory mucus. These properties are largely determined by the major macromolecular constituent, mucus glycoproteins (mucins). The other mucus components contribute to the mucous barrier character (Lethem, 1993; Khanvilkar *et al.*, 2001).

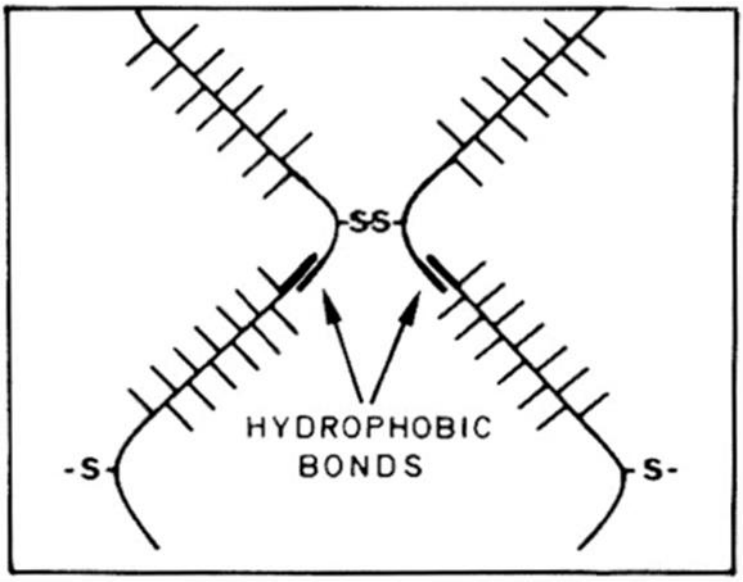

Figure 1.4. Model of mucin structure: Oligosaccharide chains project from the protein core, disulfide bonds cross-link naked protein regions and hydrophobic interactions add additional intermolecular associations (*Adapted from Khanvilkar et al., 2001*).

Chemically, mucus is an integrated structure of biopolymers. The most important physicochemical property of mucus is its viscoelasticity. Its physical behaviour is complex (non-Newtonian), while its properties can vary between those of an elastic solid and a viscous liquid (Lai *et al.,* 2009).

Mucus is constantly produced and when dilute, escapes with aqueous phase. As a sol-gel, for example respiratory mucus of the pulmonary and nasal systems, the longitudinal epithelial cells are ciliated, and their movement contributes to propulsion of the mucus blanket. By placing radioactive markers on the mucus, the rates of clearance can be assessed (Hardy *et al.,* 1985). Many studies show that although the mucus layer affords protection, it can also prevent drug reaching its target site by acting as a potential barrier to drug diffusion, especially as the

physicochemical properties of mucus are often altered in disease states (Widdicombe, 1997).

1.2.3. Properties of mucus in disease state

Mucus hypersecretion is a property shared by all obstructive pulmonary diseases such as asthma, chronic obstruction pulmonary disease (COPD) and cystic fibrosis (CF). In these diseases, mucus hypersecretion may result from either elevated intracellular mucin production contained within airway secretory cells or from elevated mucin exocytosis which increases the thickness of the extracellular mucus, or both (Olatunji *et al.,* 2006).

It has been found that the nature of the airway surface liquid constitutes a very important factor for efficient tracheobronchial drug delivery. For example, CF mucus is thicker, more tenacious, and much less penetrable than normal mucus (Garcia-Contreras and Hickey, 2002). The thick mucus obstructs airways and allows bacterial infection and inflammation and causes hyper secretion of infected sputum, which the patient finds difficult to clear (Lethem *et al.,* 1990). In pathological situations, associated with CF, the solids concentration can be in excess of 10% (Lethem *et al.,* 1990). In addition, the biochemical nature of airway mucins of patients with CF differs than that of normal subjects. CF mucins have a higher degree of sialylation and sulphation of the carbohydrate side chains. Sulphation of mucins commonly occurs in CF, mediated through excessive sulphation of mucus, encouraging colonization by *P. aeroginosa* and *S. aureus* (Cheng *et al.,* 1989).

Diversity in the biochemical structure and rheological properties of the mucus also results from the variety of mucin peptides encoded by mucin genes. Variable expression of mucin genes may lead to heterogeneous mucus in hypersecretory conditions. Therefore, sputum, a mixture of saliva, mucus and pus, has altered macromolecular composition and biophysical properties which vary with disease. Mucin glycoprotein overproduction and hypersecretion are common features of chronic inflammatory airway disease. However, in some pathologic conditions such as CF, airway sputum contains little intact mucin and has increased content of several macromolecules including DNA, filamentous actin, lipids, and proteoglycans (Judith *et al.,* 2009).

1.2.4. Barriers to nasal absorption

1.2.4.1. Mucociliary clearance

An important barrier is the general rapid clearance of the formulation administered intra-nasally due to the mucociliary clearance mechanism. As a result, the retention time within the nasal cavity is shortened and thus drug absorption is reduced. Any liquids or powder formulations that are not mucoadhesive will have a clearance half-life of 15-20 min (Soane *et al.,* 1999). The mucociliary clearance is a process which depends upon the viscoelastic properties of mucus and composition of the epithelial lining fluid.

1.2.4.2. Mucus barrier

Mucus is present as a viscoelastic layer in the nasal cavity and the tracheobronchial region but does not exist in the alveolar region. Mucus in the nasal cavity exerts a normal defence mechanism by acting as a physical barrier that protects the nasal epithelium (Lansley and Martin, 2000). Mucus filters and warms the inhaled air before it reaches the lower airways. Consequently, any inhaled particles or microorganisms are entrapped by the nasal hairs or the mucus layer, and the mucus layer will participates in the removal of particulates via mucociliary clearance by slowly move such particles to the back of the throat, and further to the gastrointestinal tract. This is particularly important in case of larger molecular weight molecules as peptides and proteins, which require extended mucosal contact to allow maximum uptake and avoid systemic side effects (McInnes *et al.*, 2005). Furthermore, the nasal mucosa has its own metabolic process (enzymatic barriers) where it converts endogenous materials into more easily eliminated compounds (Illum, 2003).

1.2.4.3. Drug nature

Despite the large surface area of the nasal cavity and the rich blood supply, the permeation of drugs via the nasal cavity basically depends on the lipophilicity of the compound. The most important factor limiting the nasal absorption of polar drugs such as peptides and proteins is the low membrane permeability. Polar drugs with molecular weights less than 1000 Da will pass the membrane paracellularly, whereas,

larger peptide and proteins will be able to pass the nasal membrane but only in small amounts (Illum, 2003).

1.3. Naso-pulmonary delivery

The nasal cavity has been commonly used as a route for drug delivery, including the treatment of local diseases such as nasal allergy, nasal congestion and nasal infections. Recently, and due to the favourable anatomical and physiological characteristics of the nasal route, nasal drug delivery has generated a great interest in the pharmaceutical industry for the systemic delivery of drugs. Such drugs include small molecular weight polar drugs, drugs which are not easily administered other than via injection (especially peptides and proteins) and drugs requiring rapid onset of action or avoidance of enzymatic degradation and first–pass hepatic metabolism (Illum, 2003). This can be attributed to the rich vasculature of nasal mucosa which promotes the direct absorption of drugs into the blood stream (Arora *et al.*, 2002). Drugs can permeate the nasal mucosal membrane in two different pathways. The first path is transcellularly (across the cells) via simple concentration gradients, receptor mediated transport or vesicular transport mechanism. The second path is passively by paracellular pathway (between the cells) through the tight junctions between the cells.

1.3.1. The Lung and the effect of particle size on delivery

The main requirement in pulmonary drug therapy is deposition of the drug into the peripheral regions of the lungs to produce an effect and enable maximum surface area for absorption (Taylor and Kellaway, 2001). The airway diameter is about 1.8

cm in the trachea which decreases from 4 to 1 mm in the segmental bronchi, while the diameter of the bronchioles become less than 1 mm to 0.4 mm in the alveoli; however the surface area increases to about 140 m^2 (Figure 1.5) (Hickey and Thompson, 1992; Washington, et al., 2001b). The large surface area of the alveolar region and the high blood flow provide a useful route of drug administration.

Many factors influence the deposition of drug particles in the lungs. One important factor is the physiological barriers include the defence system starting in the nose, where particles over 10 µm are trapped by the hair, and mucus lining the nasal cavity. Particles larger than 5 µm are trapped in the lining mucous of the tracheobronchial region (Washington *et al.,* 2001b). Trapped particles in both regions are then cleared by the mucociliary escalator to moves the mucous towards the pharynx (Schreier *et al.,* 1993). Particles between 1-5µm deposit in the periphery, but are mainly engulfed by alveolar macrophages (Schreier *et al.,* 1993). Particles of 0.5 µm or smaller are considered to be too small to deposit and are exhaled (Oberdörster, 1993).

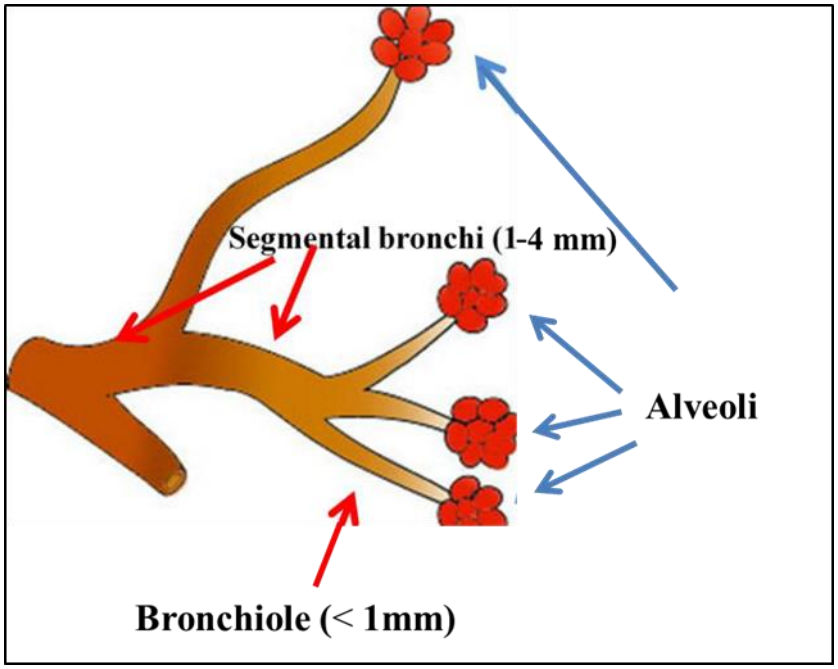

Figure 1.5. Diagram of the fractionation of particle size in each region of respiratory tract following inhalation (*Reproduced from Hicky and Thomson, 1992*).

In addition to the anatomical and physiological features of the nasal cavity and respiratory airway, there are various physicochemical and formulation factors that must be taken into consideration when designing any nasal delivery system such as concentration, pH and dosage form (Illum *et al.*, 2002). Physical properties of the aerosol such as particle size, charge, density and hygroscopicity are also important considerations in pulmonary delivery and play a role in the deposition of the drug particles (Taylor and Kellaway, 2001).

1.3.2. Absorption enhancers

In an attempt to improve the systemic absorption of drugs from the nasal cavity, several absorption enhancers have been investigated to overcome absorption problems resulting from the rapid nasal transit rate (Table 1.1, adapted from Dhakar

et al., 2011). Among those are bile salts (Illum *et al.,* 2001), chitosan (Dyer *et al.,* 2002, Illum, 2003), fusidate derivatives (Shao and Mitra, 1992) and cyclodextrins (Yang *et al.,* 2004).

Table 1.1. Mucosal absorption enhancers and mechanism of action (modified from Dhakar *et al.,* 2011).

Classification	**Examples**	**Mechanism**
Surfactants	Anionic: Sodium lauryl sulphate Cationic: Cetylpyridinium chloride Nonionic: Poloxamer, Span, Tween	Perturbation of intercellular lipids, protein domain integrity, disrupts membrane,
Bile salts	Sodium glycodeoxycholate, Sodium glycocholate, Sodium taurodeoxycholate,	Disrupts membrane, open tight junctions, mucolytic activity
Cyclodextrins	α, β, γ Cyclodextrin, Methylated β–Cyclodextrins	Inclusion of membrane compounds, open tight junctions
Fatty acids	Oleic acid , Lauric acid, Caprylic acid, Phosphotidylcholine	Increase fluidity of phospholipid domains, Disrupts membrane
Cationic compounds	Poly-L-arginine, L-lysine	Ionic interaction with negative charge on the mucosal surface
Chelators	EDTA, Citric Acid, Sodium citrate,	Interfere with tight junction integrity (Deli, 2009)
+ve charged polymers	Chitosan, Trimethyl chitosan	Ionic interaction with negative charge on the mucosal surface
Bioadhesive Materials	Carbopol, Starch, Chitosan	Reduce nasal clearance, open tight junctions

These absorption enhancers have been used to increase the nasal absorption during the brief period in which the drug becomes in contact with the nasal mucosa. This can happen either by altering the physicochemical properties of the drug or by affecting the nasal mucosal surface (Behl *et al.,* 1998). However, there were several serious concerns of mucosal damaged or impairment of the ciliary function caused by some absorption enhancers especially when chronic therapy is employed (Shao and Mitra, 1992; Witschi and Mrsny, 1999).

1.3.2.1. Bile salts

Bile salts are the most widely used surfactants to enhance the nasal absorption of drugs. Commonly used bile salts include sodium cholate (C), sodium glycocholate (GC), sodium deoxycholate (DC), sodium taurocholate (TC), sodium taurodeoxycholate (TDC) and sodium glycodeoxycholate (GDC) (Behl *et al.*, 1998, Shao and Mitra, 1992). The mechanisms by which bile salts act include increasing permeability of the membrane, formation of aqueous pore type transport pathways, inhibition of proteolytic enzymes, and solubilization of drugs in the aqueous vehicle (Behl *et al.*, 1998).

1.3.2.2. Fusidic acid derivatives

Fusidic acid derivatives mainly consists of sodium salts of fusidic acid such as sodium taurodihydrofusidate (STDHF) which is very soluble and stable in aqueous solution with no antibiotic activity. It has been extensively used for trans-nasal delivery of macromolecules e.g. growth hormones, insulin, proteins and peptides (Shao and Mitra, 1992).

1.3.2.3. Cyclodextrins

Cyclodextrins are cyclic oligomers of glucose which can form inclusion complexes with drugs without forming covalent bonds, where the drug molecules can fit into the lipophilic cavities of the cyclodextrin molecules. By forming such complexes, the physicochemical properties of drugs can be altered. The complexes can be formed by various methods such as heating, coprecipitation, damp mixing, extrusion and dry mixing. Among different types of cyclodextrins, only β-cyclodextrin is being considered as a GRAS (generally regarded as safe) material (Behl *et al.*, 1998).

1.3.2.4. Bioadhesive Materials

An alternative approach has been to increase nasal residence time using bioadhesive agents that oppose the natural mucociliary clearance protective mechanism. Bioadhesion may be defined as the state in which two materials (of which one is biological in nature) are held together for an extended period of time by interfacial forces. In pharmaceutical science, when adhesion is to the mucus membrane, this phenomenon is referred to as mucoadhesion (Gu *et al.,* 1988). This strategy aims to increase the contact time between the formulation and nasal mucosa for absorption to occur and has become of great interest as a strategy to either optimise local drug delivery by retaining the dosage form at its site of action (e.g. the gastrointestinal tract), or by retaining the formulation in intimate contact with the site of absorption (as with the nasal cavity) (Smart, 2005). The mechanism of bioadhesion basically consists of a substance adhering to the tissue by means of polymer chain interaction with the cell surface glycoprotein (Nakamura *et al.*, 1999). This process is facilitated

by water uptake from the mucosal surface and swelling which promotes the flexibility of the chain of the polymer (Alur *et al.*, 1999). This water uptake has an additional advantage of improving the drug absorption by creating a temporary osmotic opening of the tight junction in cell mucosa to facilitate the passage of drug molecules (McInnes *et al.*, 2005). The process of bioadhesion is influenced by different factors and mainly occurs as a result of a combination of more than one factor. These factors include the number of hydrophilic groups in the polymer, molecular weight, cross linking, concentration, pH, hydrogen bonding, ionic interaction and viscosity (Ugwoke *et al.*, 2001).

There are several mucoadhesive agents employed in the development of nasal formulations. The most investigated group is the hydrophilic macromolecules containing different hydrogen bond forming groups (Harding *et al.*, 1999). The presence of hydroxyl, carboxyl or amine moiety on the molecules is advantageous for adhesion. They are called wet adhesives as they are activated by moistening with the mucosa surface and then will become adherent to the surface (Smart, 2005). Chitosan is a hydrophilic linear polysaccharide that is available in a range of molecular weights. In addition to its bioadhesive properties, chitosan also has absorption enhancing effects as a result of different mechanism. Chitosan has been shown to increase the paracellular transport of polar drugs by causing transient opening in the tight junctions between the epithelial cells of the mucosa. The most widely used type of chitosan for nasal delivery is a chitosan glutamate salt (Illum, 2003).

Another example of mucoadhesive agents is hydroxypropyl methylcellulose (HPMC). It has been shown to exhibit favourable bioadhesive properties in addition to its classification as a GRAS excipient which makes it an attractive choice in formulating delivery systems to sensitive surfaces such as the nasal cavity (Kibbe 2000).

1.4. Cystic fibrosis

Cystic fibrosis (CF) is a common inherited disorder that affects the body's exocrine glands, causing them to secrete an excess of mucus. Historically, CF patients susceptible to the disease in early childhood. Around 60,000 persons globally suffer from CF of Caucasians with the greatest incidence. Approximately 1 in 1600 Caucasian births are affected and 1 in 20 people carry the gene (Welsh *et al.,* 2001; Massie and Clements, 2005). Multiple organ systems are affected by CF including the lung, the pancreas, liver, sweat glands and the gastrointestinal and reproductive tracts.

Lung disease is responsible for more than 95% of mortality in cystic fibrosis patients (Welsh *et al.,* 1994). This is due to severe deterioration of the respiratory function which involves high mucus viscosity that results in chronic infection, inflammation, and poor airway clearance. The chronic bacterial infection leads to progressive lung damage and respiratory failure (Clunes *et al.,* 2008). It has been reported that the airways of cystic fibrosis (CF) patients are colonised by pathogenic micro-organisms in infancy and majority of CF cases experience recurrent acute respiratory episodes and die of respiratory failure resulting from infection (Lyczak *et al.,* 2002).

The range of pathogens involved in respiratory tract infections arising during CF is large and diverse (Govan & Deretic, 1996). *P. aeruginosa* is considered to be the most important pathogen causing chronic respiratory infections and the principal cause of mortality in CF patients (Salunkhe *et al.*, 2005). The major nonpseudomonal CF pathogen include *Staphylococcus aureus* and *Haemophilus influenzae*, and other less common pathogens including *Streptococcus pneumoniae* and mycobacteria (Gilligan, 1991). Prevalence of these species in the airway changes over time, as illustrated in Figure 1.6. *P. aeruginosa* is characterized by a high intrinsic antibiotic tolerance, once a chronic lung infection is established, *P. aeruginosa* cannot be eradicated by antibiotic treatment. It induces a host inflammatory response by the elaboration of the bacterial products, particularly the exopolysaccharide alginate. Moreover, the complex CF mucus provides *P. aeruginosa* with carbon and energy to support high-density growth during chronic colonization.The problem of eradication of *P. aeruginosa* from chronically infected patients has also been shown to be due to bacterial mucoid secretions (Bjarnsholt *et al.*, 2009). *P. aeruginosa sp*. mutate to a mucoid type which is resistant to phagocytosis by cells of the immune system. This leads to increased tolerance to toxic oxygen radicals and antibiotics. Thus, over time, mucoid *P. aeruginosa* strains colonise the CF lung in structures referred to as biofilms, making chronic infections very difficult to treat (Hoiby, 2002).

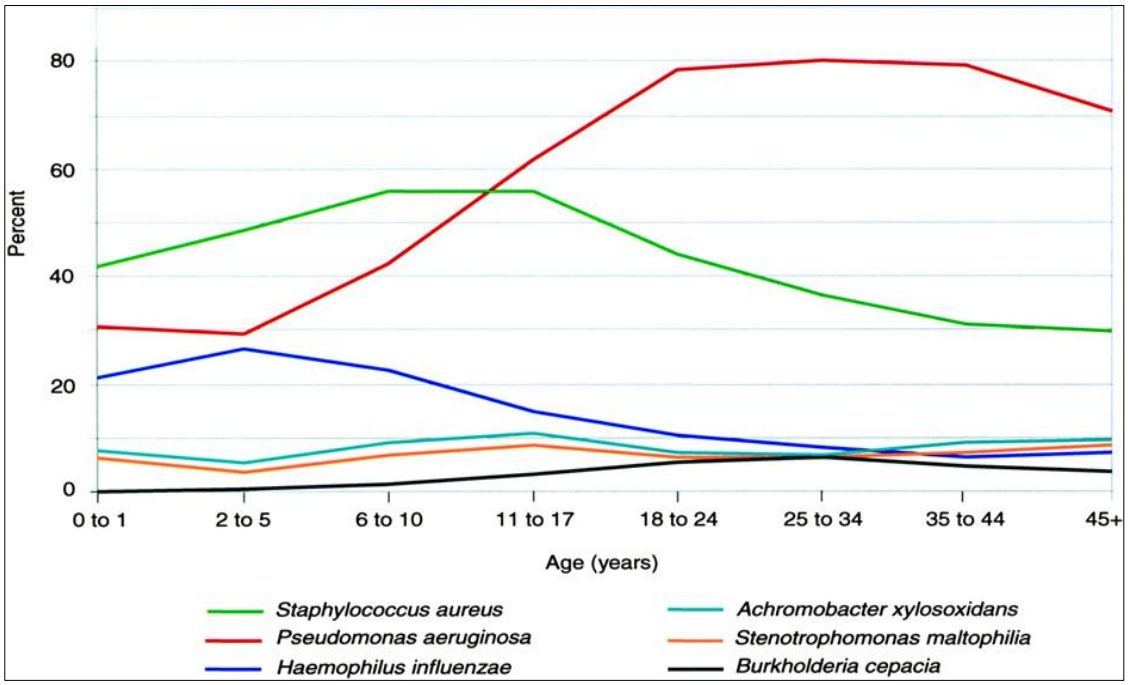

Figure 1.6. Prevalence of CF respiratory pathogens by age group (*Adapted from Harrison, 2007*).

In CF sputum, water content is reduced leading to an increase in physical entanglements and a pronounced increase in the viscoelastic nature of the sputum. When mucus becomes too thick, mucociliary clearance is reduced due to alterations in the mucus viscoelasticity and patients experience difficulty in mucus clearance. This leads to bacterial overgrowth such as chronic *P. aeruginosa* infection. Moreover, the altered mucus in CF patients acts as a diffusional barrier, reducing access of therapeutic agents to the epithelium. This is due to increased concentrations of highly-branched mucin glycoproteins, DNA, alginate, and lipopolysaccharides that form a dense mesh-like network that traps or adheres to the drug or gene carriers (Lai *et al.*, 2009).

The genetic basis of CF resides in the mutations in the transmembrane conductance regulator (CFTR) gene (Andersen, 1938). The mutations have been defined at the DNA level and affect the CFTR protein which acts as a regulator of chloride and other ion channels (Rommens *et al.,* 1989). This mutations result in a decrease of chloride transport across epithelia, fluid secretion and increased reabsorption of sodium, which causes a reduced water content of secretions and results in dehydrated, viscous mucus (Rommens *et al.,* 1989; Kerem *et al.,* 1989).

1.5. Treatment of CF

In general, CF treatments focus on reducing disease progression to delay the onset of irreversible lung damage. This can be achieved by using a number of treatment groups for a specific function, antibiotics to control the airway infection; mucolytics are used to inhance mucus clearance (Hodson *et al.,* 2003; Murphy and Rosenstein, 1998); steroids and nonsteroidal anti-inflammatory drugs are also used to control the inflammatory response (Marshall *et al.,* 2000; Murphy and Rosenstein, 1998); and α-adrenergic agonists as a bronchodilator.

1.5.1. Antibiotics

Intravenous antibiotics that are used for treatment of *P. aeruginosa* infections are usually given for 2 weeks or longer. Suggested antibiotic regimens include an aminoglycoside, such as tobramycin sulphate or amikacin sulphate, administered with broad-spectrum penicillin such as piperacillin or ticarcillin disodium (Franz *et al.,* 1994). Although intravenous (IV) antibiotic treatment of CF patients has improved in its techniques and patients live longer, chronic infection with *P.*

aeruginosa has emerged as a serious problem. In the US, 52% of patients with CF are chronically infected with *P. aeruginosa* and 51% with *S. aureus*. In the UK, the percentages are 36% and 15% respectively (Dodge *et al.,* 2007). Therefore, nebulised antibiotics have been used as an alternative to reduce levels of chronic *P. aeruginosa* infection. Nebulised antibiotics have been shown to maintain lung function between courses of antibiotics and also used as prophylaxis (Taylor and Hodson, 1993). Antibiotics that commonly used for inhalation therapy in infections with CF are colistin, tobramycin, and aztreonam (David and Madge, 2011). Lenoir and co-workers reported that high dose aerosolized tobramycin showed an improvement in lung function with a concomitant decrease in sputum density of *P. aeruginosa* (Lenoir *et al.,* 2007). However, some Pseudomonal strains become resistant to the antibiotics. For example, *P. cepacia* has emerged as a serious problem in patients with CF because this organism tends to develop resistance to multiple antibiotics. Furthermore, other study shows that the infection with *P. cepacia* has been associated with a severe pneumonia (Downey *et al.,* 2007; Paschoal *et al.,* 2007). Practically, aerosolized antibiotic agents are extensively used for patients chronically infected with *P. aeruginosa* (Banerjee and Stableforth, 2000; Geller *et al.,* 2007). It has been reported from 12 studies of nebulised antibacterials for maintenance treatment in CF patients that treatments using inhaled antibiotics can reduce the number of hospital admissions, while improving lung function (Touw *et al.,* 1995). It has also been shown that the penetration of an aerosolized solution in the human lung is more efficient when aerosolisation is preceded by physiotherapy and a bronchodilator (Kuni *et al.,* 1992).

1.5.1.1. Colistin

Colistin is a polymyxin antibiotic effective against most Gram-negative bacilli. It contains a mixture of d- and l-amino acids arranged as a cyclic heptapeptide ring with a tripeptide side chain (Figure 1.7) (Li *et al.,* 2005). More than 30 components have been isolated from colistin and the two major components are colistin A (polymyxin E1) and colistin B (polymyxin E2) (Thomas *et al.,* 1980). Colistin is commercially available in two forms: colistin sulphate which is the cationic stable form, while colistimethate is the anionic and readily hydrolysed form. Colistin is polycationic and has both hydrophilic and lipophilic moieties. These poly cationic regions interact with the bacterial outer membrane, by displacing bacterial counter ions in the lipopolysaccharide (Li *et al.,* 2005). Colistin is an old antibiotic that has been displaced by the potentially less toxic aminoglycosides in 1970s. However, due to the absence of new drugs active against resistant Gram-negative bacteria, colistin has attracted more interest recently because of its significant activity as anti-pseudomonal agent (Evans *et al.,* 1999; Li *et al.,* 2005; Schuster *et al.,* 2013). Colistin dose given for nebulisation is 1 to 2 million IU twice daily (Colistin base has an assigned potency of 30 000 IU/mg) (BNF, 2012).

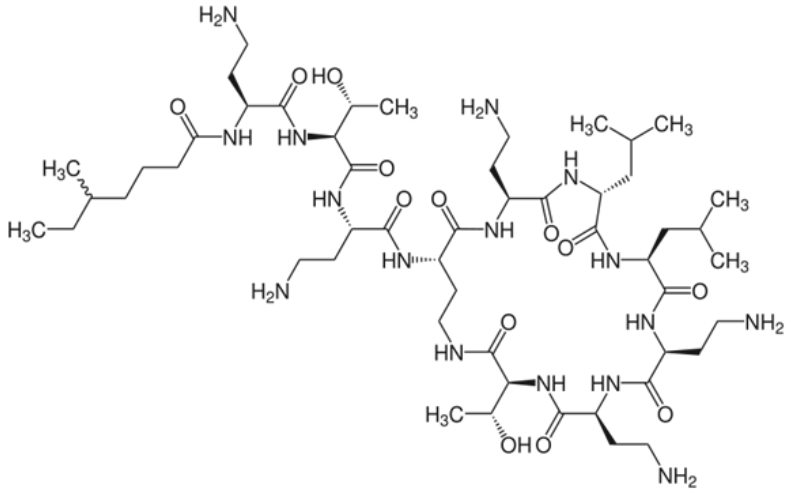

Figure 1.7. Structure of Colistin

1.5.1.2. Tobramycin:

Tobramycin is an aminoglycoside antibiotic derived from Streptomyces tenebrarius (Figure 1.8). It is effective against various types of bacteria particularly Gram-negative bacteria. Tobramycin is the aminoglycoside of choice for the treatment of confirmed Pseudomonas infections because it has higher activity against Pseudomonas species compared with other aminoglycosides such as gentamycin. It is preferred for the initial treatment of severe *P. aeruginosa*-related infections such as cystic fibrosis (Lode, 1998).

It can be given intravenously or intramuscularly and also be given in nebulised formulations for the treatment of exacerbations of chronic infection with Pseudomonas aeruginosa in patients diagnosed with cystic fibrosis. TOBI® is a tobramycin solution for inhalation given twice daily in 300 mg dose (Ramsey *et al.*, 1993). Like other aminoglycosides, tobramycin has ototoxicity and nephrotoxicity

for these reasons parenteral tobramycin needs to be carefully dosed (Lerner *et al.*, 1986).

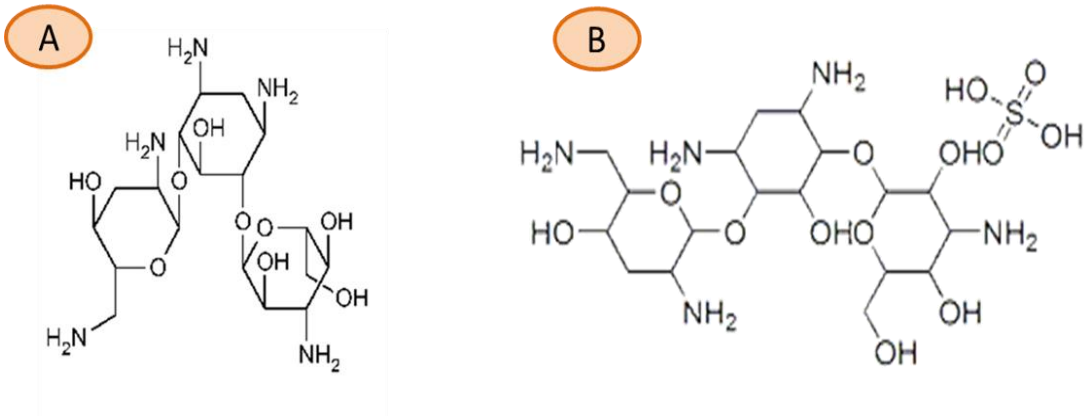

Figure 1.8. Structures of a) tobramycin, and b) tobramycin sulphate.

1.5.2. Mucolytic agents

Ideally, the aim of mucolytic therapy is to facilitate physiological clearance by adjusting the viscoelasticity of mucus. Therefore, the use of mucolytic agents as drug transport enhancers may be particularly important for diseases that have properties of abnormal viscous mucus, such as CF and COPD (Lai *et al.*, 2009). Mucolytic agents enhance drug penetration into mucus by altering the physical properties of the mucus and decrease its ability to act as a barrier to diffusion (Lethem, 1993). The most commonly used mucolytic agents are the sulphydryl reagents, e.g. erdosteine, N-acetylcysteine and S-carboxymethylcysteine. They reduce the cross-linking of mucin fibers by disrupting mucin disulfide bonds through sulphydryl exchange mechanism (Livingstone *et al.*, 1990). Sulphydryl compounds are available in an oral tablet or an

inhaled form given by a nebuliser. Mucinex® (N-acetyl-L-cysteine; NAC) is previously tested for its ability to improve the penetration of nanoparticles across CF sputum (Henke *et al.,* 2007). It has been reported that oral administration of the mucolytic agent erdosteine for one week to chronic bronchitis patients, increased the level of amoxicillin in sputum but not in serum, an effect that was associated with improved clinical outcome (Ricevuti *et al.,* 1988).

Another common mucolytic is Pulmozyme™, a Recombinant human deoxyribonuclease (rhDNase) also known as Dornase alfa. It acts enzymatically by breaking down the DNA that forms dense entanglements with mucin glycoproteins, thus reducing crosslinking and mucus viscoelasticity. It has been successfully used to treat the pathophysiological properties of CF, as a result of the viscous mucus. (rhDNase from Genentech Inc.) has been shown to improve the forced vital capacity (FVC) and the forced expiratory volume (FEV1) when administered by nebulisation (Fuchs *et al.,* 1994; Henry *et al.,* 1998; Hodson *et al.,* 2003; Frederiksen *et al.,* 2006). A study performed by Rozov and colleagues also showed that Dornase alfa inhalation is associated with an improvement in lung function of CF patients during the first year of treatment. In contrast, in patients with bronchiectasis not caused by CF, dornase alfa did not alter sputum transportability, lung function, dyspnoea or quality of life (Rozov *et al.,* 2010).

Another class of agents have attempted to increase penetration by affecting non-mucin components of mucus; EDTA, which can disperse alginate, is capable of increasing antibiotic diffusion through the alginate secreted by *P. aeruginosa*.

1.6. Lamellar bodies: Origin and function

Lamellar bodies are lipid storage and secretory organelles comprising many phospholipid layers vary greatly in size (100-2400) nm. They can be surrounded by a membrane and have a core composed of multilamellar membranes. Lamellar bodies are present in a wide variety of cell types to store and secrete certain lipids with defined functions (Schmitz & Muller, 1991). The most intensively investigated lamellar bodies are the pulmonary surfactants, a complex mixture of phospholipids and proteins synthesized by alveolar type II (ATII) cells in the lung epithelium (Kunkelmann *et al.,* 1988; Griese *et al.,* 1997) (Figure 1.9). They are also present in the bronchia and the nasal mucosa. Lamellar bodies provide a lipid film of dipalmitoyl phosphatidylcholine (DPPC) on the surface of lung alveoli to reduce surface tension during gas exchange (Villar and Slutsky, 1989), minimize alveolar fluid and function as a hydrophobic protective lining against environmental effects (Wright and Dobbs, 1991; Wang *et al.,* 2007). Furthermore, pulmonary surfactant is believed to play a role in the improvement of mucociliary clearance by physical removal of inhaled debris and particulate material including microorganisms from the alveoli and small airways (Griese, 1999).

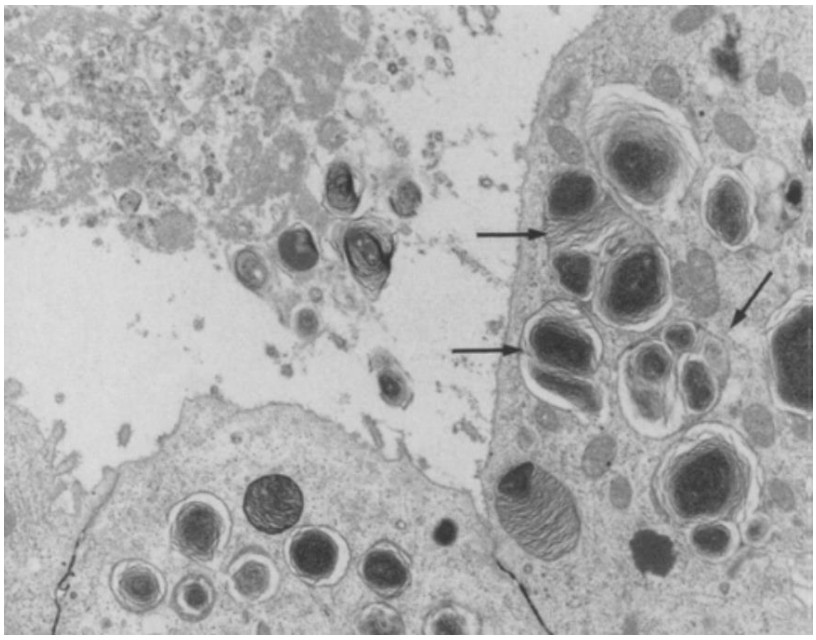

Figure 1.9. Lamellar bodies of a type II cell of a lung cell culture (*Adapted from Kunkelmann et al., 1988*).

In CF, functional and biochemical surfactant abnormalities develop with progressing disease; this is supported by correlations between surfactant parameters and lung function data (Griese *et al.,* 1997). In addition, research has suggested that a decrease in the appearance of lamellar bodies occurs in the respiratory tract of CF patients. A reduced production of lamellar bodies has been recorded in the tissue of CF mice, a defect that was reversible by replacement of CFTR gene (*Larson et al.,* 2000). In another study, an extreme decrease in phosphatidylcholine content in cystic fibrosis (CF) patients was reported (Gilljam *et al.,* 1989). Other authors have noted a lack of surfactant phospholipids in the CF airway (Puchelle *et al.,* 2002). However, the resultant deficiency of the lamellar bodies in cystic fibrosis patients can be altered. Wang and co-workers demonstrate the successful production of ATII cells by lamellar bodies formation, providing a practical source of ATII cells to explore in

disease models their potential in the repair of the injured alveolus and in the therapeutic treatment of genetic diseases affecting the lung such as CF (Wang *et al.*, 2007).

Lamellar bodies have an important function in mucociliary clearance and also in maintaining airway elasticity. So in treatment of CF patients the administration of exogenous lamellar body mimetics, as inhaled medications, could be a therapeutic approach to improve lung function.

1.7. Lamellasomes

Lamellasomes are lamellar body mimetics, composed of multilamellar vesicles of phospholipids and cholesterol, representative of lamellar bodies in the lung in both type and ratio and they have the amphiphilic nature of phospholipids (Figure 1.10 and Figure 1.11). Lamellasomes™ (LMS-611) is a formulation of multi-lamellar liposomes with a particle size ranged between 2-15 µm, suspended in normal saline (0.9% NaCl) solution to give an off white suspension of pH 4-6. It has a total lipid content of 19.6 mg /mL with a viscosity of $1.5 \times 10^{-3} \pm 0.2$ PaS and a zeta potential $\geq$ -10 mV $\leq$ -70 mV (Lamellar Biomedical). Battaglia team investigated formation of metastable multilamellar aggregates (lamellasomes) with various size ranges by spontaneous self-assembly of amphiphilic block copolymers in water. They reported that lamellasomes are stable due to the structural nature of the amphiphilic copolymer assembly, and showed the ability of these lamellasomes to transform into unilamellar vesicles (Figure 1.12) (Battaglia *et al.*, 2007).

The physico-chemical property of LMS formulation is suited to pulmonary delivery to enhance airway clearance. This is in part due to their inherent surface active and adsorptive properties which lead to the disruption of mucus, bacterial biofilms and sputum. This property is grants it to be a potential vehicle for co-formulation of drugs as it facilitates the generation of smaller aerosol droplets during nebulization. One area of therapeutic interest for such formulations is cystic fibrosis (CF), since the CF lung may harbour antibiotic-resistant bacteria such as mucoid strains of *P. aeruginosa*.

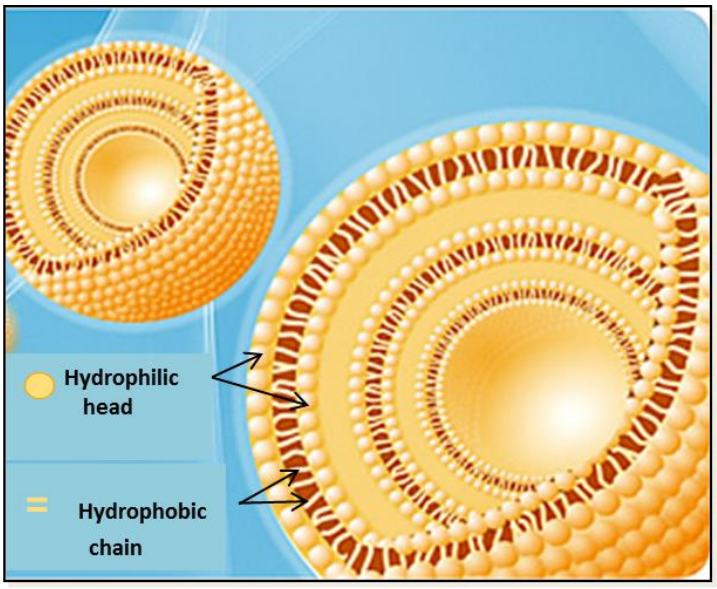

Figure 1.10. Schematic illustration of Lamellasomes.

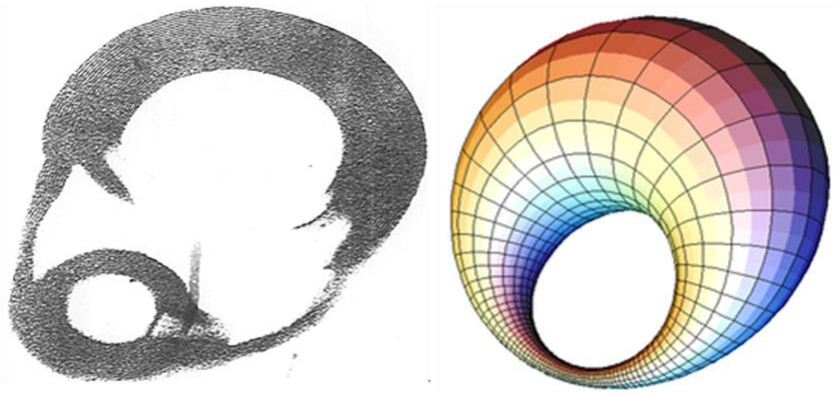

Figure 1.11. An electron micrograph of a Lamellasome™ displaying tightly-packed concentric lamellae with identical Dupin cyclides geometryto that found in naturally-occurring lamellar bodies (Left). An illustration of the inverted toroid, typical of a Dupin cycloidic geometry is shown on the right (Wikipedia commons).

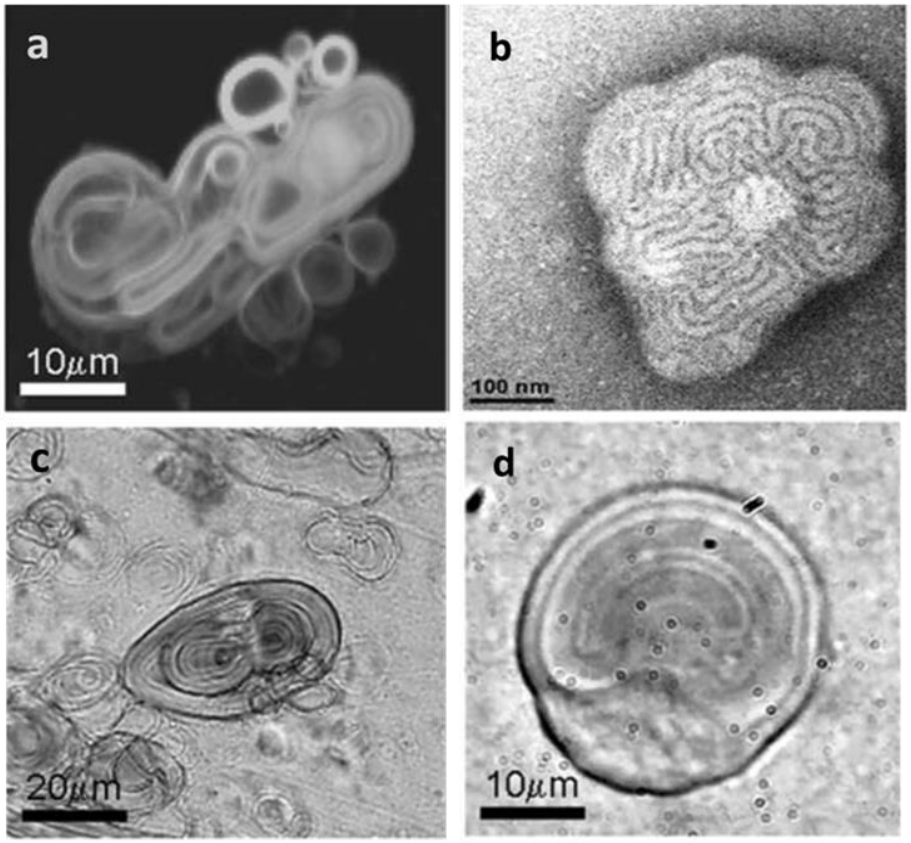

Figure 1.12. Confocal laser scanning (a), transmission electron (b) and optical (c and d) micrographs of lamellarsomes (*Adapted from Battaglia et al., 2007*).

1.8. Bacteriophages as therapeutic agents:

Recently, bacteriophage therapy has received more interest as an alternative therapy for antibiotic resistant bacterial infections. The concept of phage therapy is not new, since phages have been used for the treatment of bacterial infections, such as gangrene and dysentery, in humans over the past 90 years quite successfully in Eastern Europe and the former Soviet Union, and is still routinely used in the Republic of Georgia. The first treatment with phage was reported in 1921, when six patients with Staphylococcus skin disease were treated using phage (Sulakvelidze and Kutter, 2005). By the 1930s, anti-staphylococcal phage products were produced on the market. In the late 1930s phage preparation as well as phage therapy researches were discontinued for many reasons. The most important reason was the discovery of antibiotics; another reason was the poor understanding of phage therapy. Since the 1990s, there has been a revival in interest in phage as antibacterial agents and phage therapy is being studied now in an attempt to solve the problem of antibiotic resistance.

The word bacteriophage means 'bacteria eater' since bacteriophages (phages) are viruses that infect bacteria (Douglas, 1975). Viruses are the most numerous organisms on Earth, with an estimated number in the range of 10^{31} or more, and phages are the most numerous of viral types (Hyman and Abedon, 2009). In the environment, phages are 10 times more numerous than bacteria. They can be isolated from aquatic environment albeit that they appear wherever bacteria reside. Viruses lack the ability to replicate unless they infect a cell and gain the ability of

reproduction. Phages cannot infect mammalian cells, they specifically target bacteria, each phage typically attacks a single species, and sometimes it can become more specific and attack a single strain of bacterium. Phages infect bacteria (host cells) and use them to replicate up to 10,000 progeny which are released after the host cell is killed (Hanlon, 2007).

The structure of phage contains a head (or called capsid) composed of a protein coat of icosahedron shape with viral genome inside (mainly double-strand DNA). The capsid protects the nucleic acid and facilitates attachment of bacterial cell. The phage either has a tail with six tail fibres containing receptors that function as attachment sites on the host cell surface, if the phage does not have a tail it attaches to the bacterial cell by other attachment mechanism (Figure 1.13) (Hanlon, 2007).

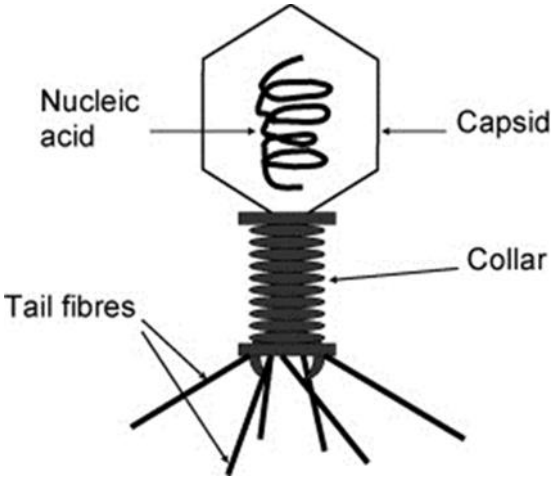

Figure 1.13. Diagrammatic representation of a typical bacteriophage (*Adapted from Hanlon, 2007*).

Bacteriophages can be divided into two types according to their life cycle: virulent and temperate. Virulent phages kill the host cell (bacterial cell) by rapid lysis to release progeny phages, whereas temperate phages form a long stable relationship with the host cell and spend part of their life cycle in a state called prophage. Viral DNA either exists as a plasmid or integrated into the host cell DNA. If the host cell genome replicates the prophage DNA also replicates and the resultant cells will inherit the viral DNA (Lenski, 1988). Because of their ability to integrate their genome into the host genome, temperate phages may cause undesirable pheno-typical changes. Therefore, they are not appropriate for use in phage therapy. On the other hand, virulent phages offer the greatest therapeutic potential due to their lethal effect on the host cell (Carlton *et al.*, 2005).

The life cycle of a bacteriophage begins when it moves toward its bacterial host in a random motion and attaches to the cell surface via receptor sites which are usually one of the cell surface components (protein, lipopolysaccharide or oligosaccharide). This attachment is followed by penetration of the nucleic acid into the host cell allowing replication of the virus and causing cell lysis and release of viral progeny (Figure 1.14).

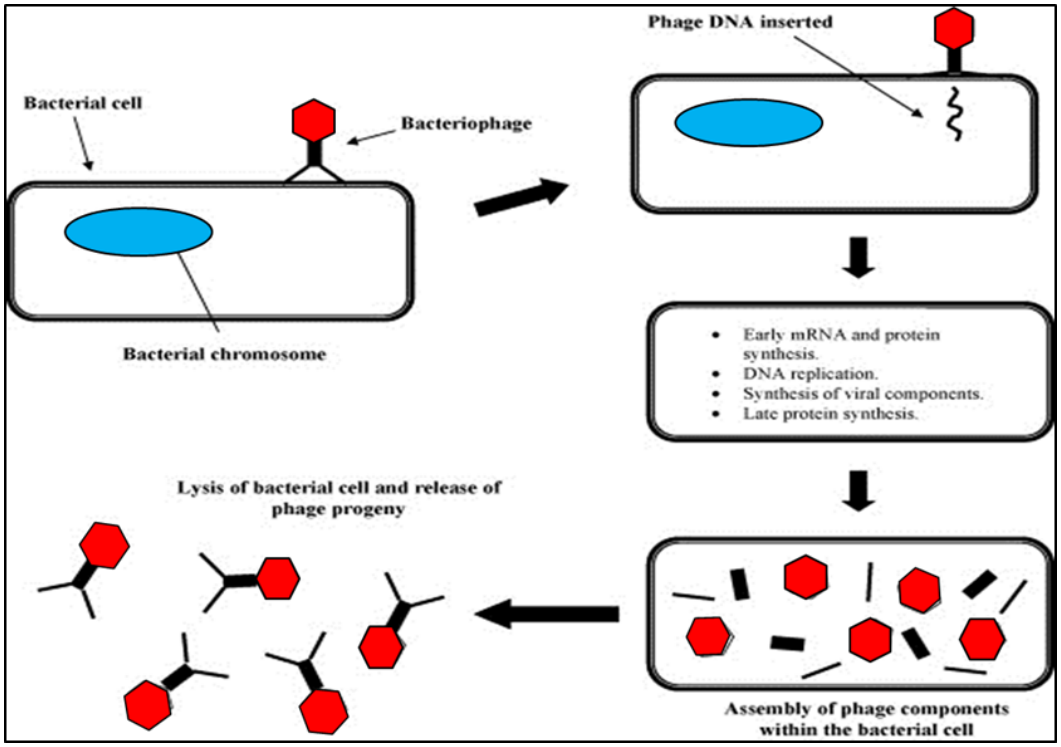

Figure 1.14. Lytic cycle of a virulent bacteriophage (*Adapted from Hanlon, 2007*).

The bacteriophage are classified according to its morphology as seen in Figure 1.15. There are various morphological types of phages with different nucleic acids including DNA, RNA, single stranded, segmented and double strand non-segmented DNA genome of tailed phage which is the most common (Table 1.2).

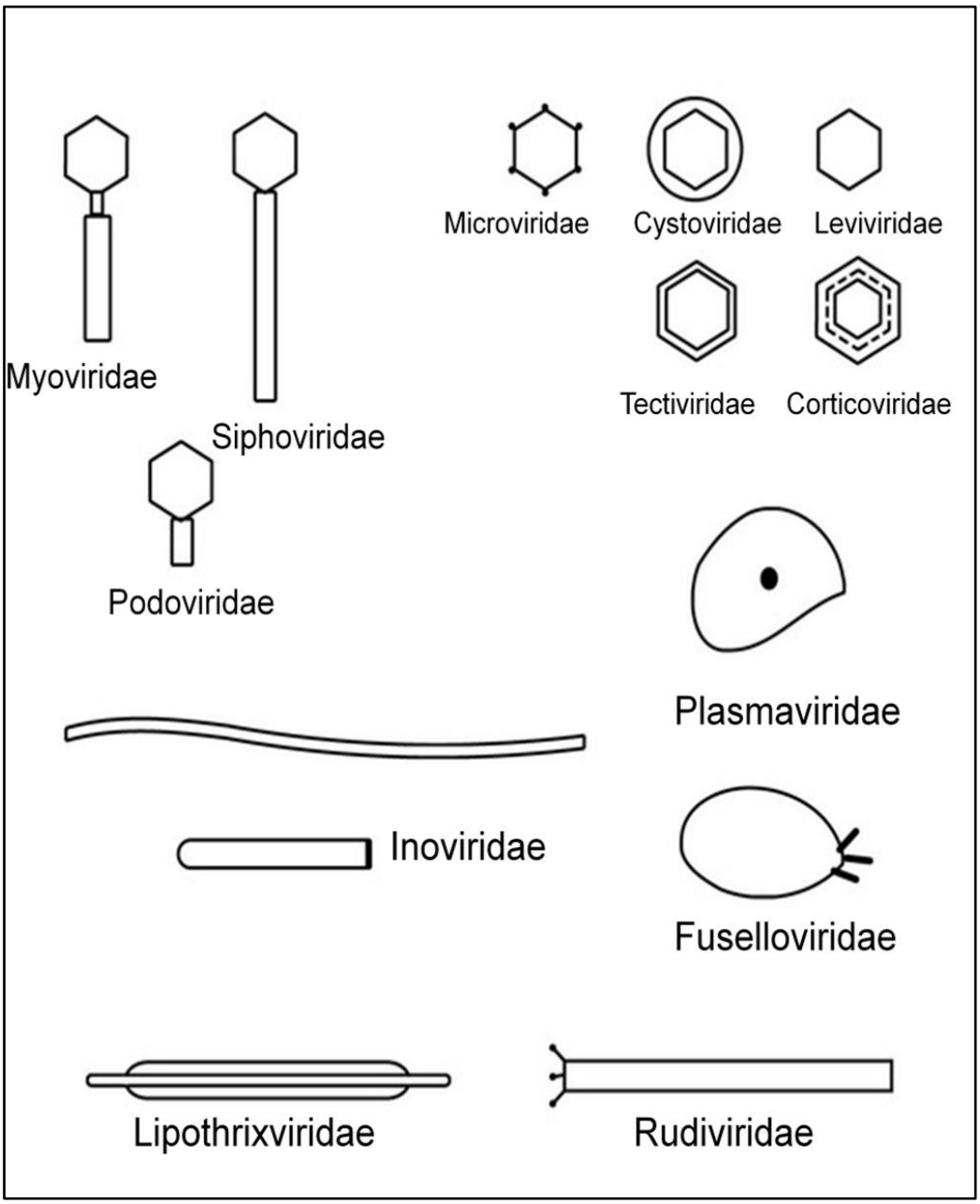

Figure 1.15. Morphological classification of bacteriophage (*Adapted from Kutter & Sulkavelide, 2005*).

Table 1.2. Bacteriophage Classification (ds: double-stranded; ss: single-stranded) (Sulakvelidze and Kutter, 2005; Hanlon, 2007).

Phage group	Family name	Morphology	Genome
Tailed phages	Myoviridae	Contractile tail	dsDNA
	Podoviridae	Short, non-contractile tail	dsDNA
	Siphoviridae	Long, non- contractile tail	dsDNA
Tailless phages Polyhedral DNA Phages	Microviridae	Icosahedral capsid	ssDNA
	Corticoviridae	Icosahedral capsid with lipid layer	dsDNA
	Tectiviridae	Icosahedral capsid with inner-lipoprotein vesicle	dsDNA
Polyhedral RNA Phages	Leviviridae	Quasi-icosahedral capsid	ssRNA
	Cystoviridae	Enveloped, icosahedral capsid, lipids	dsRNA
Filamentous phages	Inoviridae	Rod-shaped with helical symmetry	ssDNA
	Lipothrixvirdae	Enveloped filaments, lipids	dsDNA
	Rudiviridae	Helical rods	dsDNA
Pleomorphic phages	Plasmaviridae	Pleomorphic, envelope, lipids no capsid	dsDNA
	Fuselloviridae	Pleomorphic, envelope, lipids no capsid	dsDNA

A bacteriophage is specific for a particular bacterial host (Toro *et al.,* 2005). With this advantage, bacteriophages are good candidates and alternative agents for bacterial infections, particularly in antibiotic resistance. The host range of the phage is usually determined by the surface structures that are used to dock on bacteria, which are either carbohydrate or protein receptors. In Gram-negative bacteria, oligosaccharides and lipopolysaccharides can act as the receptors for some phage.

However, the complexity of Gram-positive bacteria offers a very different set of potential binding sites (Fischetti *et al.,* 2006). Some phage therapy is based on use of intact phages. Using whole phage as a therapy has the advantage that for every one phage that enters a bacterial cell replicates inside and then causes lysis, 10 to 100 phage particles are subsequently released, which can then enter other bacterial cells, etc. Sometimes, the high specificity of phages limits their potential to attack an unknown diversity of target bacteria. Another possibility is the emergence of bacterial resistance to phage attachment as a defensive way of bacterial survival. Scientists have overcome this either by careful selection and designing a cocktail of phages (different phage with different lysis ranges) to circumvent resistance (Sulakvelidze *et al.,* 2001) or by the use of a single broad host range phage that can infect most of bacteria (Carlton *et al.,* 2005). A few phages with a relatively broad host range are known, making them possibly useful for therapeutic purposes.

Phage therapy may also be based on phage components as the phage system requires specific viral proteins to target bacterial DNA and RNA during lytic proliferation of viral DNA replication (Fischetti *et al.,* 2006).

Table 1.3. Phage therapy related to diseases, Adapted from (Sulakvelidze *et al.,* 2001).

Reference(s)	Infection(s)	Etiologic agent(s)	Comments
Weber-Dabrowska, Mulczyk, Gorski (2003)	Septic infection	*S. aureus, P. aeruginosa, E. coli, K. pneumonia, P. mirabilis, M. morganii, Enterobacter*	Successful prevention and treatment of septicaemia in humans.
Marza *et al.,* (2006)	Skin burn with infection	*P. aeruginosa*	A 27-year old with 50% surface area burns. After skin graft and excision, the wound became infected. Purified phage suspension could heal the wound with no adverse effects.
Marza *et al.,* (2006)	Chronic bilateral otitis externa	*P. aeruginosa*	A 5-year-old dog presented with chronic bilateral otitis externa was given a phage suspension. After treatment the ear was dry and the inflammation disappeared.
Weber-Dabrowska *et al.,* (2006)	External ear infection	*S. homes, S. epidermidis*	A 24-year-old woman who suffered from post-influenza otitis media infection. Specific bacteriophage combined with lactoferrin administration improved the treatment of infection.
Biocontrol. Ltd.UK.(2007)	Otitis	*Pseudomonas*	The first completed phase II clinical trial testing the efficacy of phage therapy, in this case for human ear infections.
Grandgirard, *et al.,* (2008)	Meningitis	*Streptococcus pneumoniae*	Phage lysin specific for *S. pneumonia (recombinant Cpl-1)* was used with infant rat to treat pneumococcal meningitis. Cpl-1 decreases the pneumococci in cerebrospinal fluid.

Heo and co-workers characterized two new potentially lytic bacteriophages (MPK1 and MPK6) that were effective against *P. aeruginosa* infections. They found that Intramuscular and intraperitoneal administration of MPK1 and to a lesser extent MPK6, significantly protected mice from mortality caused by PAO1-induced peritonitic sepsis (Heo *et al.,* 2009). *S. aureus* has different clinically important strains (Deurenberg *et al.,* 2007). Therefore, for treatment of *S. aureus* infections, the phage(s) selected should be polyvalent which means that it should have a broad host range and have the ability to infect these strains. There are many polyvalent virulent (obligately lytic) *S. aureus* phages reported in the literature. Phage ϕ812, a member of the family Myoviridae, has been reported to kill 95% of the 782 *S. aureus* culture collection strains (Pantucek *et al.,* 1998). Phage K is another polyvalent lytic phage (Rees and Fry, 1981). It has a broad host range and effective against a range of MRSA strains including vancomycin and teicoplanin resistant strains (O'Flaherty *et al.,* 2005). Vybiral and his group in 2003 have demonstrated that phage K can infect 39 of 53 MRSA strains. Their study has shown that phage K was effective in reducing the *S.aureus* counts in the *in situ* hand wash model (Vybiral *et al.,* 2003).

Phages have many advantages over antibiotics as therapeutic agents; the most important advantage is that they are effective against multidrug resistant pathogenic bacteria (Hanlon, 2007). This may be attributed to the different mechanism of action that phages have compared to antibiotics. As a result, phages may be effective against multi drug resistance bacteria and in future could therefore be reserved as a last line of defense, either alone or, more probably, in conjunction with antibiotic

administration. In addition, phages have fewer side effects than antibiotics since phages or their products do not affect eukaryotic cells (Matsuzaki *et al.,* 2005). However, we do not yet appreciate the full value of phage-based therapy since it has not yet been extensively tested in humans under sufficiently diverse scenarios. One theoretical advantage is that due to their specificity, phages given orally will target only the gut pathogens and will not affect the normal flora of the gut, and the potential overgrowth of secondary pathogens is avoided. In addition, phage distribution within a given environment is considered a natural process since phages consists entirely of proteins and nucleic acids. Therefore, when they breakdown, they produce natural products: amino acids and nucleic acids (Carlton *et al.*, 2005). Moreover, phages are easier to produce (albeit that truly large scale bioprocessing has not yet been achieved), cheaper in cost than certain antibiotics and in theory requires less doses frequency due to the ability of phages to replicate within the target bacteria. It is also promising to see evidence showing that phages can penetrate poorly vascularised tissues and can cross the blood-brain barrier (Alisky *et al.*, 1998).

Although they have developed to tolerate difficult environmental conditions, phages are show individual variation and their strength varies over a broad range. Some phages are very stable at different conditions so they can be stored without special precautions. Others are fragile and need to be handled with care and stored in specific conditions (Ackerman *et al.,* 2004). Therefore, many variables should be considered when storing phages.

There are different methods for the storage of phage preparations. *Bacillus anthraci* specific gamma phages can be stored at 2 to 5 °C for one year, with the phage titre dropping to 30% of the original activity. Freezing at – 70/ – 80 °C or in liquid N_2 with glycerol or dimethylsulphoxide (DMSO) is another way of storage. Although phages appear to survive freezing well, this method is not suitable for phage therapy since phages need to be distributed to the end-user in a less costly manner, i.e. using refrigeration or 'room temperature' distribution. Another method for phage storage is freeze drying, which is commonly used for many pharmaceuticals including proteins and DNA. The success of freeze-drying may depend on the lyoprotectant used. Freeze-drying without protectant, such as in plain buffer or in culture medium, may be expected to result in a rapid loss of infectivity, although this is very much dependent on the phage under study. Ackermann and colleagues reported that a wide variety of bacteriophages had survived 20 years in freeze-dried ampoules that had retained the vacuum (Ackermann *et al.*, 2004).

Many researchers have investigated the use of bacteriophage in experimental infections of animals. Smith and Huggins (1982) infected mice with a toxigenic encapsulated strain of *E. coli* isolated from a baby with meningitis. They used anti-K1 phage which is specific for the K1 capsular antigen, and found that a single intramuscular dose was as effective as multiple intramuscular doses of ampicillin, tetracycline, cloramphenicol or trimethoprim with sulfafurazole. Another study was conducted by Soothill (1994) using guinea pigs for the effectiveness of phage against burn wound infections that caused by *P. aeruginosa*. He showed that the prophylactic administration of phage can prevent the destruction of skin grafts by *P.*

aeruginosa (Soothill, 1994). Biswas and group showed that upon intraperitoneal (i.p.) administration of 10^9 colony forming unit (CFU) of vancomycin resistant *Enterococcus faecium* (VRE), mice were all dead within 48 hours. By administration of i.p. injection of 3×10^8 plaque forming unit (PFU) of phage preparation after 45 minutes of VRE administration, the animals all survived (Biswas *et al.,* 2002). The results obtained from these studies provide evidence that bacteriophage therapy is an effective treatment of animal bacterial infections, and may have a role in the treatment of human infections.

A study was conducted to investigate the possibility of respiratory delivery of a *Burkholderia capacia* complex (BCC) bacteriophage by nebulized aerosol administration to treat bacterial lung infection. The results showed that BCC bacteriophages can be nebulized successfully within a reasonable delivery time (Golshahi *et al.,* 2008). Another study reported the development of microencapsulated bacteriophage Felix O1 for oral delivery using chitosan-alginate-$CaCl_2$ system. Their results revealed that these microspheres may facilitate therapeutic phage delivery to the gut (Ma *et al.,* 2008). Puapermpoonsiri *et al.,* 2009 have demonstrated that bacteriophage can be encapsulated into biodegradable polyester microspheres as controlled delivery formulation for the treatment of bacterial lung infections.

From a large amount of clinical data collected from the Institute of Immunology and Experimental therapy, Slopek and co-workers (1987) described the results obtained between 1981 and 1986 at 10 hospitals from 550 patients with conditions of wound

infections, peritonitis, respiratory tract infections and bacteraemia. Patients were treated against *Staphylococci*, *Klebsiella*, *Pseudomonas*, *E. coli* and *Salmonella* with 10 mL of bacteriophage oral suspension or topical phage-soaked dressings, results showed that about 94% of the patients completely recovered. In another study, It has been found that 20 cancer patients with concurrent bacterial infections was cured after receiving bacteriophage treatment in a dose given orally three times a day (Dabrowska *et al.,* 2005). Paisano and colleagues have described the use of human dental roots infected with *Enterococcus faecalis* to study the efficacy of bacteriophages as antimicrobial agents. They found that when different phage to bacteria ratios was used, the viability of bacteria in root canals was reduced (Paisano *et al.,* 2004). Wright's team, in their first controlled clinical trial of therapeutic bacteriophage ear drops preparation (Biophage-PA) evaluated the efficacy and safety to target antibiotic resistant *P. aeruginosa* in chronic otitis. They concluded that the therapeutic bacteriophage preparation showed enhanced efficacy combined with safety in chemoresistant patients (Wright *et al.,* 2009).

Some phage preparations have already been produced into the markets and used in clinic for treatment of topical antibiotic resistant bacterial infections. The PhageBioDerm® preparation is a biodegradable patch consisting of polymeric material incorporating phage. These have been used in Republic of Georgia for treatment of chronic skin infections that resist antibiotics (Sulakvelidze *et al.,* 2001). Moreover, it has been reported recently that a Phase I/IIa clinical trial for treatment of *P. aeruginosa* infections of the human ear was completed in November 2007 (Wright, et al., 2009).

1.9. Aims and objectives of the thesis:

The overarching aim of the thesis is to investigate novel routes to the formulation and processing of bacteriophages for non-invasive naso-pulmonary delivery, testing the antibiotic activity of selected formulations as proof of concept of their therapeutic potential:

- Formulation of lyophilised nasal insert, harbouring bacteriophage as the therapeutic agent for treatment of MRSA infections and evaluation of its therapeutic efficacy against *S. aureous* (Chapter 2).
- Present a new approach for bacteriophage bioprocessing through co-precipitation of an aqueous mixture of phage (*S. aureus* phage) and a crystallisable carrier (glutamine or glycine) with or without stabilizers (Chapter 3).
- Improve the pulmonary delivery of nebulized solutions of antibiotics or bacteriophage by dilution into Lamellasomes^{TM} (LMS) for treatment of antibiotic-resistant bacteria (mucoid strains of *P. aeruginosa*) in cystic fibrosis (Chapter 4).

Chapter 2: Formulation and evaluation of a new dosage form for bacteriophage therapy of nasal MRSA infections.

2.1. Introduction

In the past, the emergence of MRSA raised a serious therapeutic and infection control issue (Cookson, 1993). A pandemic of MRSA which resisted treatment with the currently used antibiotics, combined with the worrying lack of new antibiotics in the pipeline led researchers to investigate alternative strategies for the treatment of bacterial infections.

It is known that nasal decolonization offers an effective strategy to reduce the *S. aureus* infections generally and specifically in MRSA infections (Critchley, 2006). To our knowledge, there is limited work on the formulation of bacteriophage to be administered intra-nasally. The present study is intended to formulate a new dosage form for bacteriophage therapy of MRSA infections. It is known that the viability of bacteriophages is rapidly lost upon exposure to low pH acidic gastric fluid via oral administration (Ma *et al.,* 2008). In view of these data, we selected the nasal route to avoid the harsh gastric environment and to deliver drug directly into the systemic circulation (Mygind and Dahl, 1998). Furthermore, using the nasal route of administration would allow the nasal insert composed of bioadhesive polymers such as hydroxypropylmethyl cellulose (HPMC) to hydrate (Henriksen *et al.,* 1996). HPMC (Figure 2.1) has a high viscosity and water- withdrawing property that results in high bioadhesion, giving a long residence time in the nasal cavity allowing higher

absorption than conventional nasal formulations (McInnes *et al.,* 2005). From this, the disadvantage of rapid mucociliary clearance from the nasal cavity was minimised. Mannitol was added to some of the formulations. It was selected as an excipient because it is a non-hygroscopic material that is accepted for use extensively in the pharmaceutical formulations (Kibbe, 2000). It is also used widely as a protein stabilizer in dried protein formulations (Bakaltcheva *et al.,* 2007; Schule *et al.,* 2007). The administration of highly viscous polymer solution or gel to the nasal cavity is far from straight forward and such delivery systems may need a special device for application (McInnes *et al.,* 2007). The polymer plug described by McInnes and colleagues was designed to assist manual application of the nasal insert. It works in the following way: on contact with the moist nasal mucosa surface, the lyophilisate will hydrate to form a HPMC gel concentration higher than that measured originally prior to the lyophilisation. This re-hydrated, highly concentrated HPMC gel should result in greater bioadhesion and longer residence time in the nasal cavity, combined with the improved absorption attributed to the transient dehydration effect on the nasal mucosa, leading to intimate contact with the bacteriophageal formulation.

Lyophilised nasal inserts were prepared using *S. aureus* bacteriophages. The effect of lyophilisation on the phage viability and the activity of preparation on storage were evaluated. The polymer was selected on the basis of its inert nature and thus it should not be compromise the biological activity of bacteriophages. Physical properties including porosity, the extent of hydration and water absorption were investigated.

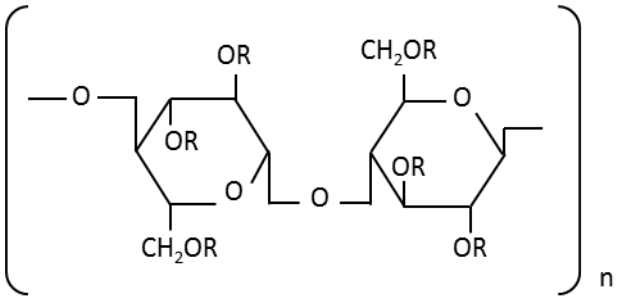

Figure 2.1. Chemical structure of HPMC. The substitution R represents either a $–CH_3$, or a $–CH_2CH(CH_3)OH$ group or a hydrogen atom (*Adapted from Siepmann and Peppas, 2001*).

2.2. Materials and Methods

2.2.1. Materials

Hydroxypropyl methylcellulose (HPMC) powder K4MP grade was obtained from Dow Chemicals (Michigan, IL, USA). The letter K represents a hydroxypropyl substitution of 8.1% and a methoxyl substitution of 22%. The number 4 indicates the viscosity of 2% HPMC aqueous solution at 20ºC. The letter P identifies premium grade product. D-mannitol powder was purchased from VWR International, Lutterworth, UK.

Granulated agar, tryptone, yeast extract and sodium chloride were all purchased from Melford Laboratories Ltd., Ipswich, UK. Gelatin, fluorescein isothiocyanate (FITC), Trizma base and magnesium sulphate heptahydrate were purchased from Sigma-Aldrich Chemical Company (Dorset, UK). Dichloromethane (DCM) and methanol were purchased from Fischer Scientific, Leicestershire, UK. All other chemicals were at analytical grade or equivalent.

2.2.2 Bacterial and bacteriophage strains

The bacterial strain used as a model for MRSA was the *S. aureus* FDA209P variant, acquired from the National Collection of Industrial, Food and Marine Bacteria (NCIMB), Aberdeen, UK (strain 8588; (American Type Culture Collection (ATCC) ref: 11522). The bacteriophage selective for this *S. aureus* strain is of the family Siphoviridae and was acquired from the National Collectional Industrial, Food and Marine Bacteria (NCIMB), Aberdeen, UK (cat. no. 9563; ATCC ref: 6538-B).

2.2.3. Methods

2.2.3.1. Bacteria

2.2.3.1.1. Preparation of media

Luria Bertani (LB) broth

9 g of NaCl, 4.5 g of yeast extract and 9 g of tryptone were dissolved in 700 mL of water and adjusted to 900 mL (pH ~7.4). The broth was sterilised by autoclaving at 120 °C for 20 min and subsequently stored at room temperature.

Luria Bertani (LB) agar

13.5 g of bacterial grade agar was included in the LB broth mixture described above. For 'soft' top agar (used in plaque assays, 6.7 g of agar was included). After sterilisation, the mixture was cooled to 45-50 °C and ~25 mL of this molten agar poured into an aseptic polystyrene Petri dish. The agar plate was kept in a laminar flow cabinet for few hours until solid and then stored at 4 °C for no more than 1 week.

Storage medium

5.8 g of NaCl, 0.98 g of anhydrous MgSO4, 0.1 g of gelatin and 50 mL of 1 M Tris HCl (pH 7.5) were dissolved in 900 mL of water which was adjusted to 1 L (pH 7.5). The solution was autoclaved and stored at room temperature.

2.2.3.1.2. Bacterial culture

S. aureus bacterial cultures were grown in LB medium (9 g of tryptone, 4.5 g of yeast extract, 9 g of NaCl dissolved in 900 mL of water). Frozen stocks were initially streaked and grown on LB medium containing 1.5% agar, to select for individual

colonies. Cells were cultured by inoculating 5 mL of LB medium with a single colony of *S. aureus* bacteria and incubating overnight at 37 ºC with vigorous shaking. These overnight cultures were then used for bacteriophage preparation.

2.2.3.2. Bacteriophage

2.2.3.2.1. Bacteriophage preparation

A mixture of 300 µLbacterial culture and 450 µLbacteriophage stock solution (10^9-10^{10} plaque forming unit per mL (pfu/mL) was incubated for 20 minutes at 37 ºC and 200 µLwas added to 4 mL of partially cooled LB agar (LB broth containing 1.5% agar). This was poured onto a cooled LB agar plate which was incubated at 37 ºC overnight (Sambrook and Russell, 2001).

Bacteriophages were collected by adding 5 mL of storage medium (SM) buffer to flood the plates which were kept at 4 ºC for 3 to 4 h and swirled gently every 0.5 h. Bacteriophage was then collected by decanting the storage medium from the plates which then filtered by using 0.22 µm pore size filter (Millipore Ltd., Watford, UK), and stored at 4 ºC.

2.2.3.2.2. Bacteriophage titration (plaque assay)

The lytic activity of the bacteriophage (the phage titre) was determined by plaque assay. To determine the phage titre, a phage stock solution was titrated by ten-fold serial dilutions in SM buffer and 100 µLof each dilution was mixed with 100 µLof overnight bacterial culture. The mixture was added to 4 mL of partially cooled LB agar and poured onto LB agar plate. Plates were then incubated overnight at 37 °C. The number of plaques was counted the following day and used to calculate the

concentration of bacteriophage (pfu/mL) (Figure 2.2). A negative control (bacterial culture without bacteriophage) and positive control (bacterial culture with a known concentration of bacteriophage) were also prepared for comparison. To determine the residual lytic activity of the lyophilized bacteriophage in the nasal inserts, each lyophilisate was reconstituted in 1 mL sterile water and the plaque assay was performed from the serial dilutions as above. Phage titres were calculated from the dilutions giving a countable number of plaques (< 300) per plate, this was generally around a dilution of 10^6. Bacteriophage formulations before lyophilisation were also tested for lytic activity, in order to evaluate the effect of lyophilisation and storage on phage integrity. The lytic activity of the bacteriophage from the lyophilisate was tested at day 1, 4, 7, 14, 30, 60, 180, 240 and 360.

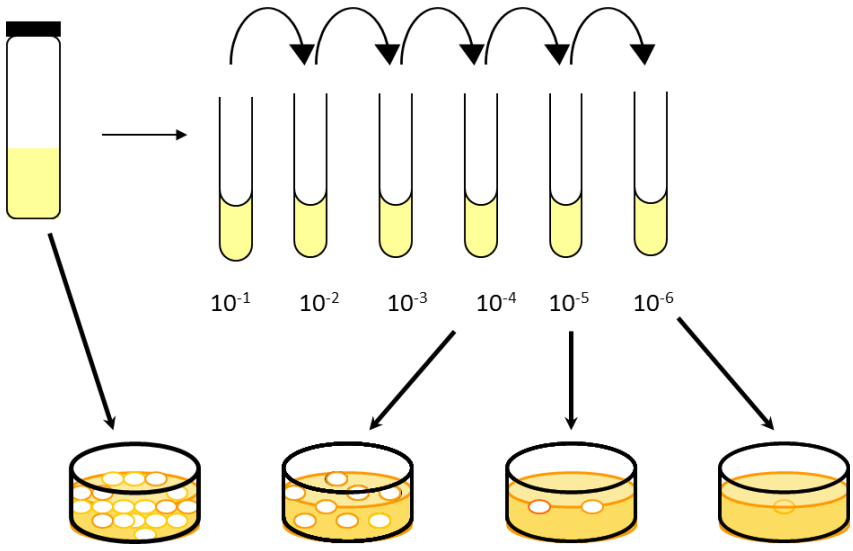

Figure 2.2. Plaque assay method.

2.2.3.2.3. Bacteriophage purification

Purified bacteriophages were prepared using a modified method (Sambrook and Russell, 2001). Briefly, 0.5 g caesium chloride (CsCl) was added to each mL of bacteriophage solution and allowed to dissolve. A step gradient was prepared by pouring 2 mL of CsCl solutions of decreasing density (1.7, 1.5, and 1.4 g/mL) on top of one another in a thick-walled 38 mL polycarbonate centrifugation tube (Beckman-Coulter, High Wycombe, UK). The aqueous preparation of bacteriophage in CsCl was then carefully poured on top of these layers, and the interface between the layers was marked on the outside of the tube. After centrifugation at 22,000 rpm in a Beckman SW 28 rotor (64,000 x g) at 4 ºC for 2 h a visible bluish band was formed at the interface between CsCl solutions of 1.4 and 1.5 g/mL densities which was carefully collected using a syringe with small size bore needle (21G) and stored at 4 ºC to use for labelling or formulation. The lytic activity (titre) of bacteriophage solution after purification was also tested by plaque assay as above.

2.2.3.2.4. Fluorescence labelling

Fluorescein isothiocyanate powder (FITC) 0.5 g was added to 1 mL of purified bacteriophage solution which then equilibrated in 10 mL of 46 mM $NaHCO_3$ (pH 9) and shaken gently for 2 h. The resulting suspension was centrifuged and dialyzed extensively in phosphate buffered saline (PBS), pH 7.4, by 3× exchange over 24 h using a cellulose dialysis bag with a MW cut-off at 12,400 Da (D9777, Sigma-Aldrich, UK) to remove free FITC.

2.2.3.3. Formulations

2.2.3.3.1. Preparation of formulations

Control samples (labelled ‘C’) were prepared by dissolving the required amount of HPMC powder in one third of the final volume of sterile distilled water (at 80 to 90 ºC), by slow addition of HPMC with stirring until a consistent dispersion was obtained. The remaining amount of sterile water was then added (using water at room temperature) and stirring was continued until a uniform gel of 1% and 2% (w/v) HPMC was obtained. The required mass of mannitol powder was also added, where appropriate, to produce a concentration of 1%. The gel was stored at 4 ºC overnight to partially degas the gel and allow complete hydration of the polymer chains. Blank samples (labelled ‘B’) were prepared as above using sterile SM instead of sterile distilled water. Formulated samples (labelled ‘F’), for inserts containing the bacteriophages, were prepared as for the blank samples, the required amount of stock phage solution being added to the aqueous HPMC dispersion with gentle stirring. Gel formulations and blanks were prepared as outlined in Table 2.1.

Table 2.1. Composition of HPMC gels used to manufacture lyophilised formulations

Notation/ formulation	**Control samples (without gelatin)**				**Blank samples (with gelatin)**				**Formulation samples (with gelatin)**			
	C1	C2	C3	C4	B1	B2	B3	B4	F1	F2	F3	F4
HPMC	1%	1%	2%	2%	1%	1%	2%	2%	1%	1%	2%	2%
Mannitol	-	1%	-	1%	-	1%	-	1%	-	1%	-	1%
Phage stock (10^{10}pfu/mL)	-	-	-	-	-	-	-	-	10%	10%	10%	10%
Diluent	Sterile water				Storage media				Storage media			

C, control sample; B, blank sample; F, formulation sample.

2.2.3.3.2. Lyophilisation of formulations

Nasal inserts were prepared by lyophilising 1 mL of formulation solution (HPMC gel containing the bacteriophage solution) in a freeze-drying micro-tube 1.5 mL Eppendorf tube using a VirTis Advantage Freeze-dryer (VirTis, USA). The freeze-drying protocol was carried out following the method as described by Puapermpoonsiri *et al.,* 2010). The freezing steps was initiated with cooling the samples to 5 ºC for 30 min, followed by cooling to -5 ºC at a rate of 1 ºC/min for another 30 min and then to -30 ºC at 1 ºC/min for 1 hr. primary drying was started at -30 ºC with a chamber pressure of 100 millitorre for 1000 min and secondary drying involved subsequent heating to 25 ºC at 0.1 ºC/min, maintained for 6 h under vacuum. After lyophilisation samples were collected and stored in container with silica gel at 4 ºC (Table 2.2).

Table 2.2. Freeze Drier cycle.

Thermal Treatment

	Temp (°C)	**Time (minutes)**	**Vacuum (mTorr)**	**R/H**
Step 1- Cooling	5	30		H
Step 2- Freeze	-5	30		H
	-30	60		R
Extra Freeze	-60			
Condenser	-55		100	
Primary Drying	-30	1000	100	H
Post Heat (secondary drying)	25	360	150	

To investigate the effect of the freezing and drying protocol on lyophilisate morphology, a simple rapid freeze/dry protocol was also used, involving freezing of gels to -80 °C over 30 min and subsequent drying at 10 °C for 24 h under vacuum (MicroModulyo, Thermo Scientific Ltd., UK).

2.2.3.4. Disc diffusion method

Sterile discs (p.no. 74146, Sigma-Aldrich, UK) were placed on the surface of agar plates and impregnated with 80 µLof lyophilisate solution prepared from serial dilutions. The agar plates inoculated with 80 µLof bacterial culture that was mixed with 4 mL of partially cooled LB agar. After overnight incubation at 37 °C, the resulting visible zones of growth inhibition that surround the discs were inspected for clarity.

2.2.3.5. Scanning electron microscopy (SEM)

Lyophilised samples were prepared by cutting a section of the sample with a sharp scalpel blade, fixed onto metal stubs using double-sided adhesive copper tape and coated with gold under vacuum. Samples were imaged using a Jeol JSM-6400 scanning electron microscope at 10 kV intensity.

2.2.3.6. Confocal laser scanning microscopy (CLSM)

The Confocal Laser Scanning Microscope (CLSM) allows an image to be obtained at various focal planes from within an optically transparent sample. A scanning beam and light source both are focussed on the same point which enables a high resolution image to be acquired.

Lyophilisates for CLSM were prepared as above but using fluorescein labelled bacteriophage during formulation. A small section of the lyophilisate for each formulation was placed on glass slide and covered with a cover slip. Samples were analysed and imaged on a Leica DM 6000B microscope using an Argon laser line at 488 nm with an emission bandwidth of 521-616 nm. Scans were performed using 10× and 20× objectives and images were converted with Volocity® software (Improvision, PerkinElmer, Cambridge, UK).

2.2.3.7. Residual water content

Gel samples of 1 g were formulated as above but lyophilized in 10 mL, tared glass vials. The mass of the dried cakes was calculated from the weight difference and the vials were stored in an air-tight box at 4 °C. For residual water determination, the dried cakes were reconstituted with 4 mL solvent mixture (dichloromethane and

methanol 50:50). The mass of the solvent for each sample was obtained and a blank sample containing a known solvent mass was also prepared. The water content of each cake was determined by the Karl Fischer (KF) titration method (Mettler Toledo DL 37, Leicester, UK). After calibration with a Karl Fischer water content standard (Hydranal, Sigma–Aldrich, Gillingham, UK), the apparatus was used to determine the water content of the blank solvent mixture. The water content for each formulation was determined twice from four independent samples and the result of the titration was expressed as a percentage.

2.2.3.8. Dynamic vapor sorption (DVS)

The isothermal sorption behaviour was studied using a DVS 1000, Surface Measurement Systems, Cheshire, UK (Figure 2.3). The DVS apparatus consists of a highly sensitive Cahn microbalance and a chamber within which the humidity and the temperature can be regulated as required via a computer system (Figure 2.4) to measure any changes in the mass of the sample as a result of sorption or desorption of water vapour. The method of McInnes et al. (2007) was followed. Briefly, samples were subjected to a controlled cycle of relative humidity (RH) ranging from 0% to 95% in stepwise increments of 10%. RH was then decreased through the same steps. Changes in the mass of the sample due to sorption or desorption of moisture are expressed as a percentage of its dry mass.

Figure 2.3. Dynamic vapour sorption apparatus (DVS).

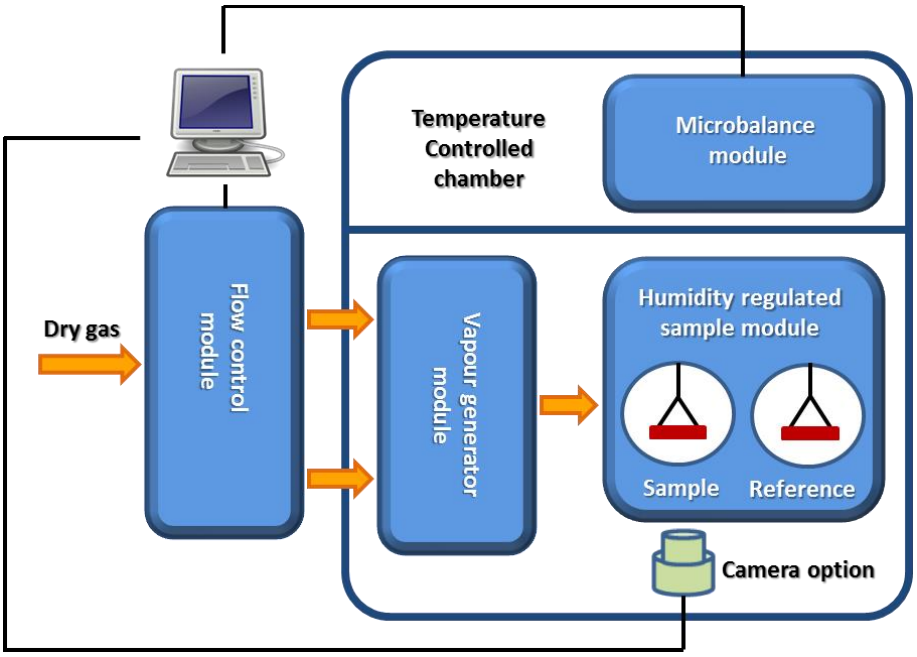

Figure 2.4. Schematic representation of the dynamic vapour sorption system, reproduced from Surface Measurement Systems website.

2.2.3.9. Differential scanning calorimetry (DSC)

Samples of 4–6 mg were accurately weighed into 40 µLaluminium pans, hermetically sealed with pin-hole lids, and heated under a nitrogen purge in a Mettler Toledo DSC822e (Mettler–Toledo, Leicester, UK). Thermal transitions for the blank and test lyophilized samples were analysed using a modulated DSC method for determination of the glass transition (T_g) of HPMC, and a standard linear DSC method to determine the crystallization and melting events of mannitol. The T_g of HPMC was represented in the reversing signal and the mid-point of the T_g determined at a heating rate of 2 °C/min from 25 to 240 °C. A quench-cool method was used for determination of the enthalpy of crystallization (ΔH_c) for mannitol from

25 to 200 °C at a heating rate of 10 °C/ min. The data analysis was performed using Mettler STARe software.

2.3. Results

2.3.1. Lyophilisate shape and texture

Lyophilisation of the formulated gels produced a torpedo shape nasal insert with a smooth surface texture (Figure 2.5). On handling, the formulation that was obtained from a 1% HPMC concentration was very soft and easy to deform. Increasing the concentration of HPMC polymer along with the addition of mannitol decreased the deformation and resulted in a firm insert with a more fibrous structure.

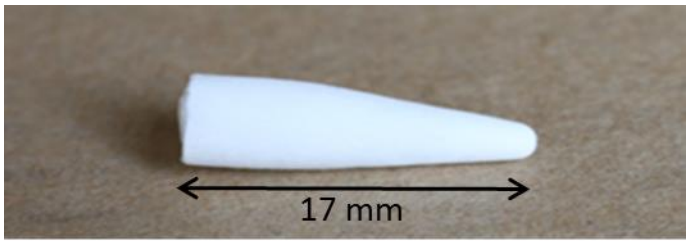

Figure 2.5. The lyophilised nasal insert

2.3.2. Scanning electron microscopy (SEM)

Morphological examination of HPMC lyophilisate displays a sponge-like structure wherein individual 'leaflets' were layered. It was observed from SEM images for all formulations that HPMC lyophilisate gives a highly porous internal structure which could be readily distinguished from the less porous external surface for all formulations (Figure 2.6). High magnification of the internal surface shows layers of a thin leaflets structure that surround the pores of the lyophilisate containing 1% HPMC concentration which appear to be more evident for the lyophilised 2% HPMC

formulation , i.e. the porous structures were largely indistinguishable for the 2% formulations (Figure 2.7 a-c). The addition of mannitol to the formulations did not appear to cause a noticeable effect on the structure of the lyophilisates (Figure 2.7 b-d). Furthermore, there was no difference observed between the blank lyophilisate, that contains HPMC or HPMC and mannitol only, and the formulation lyophilisate that contains phage solution.

To investigate the effect of the lyophilisation protocol on lyophilisate morphology, a rapid freezing/rapid drying protocol was used. The SEM images show that the structure of the lyophilisate remained composed of individual leaflets but the porous structure had been changed to a structure better described as lamellar (Figure 2.8).

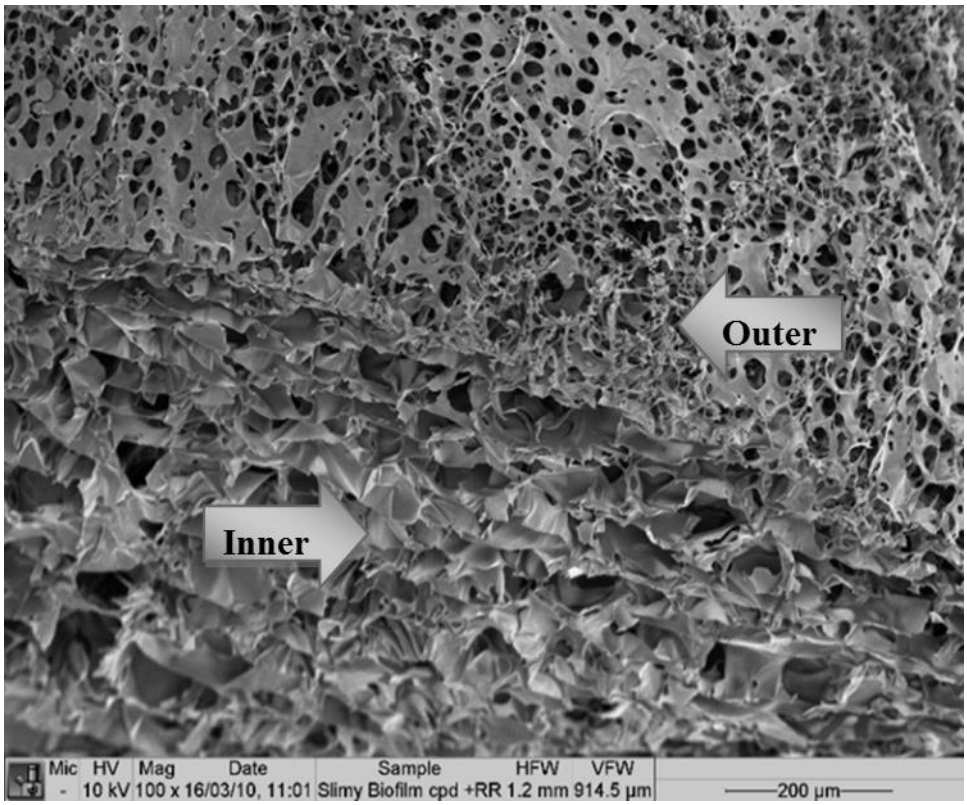

Figure 2.6. Representative scanning electron micrograph of the blank lyophilized nasal insert showing the difference between inner and outer surfaces.

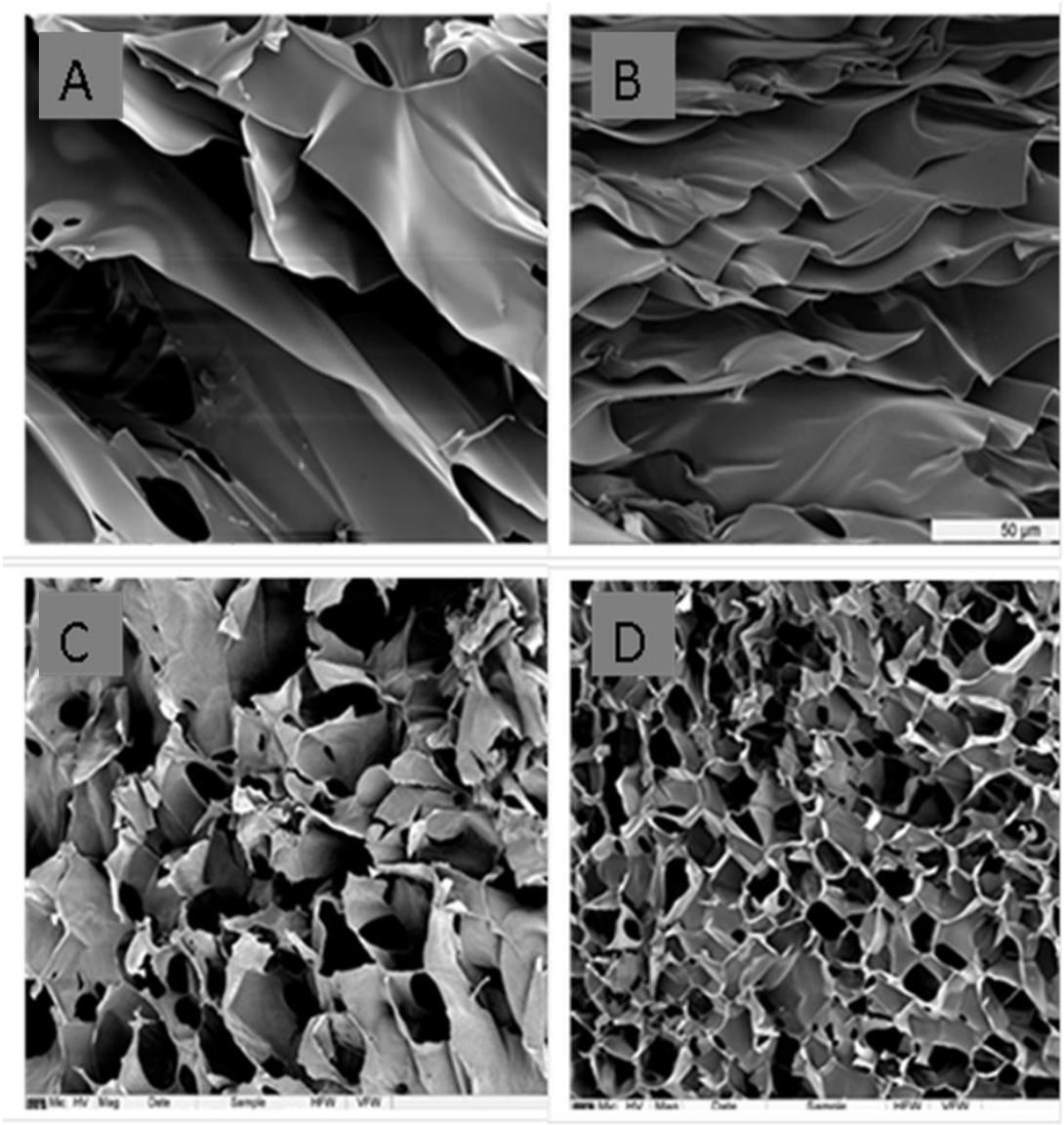

Figure 2.7. Scanning electron micrographs for blank lyophilized nasal inserts. A, 1% HPMC; B, 1% HPMC/1% mannitol; C, 2% HPMC; D, 2% HPMC/1% mannitol.

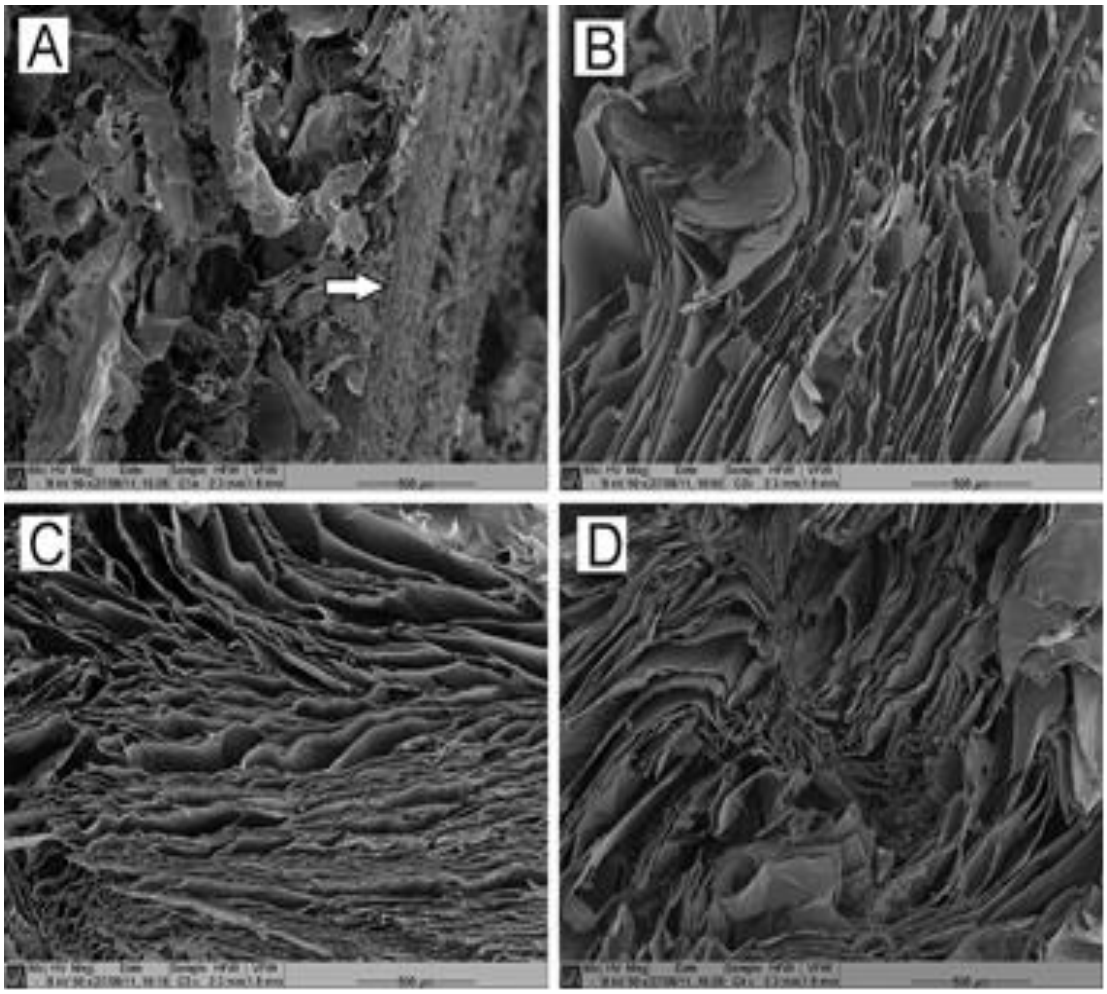

Figure 2.8. Representative scanning electron micrographs for blank lyophilized nasal inserts following a rapid freeze/dry protocol. A, 1% HPMC; B, 1% HPMC/1% mannitol; C, 2% HPMC; D, 2% HPMC/1% mannitol. The white arrow points from the internal matrix to the boundary with the surface of the insert. The scale bar (500 µm) is shown in bottom right of each pane.

2.3.3. Confocal laser scanning microscopy (CLSM)

To examine possible aggregation and/or localization of the bacteriophages during the freeze-dry steps, the distribution of fluorescein-labelled bacteriophages was visualized by CLSM. Confocal micrographs show the bacteriophages to be distributed in a homogenous manner throughout the lyophilisate (Figure 2.9), which

reflects the overlapping of the leaflets and pore structure observed by SEM (Figure 2.7). Although it is not possible to resolve nanometer-sized aggregates of small numbers of bacteriophages in these images, there is no evidence of gross aggregation or localization of the bacteriophages, i.e. the freezing step would appear to have avoided slow formation of ice crystals and supersaturated regions of liquid.

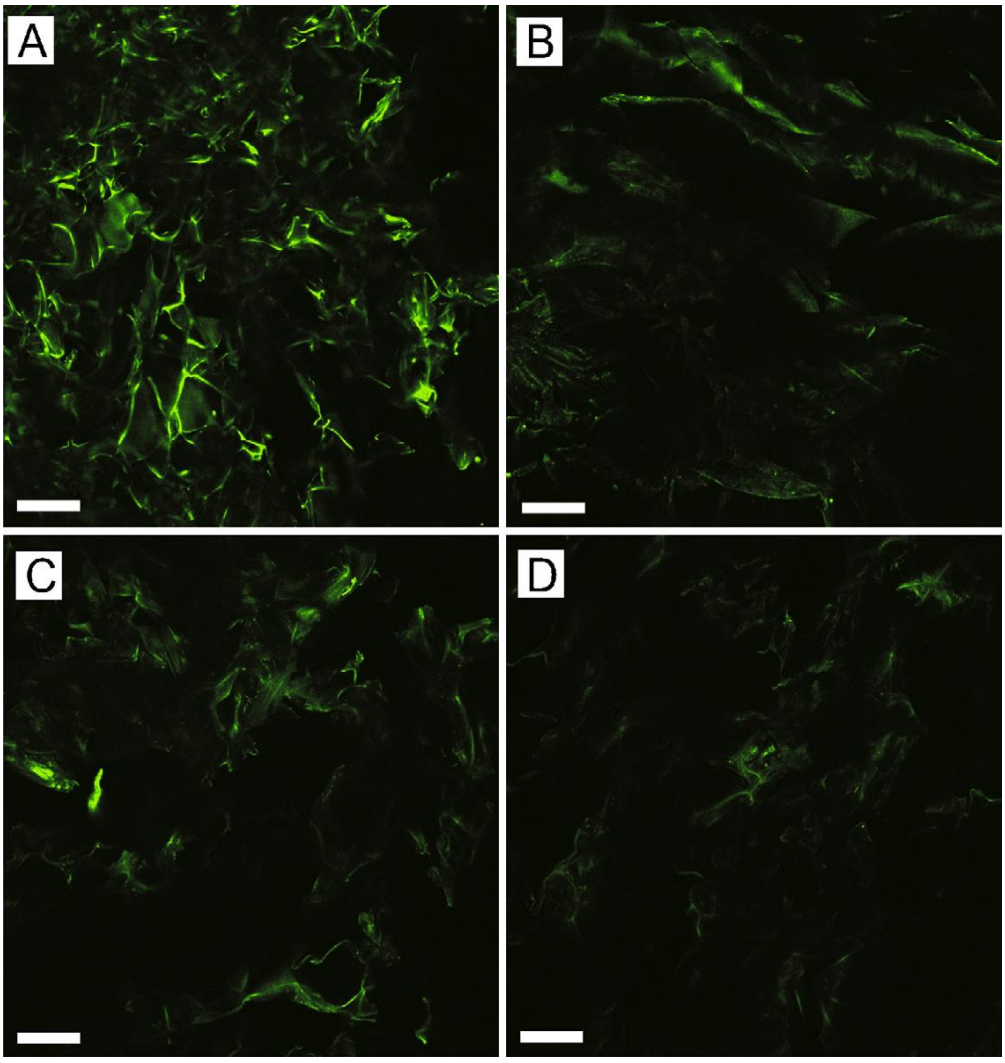

Figure 2.9. CLSM images of fluorescein-labelled bacteriophage distributed through the lyophilized formulations, (A) 1% HPMC; (B) 1% HPMC/1% mannitol; (C) 2% HPMC; (D) 2% HPMC/1% mannitol. Bar = 250 µm.

2.3.4. Lytic activity measurement of formulated bacteriophages by plaque assay method

The plaque assay method was used for the determination of the lytic activity of the bacteriophage by counting the observed plaques, which each represent a single phage particle. The results presented in Table 2.3 show the lytic activity of the bacteriophages before and after lyophilisation of the formulations. Enumerating the plaques per agar plate for a given dilution enabled calculation of the bacteriophage titre that would have been present in each undiluted sample tested (Table 2.4). For comparison, formulations before lyophilisation (i.e. as the gel) were tested for lytic activity, in order to evaluate the effect of resuspension on phage integrity. For formulations before lyophilisation samples, given that the typical number of plaques observed on an agar plate from a phage dilution of 10^{-6} was > 300 (i.e. too many plaques to count), the concentration of phage in each test sample was calculated from the number of plaques observed following a dilution of 10^{-7}. A titre of 10^{9} pfu/mL was calculated for the HPMC/mannitol gel formulations prior to lyophilisation, indicating that there was no loss of lytic activity during mixing of the bacteriophages into the gels (since the phage titres added to the gel were consistently10^{10} pfu/mL, and a 10-fold dilution of the bacteriophage stock was made). In contrast, lyophilisation of formulations resulted in phage titre of 10^{8} pfu/ mL, which implied that the lytic activity loss of the bacteriophages following lyophilisation was 10 % of the original lytic activity. Nevertheless, a titre of 10^{8} pfu/ mL was considered sufficient and long term stability testing was therefore determined.

Performing plaque assay for lyophilised formulations without dilution resulted in clear plates due to confluent lysis of *S. aureus* bacteria by phage. Therefore, serial dilutions of samples were prepared and dilution 10^{-6} was selected for determination of phage concentration as it gives countable plaques (Figure 2.10). The data reported in Table 2.3 shows that the number of plaques gradually decreases within time. However, Table 2.4 shows that the lytic activity decreased from 10^{8} pfu/mL on day 1 to around 10^{7}, 10^{6} and 10^{5} pfu/mL after 1, 2 and 12 months, respectively. Calculated phage titre for formulations containing only 1% mannitol before and after lyophilisation was $(1.30 \pm 3.0) \times 10^{9}$ and $(3.87 \pm 2.08) \times 10^{3}$ respectively.

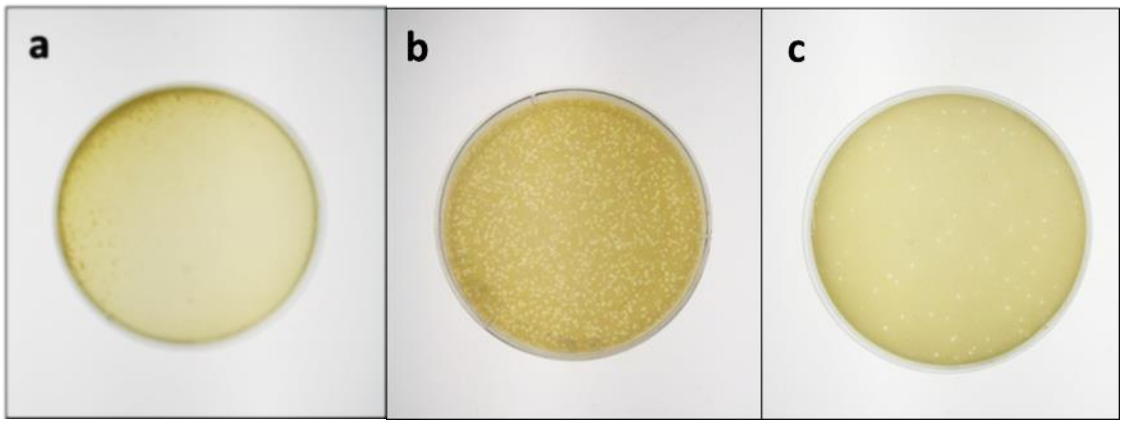

Figure 2.10. Plaque assay showing the lytic activity of bacteriophage for the lyophilisate: a) confluent lysis for undiluted sample; b) uncountable plaque for dilutions from10^{-2} to 10^{-5} and c) countable plaque for dilution 10^{-6} and 10^{-7}.

Table 2.3. Lytic activity of bacteriophage before and after lyophilisation.

Formula	**Lytic activity**										
	Before lyophil.		After lyophil.								
	Dilution		Dilution (10^{-6})							(10^{-5})	(10^{-4})
	(10^{-6})	(10^{-7})	Day 1	Day 4	Day 7	Day 14	Day 21	Day 30	Day 60	Day 60	Day 180
F1	+ P	89 ± 7	P(44 ± 5)	P(42±2)	P(35±17)	P(5±2)	P(8±1)	P(26±2)	−P	P(7±1)	P(9±2)
F2	+ P	55 ± 8	P(85±14)	P(14±4)	P(32±12)	P(10±3)	P(13±7)	P(6±4)	−P	P(9±5)	P(27±2)
F3	+ P	29 ± 4	(nd)	P(39±26)	P(39±11)	P(57±15)	P(15±10)	P(3±2)	−P	P(6±5)	P(18±3)
F4	+ P	40 ± 4	P(87±12)	P(73±4)	P(42±7)	P(121±8)	P(66±7)	P(40±14)	−P	P(50±8)	P(141±9)

+P: plaques >300 per plate; P (number): number of individual plaques; −P: no plaques observed; nd: not determined.
F1, 1% HPMC; F2, 1% HPMC/1% mannitol; F3, 2% HPMC; F4, 2% HPMC/1% mannitol.
Data are expressed as the mean ± SD for three independent experiments.

Table 2.4. Concentration of active bacteriophage in the lyophilisates calculated from table 2.3.

Time	Dil	F1	F2	F3	F4
Before lyophilisation					
	10^7	(8.90 ± 7.5) ×10^9	(5.53 ± 8.5) ×10^9	(2.90 ± 8.4) ×10^9	(4.00 ± 4.5) ×10^9
After lyophilisation					
Day 1	10^6	(4.40 ± 5.2) ×10^8	(8.53± 1.4)×10^8	nd	(8.70 ± 1.2) ×10^8
Day 4	10^6	(4.27 ± 2.2) ×10^8	(1.47 ± 4.7) ×10^8	(3.93 ± 2.6) ×10^8	(7.37 ± 4.0) ×10^8
Day 7	10^6	(3.53 ± 1.7) ×10^8	(3.20 ± 1.2) ×10^8	(3.90 ± 1.1) ×10^8	(4.20 ± 7.9) ×10^8
Day 14	10^6	(5.00 ± 2.0) ×10^7	(1.03 ± 1.0) ×10^8	(5.77 ± 1.5) ×10^8	(1.21 ± 8.8) ×10^9
Day 21	10^6	(8.00 ± 1.4) ×10^7	(1.33 ± 7.5) ×10^8	(1.53 ± 1.0) ×10^8	(6.60 ± 7.0) ×10^8
Day 30	10^6	(2.60 ± 2.7) ×10^8	(6.00 ± 4.3) ×10^7	(4.33 ± 2.5) ×10^7	(4.00 ± 1.4) ×10^8
Day 60	10^5	(7.33±1.1) ×10^6	(9.00±5.5) ×10^6	(8.67±5.1) ×10^6	(3.47±8.5) ×10^7
Day 180	10^4	(8.07±9.5) ×10^6	(4.13±2.3) ×10^6	(3.25±3.5) ×10^6	(8.87±1.0) ×10^6
Day 240	10^4	(5.33±8.5) ×10^6	(5.67±8.9) ×10^6	(6.00±1.9) ×10^6	(1.32±3.1) ×10^7
Day 360	10^4	(2.23±1.2) ×10^6	(4.67±1.5) ×10^5	(8.00±4.5) ×10^5	(2.30±7.9) ×10^6

F1, 1% HPMC; F2, 1% HPMC/1% mannitol; F3, 2% HPMC; F4, 2% HPMC/1% mannitol. Data are expressed as the mean ± SD for three independent experiments.

2.3.5. Disc diffusion method

The results are given on the basis of comparison of the zone clarity with the negative control bacterial culture (C-neg). When the lyophilised formulations which contained 1% and 2% HPMC were used without dilution, the viscosity of gel prevented the solution from spreading completely around the sterile disc. Lyophilisates containing 1% HPMC and 1% mannitol allow spreading of the gel around the disc, whereas increasing the HPMC concentration to 2% decreased the mannitol effect due to the increase in the viscosity of HPMC polymer.

No conclusive results could therefore be obtained as the formulations had not spread around the discs and for this reason diluted samples were used. On day 1 post-lyophilisation, all formulations yielded clear zones around the disc indicating inhibition of bacterial growth in an otherwise continual bacterial lawn. Larger dilutions (10^{-3} to 10^{-6}) produced a smaller clear zone which also appeared 'punctate' (i.e. not a continuous clear band) and this was also observed on days 7 and 14 post-lyophilisation. On day 30, when the last experiment was done, the zones continued to be punctuate and less clear comparing to the first day. However, the sample was less turbid than the cloud negative control zone (Figure 2.11).

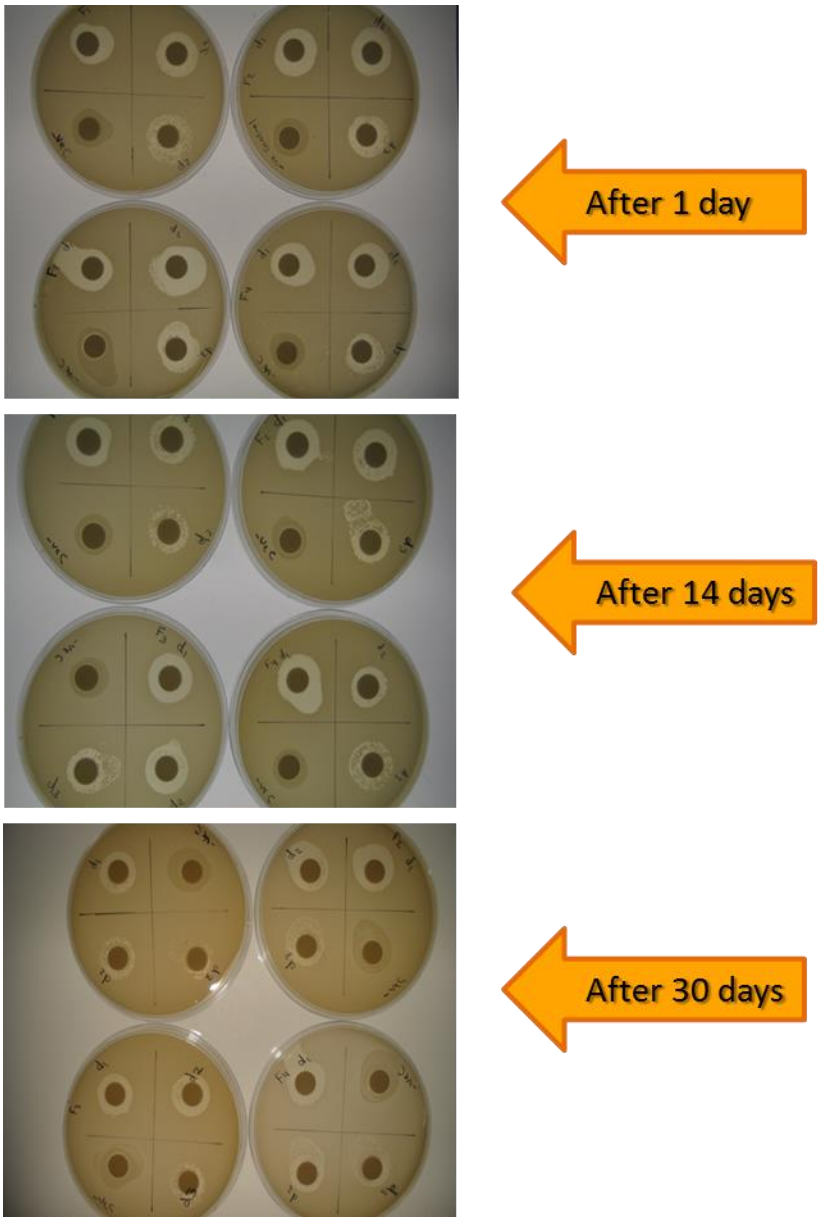

Figure 2.11. Disc diffusion test of lyophilisates.

2.3.6. Water content

Figure 2.12 shows the freeze dried cakes that were used for water content test. To determine the residual moisture contents in the lyophilised formulations, Karl-Fischer titration was performed. Figure 2.13 shows that the formulation which

contained HPMC at 2% w/w concentration (F3) had the highest percentage moisture content. Addition of mannitol to the formulation resulted in lower residual moisture contents. However, in the formulation that contains 2% HPMC (F4) mannitol does not appear to have a high effect on the water content of the lyophilisate. Overall, except for the 1% HPMC/1% mannitol lyophilizate, the residual moisture content in these formulations was comparatively high.

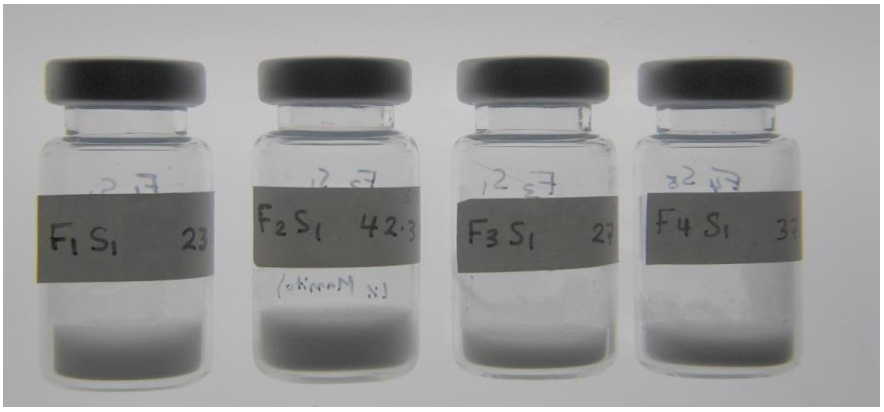

Figure 2.12. The lyophilised samples for water content determination.

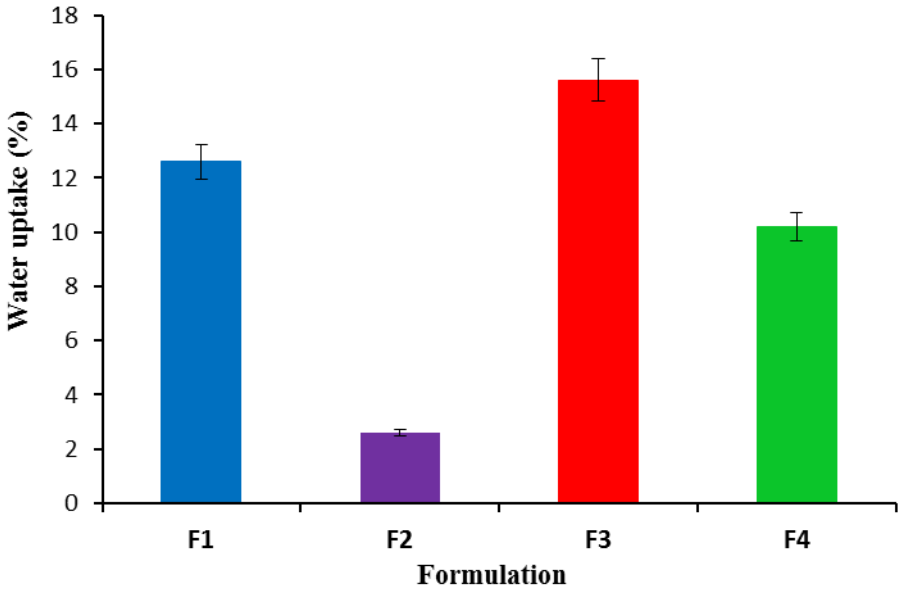

Figure 2.13. Residual moisture content of the lyophilized bacteriophage formulations: F1, 1% HPMC; F2, 1% HPMC/1% mannitol; F3, 2% HPMC; F4, 2% HPMC/1% mannitol. The data shown as mean ± SD for n=4.

2.3.7. Dynamic vapor sorption (DVS)

DVS was used to mimic the water sorption that may occur when the lyophilized inserts are placed in the nose. The sorption profiles results gathered from the dynamic vapour sorption analysis show the effect of changing the target humidity (blue line) on the weight of the sample (red line) over time. The water sorption profiles showed an increase in mass as a result of exposure to increasing relative humidities (RH) to 95%, and corresponding drying as RH returned to zero. It is clear from the profiles that the sorption and the desorption behaviours of HPMC formulations are stable. Table 5 compares the water vapour sorption values as a percentage of the dry weights. A marked difference was observed between inserts formulated with water (28–52% mass increase), storage media (67–103% mass increase) and bacteriophage (101–141% mass increase). Sorption capacity for the control samples ranged between 28% and 51% of the dry weight, Figure 2.14 has been shown as an example of sorption capacity for the control samples. Lyophilisate formulations that contain HPMC only were seen to absorb water to a greater extent than those which contained mannitol. In contrast a substantial increase in weight for all formulations containing the phage was observed (Figure 2.15). For lyophilizates containing mannitol, a small but noticeable mass loss was observed during the water sorption phase between 5 and 10% RH (Figures 2.16 a; 2.16 b). This was due to the transformation of amorphous mannitol to the crystalline form, with concomitant loss of water from the lyophilizate. Mannitol itself adsorbed very little water vapor during the same cycle: showing only a 0.3 and 1% mass increase for the powder as received and lyophilized, respectively. In contrast, HPMC powder (as received) displayed a

30% increase in mass for the same cycle. The addition of mannitol reduced water sorption for the control samples and, to a lesser extent, for the blank and bacteriophage formulations.

Table 2.5. DVS results of the lyophilisates containing different concentrations of HPMC and mannitol.

Formulation	**% Change in dry weight**		
	C	**B**	**F**
1%HPMC	50	103	141
1%HPMC 1%Mannitol	28	74	123
2%HPMC	52	70	101
2%HPMC 1%Mannitol	39	67	102

C, control sample that contain water; B, blank samples that contain storage media; F, formulation samples that contain phage solution.

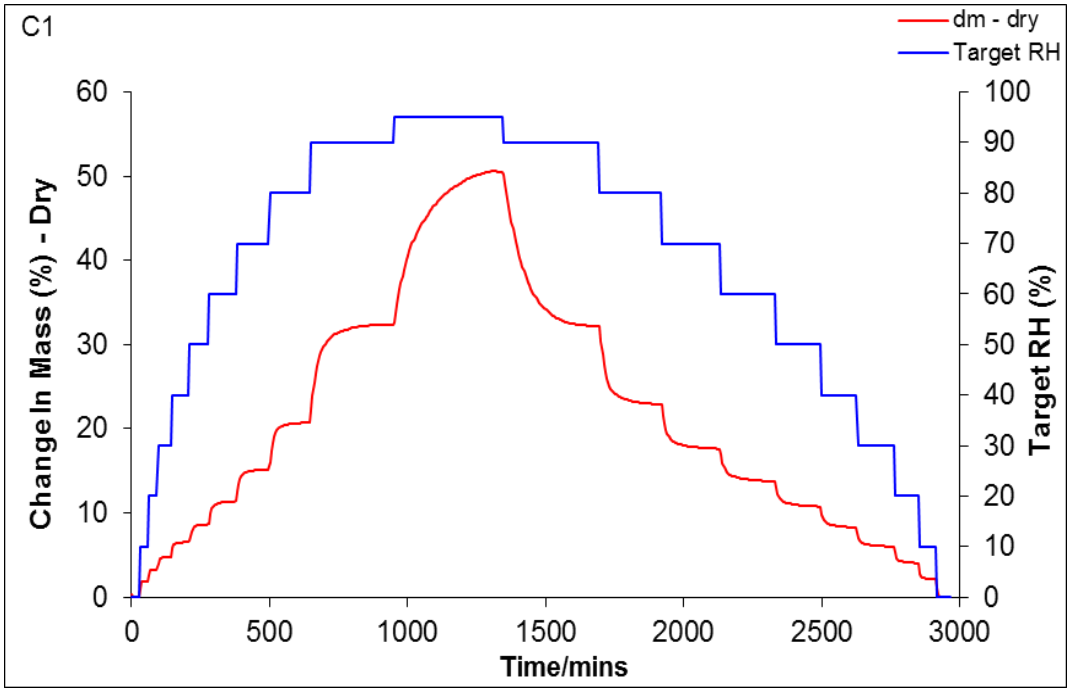

Figure 2.14. Example profile of the percentage change in sample mass (red lines) versus RH (blue lines) for the control sample, C1.

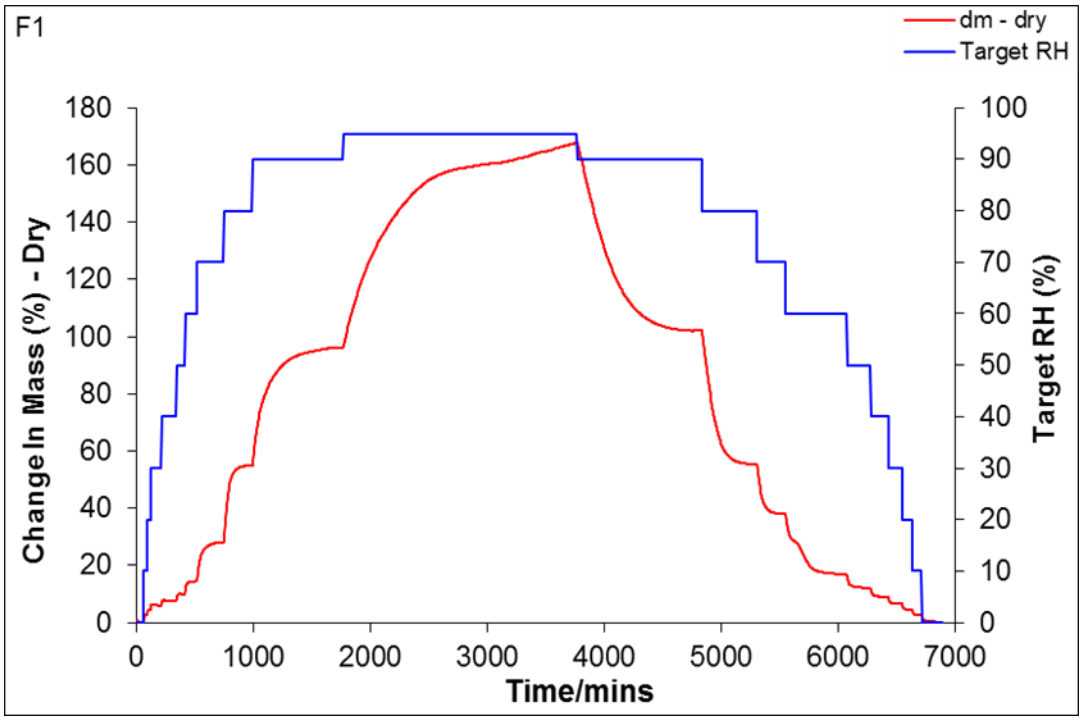

Figure 2.15. Example profile of the percentage change in weight for a formulation sample.

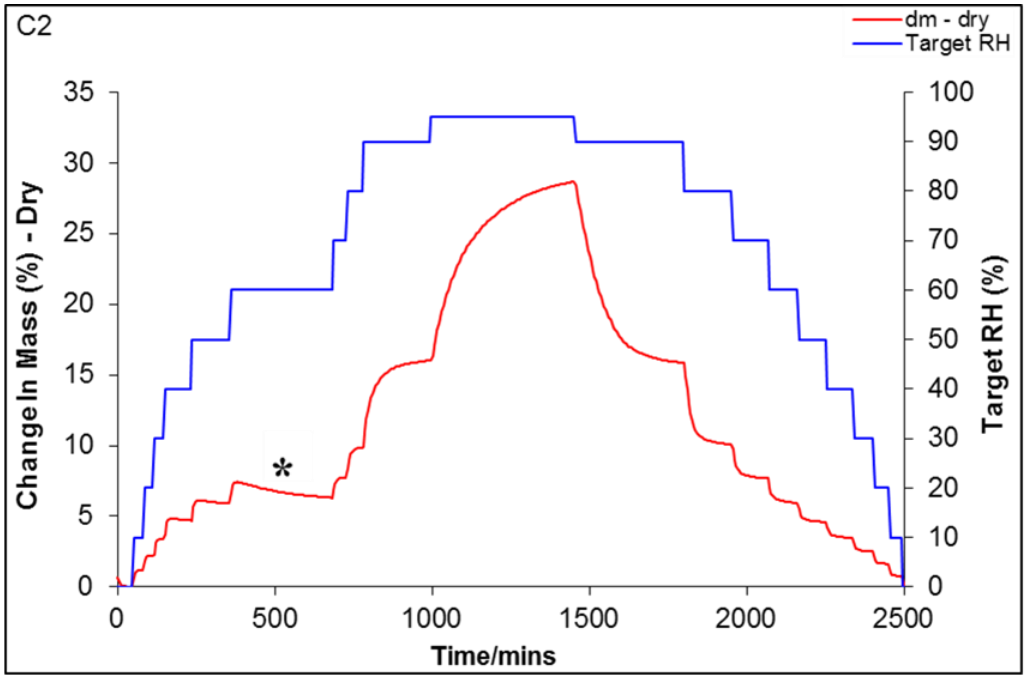

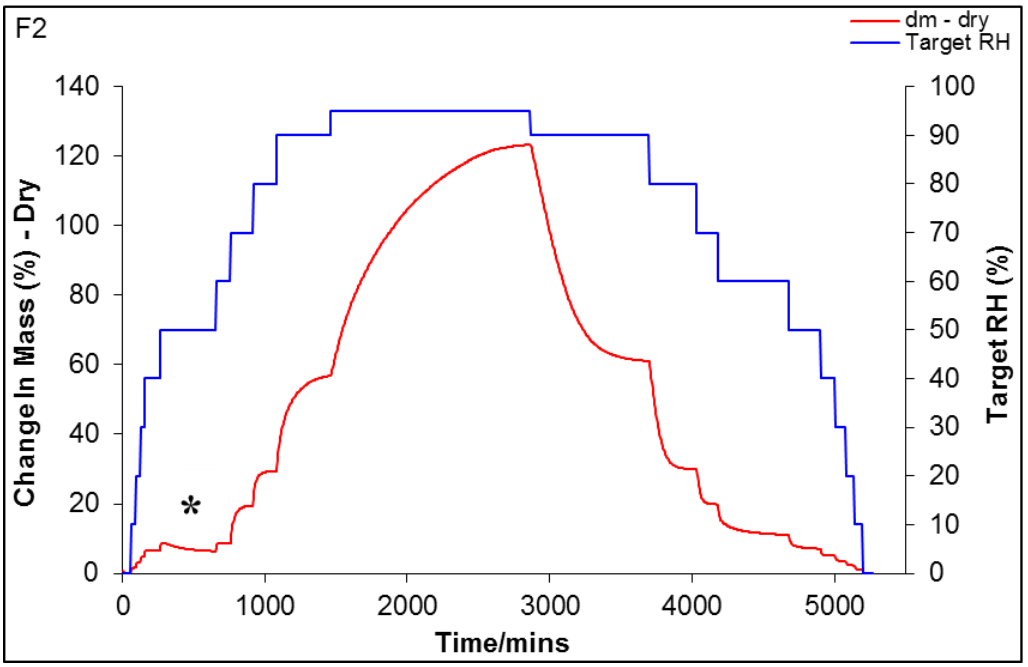

Figure 2.16. Example profiles of the percentage change in sample mass versus RH for formulations that contain mannitol: a) C2, control sample that contains water and b) F2; formulation sample that contains phage, the * indicates the loss of mass as a consequence of the change from amorphous to crystalline mannitol.

2.3.8. Differential scanning calorimetry (DSC)

Table 6 shows the midpoint of the T_g of HPMC for all formulations. The T_g values for formulations without mannitol was consistent, varying around 186 ± 7 °C. The heat of crystallization (ΔHc) was determined for each formulation after normalization of the thermograms (Table 7). A clear decrease in the ΔHc for mannitol was observed upon the addition of HPMC in simple powder blends, dependent on the relative amount of HPMC added. ΔHc values for the corresponding lyophilized mixtures (C2 and C4) also indicated that re-crystallization of mannitol was directly inhibited by HPMC. The addition of storage media containing gelatin further decreased the ΔHc (B2 and B4), with the presence of bacteriophage in the 2% HPMC formulation (F4) almost completely attenuating mannitol re-crystallization.

Table 2.6. Glass Transition Temperature (T_g) of HPMC polymer for different formulations.

Formulation	HPMC powder	C1	C3	B1	B3	F1	F3
T_g (˚C)	187	190	188	192	188	179	186

Table 2.7. Heat of crystallisation (ΔH_c) values for mannitol in different formulations

Formulation	ΔH_c (mJ)
Mannitol powder	1120
Mannitol lyophilisate	798
HPMC/mannitol physical mixture 1:1	488
HPMC/mannitol physical mixture 2:1	251
C2	360
C4	99
B2	231
B4	44
F2	58
F4	9

2.4. Discussion

The lamellar structure of the leaflets presumably results from the formation of large sheet-like ice crystals during the rapid freezing step, since similar structures have been described as a consequence of changes in ice nucleation (Searles et al., 2001). Thus, the morphology of the nasal insert would appear to be reproducible so long as careful control over freezing and drying steps can be maintained throughout the lyophilization process.

It was observed from the SEM images that the surface morphology of the bacteriophage containing lyophilisate has no significant (clear) difference from that without bacteriophage. All of the samples show a smooth surface with a porous internal structure. It is obvious that as concentration of the HPMC polymer increases, the leaf-like structure that surrounds the pores also increases due to increase the

viscosity of the gel solution giving less porous lyophilisate. On comparing the CLSM and SEM micrographs, the bacteriophages appear to be homogenously distributed throughout the lyophilised nasal insert and no evidence of aggregation is apparent. This would suggest that the phages are fully dispersed throughout the nasal insert. The highly porous structure of lyophilizates is suggested to provide an ideal route for rehydration of the lyophilizate within the nasal cavity (McInnes *et al.,* 2007). The formation of the pores can be attributed to the space that was occupied by ice crystals during the freezing drying. Fast and slow cooling protocols have been used for the lyophilization of carboxymethyl cellulose in order to control the pore structure and strength of the resultant lyophilizate (Yuan *et al.,* 2009). The cooling rate adopted here (1 °C/min) was very similar to the slow cooling rate reported by Yuan et al. (0.83 °C /min), who described 60–100 μm pore sizes for carboxymethyl cellulose. The same size range can be observed for the lyophilizates in this study: Figure 5B showing pore sizes ranging from 50 to 100 μm. Imaging at the boundary of the inner matrix and surfaces, shows that the individual leaflets forming the pore walls can be much closer together (Figure. 5A and C). The addition of bacteriophage did not appear to change pore size when comparing Figure 7A/C and B/D.

The initial bacteriophage titre that is sufficient for successful treatment is not known. However, it has been reported that in mice treatment, phage therapy failed for doses less than 3×10^3 pfu/mL and 3×10^4 pfu/mL for intramuscular and intravenous delivery respectively (Payne and Jansen, 2003). According to (Sulakvelidze *et al.,* 2001) high doses of bacteriophages can be used without any risk. It has also been found by (Capparelli *et al.,* 2007) that a titre of 10^9 pfu of bacteriophages (M^{Sa}) is

sufficient for treatment of mice infected with *S. aureous* strain A170. Therefore, the phage titre of 10^9 pfu was used for the study.

It is known that lyophilisation may affect the activity of bacteriophages. The plaque assay was performed to typify the lytic activity of bacteriophage. lyophilization of formulations resulted in a titre of 10^8 pfu/mL, which implied that 90% of the original lytic activity had been lost. Although this may seem high, this loss was less than or equivalent to previous losses following encapsulation (Puapermpoonsiri *et al.*, 2009), or lyophilization with high concentrations of sucrose (Puapermpoonsiri *et al.*, 2010). A titre of 10^8 pfu/mL is still considerable, comparable with bacteriophage doses of 10^7–10^8 pfu for inhalation (Golshahi *et al.*, 2010) and 6×10^5 pfu for dosing of the ear (Wright *et al.*, 2009); this warranted long term stability testing of the lyophilized inserts. The low phage titre loss during lyophilisation was suggesting that the phage was efficiently dispersed in the gel and lyophilised without significant detrimental effects on phage viability.The lytic activity was seen to decrease around 10 to 1000-fold over 1–12 months storage at 4 °C. The stability of the bacteriophage in the lyophilized nasal inserts was therefore far greater than for encapsulated phage in polyester matrices, wherein no lytic activity was observed after one week (Puapermpoonsiri *et al.*, 2009). This was encouraging, particularly since the bacteriophage titre in the inserts after 12 months may still represent a therapeutic dose (Wright *et al.*, 2009). No particular correlation could be observed between the formulations and the bacteriophage titres; i.e. neither the addition of mannitol nor the higher HPMC concentration conferred any additional benefit as regards long-term stabilization of the bacteriophages. The addition of HPMC at either 1 or 2% brings

about 'molecular crowding' through excluded volume effects experienced by the bacteriophage, a phenomenon well understood through studies using macromolecules such as polyethylene glycol (PEG), dextran and Ficoll, or sol–gels (Eggers and Valentine, 2001). The concentrations required to bring about molecular crowding using PEG or dextran are equivalent to the HPMC concentrations used here (Dominak *et al.,* 2010). While the excluded volume experienced by the bacteriophage increases for further addition of HPMC and/or mannitol, this does not necessary imply further change to the lytic activity since the effect of a concomitant increase in viscosity in these systems remains unknown. A 1% HPMC concentration would therefore appear to be sufficient as regards cryo- and lyoprotection of the bacteriophages. The lytic activity data reported in the tables (Tables 2.3 and 2.4) prove that phage remained stable within the formulation for 12 months. Therefore, the stabilizing effect of HPMC is greater than the stabilization of bacteriophage by PEG 6000 (Puapermpoonsiri *et al.,* 2010), and would suggest that high molecular weight, polyol polymers are useful formulation excipients for bacteriophages. However, a simple explanation involving stabilization of protein (bacteriophage coat) structure via polyols, is not complete. This is because sucrose conferred no additional stability to lyophilized bacteriophages tested over 30 days (Puapermpoonsiri *et al.,* 2010). Similarly, the lytic activity of the bacteriophages lyophilized from 1% solutions of mannitol, i.e. without the addition of HPMC, showed a large loss of around 6 log cycles by day 1. A further consideration involves the possible adsorption of the bacteriophages to crystalline domains of mannitol within the lyophilizate. This method of surface stabilization would reflect that

proposed for protein coated microcrystals which have been shown to stabilize both enzymes and DNA through surface adsorption to the crystalline carriers during dehydration (Kreiner et al., 2005; Moore *et al.,* 2010; Alvarez *et al.,* 2011). However, given that mannitol conferred no additional stabilizing effect, this mechanism is unlikely to play a significant role in these studies. The addition of mannitol is therefore only justified in order to improve the strength of nasal inserts, as previously described (McInnes *et al.,* 2007). Stabilization conferred through immobilization of the bacteriophages onto the HPMC matrix is also unlikely since immobilization onto polyester matrices retained lytic activity for only 7 days (Puapermpoonsiri *et al.,* 2009). Molecular crowding is well known to increase the conformational stability of proteins (Eggers and Valentine, 2001) and this effect may have contributed to the observed stabilization of the bacteriophage by HPMC. Another explanation for the observed lytic activities is to compare the T_g of the amorphous materials: the T_g of the polyester used was ~45 °C (Rouse *et al.,* 2007), while the T_g for sucrose is ~72 °C (Puapermpoonsiri *et al.,* 2010). Differential scanning calorimetry (DSC) is widely used for the determination of the T_g of amorphous materials and modulated temperature DSC (MTDSC) has been shown to be applicable to the study of HPMC blends (Nyamweya and Hoag, 2000). We also chose MTDSC since the T_g of HPMC can be obscured by an associated enthalpic relaxation peak, which for some amorphous materials can be considerable (Rouse *et al.,* 2007). The midpoint of the T_g of HPMC for formulations without mannitol was consistent, varying around 186 ± 7 °C (Table 6). The T_g values are also in agreement with previous data, reporting the T_g of HPMC K4M powder to be 184 °C (Doelker, 1993). The range in the T_g values

reported is reasonable given that the change in the heat capacity of HPMC during the transition event was small, making the extrapolation of the baseline less certain. The difference in the values may also reflect the difference in the water content of the samples, since water is well known plasticizer of amorphous materials, with a general tendency to decrease the T_g (Hagens *et al.,* 2004; Bouissou *et al.,* 2005). It was not possible to observe the small T_g for HPMC when mannitol was added to the formulations. The T_g of the excipient may therefore relate to the resultant stability of the formulated bacteriophage in the solid state; i.e., the more stable the amorphous state of the excipient, the more stable the lyophilized bacteriophages.

The disc inhibition method is a rapid, simple and reliable method which we used to confirm the results of the plaque assay test. In this method, the resulting zone that surrounds the disc gives an indication of the effectiveness of phage against bacteria. The results of the first day show clear zones around the discs. Following 30 days the clear zones were still observed which indicated that the phages remain infective for more than 30 days at the storage conditions. The addition of mannitol to the formulation that contains HPMC concentration 1% has a clear effect on the formulation as it allows a consistant gel that spread more easily out of the disc. However, it has no effect on the lytic activity of the bacteriophage.

The hydration property of the lyophilised formulation is an important factor in the bioadhesion process between the polymer gel and the mucus layer (Mortazavi, 1995). In addition, residual moisture content is an important consideration for both the stability of the bacteriophage and amorphous polymeric materials. Therefore, the

hydration of the lyophilised formulations was assessed by KF titration. The data produced provided information on the residual moisture contents for lyophilised formulations. The extent of hydration of the four formulations was low. A high porous structure gives low residual moisture contents. The addition of mannitol to the HPMC gels appeared to promote the drying of the lyophilizate, particularly for the 1% HPMC formulations, because mannitol absorbs little water either in powder or lyophilised form (McInnes *et al.,* 2005). This may be due to its non-hygroscopic nature; although the difference between formulations F3 and F4 was not statistically significant ($P > 0.01$).

SEM images show that the presence of mannitol in the formulations does not appear to be evident particularly with high concentration of HPMC. This could however, correspond to incorporation of mannitol into the HPMC structure. Previous studies with lyophilized bacteriophages suggested that a more porous cake resulted in better mass transfer and lower residual moisture, with a value of 4–6% correlating to maximum retention of bacteriophage titre (Puapermpoonsiri *et al.,* 2010). The resultant stability of the formulations over 12 months storage would therefore not have been predicted, and corroborates the suggestion that the high T_g of the HPMC is more important in maintaining the stability of the bacteriophages. These HPMC/mannitol formulations are therefore not comparable to lyophilized formulations designed for reconstitution to yield non-viscous fluids for injection or nebulization, for example.

It is pertinent to note that the high humidity environment in the nasal cavity means that it was highly important to study the behaviour of the samples under similar conditions and this was an important requirement in characterising a formulation. The DVS analysis provides information on the behaviour of the lyophilisates at particular humidities. Starting the cycle with an initial drying phase at 0% RH allowed the removal of the residual water content that may have been gained from the drying process or the atmosphere (McInnes *et al.,* 2005). The sorption capacity is varied depending on the physico-chemical properties of the formulation contents. This explains the difference in the results among the lyophilisates. The typical water sorption and desorption profiles of 1% HPMC lyophilisate give indication of the polymer stability due to its presence in the amorphous form. While the decrease in the weight of the formulation that contains 1% HPMC 1% mannitol is due to the change in the formulation properties as a result of crystallisation of mannitol. However, this transformation is reversible during desorption phase in which the mannitol was return to the amorphous state. It has been reported that when mannitol was spray dried with 2 different proteins, it produced two different forms. The mannitol with trypsin produced an amorphous product whilst when sprayed with lysozyme the product indicated some crystallinity (Hulse *et al.,* 2009). Thus, the behaviour of mannitol may depend on the amount of residual moisture content. The high percentage the mass changed of the formulation contain 2% HPMC attributed to the high water sorption capacity of the polymer under conditions of high humidity due to its hygroscopic property. However, the water sorption profile was not determined only by HPMC since a marked difference was observed between inserts

formulated with water (28–52% mass increase), storage media (67–102% mass increase) and bacteriophage (101–143% mass increase). Since the storage medium contained buffer salts and gelatin, the gelatin component is most likely responsible for the difference between the control and blank samples, since proteins are well known to retain 'bound' water and gelatin powder is deliquescent. This was confirmed by DVS analysis for gelatin powder alone, which demonstrated a 41% mass increase over the same cycle. The difference between the blank and bacteriophage samples is therefore due to the bacteriophage themselves, presumably for the same reason of bound water associated with the protein capsule coat. Our results agree well with those for comparable lyophilized formulations in the study by McInnes *et al.* (2005), who showed that HPMC absorbs more than 50% of its dry mass while mannitol demonstrated very low water vapor sorption.

Our results agree well with the findings of a study of McInnes *et al.*(2005) which show that in the lyophilised form, HPMC absorbs more than 50% of its dry weight while mannitol absorbs very little water vapour. Overall, the water content results obtained by Karl Fischer titration correlated well with the water sorption results of the DVS.

Since it has been reported that polymeric excipients inhibit crystal transformation by slowing crystal growth or by removing excess water by absorption (Tian *et al.*, 2007), we investigated if this was also true for the lyophilizates. Following a quench-cool cycle in order to transfer the mannitol into its amorphous state, DSC thermograms showed an exothermic re-crystallization peak followed by an

endothermic melting peak at 166 °C, corresponding to previous data (Torrado and Torrado, 2002). The heat of crystallization (ΔH_c) values of mannitol in the formulations indicate that re-crystallization of mannitol was directly inhibited by HPMC. The inhibition of mannitol re-crystallization by proteinaceous material has been previously reported (Hawe and Friess, 2006), consistent with the respective changes to ΔH_c of mannitol seen between the control, blank and bacteriophage formulations. Given these data, it is reasonable to assume that the amorphous form of mannitol is stabilized to varying extents in the lyophilizates, dependent on the original percentage of HPMC in the gel and the presence of gelatin and bacteriophages.

Chapter 3: Bioprocessing of Bacteriophages via Rapid Drying onto Micro-crystals

3.1. Introduction

Recently, with the rapid development of therapeutic protein products, the issue of macromolecular stability has gained increased importance in the biopharmaceutical industry, particularly regarding bioprocessing. Various stages (aspects) of bioprocessing can cause tremendous stresses on macromolecular- based products (Harding, 2010). Protein aggregation is a particular problem in biopharmaceutical processing as it is routinely encountered during fermentation, refolding, purification, sterilisation, lyophilisation, shipping, and storage (Brange, 2000; Wang, 2005). An interesting finding of Lu et al. (2008a) study was that aggregation of proteins during bioprocessing could be monitored as the change in the sedimentation coefficient of monomer and lower order species.

In recent years, several methods have been developed providing the biopharmaceutical industry with the necessary tools to assess the physicochemical stability of macromolecular drugs. These techniques include the determination of structural integrity and colloidal stability of products against the stresses that may be encountered in bioprocessing, such as shear stresses (Harding, 2010). If bacteriophages are to be considered as drug candidates, then similar techniques will need to be brought to bear on the monitoring of adverse effects to bacteriophage integrity during bioprocessing (Moineau *et al.*, 2002). In this project, the deliberate

production of an enriched bacteriophage preparation that has maximum stability is a key research objective.

As for any biomacromolecule, key steps in the bioprocessing stages involve concentration and storage conditions (Harding 2010), particularly with respect to possible aggregation of proteins (Cromwell et al., 2006). Phages, as individual strains, have a wide range of stabilities; thus, some strains do not require special conditions for storage, but others do (Skurnik *et al.,* 2007). Comparison of various methods of preservation such as freezing and lyophilisation indicate that phages become inactivated over a period of six weeks to two years, dependent on the method and strain (Clark and Geary 1973). Nevertheless, long-term stability (i.e. retention of high phage titres) is desirable in terms of practicality (Alfadhel *et al.*, 2011). This would depend on the type of phage, the formulation method and the choice of excipients to be chemically compatible with the phage (Golshahi *et al.,* 2010). Bacteriophages may be stable for up to several years if kept at 4 ºC in filter-sterilised broth; common media used are Trypticase Soy Agar and Brain Heart Infusion broth (Ackermann *et al.,* 2004). Additives can be used to assure sterility of the media, such as chloroform in the case of non-lipid enveloped phages (Gould 1999). Phage-lysates are then kept at 4 ºC or at ultra-low temperatures (below -60 ºC) or in liquid nitrogen without further treatment; glycerol and DMSO may be used as cryoprotectants (Skurnik *et al.,* 2007).

Lyophilisation (freeze-drying) has been reported as a feasible technique for the preservation of phages (Puapermpoonsiri *et al.,* 2010), which may retain their

viability up to 20 years when vacuum-packed in the storage ampoule (Ackermann *et al.,* 2004). Additives reported to retain the stability of lyophilised phages include bovine serum albumin (Ackermann *et al.*, 2004; Gould 1999), carbohydrates such as sucrose and lactose (Puapermpoonsiri et al. 2009; Skurnik *et al.,* 2007), glycerol (Ackermann *et al.,* 2004), skimmed milk and peptone (Clark and Geary 1973). However, studies reveal a wide variability in the storage requirements for individual phages and there is probably not a universal method for long-term preservation. One recently reported, novel method for the long-preservation of tailed phages, involved storage in frozen infected cells at -80 ºC (Golec *et al.,* 2011). These results suggested that the viability of the tailed phages using this method was generally improved, compared to the earlier storage methods.

As mentioned earlier, with the increasing importance of biomolecules as therapeutic agents more attention is being directed towards the development of improved methods for formulation and delivery of proteins. Stabilization of biologics in the form of dry powder has been reported for vaccines (Murdan *et al.,* 2005) and for nasal and pulmonary delivery systems (Mohammed and van der Walle, 2006). An important requirement is the prevention of loss of bioactivity as the biomolecule is transferred to the dry state.

A straightforward method for attaining controlled dehydration of biomolecules employs co-precipitation: a process of generating protein-coated microcrystals (PCMC). It is a rapid, cost-efficient technique to immobilise biomolecules onto the surface of water-soluble crystal forming carrier. In this process, an aqueous solution

containing the target biomolecule and the carrier (generally an amino acid) is rapidly mixed with an excess of water-miscible organic solvent. A very rapid dehydration takes places, as the water surrounding the biomolecule dissolves into the water miscible solvent and co-precipitation of the carrier and the biomolecule occurs (Moore *et al.*, 2000) (Figure 3.1). The particles can be isolated from the solvent by filtration or simple isothermal vacuum drying and so costly processes such as lyophilisation and spray-drying can be avoided. The fine powders obtained have useful properties including ease of handling and accurate dispensing in a suspension form. PCMC techniques have been successfully applied to biomolecules such as proteins (Moore *et al.*, 2000), DNA (Kreiner *et al.*, 2005), enzymes (Kreiner *et al.*, 2001), and nanoparticles (Murugesan *et al.*, 2005).

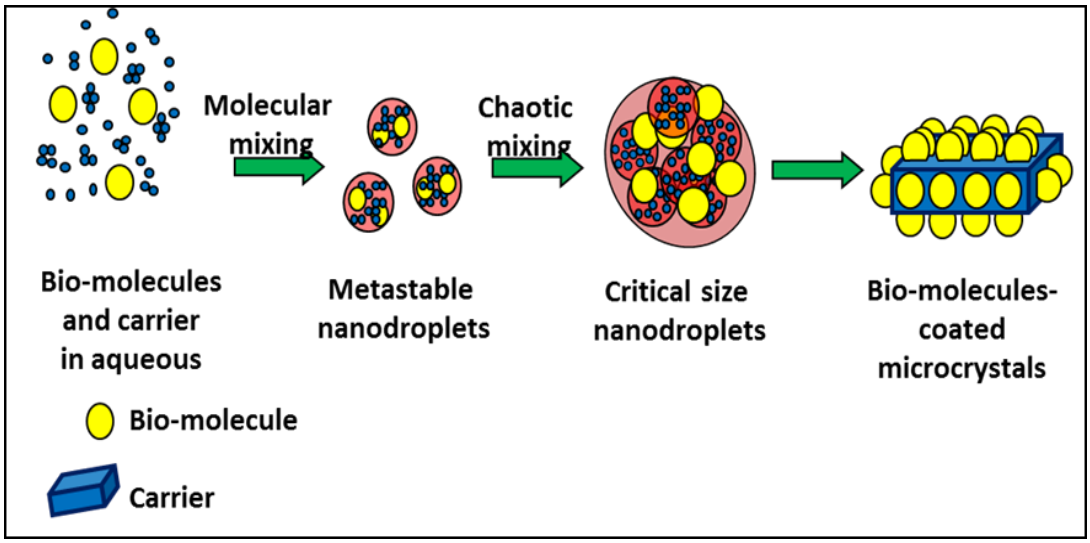

Figure 3.1. Schematic diagram of protein coated microcrystals (PCMC) preparation method.

In this work, we present a new approach for the rapid drying of phage from solution and subsequent storage at room temperature (or below) in the form of dry powders, with the phage bound onto the surface of an inert excipient. The approach draws from the PCMC process. Bacteriophages present unique challenges for the PCMC process on account of their complex self-assembled structure and resultant lability. To adopt a widespread use of this process, a good retention of bacteriophage activity is of prime importance. Therefore, our focus in this study is screening of the key variables in the PCMC process in order to try to maintain maximal lytic activity during storage. The processing variables include drying the formulations at different relative humidities (RH), using different organic solvents and also adding stabilising additives to the formulations. The additives chosen in the reported study included trehalose, since non-reducing sugars are widely accepted to be protein stabilisers (Pereira *et al.*, 2007), and BSA, since this is an exceptionally stable and surface active protein (Annan *et al.*, 2006). Amino acid carriers that were used in this study were glutamine and glycine.

Glutamine is a non-essential amino acid with MW 146.15 with solubility in water of 2.5 g/ 100 mL H_2O at 25 °C. Glutamine was chosen because of its relatively low aqueous saturated concentration, 36 mg/mL at 25°C. This was expected to lead to an efficient precipitation process comparing to other carriers and to increase protein yields. By washing the recovered crystals with a saturated aqueous solution of the same amino acid, lower quantities of amino acid would be required which would minimize costs during scale-up of the process (Brown, 1991).

Glycine is the starting material for many other proteins and amino acids. It has MW 75.07 and a solubility of 25g per 100 mL H_2O at 25 °C. Glycine dissolves in both water and other organic solvents as it has both hydrophobic and hydrophilic properties. The structure of glycine (Figure 3.2) shows that it contains both carboxylic acid and amine group in the same carbon atom. This is important category of amino acids called as α-amino acids (O'Neil, 2001).

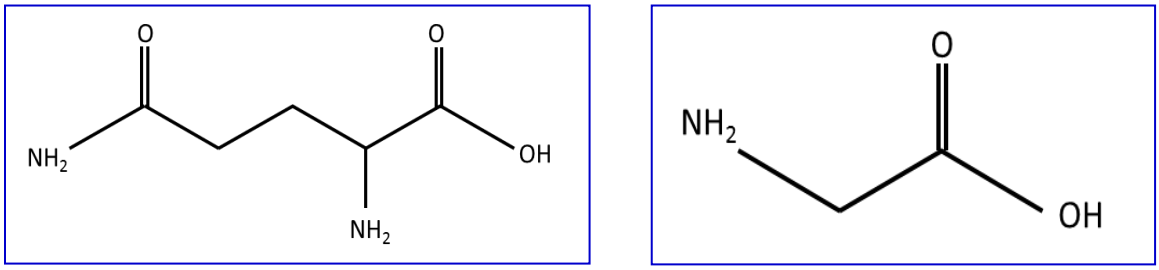

a) Glutamine **b) Glycine**

Figure 3.2. Chemical structures of glutamine and glycine.

3.2. Materials and Methods

3.2.1. Materials

Glutamine, bovine serum albumin (BSA), trehalose, gelatine, magnesium nitrate hexahydrate, sodium chloride, and organic solvents: methanol, isopropanol and isobutanol (2-methyl-1-propanol), were purchased from Sigma-Aldrich Chemical Company (Dorset, UK) Water was purified to > 16 MΩ cm. Granulated agar, yeast extract, tryptone and glycine were supplied by Melford Laboratories Ltd., UK. Trizma base and magnesium sulphate heptahydrate were purchased from Fluka, UK. All chemical and solvents were of analytical grade or equivalent.

3.2.2. Bacterial and bacteriophage strains

Staphylococcus aureus FD209 P variant (strain 8588) was acquired from NCIMB, Aberdeen, UK (ATCC ref. 11522). The bacteriophage specific for this strain of *S. aureus* belongs to the *Siphoviridae* family and was also obtained from NCIMB, Aberdeen, UK (Cat. No: 9563; ATCC ref. 6538-B).

3.2.3. Bacteriophage preparation and harvest.

The bacteriophage preparation and harvest method used as discussed in chapter 2.

3.2.4. Preparation of Phage-coated microcrystals

Glutamine and glycine were diluted into the corresponding volume of bacteriophage stock to sub-saturation concentrations of 15 mg/mL and 112.5 mg/mL, respectively. Stabilising additives, where used, were also added to the bacteriophage stock at a concentration yielding 5 % w/w relative to the mass of amino acid. This aqueous

phase was added drop-wise into the organic solvent while stirring with a magnetic bar at 1100 rpm for 1 minute (magnetic stirrer KMO2 basic from IKA® Werke GmbH & Co. KG) (Figure 3.3). Isopropanol and or isobutanol were used as the organic phase. The aqueous phase to organic solvent ratio by volume was found to be optimum at 1:9 (10 % aq. sol.) for isopropanol and 1:19 (5 % aq. sol.) for isobutanol, based on their full and partial miscibility with water, respectively. The crystalline precipitate formed immediately on mixing and was harvested by vacuum filtration across a hydrophobic membrane filter with 0.45 µm pore-size (Millipore, Ireland). The harvested phage-coated microcrystals (ϕ-CMC) were then dried and stored at a constant temperature of 25 °C. ϕ-CMC were dried until constant weight and, for plaque assay, reconstituted in distilled water to amino acid concentrations originally used in their preparation. The titre of the phage in the reconstituted ϕ-CMC was compared to the titre of the neat phage used in their preparation, in order to determine the preservation of integrity of the phage after processing.

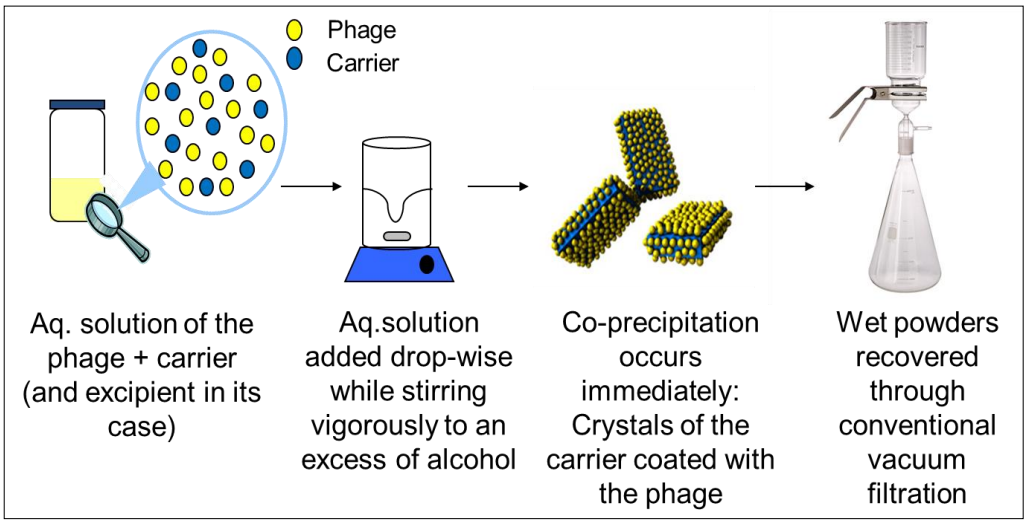

Figure 3.3. Preparation method of ϕ-CMCs.

3.2.5. Drying/storage conditions at varying humidity.

ϕ-CMC containing stabilizers were prepared as above and dried until constant weight at 25 °C and constant relative humidity (RH) of 52 % and 75 % RH, with the latter were obtained using saturated solutions of $Mg(NO_3)_2 \cdot 6H_2O$ and NaCl in sealed containers, respectively. The dried powders then were redispersed in 1 mL distilled water and lytic activity determined by plaque assay as above. Experiments were repeated for three independently prepared batches.

3.2.6. Plaque assay

A serial ten-fold dilution of the bacteriophage stock was made in triplicate. A 100 µL aliquot of each dilution and an equal volume of overnight-incubated bacterial culture were added to 4 mL of partially cooled 0.75 % LB agar, and poured onto a 1.5 % LB agar plate, kept at 37 ºC for 18 h. Positive and negative controls were prepared in the same way by adding bacterial culture and a known concentration of bacteriophage and solely bacterial culture respectively. Following overnight incubation, the number of plaques was counted for each dilution and the phage titre given in units of plaque forming units per mL (pfu/mL). The titre of the phage was calculated from the last dilution containing between 30 and 300 plaques: less than 30 plaques per plate are considered to be too few to count (TFTC) and more than 300 plaques are considered to be too many to count (TMTC) (Cappuccino and Sherman 2011). For each formulation the plaque assay was performed in triplicate (three serial dilutions), therefore the final titre results are presented as the mean of the three values obtained for each formulation together with the derived standard deviation.

3.2.7. Characterization of dried powder

3.2.7.1. Percentage yield of Φ-CMC dry powder

The yield of the dry powders was calculated as: (Mass of dried powder recovered) / (Mass dissolved in aqueous phase) × 100; where 'mass' included additives (BSA or trehalose) but not phage since the latter was considered to be negligible.

3.2.7.2. Particle size analysis and zeta potential (ζ)

Sizing of the powders was performed by laser diffractometry (Mastersizer 2000 Version 5.00, Malvern Instruments Ltd., UK). The powder was dispersed in isopropanol (non-solvent) in the chamber until a laser obscurity around 10% was reached and data acquired. Size distribution was evaluated using Mie scattering theory and the median diameter was measured for three independent batches, calculating the average median diameter and standard deviation.

The zeta potential (ζ**)** of the powders was measured by photon correlation spectroscopy using a Malvern Zetasizer Nano-ZS (Malvern Instruments, Malvern, United Kingdom) at 25˚C, using methanol as the dispersant.

3.2.7.3. Scanning electron microscopy (SEM)

The morphology of the powders was imaged by scanning electron microscopy (SEM), using a JEOL 6400 scanning electron microscope, scandium imaging platform (University of Glasgow, UK) at either 2.5 kV or 6 kV and at different magnifications. Dry powders were fixed onto metal stubs using double-sided

adhesive copper tape. Stubs were coated with gold under vacuum for 30 min using a sputter coater (Polaron SC515) before imaging.

3.2.7.4. Moisture content

The residual water content of the dry powders was determined by Karl Fischer titration (Mettler Toledo DL 37, Leicester, UK). 50 mg of dried powders were suspended in 500 µLof anhydrous methanol. Samples were centrifuged with the aim of obtaining a clear supernatant. The apparatus was calibrated with Karl Fischer water standard (2-methoxy ethanol) and blanked with the addition of anhydrous methanol. The water content was determined for each formulation in duplicate for each independently prepared sample and expressed as the percentage.

3.3. Results

3.3.1. Phage lytic activity of the ϕ-CMC powders.

3.3.1.1 Phage lytic activity without the addition of excipients

Phage-coated microcrystals (ϕ-CMC) were first produced by immobilisation of phages onto an amino acid carrier, precipitated by mixing with isopropanol. This simple method was found to be inadequate since the phage titres following reconstitution of the ϕ-CMC had fallen by ~10^9 and ~10^{11} for the glutamine and glycine carriers, respectively (Table 3.1).

Table 3.1. Phage titre following initial immobilisation of phage to amino acid carriers without additives.

Formulation	Titre of the neat phage (pfu/mL)	Titre of the reconstituted powder (pfu/mL)
Gln (15 mg/mL)	$(1.7 \pm 0.9) \times 10^{13}$	$(1.4 \pm 0.4) \times 10^{4}$
Gly (112.5 mg/mL)	$(1.7 \pm 0.9) \times 10^{13}$	$(7.1 \pm 2.2) \times 10^{2}$

3.3.1.2. Effect of drying/storage conditions at varying humidity on lytic activity of phage in the formulations.

Figure 3.4 summarises the results obtained for ϕ-CMC formulations containing stabilizers dried at 25 °C and relative humidities (RH) of 52 and 75 %. The most noticeable difference arises from the humidity at which the ϕ-CMC were dried: at 52 % RH a fall in the lytic activity of $\sim 10^{13}$ was observed despite the addition of trehalose to the carrier, while for the same formulations dried at 75 % RH, a fall of $\sim 10^{7}$ was observed.

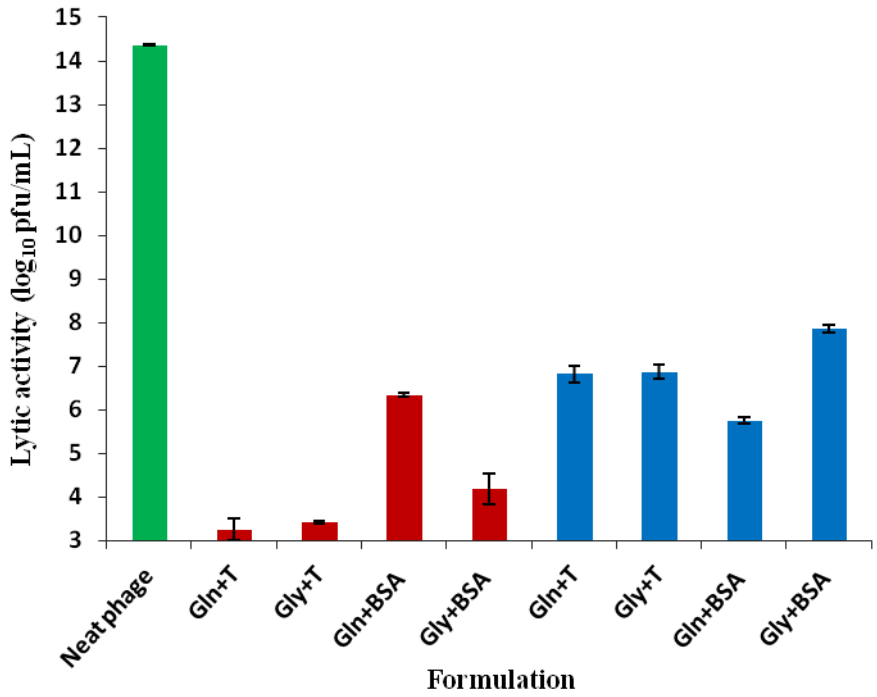

Figure 3.4. Lytic activities of the ϕ-CMC generated from mixing with isopropanol and reconstituted in water. The core substrate of the ϕ-CMC were composed of: Gln = glutamine, Gly = glycine, T = trehalose, BSA = bovine serum albumin. Red and blue bars represent drying at 52 and 75 % RH, respectively. The green bar indicates the titre of the phage stock from which the ϕ-CMCs were generated. Data show mean ± S.D. for n = 3.

3.3.1.3. Effect of type of organic solvent on the lytic activity of phage.

To investigate the effect of solvent on increasing phage lytic activity, the same ϕ-CMC process was used but with the substitution of isobutanol for isopropanol during the mixing step. However, due to the low miscibility of isobutanol in water, the aqueous:organic solvent ratio (by volume) was changed to 1:19 during the mixing step, compared to 1:9 for isopropanol. Figure 3.5 illustrates that for powders dried at 52 % RH, the reconstituted glutamine ϕ-CMC showed a complete loss of lytic

activity, irrespective of the addition of trehalose or BSA. In contrast, reconstituted glycine ϕ-CMC retained high lytic activity, with the titre remaining at between 6 log_{10} and 8 $log_{10.}$ When the ϕ-CMC were dried at 75 % RH, the same difference between glutamine and glycine carriers was observed. In addition, the reconstituted glycine ϕ-CMC showed a higher lytic activity (10 $log_{10)}$ than those dried at 52 % RH.

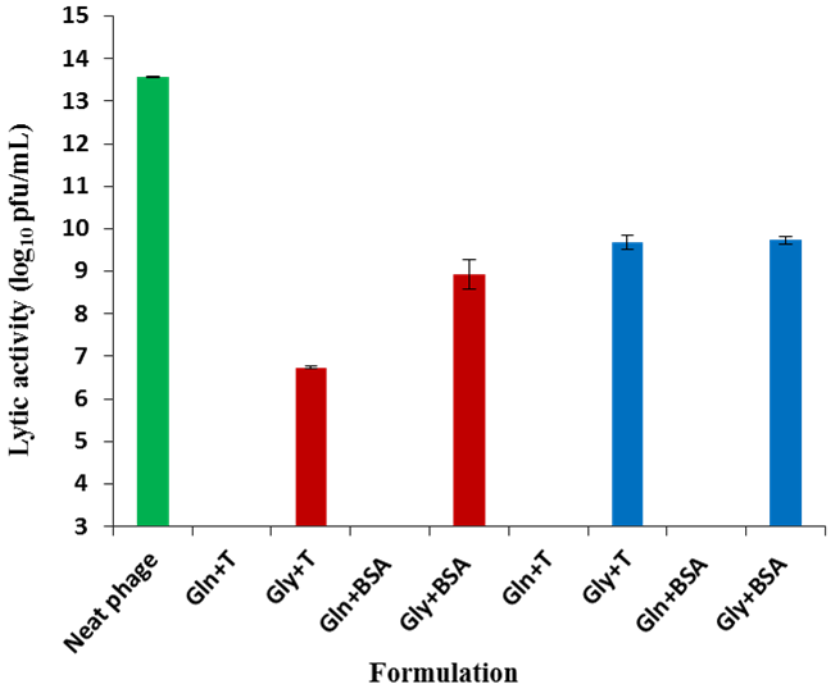

Figure 3.5. Lytic activities of the ϕ-CMC generated from mixing with isobutanol and reconstituted in water. The core substrate of the ϕ-CMC were composed of: Gln = glutamine, Gly = glycine, Trh = trehalose, BSA = bovine serum albumin. Red and blue bars represent drying at 52 and 75 % RH, respectively. The green bar indicates the titre of the phage stock from which the ϕ-CMCs were generated. Data show mean ± S.D. for n = 3.

To investigate the effect of storage conditions on lytic activity of phage, the formulation containing glycine with trehalose/ BSA as stabiblizer has been chosen.

The stability testing of formulations stored at 52% and 75% RH showed that the phage partially lost their lytic activity over 1 month period (Figure 3.6).

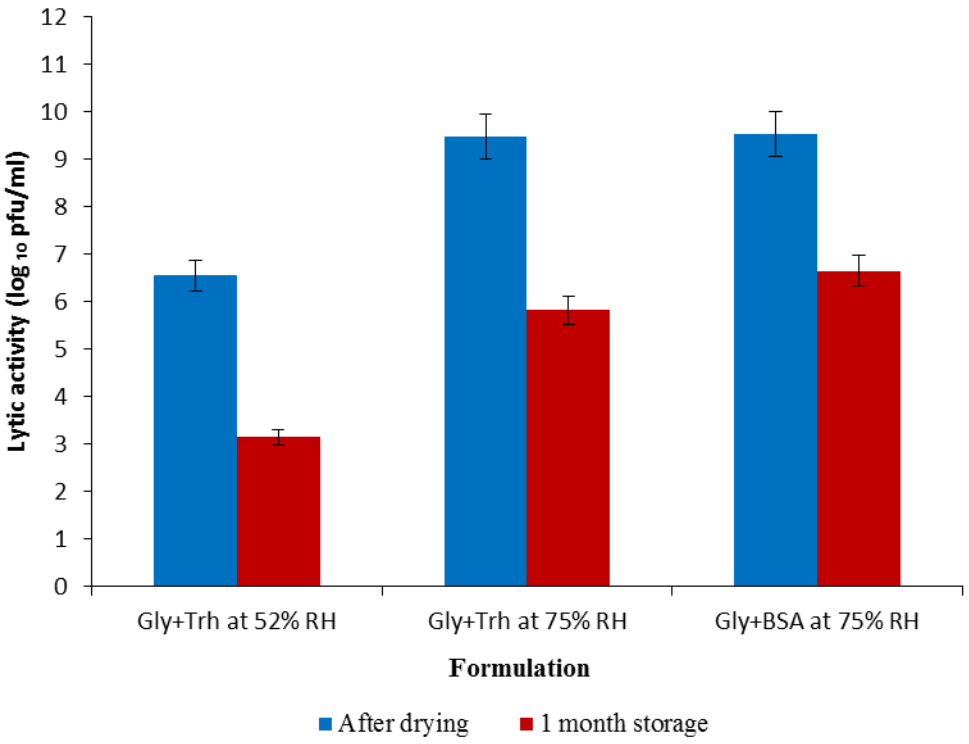

Figure 3.6. Comparison between the lytic activities of the ϕ-CMC with glycine generated from mixing with isobutanol and reconstituted in water, after drying and after one month storage, data show mean ± S.D. for n = 3.

3.3.2. Characterization of ϕ-CMC dry powders.

3.3.2.1. % yield of Φ-CMC dry powder.

The percentage yield calculated for the ϕ-CMC powders without excipients after drying at 25°C is 90.33% and 96.54 for glutamine and glycine respectively. Table 3.2 shows that the yield produced after addition of excipients was also above 90% for all measured powders, with most powders having around 95-100% yield.

Table 3.2. Percentage yield calculated for the ϕ-CMC with excipients precipitated from isopropanol after drying at 25 °C.

Formulation	RH for drying (%)	Yield (%)
Gln + Trh	52	101.35
Gln + Trh	75	-
Gly + Trh	52	-
Gly + Trh	75	94.60
Gln + BSA	52	96.53
Gln + BSA	75	94.33
Gly + BSA	52	97.68
Gly + BSA	75	103.16

Table 3.3. Percentage yield calculated for the ϕ-CMC with excipients precipitated from isobutanol after drying at 25 °C.

Formulation	RH in storage (%)	Yield (%)
Gln + Trh	52	89.98
Gln + Trh	75	84.93
Gly + Trh	52	98.65
Gly + Trh	75	90.14
Gln + BSA	52	98.59
Gln + BSA	75	95.31
Gly + BSA	52	96.80
Gly + BSA	75	96.81

3.3.2.2. Surface characteristics and morphology of the Φ-CMC by SEM

Figure 3.7 shows the SEM micrographs of dried ϕ-CMC generated from mixing with isopropanol. With glutamine as the carrier, in the presence of both trehalose and BSA, ϕ-CMC presented a thin-layer morphology, with overlap of different layers and sizes arranged apparently randomly (Figure 3.7 A and B). For ϕ-CMC made with glycine as the carrier, well-defined, discrete spherical aggregates were observed, among other sections of the material, which formed random clusters, and aggregates of particles (Figure 3.7 C and D).

Micrographs of the ϕ-CMC generated from mixing in isobutanol indicated that the nature of the organic solvent did not have a major influence on particle morphology (Figure 3.8). As for precipitation from isopropanol, the glycine ϕ-CMC tended to aggregate into spheres with diameters ≥ 10 μm (Figure 3.8 C and D), although the use of isobutanol appeared to be cause a slight tendency of the glutamine ϕ-CMC to aggregate as well (Figure 3.8 A and B).

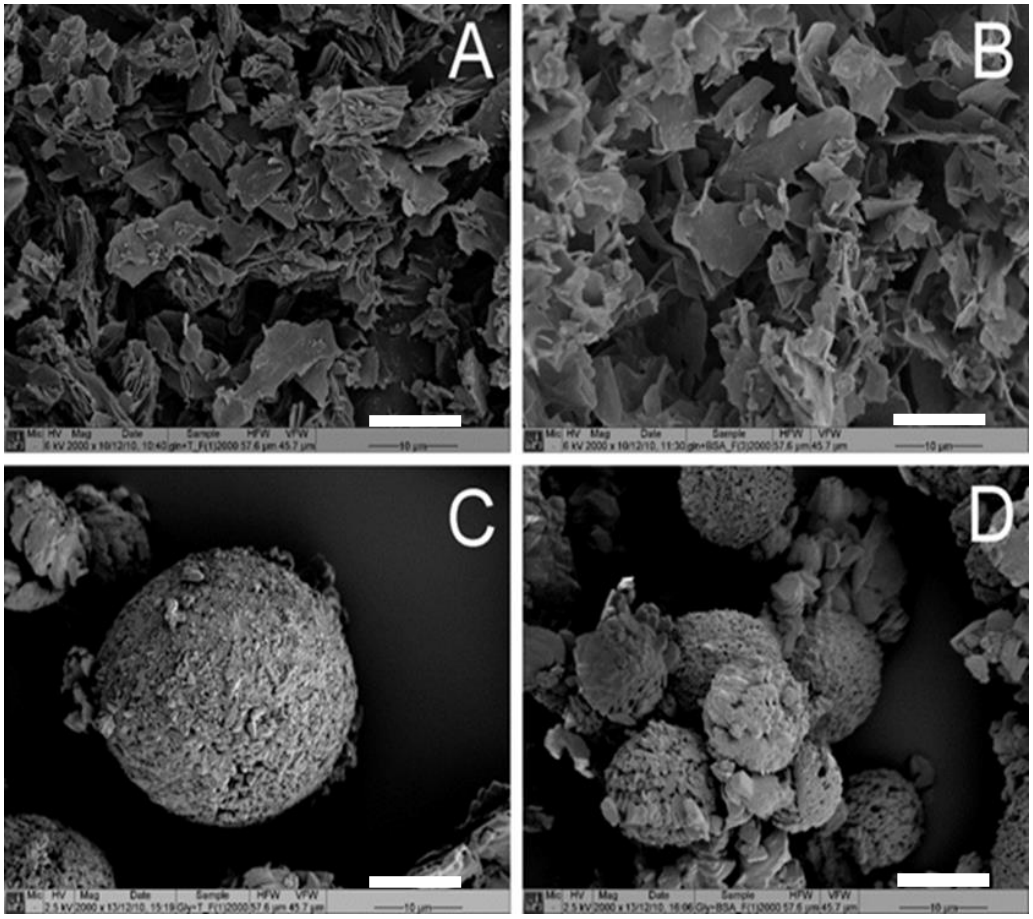

Figure 3.7. SEM micrographs of dried ϕ-CMC generated from mixing with isopropanol. The core substrate of the ϕ-CMC being composed of Gln and 5 % w/w trehalose (A), Gln and 5 % w/w BSA (B), Gly and 5 % w/w trehalose (C), Gly and 5 % w/w BSA (D). Magnification = 2000×; scale bar = 10 μm.

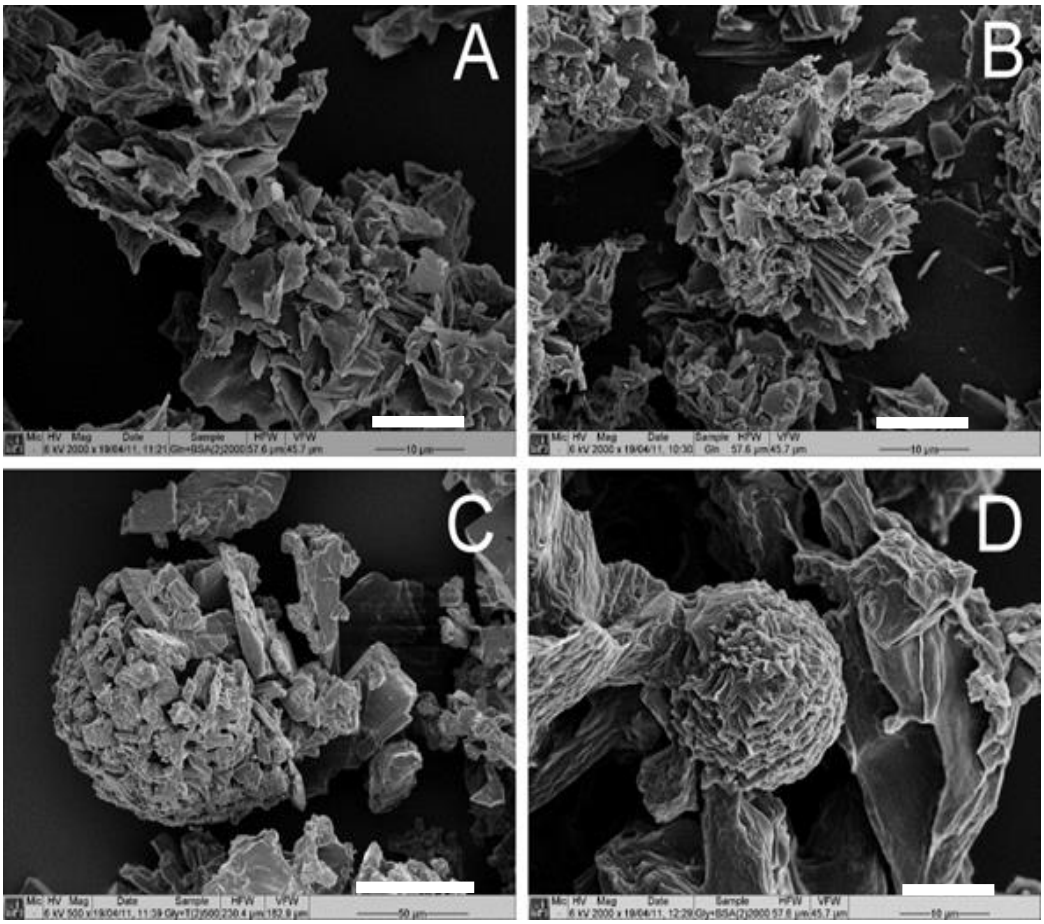

Figure 3.8. SEM micrographs of dried ϕ-CMC generated from mixing with isobutanol. The core substrate of the ϕ-CMC being composed of Gln and 5 % w/w trehalose (A), Gln and 5 % w/w BSA (B), Gly and 5 % w/w trehalose (C), Gly and 5 % w/w BSA (D). For A, B, and D, magnification = 2000×; scale bar = 10 µm. For C, magnification = 500×; scale bar = 50 µm.

3.3.2.3. Residual moisture content of Φ-CMC formulations

When using the same phage stock solution for all formulations, high and low phage loadings per unit mass of glutamine and glycine will result, since the concentration of glutamine and glycine in the aqueous phase was 15 and 112.5 mg/mL, respectively. Therefore, formulations having the same phage loading were also prepared and Karl Fischer analysis was performed on all formulations for better

comparison. Comparing the residual moisture content of ϕ-CMC incorporating trehalose or BSA for high and low phage loadings, it can be seen that glutamine ϕ-CMC had a significantly higher residual moisture content than the equivalent glycine ϕ-CMC, irrespective of whether the ϕ-CMC were dried at 52 or 75 % RH (Table 3.4). Also for glutamine formulations the residual moisture content for ϕ-CMC incorporating BSA was higher than ϕ-CMC incorporating trehalose. However, when the same phage loading was used for the formulations, no significance difference in the residual moisture content was observed.

Table 3.4. Residual moisture content of the ϕ-CMC precipitated from isopropanol after drying at 25 °C.

Formulation	**% RH for drying**	**% water content**	
		High (Gln) and low (Gly) phage-loading[a]	Same phage-loading[a]
Gln[b] + Trh[c]	52	5.27 ± 0.67	1.02 ± 0.05
Gln + Trh	75	14.65 ± 0.81	1.93 ± 0.07
Gly[d] + Trh	52	2.02 ± 0.28	1.64 ± 0.08
Gly + Trh	75	4.15 ± 0.22	3.19 ± 0.98
Gln + BSA[c]	52	6.29 ± 0.22	1.51 ± 0.07
Gln + BSA	75	17.60 ± 0.68	2.62 ± 0.68
Gly + BSA	52	1.62 ± 0.26	1.92 ± 0.09
Gly + BSA	75	4.07 ± 0.07	3.77 ± 0.16

[a], defined as pfu per mg of carrier; concentration in aqueous phase = 15 mg/mL[b], 5% w/w[c] and 112.5 mg/mL[d].

Moreover, effect of organic solvent on the moisture content for all formulations has also been investigated in this work. For ϕ-CMC with the same phage loadings but precipitated in isobutanol, the residual water content was observed to be strongly dependent on the % RH during drying. Table 3.5 shows that at 75 % RH, the residual

moisture content was between 13 and 17 % (except glycine/trehalose formulation), whereas at 52% RH the residual moisture content was between 1.9 and 3.3 %.

Table 3.5. Residual moisture of the ϕ-CMC precipitated from isobutanol after drying at 25 °C.

Formulation	% RH for drying	% water content for ϕ-CMC with the same phage-loading[a]
Gln[b] + Trh[c]	52	3.29 ± 0.19
Gln + Trh	75	17.1 ± 0.73
Gly[d] + Trh	52	1.26 ± 0.02
Gly + Trh	75	3.71 ± 0.03
Gln + BSA[c]	52	3.12 ± 0.11
Gln + BSA	75	13.0 ± 0.22
Gly + BSA	52	1.88 ± 0.06
Gly + BSA	75	13.8 ± 0.19

[a], defined as pfu per mg of carrier; concentration in aqueous phase = 15 mg/mL[b], 5% w/w[c] and 112.5 mg/mL[d].

3.4. Discussion

When either of the amino acids (glutamine or glycine) were used alone as a carrier for co-precipitation of phage, the phage titre dramatically decreased. The efficiency of various amino acids as carriers has been previously reported (Moore *et al.,* 2000; Kreiner *et al.,* 2005) and it appears that the high loss of phage lytic activity is due to the effect of organic solvents. Generally, a water-miscible organic solvent disrupts the protein conformation due to replacement of structural water molecules on the surface of protein with the surrounding organic solvent (Khmelnitsky *et al.,* 1991). As a result, a high loss of phage infectivity in isolation by this simple method is likely to occur upon exposure to the water miscible organic solvents and is also

likely to occur during adsorption-induced unfolding of the phage protein coat at the carrier surface. Matsubara and co-workers (2007) showed that phage lytic activity decreased in presence of water-miscible organic solvents and the loss of phage infectivity was directly related to the solvent concentration. Such a large loss of phage lytic activity in the formulations would clearly be unacceptable for phage bioprocessing and additives were therefore sought which would stabilise the phage. By addition of trehalose and BSA, two mechanisms were investigated for the stabilisation of the phage during the PCMC process. First, by using trehalose to thermodynamically favour the folded state by preferential exclusion of non-reducing sugars from the protein domains of the phage (Lee and Timasheff 1981). Second, minimisation of adsorption to the water/organic solvent interface through competition with BSA and subsequent attenuation of adsorption-induced unfolding (Annan *et al.*, 2006).

We also investigated the effect of drying/ storage conditions on lytic activity, since storage of medicines at varying humidities is a commonly used technique to determine the stability of a drug in a particular formulation. The intention of drying at different humidities was not to specifically generate ϕ-CMC with low/high residual moisture content but rather to accelerate the rate and extent of removal and/or exchange of residual organic solvent from the phage on the carrier surface (Wang *et al.*, 2002). In this respect, it is clear that a rapid removal of residual organic solvent from the ϕ-CMC by exchange with water vapour present at 75 % RH prevented further loss of lytic activity; i.e. minimising the exposure of the phages to

residual organic solvent better maintained their integrity. This result is in agreement with previous work showing that inactivation of filamentous phages is accelerated on exposure to water-miscible organic solvents in a concentration dependent manner (Matsubara *et al.*, 2007). The addition of BSA to the amino acid carrier improved the lytic activity of the reconstituted ϕ-CMC compared to carriers including trehalose, particularly when dried at 52 % RH. However, the extent of BSA-mediated stabilisation of phage immobilised to the two amino acid carriers was more variable than that afforded by trehalose (Figure 3.4). This may reflect the more complex, macromolecular nature of BSA, whose chemical and physical structure will be expected to change during exposure to solvent and also to increasing RH. Examples of detrimental and advantageous effects on proteins exposed to differing RH can be found in the literature. For example, the physical (conformational) stabilisation of dried lactate dehydrogenase and granulocyte colony-stimulating factor by amino acids was compromised by uptake of residual moisture (Mattern *et al.*, 1999). In contrast, the enhancement of physical stability has been observed for antibodies in the presence of high residual moisture (Breen *et al.*, 2001). The same enhancement of physical stability would therefore appear to be true for phage, with respect to their proteinaceous head group and tail. Given these considerations, trehalose may be preferable over BSA for the stabilisation of phage during the ϕ-CMC process, since the outcome with regard to lytic activity is less variable.

Although the effect of additives and increasing RH on ϕ-CMC lytic activity was encouraging, the phage titres remained below what could be considered practically

useful. Thus, after reconstitution of ϕ-CMC, it would be expected that the resultant phage titres remain sufficiently high for further formulation for a particular phage therapy. One such example would be the clinical trial testing the efficacy and safety of bacteriophages targeting *Pseudomonas aeruginosa* in chronic otitis in humans (Wright *et al.* 2009). In that clinical trial, 10^5 pfu of each of six bacteriophages in 0.2 mL liquid were applied into the ear. Taking this titre as a guide leads to the conclusion that reconstitution of ϕ-CMC should yield a titre in the order of at least 10^6 pfu/mL.

While the ϕ-CMC process allows for concentration of the phage by reconstituting the dried powder into a smaller aqueous volume than that originally containing the phage, there is a limit to this due to the solubility of the amino acid carrier. For ϕ-CMC precipitated from isopropanol, containing trehalose or BSA and dried at 75 % RH, phage titres from reconstituted powders were around 10^7 pfu/mL. These titres may be at the lower limit for subsequent formulation, at least with respect to the clinical trial by Wright et al. (2009). Higher titres following ϕ-CMC reconstitution would therefore be desirable.

To this aim, isopropanol was replaced by isobutanol during the mixing step. The logic behind this decision was that the nature of the solvent in aqueous-organic mixtures is known to effect the extent of protein denaturation (Griebenow and Klibanov 1996). However, due to changing the aqueous/organic solvent ratio, the results showed that the lytic activity of the phage was very much dependent on the amino acid carrier (Figure 3.5). There is a large discrepancy in the titre between

glycine and glutamine ϕ-CMC formed with isobutanol nevertheless if powders were dried at 52 % or 75 % RH). The reason for that can be related in part to the efficiency of the process and yield. Table 3.3 shows that the yield of glutamine/trehalose powders was below 90%, distinct from glutamine/BSA and all glycine powders which retained the high yields also observed for precipitation in isopropanol. The relatively poor efficiency glutamine/trehalose precipitation would be expected to attenuate the immobilisation of phage on the carrier surface and thereby bring about a perceived loss of lytic activity. Process efficiency is not sufficient however to explain the loss of lytic activity for glutamine/BSA powders. Here, consideration of the 'solid-state buffering capacity' may be relevant. When proteins (and therefore phage) are immobilised onto a crystal carrier through mixing with non-solvent, their ionisation state will change according to the nature of the carrier and its buffering capacity. Previous studies of PCMC using various crystal carriers have demonstrated this *in situ* control of ionisation-state for an immobilised enzyme, showing large differences in enzyme activity dependent on the nature of the carrier (Kreiner and Parker 2004). Thus, the combination of the low glutamine concentration (15 mg/mL, *cf.* 112.5 mg/mL glycine) and reduced aqueous: organic solvent ratio in isobutanol, may not only have reduced process efficiency but also been insufficient for *in situ* control of the phage ionisation-state.

When the ϕ-CMC produced from isobutanol were dried at 75 % RH, the same discrepancy between glutamine and glycine carriers was observed, but of particular interest was that the reconstituted glycine ϕ-CMC showed a fall in titre of only $< 10^4$.

This was encouraging, since the resultant titre of the powders was almost 10^{10} pfu/mL, well within the range which could be considered practically useful for formulation, as described above. Given that all other parameters except the choice of solvent remained the same, this result also demonstrates that a key driver of phage inactivation in this bioprocess is exposure to organic solvent. An optimised bioprocess method was therefore identified in this study, wherein ϕ-CMC were generated from glycine as the core substrate following mixing with isobutanol and drying at 75 % RH. There did not appear to be a preferred mechanism for stabilisation of the phage during this bioprocess since there was no statistical difference between titres for glycine ϕ-CMC incorporating trehalose or BSA, at least at 75 % RH (Figure 3.5). At 52 % RH, BSA would appear to have some advantage over trehalose as regards phage stabilisation, but this is a secondary effect compared to the importance of RH.

Stability testing of the ϕ-CMC generated from glycine with trehalose/BSA as stabiliser and drying at 52/75 % RH showed that the phage partially lost their lytic activity over a one-month period (Figure 3.6). The fall in titre was between 3 and 4 $\log_{10}$ for all ϕ-CMC tested, irrespective of the initial titre, stabiliser and RH. This rate of loss of titre for phage immobilised to crystal carriers was however much less than that observed for phage immobilised to amorphous polyesters, also in the solid state following lyophilisation (Puapermpoonsiri *et al.,* 2009). This would suggest that the mobility of the carrier plays a role in the inactivation of immobilised phage during storage, with crystalline materials being preferred over amorphous materials.

An important measure of the PCMC process is the overall yield of dry powder. For the process to be commercially viable, the yield would be expected to be near 100%. The high percentage yield obtained for all ϕ-CMC formulations indicates that the mixing of the aqueous and solvent phases, and subsequent precipitation of the carrier (and additive where used), was very efficient at this micro-scale. In the cases where the yield was slightly above 100%, this may have been due to errors in weighing at the micro-scale or incomplete drying of the powder. Scale-up of the process would be expected to reduce the effect of small variances in weighing measurements on the calculation of yield. Scale-up of the process could be envisaged using in-line pump mixing and would be expected to at least match, or better, the yields obtained here.

Physical characterization of the powders by SEM indicated that the ϕ-CMC morphology was highly dependent on the amino acid carrier. The use of glutamine produced particles of different thin layers while spherical aggregates where produced when glycine is the amino acid used.

The zeta potential is often used as an indication on the storage stability of a colloidal particulate system. The stability depends on the forces of interaction between the colloids particles. The Derjaguin-Landau-Verwey-Overbeek (DLVO) theory is one of the common principles for quantification of forces in colloidal sciences (Sabin *et al.*, 2010). The DLVO theory is built on the hypothesis that the forces between two surfaces are determined by the sum of two forces: the electrical double layer repulsive force and the London-van der Waals attractive force (Kayes, 1988). When particles come close to each other due to Brownian motion these forces determine

whether the particles will repulse or aggregate. The magnitude of ZP should be high enough to prevent aggregation. It was suggested that zeta potential value ≥ 30 mV or ≤ -30 mV (optimum 60 mV) are required for full electrostatic stabilization (Malvern, 2004). Therefore, as the zeta-potential decreases we can expect less electrostatic repulsion which, according to the DLVO theory, will then favour aggregation of the particles. As a result, the tendency of the glycine ϕ-CMC to aggregate can be associated with the smaller zeta potential of the particles (-11.1 ± 1.2 mV) compared to glutamine ϕ-CMC (-47.4 ± 1.2 mV). Although the amide side chain of glutamine does not carry a charge, delocalisation of the lone electron pairs gives a strong dipole moment, and hence the greater zeta potential of glutamine ϕ-CMC over glycine ϕ-CMC. It is possible that the slight aggregation observed for glycine ϕ-CMC was an artefact of the sample preparation for SEM. However, sizing of the ϕ-CMC suspended in isopropanol by light scattering showed bimodal profiles corresponding to dispersed and aggregated crystal particles (between 8 and 130 µm diameter) for all samples tested, irrespective of the solvent. For the purposes of bioprocessing, the aggregation of the particles is not expected to be problematic since this does not have any effect on reconstitution into aqueous buffer. As regards powder handling, a bimodal distribution of particle sizes in a powder is often beneficial. For example, in pharmaceutical processes such as tableting, Emcompress® (calcium hydrogen phosphate dihydrate and dibasic calcium phosphate) is used because of good flowability on account of its agglomeration and resultant bimodal size distribution (*ca*. 30 and 180 µm diameter) (Schussele and Bauer-Brandl 2003), approximating that for the ϕ-CMC powders.

The residual moisture analysis was used to indirectly demonstrate that the phage were immobilised onto the surface of the ϕ-CMC not within the crystal carriers. For a high and low phage loadings formulations, the higher residual moisture content of glutamine ϕ-CMC compared to glycine ϕ-CMC probably explained by the nature of phage. The phages are proteinaceous and will therefore be associated with hydrogen-bonded water after drying (the bulk water evaporating off the surface). The same reasoning can be used to explain why the residual moisture content for ϕ-CMC incorporating BSA was higher than ϕ-CMC incorporating trehalose. The residual water measured must be associated with the surface of the ϕ-CMC since the amino acid carriers are practically insoluble in the methanol used for Karl Fischer analysis. When the number of phages loaded onto the ϕ-CMC was such that the ratio of phage (pfu): amino acid (mass) was equivalent for glycine and glutamine formulations, the residual moisture levels also approached equivalence. Thus, for the ϕ-CMC precipitated in isopropanol, the residual moisture content was largely determined by the relative phage loading the effect of RH on moisture content was much weaker (Table 3.4). This is in contrast to ϕ-CMC with the same phage loadings precipitated from isobutanol, where the residual water content was observed to be strongly dependent on the % RH during drying. This difference most probably reflects the miscibility of the two solvents with water condensing at the carrier surface from high (75 %) RH and the effect this has on the vapour pressure. Isobutanol is only 8.5% miscible with water, whereas isopropanol is entirely miscible and so results in a greater weakening of the intermolecular forces, generating a mixture with a higher

vapour pressure than the pure components (positive deviation from Raoult's law) and therefore a drier surface as measured by the Karl Fischer technique. In principle, it would be interesting to use a wide range of solvents, but there are limitations with respect to scale-up and introduction to the biopharmaceutical industry and nowadays isopropanol and isobutanol are known to be the most promising candidates for the PCMC process.

Chapter 4: Improved pulmonary delivery of antibiotics and bacteriophage using Lamellasome™

4.1. Introduction

Pulmonary delivery is well established as an effective route for the administration of small molecules such as β_2 adrenoreceptor agents and steroids in the treatment of asthma and other pulmonary diseases. The direct exposure of these drugs to the small (peripheral) airways leads to a passive targeting, reducing the dose and minimising side effects. Larger, more complex biomolecules (enzymes, peptides and proteins) are also administered directly to the airways by inhalation. This class includes DNases (e.g. Pulmozyme®, rhDNase produced by Genentech Inc.) to tackle mucus thickening in cystic fibrosis (Fuchs *et al.,* 1994) and insulin (e.g. Exubera®, that was withdrawn) (Rosenstock *et al.,* 2008).

It has been suggested that only about 10-30% of the inhaled dose reaches the lungs when delivered from inhalation devices, the rest being swallowed (Newman, 1984). However, the direct targeting of the lungs allows a higher concentration of drug in the airway at a lower initial dose compared to systemic administration. Moreover, pathways of metabolism are different and drugs delivered directly to the lung do not undergo first pass extraction. Thus the overall efficiency of a dose administered by inhalation may be considerably higher than that given by systemic route.

In particular, CF patients with chronic pulmonary infection of *P. aeruginosa* benefit from the inhalation of antibiotics (Touw *et al.,* 1995; Mukhopadhyay, 1996).

Nebulizers are commonly used for the delivery of drugs in the treatment of cystic fibrosis, asthma, COPD and other respiratory diseases, in order to direct the antibiotic to the endobronchial site of infection. This maintains low serum concentrations of the drug, thus reducing the risk of systemic toxicity (Cheer et al, 2003).

The therapeutic efficacy of aerosolized drug depends on its deposition site in the target airway, coincident with a maximum deposition in the site of action. One important factor that affects the pattern of deposition is the size, density and shape of the inhaled particles. In general, larger-size particles (above 5 μm) will tend to be deposited in the larger airways while those of smaller diameter will target the smaller airways. Most aerosols used therapeutically contain a range of particle size from 3-5 μm which, in theory, permits a drug to reach all regions of the airway with minimum drug loss (Newman, 1984).

In general, CF treatments focus on reducing disease progression to delay the onset of irreversible lung damage (Mogayzel *et al.,* 2013). This can be achieved by using a number of agents with a specific function, e.g. antibiotics to control the airway infection; mucolytics to enhance mucus clearance (Hodson *et al.,* 2003; Murphy and Rosenstein, 1998); steroids and nonsteroidal anti-inflammatory drugs to control the inflammatory response (Lands and Stanojevic, 2000); and β_2 -adrenergic agonists as bronchodilators. Since the lungs are a major therapeutic target in CF, inhaled drug remains a key target for delivery because it ensures deposition of the drug at the site

of action, increasing local availability and decreasing systemic side effects (Yang *et al.*, 2010).

Phage therapy would be particularly useful in treating chronic bacterial infections that are resistant to antibiotics and possibly in the control pandemics (Skurnik *et al.*, 2007). By nebulising concentrated phage populations, targeted pulmonary delivery could be achieved. Nebulizers are commonly used for the treatment of cystic fibrosis, asthma, COPD and other respiratory diseases, and could be used for delivery of phage and Lamellar bodies. In chapter one, the use of lamellar bodies, which consist of a lipoprotein complex of dipalmitoyl phosphatidylcholine (DPPC) was described. Lamellar bodies, by reducing lung surface tension, have an important function in mucociliary clearance and in maintaining airway elasticity. To improve mucociliary clearance in CF patients, a formulation containing exogenous lamellar body mimetics, administered as an inhaled medication might be beneficial. The second function of the lamellar body would be as an efficient surfactant vehicle, increasing solubility or dispersion of the active ingredient.

The aim of the work in this chapter was to: (1) investigate the potential of phage therapy alone or as adjunctive therapy with aerosolized antibiotics to treat the drug resistant bacterial infections such as *P. aeruginosa*, (2) improve the pulmonary delivery of nebulized solutions of antibiotics or bacteriophage by dilution into Lamellasome^{TM} preparation.

4.2. Material and Methods

4.2.1. Materials

Lamellasome™ preparation in suspension form (LMS-611) Batch No: 150610 was a kind gift from Lamellar Biomedical Ltd (Dr Graham Park, Lamellar Biomedical Ltd, Bellshill, UK). Tobramycin sulphate, Colistin sulphate, fluorescein isothiocyanate (FITC), tetramethylrhodamine B isothiocyanate (TRITC), polyethylene glycol MW 6000 (PEG6000), sterile filter paper discs of 6 mm diameter, mucin from porcine stomach type II, mueller hinton broth were purchased from Sigma-Aldrich Chemical Company (Dorset, UK). Casamino acids powder was obtained from Fischer Scientific, UK. Sodium chloride was obtained from Melford Laboratories Ltd., Suffolk, UK. All other chemicals were purchased from either Sigma-Aldrich or Fischer Scientific at analytical grade or equivalent.

4.2.2. Bacterial and bacteriophage strains

P. aeruginosa strain 217M was kindly donated by Dr. Tyrone Pitt, Laboratory of HealthCare Associated Infection, Health Protection Agency, Colindale, London, UK. *P. aeruginosa* strain 39324 was obtained from the ATCC. The bacteriophage for both *P. aeruginosa* strains was isolated from Clyde river water by Dr McColm, University of Strathclyde, UK.

4.2.3. Bacterial culture and phage preparation

Bacterial cultures, bacteriophage harvest and plaque assay were performed as described in sections 2.2.3.1 and 2.2.3.2).

4.2.4. Characterisation of Lamellasome™

4.2.4.1. LMS-611 absorbance measurement

Optical density was measured at 550 and 600 nm to quantify the amount of LMS-611 at each stage of the MSLI following nebulisation. LMS-611 was diluted in saline and the dispersion measurement performed using a UV-vis. spectrophotometer (ThermoSpectronic, Cambridge, UK).

4.2.4.2. Nebulisation of LMS-611 using the Pari Boy and eFlow® nebulisers.

Two nebulisers were used in the study (Figure 4.1): PARI BOY® SX compressor in combination with PARI LC SPRINT® Nebuliser and the battery-driven PARI eFlow® rapid nebuliser with no compressor, PARI GmbH., Germany. A description of each nebuliser and manufacturer's data for aerosol characteristics are shown in Table 4.1. The differences between the two nebulisers such as nebulisation times and drug deposition of the lamellarsome formulations were assessed here by experiment.

Table 4.1. Comparison between the characteristics of Pari Boy and eFlow nebulisers.

Total output rate	**PARI BOY®SX nebuliser**	**PARI eFlow® nebuliser**
	590 mg/ min	500 mg/ min
Mass median diameter	3.5 µm	4.1 µm
Mass % below 5µm	67%	64%
Fill volume	3 mL	2-6 mL
Nebulisation time	10 min	5 min
	Switch off manually	Automatic switch off at the end of treatment
Nebulisation principle	Oscillating membrane	Perforated oscillating membrane
Application	Upper and lower airways	Lower airways

PARI BOY® SX nebuliser

eFlow® nebuliser

Figure 4.1. Pictures of Pari-Boy and eFlow nebulisers:http://www.parimedical.co.uk.

4.2.4.3. Evaluation of the aerodynamic particle size distribution of nebulised LMS-611 by cascade impaction.

4.2.4.3.1. Cascade impaction

Cascade impaction was employed for LMS-611 particle size measurement using a Multi-stage Liquid Impinger (MSLI) (Copley Scientific, UK), with a high capacity pump (model HCP4, Copley Scientific, UK), a Critical Flow Controller (CFC) (model TPK, Copley Scientific, UK), a flowmeter (model DFM2, Copley Scientific, UK), an adapter to the induction port (Copley Scientific, UK) and a mouthpiece adaptor fashioned from Silastic S Base used with Silastic S Curing agent green (Dow Corning, USA) (Figure 4.2). The CFC was connected to the vacuum pump and MSLI

via the silicone tubing (with inner diameter (ID) = 8 mm, outer diameter (OD) = 14 mm). Pressure tab tubing (P1: 2.2 mm ID, 3.1 mm OD, 59 mm length) at the back of CFC was inserted to the hole of the fourth stage. When the system was enclosed, the pressure (P1) was adjusted to give the required flow rate (Q). Commonly, the air flow rate (Q) was 60 ± 5 L/min, so that the effective cut-off diameters at stages 1, 2, 3, 4, 5 were 13, 6.8, 3.1, 1.7, and < 1.7 microns, respectively. Once the time was established and the pump on, the mouthpiece with adapter replaced the flowmeter. 20 mL of normal saline 0.9% was dispensed into each stage (stage 1-4) and the glass fibre filter (Gelman Sciences, USA) placed onto stage 5. Three independently prepared samples of 3 mL were tested for each formulation. The nebuliser (eFlow nebuliser or Pari Boy nebuliser) was connected and switched on. The LMS-611 formulation was aerosolized from the nebuliser device and directed through the induction port via the mouthpiece adaptor to the MSLI stages as shown in Figure 4.3. When the nebulising solution had been completely nebulised (this took~10 min for Pari Boy-nebuliser and ~5 min for eFlow nebulisers), the nebuliser was switched off and the suspension from each stage was collected.

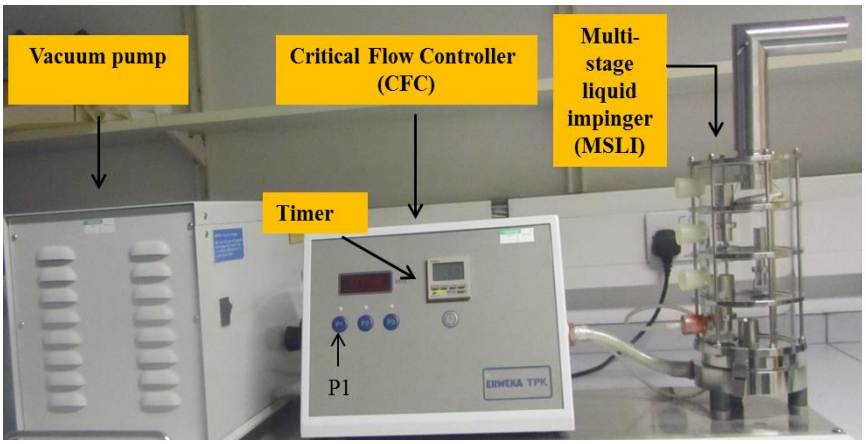

Figure 4.2. Picture of the particle sizing apparatus units (Cascade Impaction).

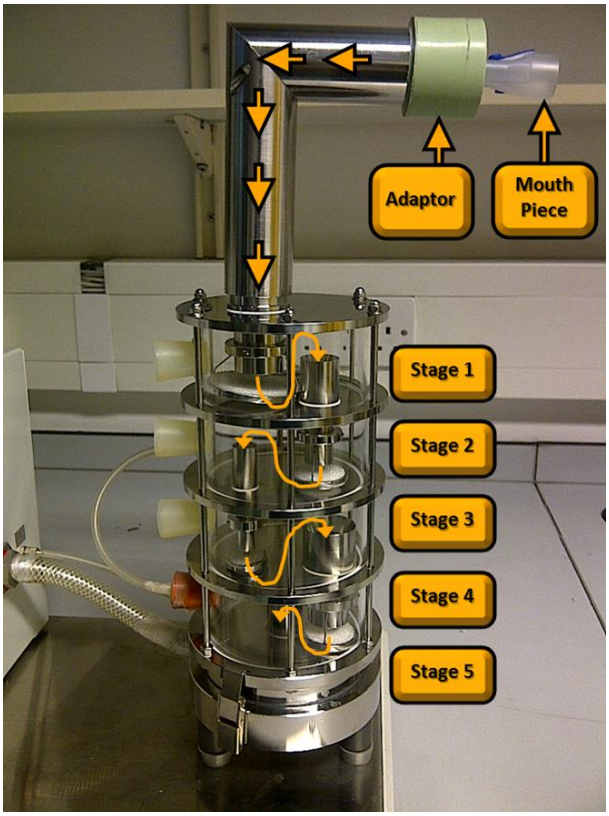

Figure 4.3. Picture of the Multi stage liquid impinger (MSLI), arrows show the flow of nebulisation fluid into stages: from stage 1 to 5.

4.2.4.3.2. Determination of the Mass Median Aerodynamic Diameter (MMAD) of LMS-611.

Calculation of the mass median aerodynamic diameter (*MMAD*) and the geometric standard deviation (GSD) was made from the log-probability plot for cumulative % frequency undersize versus particle size, as described by Martin (Martin *et al.*, 1983). GSD is a measure of the spread of the particle sizes measured by cascade impaction.

The mass of LMS-611 on each stage was determined by UV spectrophotometry, measuring the absorbance of a particulate liquid at 550 and 600 nm (all results are with reference to these two wavelengths).

4.2.4.4. Particle size and zeta potential measurements

LMS-611 particle size and the zeta potential were measured using a Malvern Zetasizer Nano-ZS (Malvern Instruments, Malvern, United Kingdom) at 25°C, using water as the dispersant.

4.2.5. Transmission electron microscopy (TEM)

10 µL of sample was dropped onto the surface of a Formvar/carbon coated 300 mesh grid and allowed to settle for 30 s. The excess sample was then removed and the sample was stained with 10 µLmethylamine vanadate negative stain (NanoVan®, Nanoprobes, Universal Biologicals, Cambridge, Ltd.), the sample left to dry before imaging.

The following LMS-611 samples were prepared for TEM:

1- LMS-611, neat (as supplied)

2- The supernatant of neat LMS-611 following centrifugation at 10,000 × *g*.

3- LMS-611 diluted with 0.9% saline 1:10

4- LMS-611 diluted with 0.9% saline 1:100

5- LMS-611 diluted with 200 mmol (1.2%) saline 1:10.

4.2.6. Determination of LMS-611 activity against bacteria

LMS-611 was tested for inhibition of *P. aeruginosa* growth in the context of a plaque assay by mixing with *P. aeruginosa* bacterial culture in 'top' agar. LMS-611 was added in 3 concentrations: neat (without dilution), dilution with 0.9% w/v NaCl ('saline' hereafter) 1 to 10 (100 µL LMS-611 + 900 µL saline) and dilution with saline 1 to 100 (10 µL LMS-611 + 990 µL saline). 100 µL of each concentration was mixed with 100 µL of overnight *P. aeruginosa* bacterial culture and added to partially cooled LB agar (0.75%, 'top' agar) which was poured onto a 1.5% agar plate and kept at 37 ºC for 18 h.

4.2.7. Formulation of LMS-611 with colistin for absorbance measurement

30 mg of colistin sulphate powder was dissolved in 0.5 mL saline and mixed with 2.5 mL of LMS-611. The mixture was centrifuged for 30 min at 13,000 × *g* and 100 µL supernatant diluted with 900 µL saline. The absorbance was measured at 230 nm by UV spectrophotometer, first generating a calibration curve of concentration versus absorbance using serial dilutions of a 1 mg/mL stock saline ranging from 100 µg/mL to 800 µg/mL.

4.2.8. Formulation of bacteriophage and/ or antibiotics into LMS-611 and characterisation of these formulations.

Saline (control), bacteriophage and/ or antibiotic (colistin, tobramyin) was diluted 1:6 into LMS-611 and nebulized using either a Pari Boy or eFlow nebulizer (PARI GmbH). The concentration of the phage stock solution used was 8.5 x 10^9 pfu/mL. By adding 0.5 mL of phage stock to 2.5 mL saline, the phage concentration was diluted to 1.4 x 10^9 pfu/mL. Formulations were prepared as outlined in table 4.2.

Table 4.2. Composition of the nebulised formulations used.

Formulation	Phage (mL)	Antibiotic (mL)	Saline (mL)	LMS-611 (mL)
Phage/LMS-611	0.5	−	−	2.5
[a] Control	0.5	−	2.5	−
Anibiotic/LMS-611	−	0.5	−	2.5
[b] Control	−	0.5	2.5	−
Phage/antibiotic/LMS-611	0.25	0.25	−	2.5

[a], control sample used for phage formulations; [b], control sample used for the antibiotic formulations.

4.2.8.1. Measurement of the lytic activity of bacteriophage in the LMS-611 fractions collected from each stage of the MSLI.

Following nebulisation, the lytic activity of bacteriophage from each stage of the MSLI was examined by plaque assay method (Plaque assay method as described in chapter 2 section 2.2.3.2.2)

4.2.8.2. Measurement of antibiotic concentration in the LMS-611 fractions collected from each stage of the MSLI (Disc inhibition method)

The antibiotic concentration from each stage of the MSLI was determined indirectly by inhibition of *P. aeruginosa* growth using disc inhibition method.

4.2.8.2.1. Disc inhibition method

Plates were poured to a depth of 4 mm with Mueller Hinton agar. After drying, an inoculum in sterile saline from colonies was made and diluted with an equal volume of saline (to read between 0.16 and 0.20 at 600 nm). 200 µL of culture was pipetted onto the plates and spread evenly with an L shaped spreader. Once the plates were dry the discs were attached and a 10 µL of formulation was added to each disc. The plates were incubated at 37 °C and the halo diameter was measured after 20 h.

4.2.9. Fluorescence labeling of BSA and LMS-611

A 2 mg/mL solution of BSA in 0.1 M $NaHCO_3$ (pH 9) was prepared. 1 mg of fluorescein isothiocyanate powder (FITC) was dissolved in 1 mL of dimethylsulphoxide. For each 1 mL of protein solution, 50 µL of FITC solution was added very slowly in 5 µLaliquots while gently stirring. The resulting solution was dialyzed extensively in phosphate buffer saline, pH 7.4, (PBS) by 3 × exchange over 24 h, using a cellulose dialysis bag with a MW cut-off of 12,400 Daltons (D9777, Sigma-Aldrich, UK). Rhodamine–doped LMS-611 was prepared in the same manner as above, by partition of the hydrophobic rhodamine dye into the LMS-611 from the aqueous media, rather than covalent conjugation as in the case of BSA-FITC.

4.2.10. Formulation of labelled LMS-611 with bovine serum albumin (BSA).

LMS-611 labelled with rhodamine and BSA-fluorescein were mixed 1:1 vol. equiv. and stirred gently for 1 h before centrifugation at 10,000 × *g* for 15 min. The pellets were collected and reconstituted in 1 mL PBS. The samples were measured by fluorescence spectroscopy using excitation wavelengths of 490 and 540 nm, corresponding to the excitation maxima of fluorescein and rhodamine, respectively.

4.2.11. Preparation of LMS-611-PEG formulations for determination of particle size

PEG 10000 was used in this study, 20% w/v PEG solution was prepared by dissolving 20 g of PEG in 100 mL distilled water. This solution was used as the stock solution for the preparation of different concentrations (10%, 5% and 2%). Samples were prepared as follow:

a- Mixture of 1 mL LMS-611 + 100 µL of PEG solution.

b- Control sample which was prepared by adding 100 µL saline to 1 mL LMS-611.

c- Mixture of 1 mL LMS-611 + 100 µL PEG centrifuged at 10,000 rpm for 15 min then the pellets were reconstituted with 1 mL of saline.

d- Mixture of 1 mL LMS-611 + 100 µL PEG centrifuged at 10,000 rpm for 15 min then the pellets were reconstituted with 1 mL phosphate buffer.

e- LMS-611 / PEG mixture diluted with saline 1:10.

f- LMS-611 diluted with saline 1:10 (control).

4.2.12. Particle size and zeta potential measurements of LMS-611-PEG formulations

LMS-611-PEG formulations were sized by laser diffractometry using a Mastersizer 2000 (Malvern Instruments Ltd., UK). Samples were dispersed in 100 mL saline and the mean diameter and standard deviation were measured (values are given as the average of two measurements). LMS-611 particle size and zeta potential were also measured using a Nano-ZS (Malvern Instruments) at 25 °C, using water as the dispersant.

4.2.13. Confocal laser scanning microscopy (CLSM)

Fluorescently labeled samples for CLSM were prepared as described in section 4.2.10, yielding the following samples for imaging:

1, LMS-611-rhodamine pellet undiluted, and LMS-611-rhodamine pellet reconstituted in PBS.

2, LMS-611-rhodamine/BSA-FITC pellet undiluted, and LMS-611-rhodamine/BSA-FITC pellet reconstituted in PBS.

3, LMS-611-rhodamine/BSA-FITC pellet reconstituted in 3 % w/v PEG 10000 solution.

For each sample a drop of 40 µL was placed onto a clean glass slide and covered with a cover slip. Samples were analyzed and imaged on a Leica DM 6000B microscope. The fluorescein conjugates were excited with an Argon laser line at 488 nm with an emission bandwidth of 557-624 nm. Scans were performed using 10×

and 20× objectives and images were converted with Volocity® software (Improvision, PerkinElmer, Cambridge, UK).

4.2.14. Rheology studies

4.2.14.1. Preparation of artificial mucus (AM)

Fifty milliliters of AM was prepared by dissolving 500 mg of DNA in 32.5 mL DNase-free water, complemented with 250 µL of egg yolk emulsion. Separately, 250 mg mucin (mucin from porcine stomach type II) was dissolved in 5 mL water, and 0.295 mg diethylenetriaminepentaacetate (DTPA), 250 mg NaCl, 110 mg KCl, 12.5 mg amino acids dissolved in 12.5 mL water. The three solutions were then mixed, and the pH of the AM was adjusted to 7.0 using NaOH solution (Yang, 2010).

4.2.14.2. Preparation of formulations for rheological studies

Samples were prepared by adding and mixing LMS-611with AM solution in different LMS-611 to AM ratios (1:100, 1:50, 1:20, 1:10, 1:5 and 1:2) and samples were incubated for 30 min at 37 °C. Equal volumes of saline were added to AM as control samples and also incubated at the same temperature for the same length of time. The viscosity of all samples was tested and each formulation was analysed in triplicate.

4.2.14.3. Rheological analysis of artificial mucus

The effect of LMS-611 on the apparent viscosities of the artificial mucus (AM) was performed using a Carrimed CSL2 100 controlled stress rheometer (TA Instruments, Dorking, UK), equipped with a 4 cm steel plate geometry with a fixed gap of 57

microns under controlled shearing stresses at physiological conditions (37±0.1°C and pH 7). The samples were spooned onto the Peltier plate and the cone lowered to the fixed gap of 57 microns. Excess sample was trimmed from the edge of the cone by a flat edged spatula to avoid sample overloading. The samples were allowed to condition and equilibrate for 180 s and flow data was generated with maximum shear rates of 200 s^{-1} and 1000 s^{-1}.

4.3. Results

4.3.1. LMS-611 calibration curves

High dilutions of LMS-611 in saline were required before the optical density came with the range corresponding to the Beer Lambert Law (i.e. AU < 1). At these dilutions, a linear relationship between LMS-611 dilution and absorbance was found (Figure 1). Therefore, these calibration curves could be used to quantify the amount of LMS-611 at each stage of the MSLI. The measurement of optical density of the LMS-611 dispersion could be made at either 550 or 600 nm, since both yielded a linear relationship over the range of LMS-611 concentrations measured. Therefore, quantification of LMS-611 following nebulisation is given using both wavelengths.

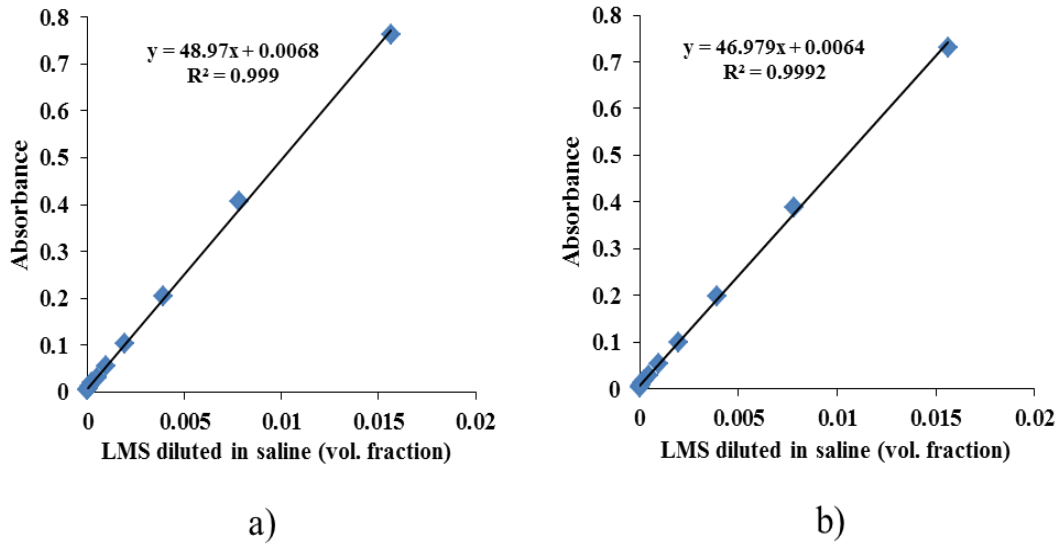

Figure 4.4. Calibration curves for LMS-611 measured using UV spectroscopy at a) 550 nm and b) 600 nm.

4.3.2. Determination of the Mass Median Aerodynamic Diameter (MMAD) of LMS-611.

The probability of the cumulative percentage of mass less than the stated particle size was plotted against the log of the aerodynamic diameter (µm) and a line of best fit was drawn. The mean cumulative percentages of mass less than stated size in each stage are shown in Table 4.3. No mass was observed on the pre-stage (throat and mouthpiece) and stage one. The MMAD was estimated from the value of aerodynamic diameter at the 50% cumulative percentage less than the stated particle size, shown in Table 4.4. The corresponding Geometric Standard Deviation (GSD) for each determined MMAD value was calculated by equation (1) (Figure 4.6).

$$Geometric\ standard\ deviation\ (GSD) = \frac{50\ \%\ size}{16\ \%\ undersize} \qquad \textbf{Eqn.1}$$

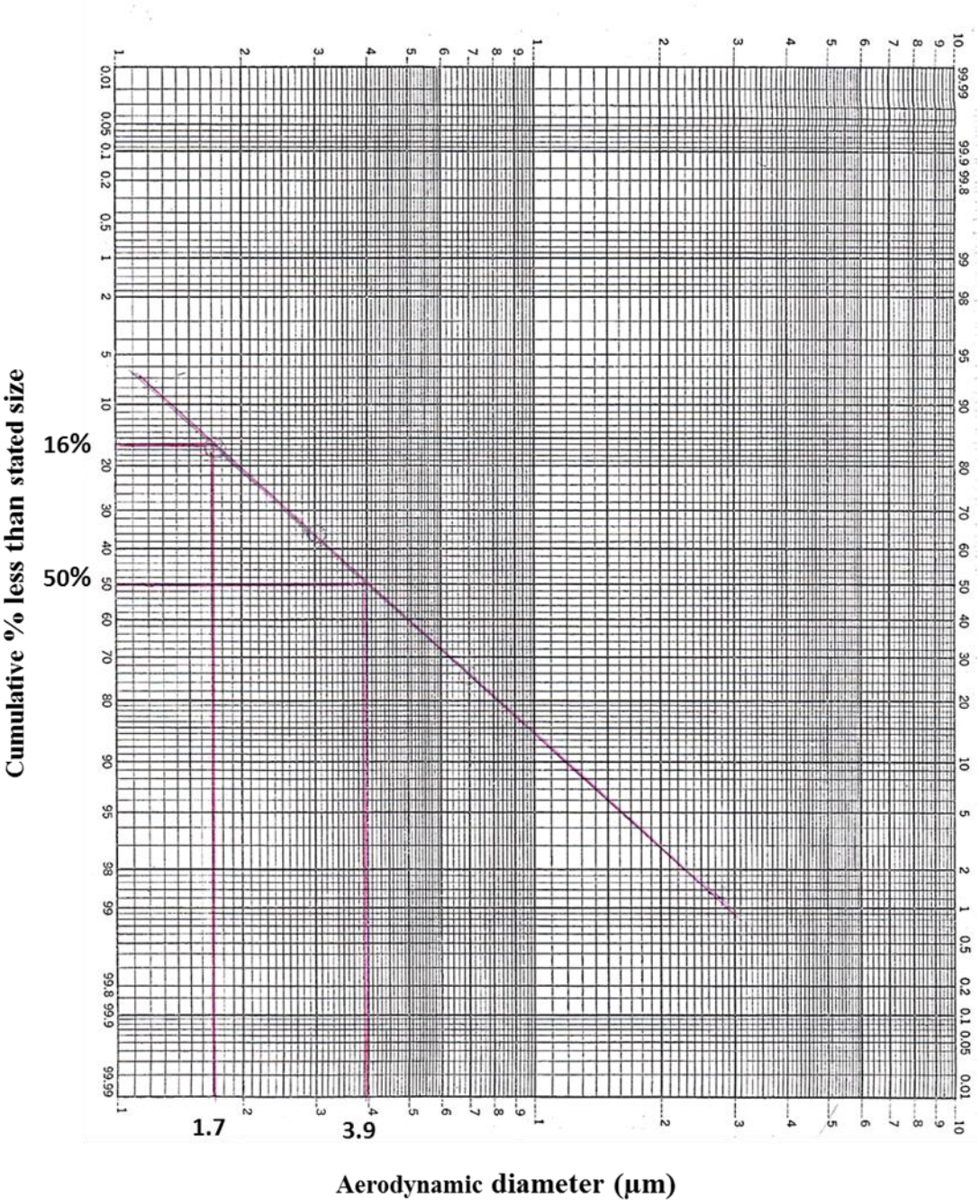

Figure 4.5. Example of Log probability graph plot for calculation of MMAD and GSD values.

Table 4.3. Mean cumulative percentage of LMS-611 mass less than stated size for each stage of the MSLI.

Stage	Size (µm)	eFlow nebuliser		Pari Boy nebuliser	
		λ 550	**λ 600**	**λ 550**	**λ 600**
Stage 2	< 13.0	100 ± 0.00	100 ± 0.00	100 ± 0.00	100 ± 0.00
Stage 3	< 6.8	85.81 ± 1.77	85.70 ± 1.77	73.23 ± 1.92	72.83 ± 2.15
Stage 4	< 3.1	45.34 ± 1.93	45.22 ± 2.09	32.91 ± 1.91	32.67 ± 2.08
Stage 5	< 1.7	17.91 ± 5.81	18.58 ± 6.36	16.61 ± 1.79	17.12 ± 1.92

Table 4.4. Determined MMAD and GSD of LMS-611 nebulised by the Pari Boy and eFlow nebulisers.

Nebuliser Type	eFlow nebuliser				Pari Boy nebuliser			
Wave-length (nm)	λ 550		λ 600		λ 550		λ 600	
	MMAD (µm)	GSD	MMAD (µm)	GSD	MMAD (µm)	GSD	MMAD (µm)	GSD
Exp 1	3.1	2.21	3	2.3	4.2	2.62	4.1	2.73
Exp 2	3.4	1.88	3.3	1.83	4.2	2.33	4.3	2.38
Exp 3	3.5	2.00	3.5	2.05	3.9	2.29	3.9	2.51
Mean ± (SD)	3.3^{a} ± 0.21	2.03^{b} ± 0.16	3.26^{c} ±0.25	2.06^{d} ±0.23	4.1^{a} ± 0.17	2.41^{b} ± 0.18	4.1^{c} ± 0.2	2.54^{d} ±0.17

P values for statistical comparison of two groups using a two-tailed non-paired T-test were as follows: a = 0.01, b = 0.05, c = 0.01, d = 0.05.

Table 4.5. MMAD and GSD of diluted LMS-611 with saline 1:10 (v/v).

eFlow nebuliser				**Pari Boy nebuliser**			
λ 550		**λ 600**		**λ 550**		**λ600**	
MMAD (µm)	GSD	MMAD (µm)	GSD	MMAD (µm)	GSD	MMAD (µm)	GSD
3.9	1.9	3.9	1.9	4.5	2.25	4.5	2.25

From Table 4.4 statistical analysis shows significant differences ($P \leq 0.05$) between the MMAD and GSD of all LMS-611 aerosols generated by nebulisation from the Pari Boy and eFlow. The Pari Boy nebuliser produced larger aerosols, with a larger GSD, than the eFlow nebuliser. However, the physiological significance is not clear since the determined MMAD values for both nebulisers should still predict aerosol deposition in the lung periphery. This different MMAD values are presumably related to the relative efficiencies of the different mechanisms of nebulisation of the two devices, though there are other considerations such as the type of spacer device and electrostatic charge on the inner surfaces. Dilution of LMS-611 1:10 with saline caused a slight increase in aerosol diameter for both nebulisers (Table 4.5), but again, the determined MMAD in both cases predicts deposition in the lung periphery. There was no significant difference in optical density measurements at 550 or 600 nm.

4.3.3. Evaluation of bacteriophage lytic activity in each stage.

By performing test to determine LMS-611 activity against *P. aeruginosa*, no inhibitory effect on *P. aeruginosa* growth was observed upon co-dilution of LMS-611 with *P. aeruginosa* into top agar. These results usefully allow the bacteriophage plaque assay to proceed without interference from any potential effect on account of the LMS-611 itself.

The results of the plaque assays show that the phage delivered in the aerosols were concentrated in stages 3 and 4 for eFlow nebuliser (Table 4.7) and stages 2, 3 and 4 for the Pari Boy nebuliser (Table 4.8), corresponding to the respective MMADs. The results show the distribution of phage at each stage was different when using the Pari Boy and eFlow nebulisers, particularly stage 1, where no phage was measured with the Pari Boy. There was no significant difference between the phage titre for the sample contains LMS-611 + phage and control sample that contains saline + phage.

Table 4.6. Calculated phage (ϕ) titre for each stage of the MSLI following nebulisation with the eFlow nebuliser.

Stage	**(Titre ± SD) pfu/mL**	
	LMS-611 2.5mL + ϕ 0.5mL	**Saline 2.5 mL + ϕ 0.5 mL**
Pre*	$(2.23 \pm 0.53) \times 10^{7}$	$(6.33 \pm 0.15) \times 10^{6}$
Stage 1	$(1.07 \pm 0.25) \times 10^{7}$	$(1.02 \pm 0.40) \times 10^{6}$
Stage 2	$(9.03 \pm 1.0) \times 10^{7}$	$(1.05 \pm 0.13) \times 10^{8}$
Stage 3	$(2.02 \pm 0.41) \times 10^{8}$	$(2.97 \pm 0.57) \times 10^{8}$
Stage 4	$(1.91 \pm 0.1) \times 10^{8}$	$(3.90 \pm 0.17) \times 10^{8}$
Stage 5	$(4.8 \pm 0.26) \times 10^{7}$	$(1.15 \pm 0.05) \times 10^{8}$

* mouth-piece and the throat; the titre of the solution for nebulisation was 1.4×10^{9} pfu/mL.

Table 4.7. Calculated Φ titre for each stage of the MSLI following nebulisation with the Pari Boy nebuliser.

Stage	**(Titre ± SD) pfu/mL**	
	LMS-611 2.5 mL+ Φ 0.5 mL	**Saline 2.5mL+ Φ 0.5mL**
Pre*	$(7.17 \pm 0.8) \times 10^7$	$(9.00 \pm 2.65) \times 10^6$
Stage 1	0.0	(0.0)
Stage 2	$(2.62 \pm 0.27) \times 10^8$	$(1.19 \pm 0.18) \times 10^8$
Stage 3	$(3.05 \pm 0.14) \times 10^8$	$(3.91 \pm 0.08) \times 10^8$
Stage 4	$(2.8 \pm 0.26) \times 10^8$	$(3.68 \pm 0.29) \times 10^8$
Stage 5	$(7.5 \pm 0.56) \times 10^7$	$(9.83 \pm 0.21) \times 10^7$

* mouth-piece and the throat; the titre of the solution for nebulisation was 1.4×10^9 pfu/mL.

4.3.4. Transmission electron microscopy (TEM)

Micrographs of the lamellarsomes in the LMS-611 preparation are representative of what is already known as regards their size, size distribution and arrangement of the lipid leaflets (Figure 4.6). Dilution of LMS-611 in saline did not appear to have significant effect on morphology, or size distribution. The micrographs suggest that LMS-611 is comprised of a heterogenous population of lamellarsomes composed of multiple lipid leaflets, distinct from multilamellar liposomes.

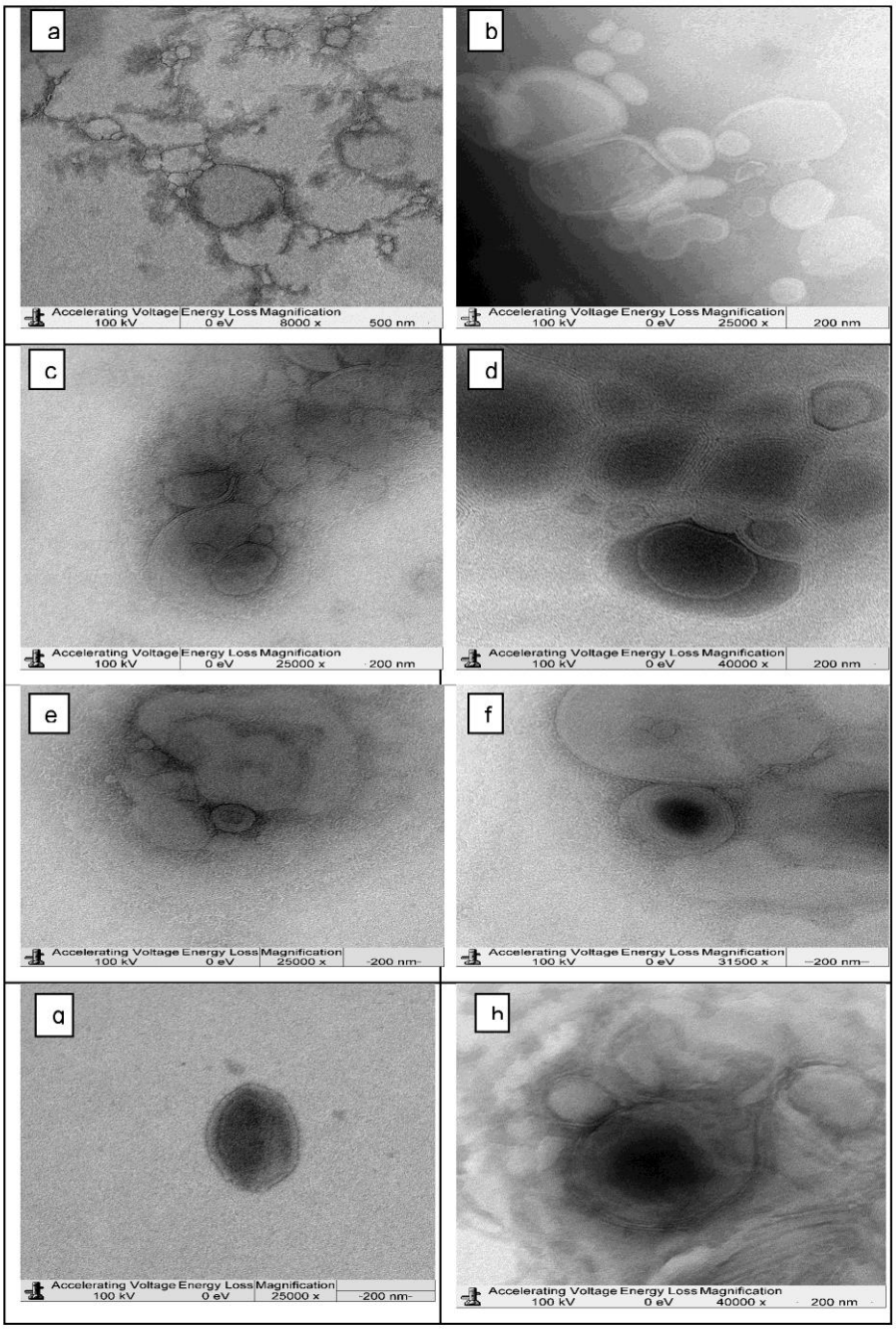

Figure 4.6. TEM of LMS-611; a and b show undiluted LMS-611 neat magnified at x8000 and x25000, respectively; c shows the undiluted supernatant of LMS-611 after centrifugation at 10,000 × *g*; d shows LMS-611 after 1:10 dilution with 1.2% saline; e and f show LMS-611 after 1:10 dilution with 0.9% saline; g and h show LMS-611 after 1:100 dilution with 0.9% saline. Scale bar bottom right corner of micrographs.

4.3.5. CLSM images

Imaging of the LMS-611 dispersed in aqueous media was confounded by movement of the individual lamellarsomes on the glass slide. However, a fraction of the material did appear to adhere to the glass surface and provided a chance to focus and image the sample. The rhodamine was clearly partitioned into the lipid lamella during the staining procedure (Figure 4.7), and while the larger lamellarsomes can be seen to be composed of more than one lipid leaflet (Figure 4.7B) the lower magnification of the CLSM (cf. the TEM) prevents detailed morphological analysis. The simple mixing of BSA-FITC into the LMS-611-rhodamine showed that there was no encapsulation of the BSA into the lamellarsomes and almost no partitioning of the BSA into the lipid leaflets (Figure 4.8). With respect to this latter, very occasional examples of yellow staining (suggesting overlap of green and red fluorescence of FITC and rhodamine, respectively) could be observed (Figure 4.8C). This would suggest loss of conformation of the globular BSA such that the lipid core of the protein may partition into the lipid leaflet. Further experiments, maybe using part/fully denatured BSA would be required to understand this better. It was not possible to use a molecular crowding agent (3% PEG 10000) to promote encapsulation of the BSA into the lamellarsomes, since no evidence of co-localisation of FITC and rhodamine stained material could be observed (Figure 4.9).

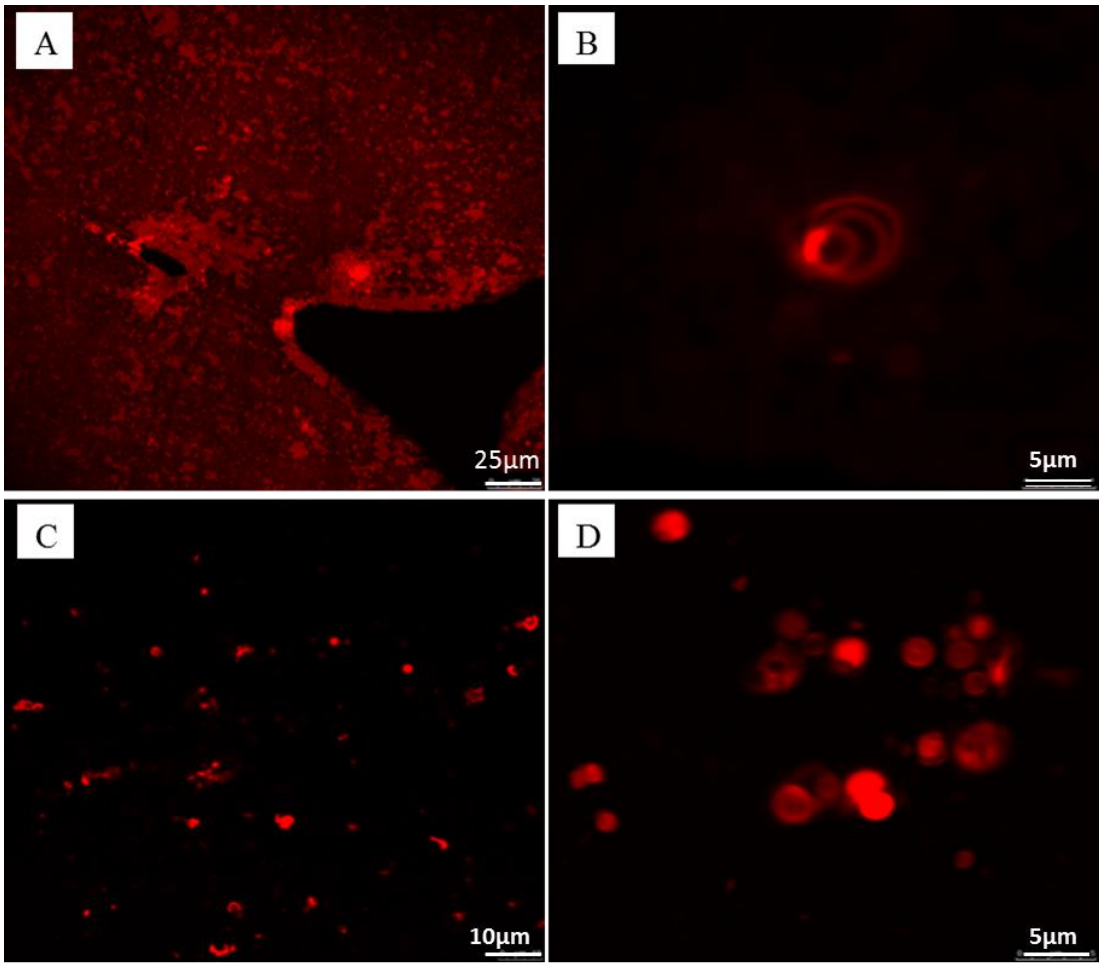

Figure 4.7. A and B show LMS-611-rhodamine pellet following centrifugation; C and D show LMS-611-rhodamine pellet diluted with PBS (scale bar bottom right corner).

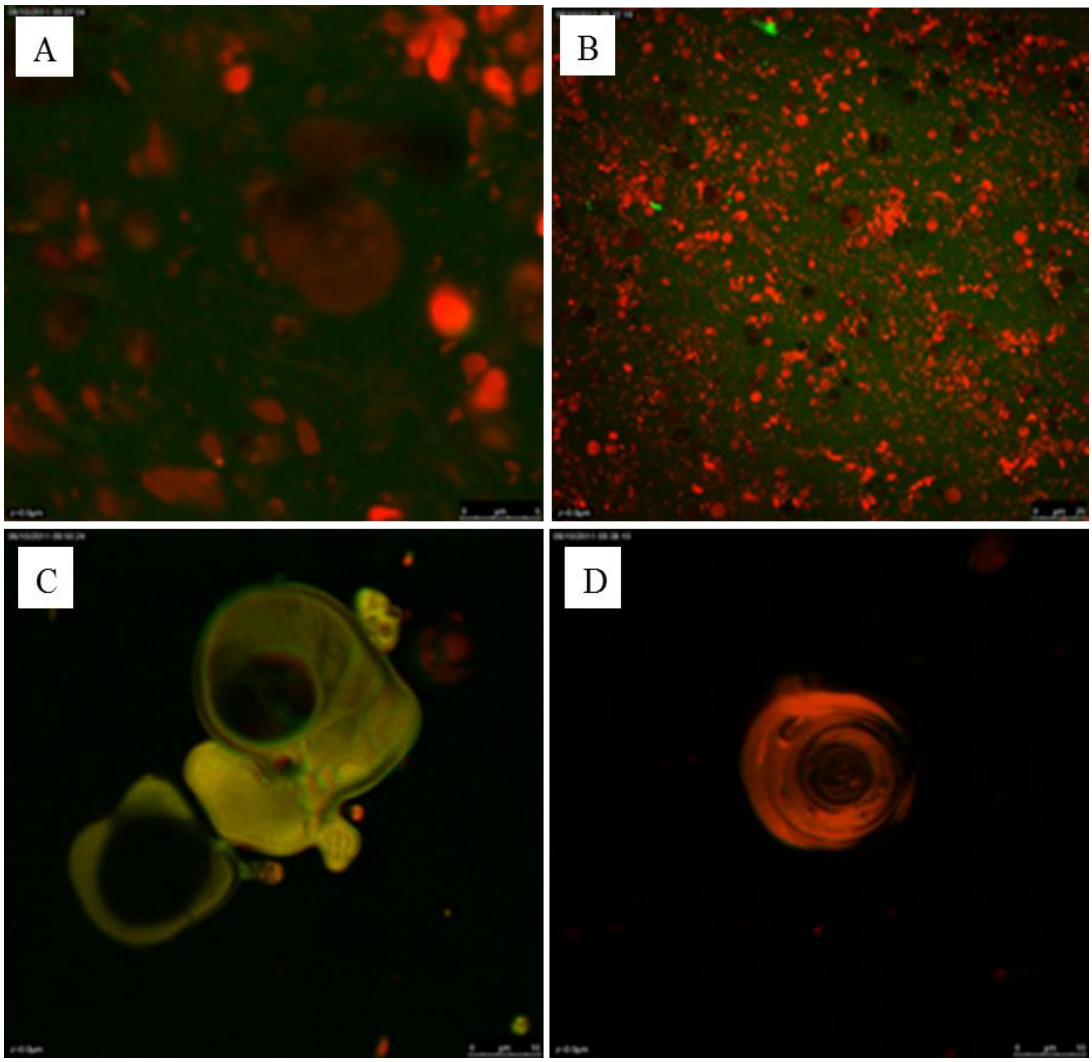

Figure 4.8. A and B show LMS-611-rhodamine/BSA-FITC pellet following centrifugation; C and D show LMS-611-rhodamine/BSA-FITC pellet diluted with PBS.

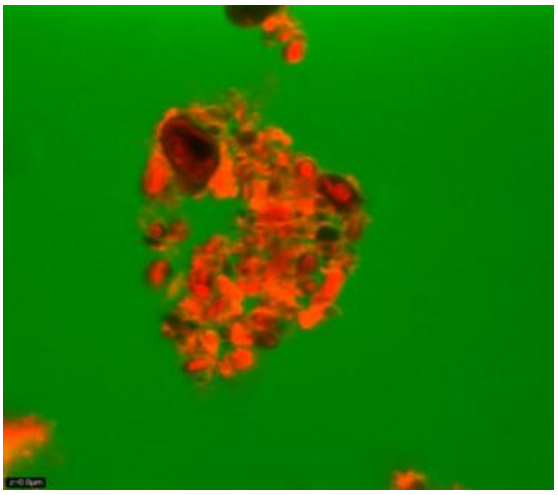

Figure 4.9. LMS-611-rhodamine/BSA-FITC pellet diluted with 3% w/v PEG 10000.

4.3.6. Fluorescence excitation and emission graphs of BSA-FITC and LMS-611-rhodamine

An alternative route to demonstrating co-localisation of BSA-FITC with LMS-611-rhodamine is to demonstrate FRET (fluorescence resonance energy transfer) in liquid samples. However, while the fluorescence emission spectrum of BSA-FITC was typical for such a solution, the emission spectrum of LMS-611-rhodamine was almost completely attenuated (Figure 4.10). This was most likely due to the large amount of light scatter that would be inevitable for a suspension as LMS-611. Further dilution of the LMS-611 did not minimise the light scatter sufficiently to permit analysis of FRET, with mixtures of the BSA-FITC/LMS-611-rhodamine suffering from the same problem.

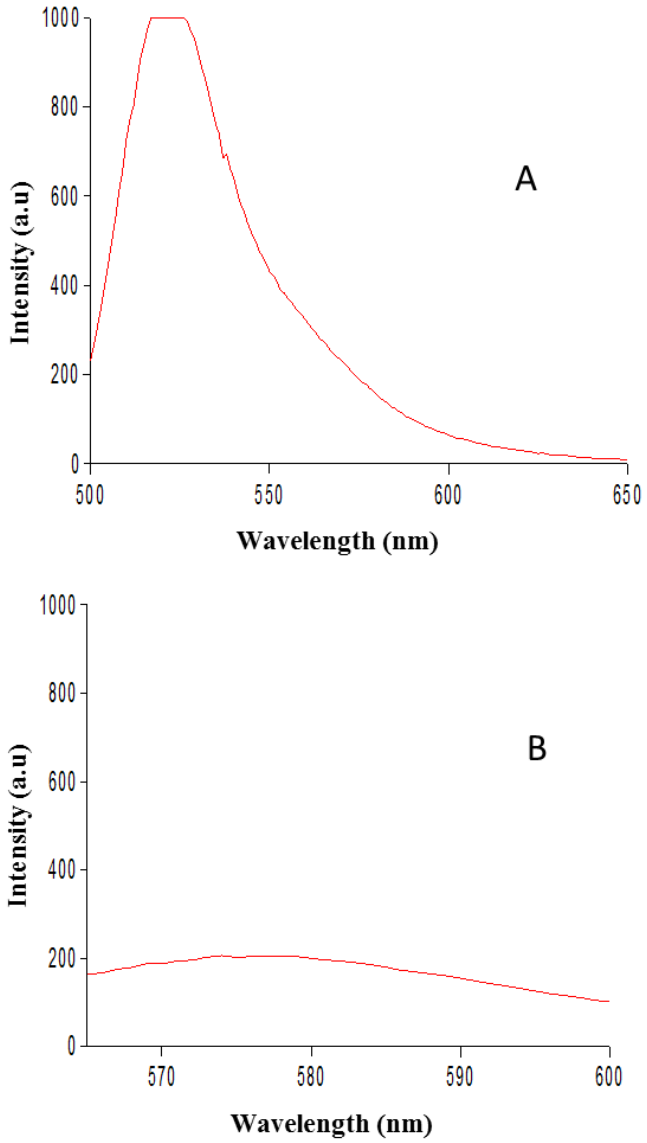

Figure 4.10. Emission spectrums of: A) BSA-FITC diluted in PBS 1:10 (λ_{ex} 490 nm) and B), LMS-611-rhodamine diluted in PBS 1:10 (λ_{ex} 540 nm).

4.3.7. Light scattering and zeta potential measurements.

The strongly negative zeta potential of LMS-611 reflects the phospholipid composition, and indicates a stable dispersion in the aqueous phase.

In 0.9% saline, the zeta potential of the LMS-611 particles was relatively small (-7 to -12 mV), irrespective of dilution and/or reconstitution in 1.8% saline (Table 4.8). In distilled water, the zeta potential was much higher since the ionic strength of the medium was very low (theoretically zero). With respect to formulation, it is generally considered that a zeta potential approaching zero should be avoided since this may otherwise lead to flocculation of the particulates. Evidence of aggregation should be relatively straightforward to determine using light scattering methods. However, measurements using the Nano-ZS were not particularly reliable since the polydispersity index was >> 0.1 and the size range was just beyond the upper limit of the Nano-ZS. A size range well above 1 µm was not predicted from the TEM images, which show lamellarsomes in the submicron range (Figure 4.7). Thus, while the size decreased for supernatant fractions from samples centrifuged at increasing *g*, the values themselves should be taken as indicative. It was therefore necessary to use the Mastersizer to measure particle diameter by light scatter, the problem here being that the sample size must be around 100 mL (cf. ~1 mL for the Nano-ZS), and this required 1:100 dilution of the LMS-611 to conserve sample. The Mastersezer 'small volume sample chamber' also uses a recirculation system, with high shear, and this may induce changes in size of a population of soft particles (such as lamellarsomes). Nevertheless, the results show that the average particle size for LMS-611 was around 6-7 µm, irrespective of dilution and/or resuspension in different buffers (saline or PBS) or PEG (Table 4.10). This size range approximates the indicative values measured by the Nano-ZS, being much larger than that predicted by TEM. It would therefore appear that a significant proportion of LMS-611 must include aggregated

lamellarsomes which form the suspension of lipid particulates observable to the naked eye.

Table 4.8. Particle size and zeta potential measurements.

Sample	**Dilution**	**Centrifugation (× *g*)**	**Mean Particle size (nm)[a]**	**Zeta-potential (mV)**
LMS-611 undiluted	-	-	3373	-7
LMS-611 undiluted	-	500	3060	-8
-	-	4000	2309	-10
-	-	10000	925	-9.5
LMS-611 / distilled water	1:10	-	6880	-34.5
LMS-611 / 0.9% saline	1:5	-	3200	-12.9
-	1:10	-	6600	-10.7
-	1:100	-	9200	-10.7
LMS-611 / 1.8% saline	1:5	-	2933	-7
-	1:10	-	5676	-7
-	1:100	-	8847	-7
LMS-611 / 5% saline	1:10	-	5000	-7
2.5 mL LMS-611 + 0.5 mL 0.9% saline [b]	5:6	-	3350	-7

[a], the high polydispersity index (>> 0.1) suggest that these readings are not robust – i.e. measurement of LMS-611 size must be made with the Mastersizer and not the Nano-ZS.
[b], to mimic the conditions used for nebulisation

Table 4.9. Particle size measurements of LMS-611-PEG formulations using the Mastersizer

Sample	PEG	diameter (µm)*
LMS-611	-	6.558
LMS-611 / PEG mixture[a]	2%	6.671
-	5%	6.652
-	10%	6.692
LMS-611 / saline (control) [b]	-	7.006
LMS-611 / PEG pellets reconstituted with 1 mL saline[c]	2%	6.428
-	5%	6.267
-	10%	6.206
-	20%	6.582
LMS-611 / PEG pellets reconstituted with 1mL phosphate buffer[d]	2%	6.156
	5%	6.227
-	10%	6.205
-	20%	6.191
LMS-611 / PEG diluted with saline 1:10[e]	2%	6.251
-	5%	6.635
-	10%	6.465
-	20%	6.529
LMS-611 diluted with saline 1:10 (control)[f]	-	9.460

*diameter value is the average of two readings, the difference between readings ≤ 0.54.

[a], mixture of 1mL LMS-611 + 100 µLPEG.

[b], 1mL LMS-611 + 100 µLsaline (control).

[c], the mixture of LMS-611 / PEG centrifuged at 10,000 rpm for 15 minutes then the pellets were reconstituted with 1 mL of saline.

[d], mixture of LMS-611 / PEG centrifuged at 10,000 rpm for 15 minutes then the pellets were reconstituted with 1 mL phosphate buffer.

[e], LMS-611 / PEG mixture diluted with saline 1:10.

[f], LMS-611 diluted with saline 1:10.

4.3.8. Determination of colistin concentrations in LMS-611

For the purposes of experiments which sought to determine the amount of antibiotic deposited at each stage of the MSLI following nebulisation, a method for measurement of colistin concentration was required. However, for antibiotics such as colistin (and others) there is no particular fingerprint wavelength which can be used which lies well away from 200-220 nm region, common to all organic compounds. The far UV region suffers from strong light scatter on account of the suspended LMS-611 particles (the same problem arose during fluorescence measurements, above), such that absorbance values acquired around this region cannot be delineated between light scatter and absorbance. Therefore, while it was possible to construct a calibration curve for colistin in saline (Figure 4.11), this needed to be repeated for colistin in LMS-611. Determination of colistin (and other antibiotic) concentrations in LMS-611 aerosols was therefore made indirectly by measurement of the relative level of antibiotic activity.

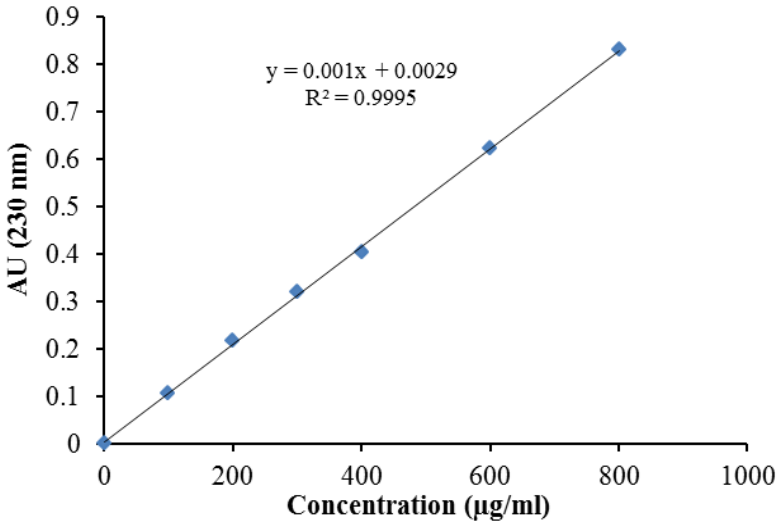

Figure 4.11. Colistin calibration curve.

Table 4.10. Particle size and zeta potential of (LMS-611/antibiotic) formulations

Sample	Mean particle size by DLS (µm)	Zeta potential (mV)
LMS-611 + Colistin	6.68	15
LMS-611 + Tobramycin	4.61	14

4.3.9. Determination of antibiotic and antibiotic/phage concentration in the LMS-611 fractions collected from each stage of the MSLI by disc inhibition method

Antibiotic activity against *P. aeruginosa* strains 217M and 39324 was examined indirectly by measuring the zone inhibition diameter resulted from the antibiotic in each plate (Figure 4.12). Therefore, antibiotic concentration in the LMS-611

fractions collected from each stage of the MSLI was calculated. Figures 4.13 and 4.14 show the antibiotic concentration (colistin and tobramycin) in the LMS-611 fractions collected from each stage of the MSLI using eFlow or Pari Boy nebulisers. For both nebulisers, dilution of colistin or tobramycin into LMS-611 increased the nebulized drug fraction deposited into the lung periphery (stages 2-5); compared with nebulization of the saline antibiotic solutions which were largely deposited in the 'throat' and upper airways (pre-stage and stage 1). This suggests that the surface activity of the LMS-611 facilitates the generation of smaller aerosol droplets during nebulization with the eFlow.

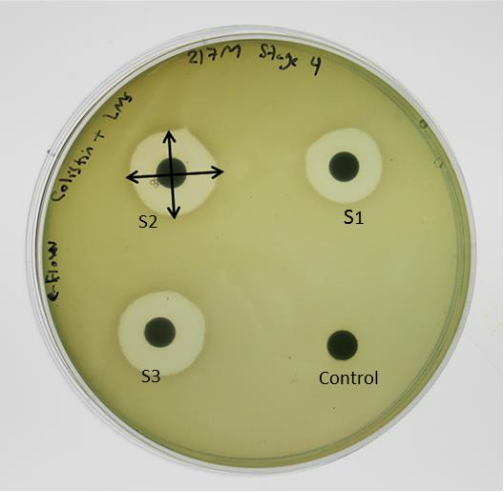

Figure 4.12. Zone diameter measurements using the disc inhibition method.

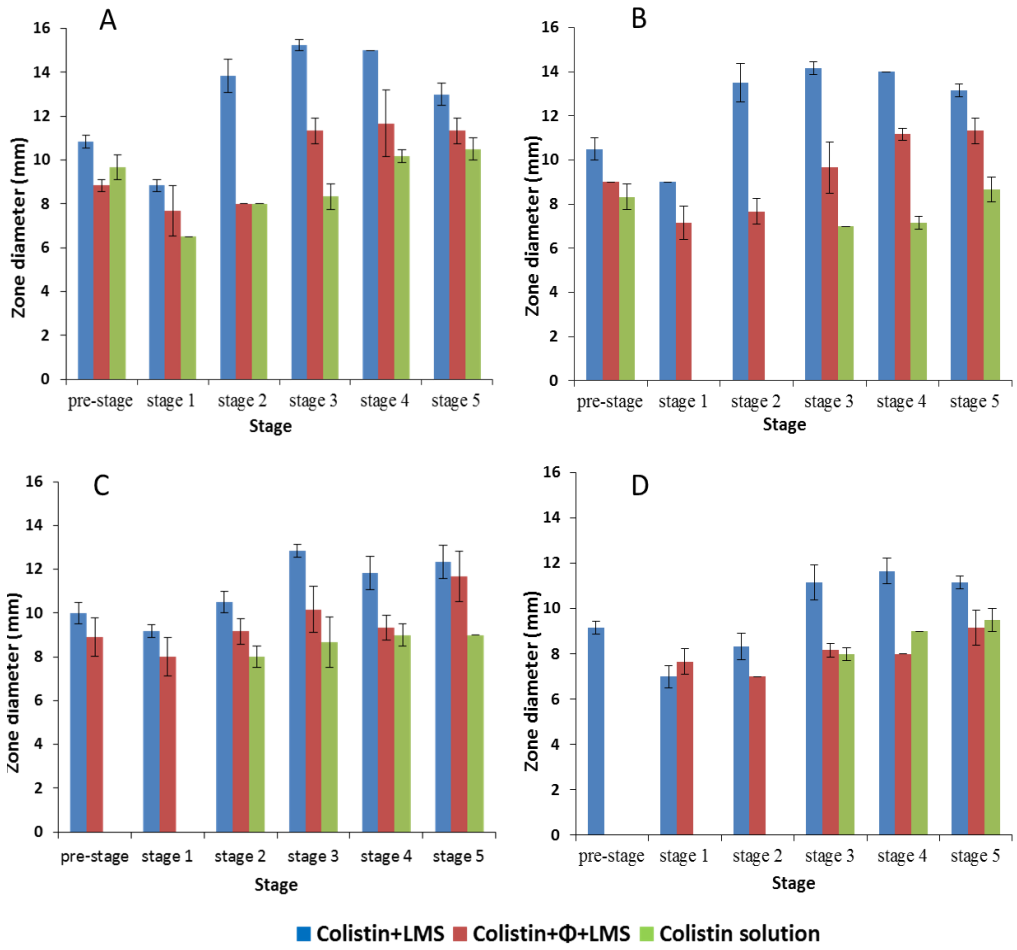

Figure 4.13. Inhibition zone diameters of colistin/LMS-611 formulations; A &B using eFlow nebuliser for *P. aeruginosa* strains 217M and 39324 respectively, C &D using Pari Boy nebuliser for *P.aeruginosa* strains 217M and 39324 respectively. The data shown as mean ± SD for n=3.

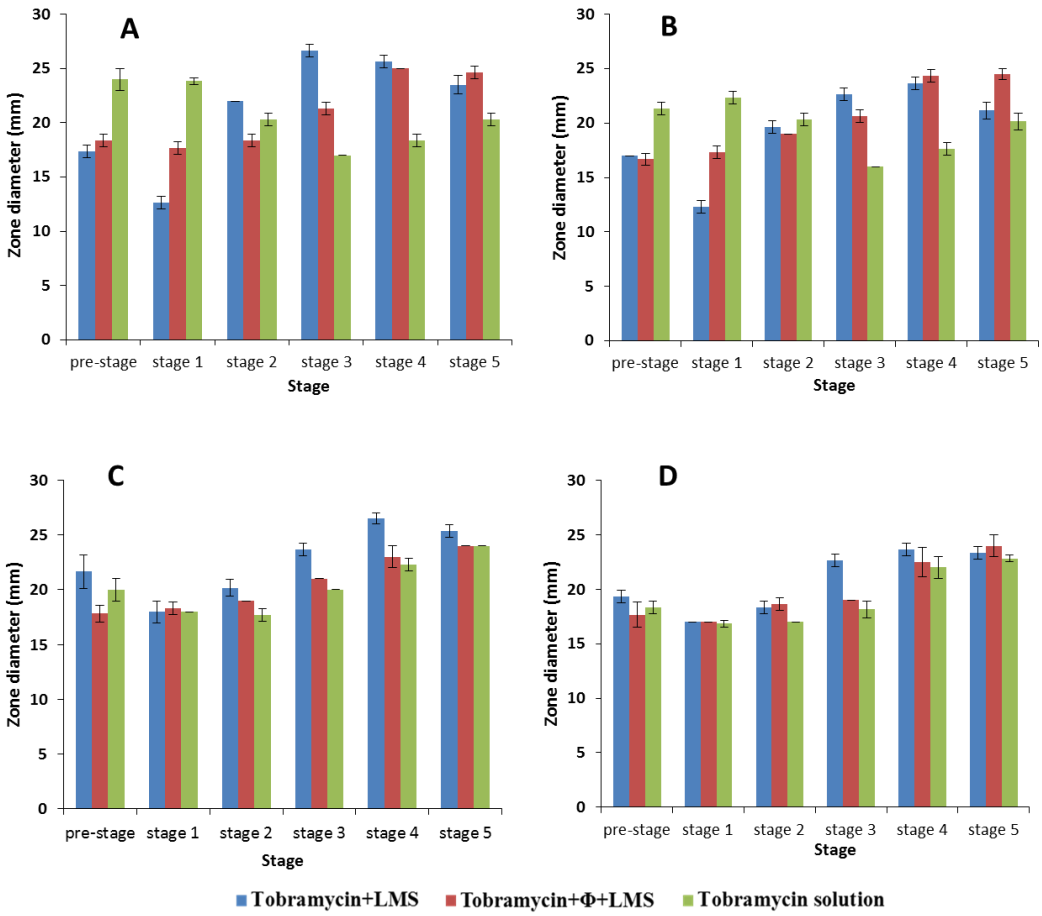

Figure 4.14. Inhibition zone diameters of Tobramycin/LMS-611 formulations; A & B using eFlow nebuliser for *P. aeruginosa* strains 217M and 39324 respectively, C & D using Pari Boy nebuliser for *P. aeruginosa* strains 217M and 39324 respectively. The data shown as mean ± SD for n=3.

4.3.10. Effect of LMS-611 on rheology of artificial mucus

Figures 4.15 and 4.16 show the effect of LMS-611 on the apparent viscosity of the AM measured at shear rates of 200 s^{-1} and 1000 s^{-1}, respectively. It can be seen from the results that the viscosity of mucus showed consistent variation with changes in the LMS-611/AM ratio: as the LMS-611 ratio in the formulation increased, the viscosity of mucus decreased. The analysis of control samples showed the same

results, which indicated that there was no apparent difference between LMS-611 and 0.9% saline regarding their effect on the extent of mucus viscosity.

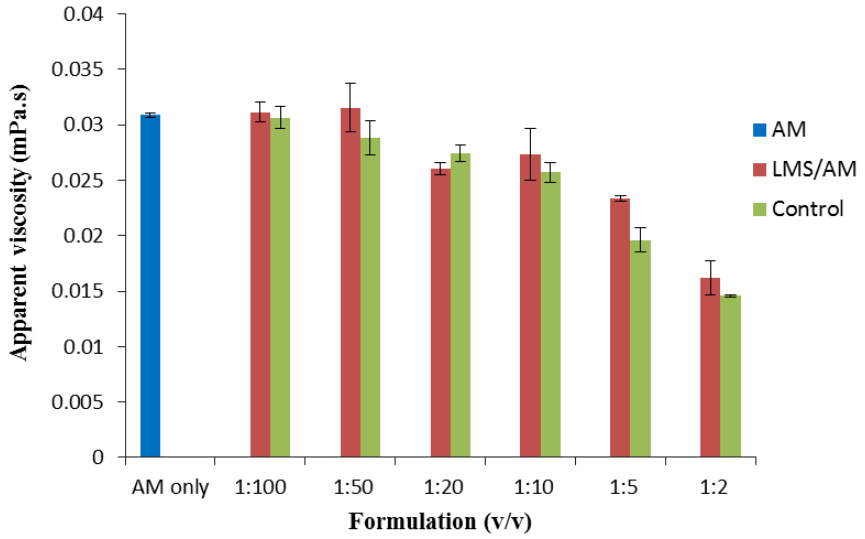

Figure 4.15. Effect of LMS-611 on the apparent viscosity of AM measured at 200 s^{-1}, Values reported as mean ± SD (n=3).

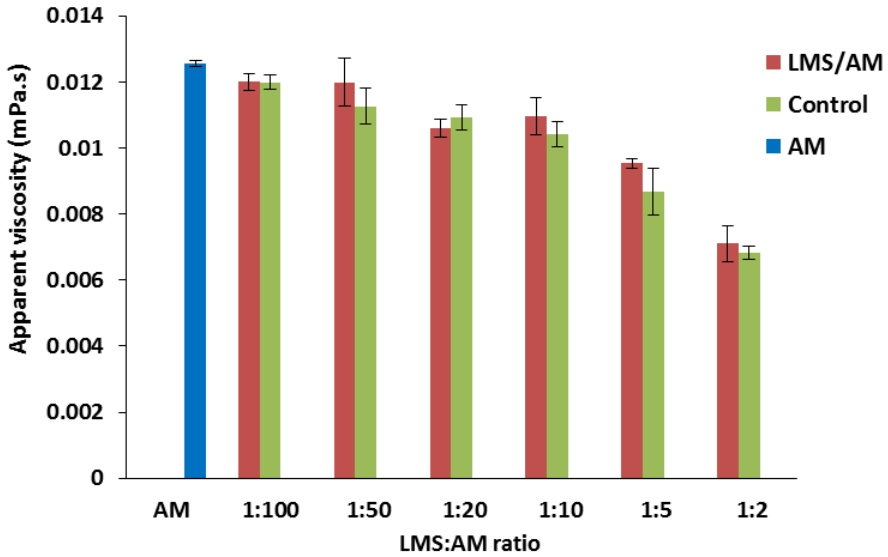

Figure 4.16. Effect of LMS-611 on the apparent viscosity of AM measured at 1000 s^{-1}, Values reported as mean ± SD (n=3).

4.4 Discussion

The physico-chemical properties of LMS-611 are suited to pulmonary delivery for the improvement of lung function. This is in part due to their inherent surface active and adsorptive properties which lead to the disruption of mucus, bacterial biofilms and sputum.

No inhibitory effect on *P. aeruginosa* growth was observed upon co-dilution of LMS-611 with *P. aeruginosa* into top agar. The absence of an anti-bacterial effect of LMS-611 in this assay is contrary to experiments for biofilms grown on glass plates or bacterial grown in planktonic form. The most likely reason is that the lamellarsomes are immobilised in an agar matrix, rather than dispersed in media. The results usefully allow the bacteriophage plaque assay to proceed without interference from any potential effect on account of the LMS-611 itself. The phage distribution data at each stage simply suggest that the phage were carried with the bulk fraction of the aerosols generated, rather than being selectively dispersed in larger or smaller aerosols, or causing a gross change in the aerosol size. The phage would most likely be dispersed in the aqueous media, existing as large hydrophilic macromolecular assemblies, rather than encapsulated within the lamellarsomes or embedded in the lipid layers. This observation can be related to the distribution of bacteriophage examined by CLSM which suggest that the phage were most likely dispersed in the aqueous media, rather than encapsulated within LMS-611. This is consistent with their large hydrophilic, macromolecular nature. The retained lytic activity of the phage is encouraging since it provides evidence that the phage have not been

denatured/inactivated following formulation with LMS-611 and subsequent nebulisation. The TEM images compare well with those acquired for the LMS-611 dispersed in aqueous media during CLSM imaging. Golshahi *et al.,* (2010) successfully developed dry powder inhaler dosage forms for bacteriophages, via lyophilisation, that were selective for *B. cepacia* complex and *P. aeroginosa*.

The standard therapy for *P. aeruginosa* respiratory infections is parenteral administration of anti-pseudomonal antibiotics. However, this route of administration gives poor penetration of the antibiotics into the endobronchial space (Hagerman *et al.,* 2007). Therefore, inhalation of aerosolised antibiotics enables delivery of high concentrations directly to the lungs with minimal systemic absorption and toxicity (Smith, 2002). The most commonly used aerosolised antibiotics are tobramycin and colistimethate sodium, which can be delivered twice daily for prolonged periods of time (Smith, 2002). It has been suggested that improvements in aerosol delivery systems have allowed shorter nebulisation times, which may improve patient compliance (Geller *et al.,* 2007) and there are a various commercially available nebulisers that have been tested as alternatives to administration of antibiotics such as tobramycin (Clavel *et al.,* 2007). The eFlow nebuliser is designed to deliver liquid or suspension formulations for inhalation more rapidly than jet nebulisers. In a study conducted by Lenney and co-workers (2011), comparing lung deposition of inhaled tobramycin via eFlow or Pari LC Plus jet nebulisation, it ws shown that the required nebulisation time was shorter for the eFlow than the LC Plus nebuliser (7 versus 20 min, respectively). However, while lung deposition in healthy subjects was comparable between both devices, in CF patients whole-lung deposition was ~40%

less with the eFlow rapid compared with the LC Plus nebuliser (8.9 versus 15.1%, respectively) (Lenney *et al.*, 2011).

In this study, two nebulisers were used and compared regarding drug deposition of the formulations. We further investigated the potential for co-formulation of antibiotics and bacteriophage by dispersion into LMS-611 and nebulization of aerosolized droplets. The results show that the antibiotics diluted into LMS-611 were predominantly deposited in stages 3-5 of the MSLI, compared to stages 1 and 2 when diluted in saline (control). The addition of LMS-611 to the antibiotic formulation shifts the deposition to the deep lung. This is particularly noticeable with the eFlow nebuliser and suggests that the surface activity of the LMS-611 facilitates the generation of smaller droplets via nebulisation, particularly nebulisation by membrane vibration (eFlow). Thus, adding LMS-611 to antibiotic solution for nebulisation means less drug is lost through impaction at the throat and upper airways. However, the addition of phage does not make a marked increase as regards bacterial kill.

Since mucus is a non-Newtonian fluid, rheological testing must be performed over a range of shear rates to give a profile of viscosity related to shear. From the viscosity data shown, it is evident that LMS-611 has an effect on the mucus viscosity. These rheological data provided an insight into the potential utility of LMS-611 as a vehicle to improve drug delivery to the airway or lung by enhancing their penetration. The results are comparable to a study conducted by Yang and co-workers for inhalable antibiotic delivery for treatment of cystic fibrosis using a dry powder. These workers

found that blank and Ciprofloxacin powder had no significant effect on the viscosity of artificial mucus, while by co-delivering of ciprofloxacin with DNase, the thick artificial mucus became a thin liquid in less than 30 min (Yang *et al.,* 2010).

Chapter 5: Conclusions and future work

5.1. Conclusions

Within this thesis, the potential of bacteriophage-loaded formulations as an alternative therapy for antibiotic resistant infections associated with MRSA or *P.aeruginosa* was explored.

Lyophilized nasal inserts harbouring bacteriophage were formulated because nasal decolonization offers an effective treatment strategy. The physical properties of the lyophilisates were measured by using suitable *in vitro* testing methods which can narrow down the most viable formulation for future studies. We concluded that lyophilized nasal inserts harbouring doses of bacteriophage, corresponding to doses used in previous clinical trials of bacteriophage therapy, can be formulated and remain stable in the fridge for up to 1 year. The addition of mannitol to the lyophilizate does not confer added stability to the bacteriophages and may be omitted if this was the sole consideration. However, given that lyophilization can be a costly step, formulations which dry to a defined percentage more rapidly may be preferred on these grounds, in which case the 1% HPMC/1% mannitol formulation would be preferred. Increasing the relative amount of HPMC in the blend with mannitol would appear to stabilize the amorphous form of mannitol in the lyophilizate, though transition of mannitol from its amorphous to crystalline form does not affect bacteriophage stability, the structure of the internal matrix, or the distribution of the bacteriophages with the matrix.

The phage-CMC formulation represents a new approach for bacteriophage bioprocessing and solid state formulation for the storage and transport of phage. The activity of the phage powders was found to depend on the type of amino acid carrier, the presence or absence of stabilizer, the organic solvent and the storage conditions. We have shown that the use of organic solvents for bioprocessing of phages is not necessarily harmful if the process is controlled, with careful selection of solvents, stabilizing additives and drying conditions. Although there are safety issues should be considered when handling large volumes of organic solvent, the practice is well established and controlled in many small molecule processes; one notable example being continuous process crystallization in the pharmaceutical industry. The phage-CMC process requires the addition of trehalose or BSA as stabilizer and drying under elevated humidities to accelerate the removal of organic solvent. Core carriers with high aqueous solubilities are required when isobutanol is used as the solvent, and other carriers such as inositol and potassium phosphate could be usefully compared against glycine. The stability of the immobilized phage decreased over time while storing the powders at room temperature or at 5 °C. Nevertheless, the lytic activity of the phage-CMC following one month storage at room temperature was comparable to doses of phage reported in the literature regarding therapeutic application in man. These results demonstrate a feasible approach for the storage and transport of phage in the solid state. It is expected that other groups aiming to bring phage therapies into mainstream Western medicine will be able to utilize the method reported here for various applications; such as rapid concentration and drying of phage stock solutions, and storage/ shipment of phages at room temperature. Further testing of

the process with other phage families would be useful since phage therapies are likely to require the use of multiple phage strains.

Lamellasome^{TM} was used in the study as a vehicle to provide stable and reliable carrier for the bacteriophages and antibiotic drugs due to its inherent surface active properties. We concluded that LMS has the potential to improve the pulmonary delivery of nebulized solutions of antibiotics or bacteriophage.

Visualisation of LMS formulations using other imaging techniques such as freeze fracture electron microscopy and magnetic resonance would be helpful to define the structure and lamellarity of the vesicles to use for further applications.

The efficiency of LMS reported here allows future work for designing other multilamellar vesicles as amphiphile-based delivery systems, either natural amphiphile using liposomes or synthetic polymeric amphiphilic membranes, to use for pulmonary delivery or for other purposes.

Further work such as *in vivo* studies could be performed with these aforementioned points taken into consideration.

5.2 Other opportunities for bacteriophage-loaded formulations

The emergence and spread of profoundly antibiotic resistant pathogens is well documented. MRSA has been known as a major source of antibiotic resistant infections in hospitals and in the community, that now needs to be treated by 'reserved' antibiotics. The European Centre for Disease Prevention & Control has collated data on the use of antibiotic doses consumed every year in the European

community. With data from 2010 (the latest year available) it shows that in the UK, every day, there are 18.7 doses of antibiotics for every 1,000 people (around 2 %). This fraction may appear reasonably high but in fact it is lower than other European countries: for instance, France, Greece and Spain have a higher frequency of antibiotic use since their health regulations allow the purchase of antibiotics as an 'over the counter' service.

Rates of MRSA have been dropping nationally as hospitals increased attention on infection control; however, the intensive and continuous use of broad-spectrum antibiotic therapy particularly cephalosporin and more recently quinolone has been implicated in incidence of *Clostridium difficile* infection, now the most common cause of hospital acquired diarrhoea (CDAD) (Meader *et al.,* 2010). *C. difficile* has become an important pathogen globally, and emergence is strongly correlated with antibiotic use: more than 90% of cases occur post-antibiotic treatment as the stable, healthy flora of the gut is destroyed. In a study of 28 hospitals in the Southeast of the USA, it was found that *C. difficile* was 25% more common than MRSA. Therefore, *C. difficile* appears to have overtaken the widely feared MRSA as the most common hospital-acquired infection.

Meader and co-workers recently reported that bacteriophage treatment significantly reduces viable *C. difficile* and prevents toxin production in an in vitro model system (Meader *et al.,* 2010).

This suggests another avenue for the use of treatment with bacteriophages to reduce bacterial infection. Moreover, prophylactic treatment with bacteriophage could

dramatically reduce the burden of infection without affecting patient's normal gut flora therefore avoiding secondary complications. Phage resistance is known but could be dealt with: cocktails of bacteriophage could be used against strains of resistant bacteria to reduce the possibility of developing resistance.

5.3. Would the community accept the use of bacteriophage as a treatment?

On the basis of public reaction to genetically modified proteins and their fear of the term 'virus', it would be expected that people would not readily accept the use of viruses as a treatment even if the treatment directed against bacteria. This psychological factor should not be a barrier. We must explain that viruses naturally exist in every ecological niche that bacteria are found including food, water and even within our bodies, existing in their bacterial host in the lower gut. Modern vaccines are attenuated live viruses but in the recent past, the MMR vaccine was rejected at the first hint of a potential problem, triggered by the media focus on poor research.

The possibilities of phage therapy has been realised in other diseases, where access to mucous membranes allows bacterial colonisation. Phage delivery to the vagina has been successfully developed to remove colonizing streptococci, the leading cause of neonatal meningitis and sepsis (Cheng 2005).

References

Ackermann, H.-W., Tremblay, D., & Moineau, S. (2004). Long-term bacteriophage preservation. *World Federation for Culture Collections Newsletter, 38*, 35-40.

Alexis, N. E., Muhlebach, M. S., Peden, D. B., & Noah, T. L. (2006). Attenuation of host defense function of lung phagocytes in young cystic fibrosis patients. *Journal of Cystic Fibrosis, 5*(1), 17-25.

Alfadhel, M., Puapermpoonsiri, U., Ford, S. J., McInnes, F. J., & van der Walle, C. F. (2011). Lyophilized inserts for nasal administration harboring bacteriophage selective for Staphylococcus aureus: In vitro evaluation. *International Journal of Pharmaceutics, 416*(1), 280-287.

Alisky, J., Iczkowski, K., Rapoport, A., & Troitsky, N. (1998). Bacteriophages show promise as antimicrobial agents. *Journal of Infection, 36*(1), 5-15.

Alur, H. H., Pather, S. I., Mitra, A. K., & Johnston, T. P. (1999). Transmucosal sustained-delivery of chlorpheniramine maleate in rabbits using a novel natural mucoadhesive gum as an excipient in buccal tablets. *International Journal of Pharmaceutics, 188*(1), 1-10.

Alvarez-Gonzalez, E., Alfadhel, M., Mane, P., Ford, S. J., Moore, B. D., & van der Walle, C. F. (2012). Bioprocessing of bacteriophages via rapid drying onto microcrystals. *Biotechnology Progress, 28*(2), 540-548.

Andersen, D. H. (1938). Cystic fibrosis of the pancreas and its relation to celiac diseasea clinical and pathologic study. *American Journal of Diseases of Children, 56*(2), 344-399.

Annan, W. S., Fairhead, M., Pereira, P., & van der Walle, C. F. (2006). Emulsifying performance of modular beta-sandwich proteins: the hydrophobic moment and conformational stability. *Protein Engineering, Design and Selection, 19*(12), 537-545.

Arora, P., Sharma, S., & Garg, S. (2002). Permeability issues in nasal drug delivery. *Drug Discovery Today, 7*(18), 967-975.

Bakaltcheva, I., O'Sullivan, A. M., Hmel, P., & Ogbu, H. (2007). Freeze-dried whole plasma: evaluating sucrose, trehalose, sorbitol, mannitol and glycine as stabilizers. *Thrombosis Research, 120*(1), 105-116.

Banerjee, D., & Stableforth, D. (2000). The treatment of respiratory pseudomonas infection in cystic fibrosis: what drug and which way? *Drugs, 60*(5), 1053-1064.

Battaglia, G., Tomas, S., & Ryan, A. J. (2007). Lamellarsomes: metastable polymeric multilamellar aggregates. *Soft Matter, 3*(4), 470-475.

Behl, C., Pimplaskar, H., Sileno, A., Xia, W., Gries, W., Demeireles, J., & Romeo, V. (1998). Optimization of systemic nasal drug delivery with pharmaceutical excipients. *Advanced Drug Delivery Reviews, 29*(1), 117-133.

Biswas, B., Adhya, S., Washart, P., Paul, B., Trostel, A. N., Powell, B., Merril, C. R. (2002). Bacteriophage therapy rescues mice bacteremic from a clinical isolate of vancomycin-resistant Enterococcus faecium. *Infection and Immunity, 70*(1), 204-210.

Bjarnsholt, T., Jensen, P., Fiandaca, M. J., Pedersen, J., Hansen, C. R., Andersen, C. B., Høiby, N. (2009). Pseudomonas aeruginosa biofilms in the respiratory tract of cystic fibrosis patients. *Pediatric Pulmonology, 44*(6), 547-558.

Bouissou, C., Begat, P., van der Walle, C., & Price, R. (2005). Study of the surface mobility of PLGA microspheres using high-resolution topography measurements with the atomic force microscope. *Journal of Controlled Release, 101*(1-3), 290-292.

Brange, J. (2000). Physical stability of proteins. *Pharmaceutical Formulation Development of Peptides and Proteins*, 89-112.

Breen, E. D., Curley, J. G., Overcashier, D. E., Hsu, C. C., & Shire, S. J. (2001). Effect of moisture on the stability of a lyophilized humanized monoclonal antibody formulation. *Pharmaceutical Research, 18*(9), 1345-1353.

Brown, M. R. (1991). The amino-acid and sugar composition of 16 species of microalgae used in mariculture. *Journal of Experimental Marine Biology and Ecology, 145*(1), 79-99.

Capparelli, R., Parlato, M., Borriello, G., Salvatore, P., & Iannelli, D. (2007). Experimental phage therapy against Staphylococcus aureus in mice. *Antimicrobial Agents and Chemotherapy, 51*(8), 2765-2773.

Cappuccino, J., & Sheman, N. (1996). Microbiology, a laboratory manual 4th edition, Benjamin/Cummings Pub. *Company, California, USA. pp*, 115-118.

Carlton, R. M., Noordman, W. H., Biswas, B., de Meester, E. D., & Loessner, M. J. (2005). Bacteriophage P100 for control of Listeria monocytogenes in foods: genome sequence, bioinformatic analyses, oral toxicity study, and application. *Regulatory Toxicology and Pharmacology, 43*(3), 301-312.

Chambers, H. F. (2001). The changing epidemiology of Staphylococcus aureus? *Emerging Infectious Disease, 7*(2), 178-182.

Cheer, S. M., Waugh, J., & Noble, S. (2003). Inhaled tobramycin (TOBI): a review of its use in the management of Pseudomonas aeruginosa infections in patients with cystic fibrosis. *Drugs, 63*(22), 2501-2520.

Cheng, P. W., Boat, T. F., Cranfill, K., Yankaskas, J. R., & Boucher, R. C. (1989). Increased sulfation of glycoconjugates by cultured nasal epithelial cells from patients with cystic fibrosis. *Journal of Clinical Investigation, 84*(1), 68-72.

Cheng, Q., Nelson, D., Zhu, S., & Fischetti, V. A. (2005). Removal of group B streptococci colonizing the vagina and oropharynx of mice with a bacteriophage lytic enzyme. *Antimicrob Agents Chemother, 49*(1), 111-117.

Clark, W. A., & Geary, D. (1973). Proceedings: Preservation of bacteriophages by freezing and freeze-drying. *Cryobiology, 10*(5), 351-360.

Clavel, A., Boulaméry, A., Bosdure, E., Luc, C., Lanteaume, A., Gorincour, G., Dubus, J. C. (2007). Nebulisers comparison with inhaled tobramycin in young children with cystic fibrosis. *Journal of Cystic Fibrosis, 6*(2), 137-143.

Clunes, L. A., Bridges, A., Alexis, N., & Tarran, R. (2008). In vivo versus in vitro airway surface liquid nicotine levels following cigarette smoke exposure. *Journal of Analytical Toxicology, 32*(3), 201-207.

Coelho, J., Woodford, N., Turton, J., & Livermore, D. (2004). Multiresistant acinetobacter in the UK: how big a threat? *Journal of Hospital Infection,*

58(3), 167-169.

Committee, J. F., & Britain, R. P. S. o. G. (2012a). *British national formulary (BNF)* (Vol. 64): Pharmaceutical Press.

Cookson, B. (1993). MRSA: Major problem or minor threat? *Journal of Medical Microbiology, 38*(5), 309-310.

Critchley, I. A. (2006). Eradication of MRSA nasal colonization as a strategy for infection prevention. *Drug Discovery Today: Therapeutic Strategies, 3*(2), 189-195.

Cromwell, M. E., Hilario, E., & Jacobson, F. (2006). Protein aggregation and bioprocessing. *The AAPS Journal, 8*(3), E572-E579.

Dabrowska, K., Switała-Jelen, K., Opolski, A., Weber-Dabrowska, B., & Gorski, A. (2005). Bacteriophage penetration in vertebrates. *Journal of Applied Microbiology, 98*(1), 7-13.

Deli, M. A. (2009). Potential use of tight junction modulators to reversibly open membranous barriers and improve drug delivery. *Biochimica et Biophysica Acta (BBA)-Biomembranes, 1788*(4), 892-910.

Deurenberg, R., Vink, C., Kalenic, S., Friedrich, A., Bruggeman, C., & Stobberingh, E. (2007). The molecular evolution of methicillin-resistant Staphylococcus aureus. *Clinical Microbiology and Infection, 13*(3), 222-235.

Dhakar, R. C., Maurya, S. D., Tilak, V. K., & Gupta, A. K. (2011). A review on factors affecting the design of nasal drug delivery system. *International Journal of Drug Delivery, 3*(2), 194-208.

Dodge, J., Lewis, P., Stanton, M., & Wilsher, J. (2007). Cystic fibrosis mortality and survival in the UK: 1947–2003. *European Respiratory Journal, 29*(3), 522-526.

Doelker, E. (1993). Cellulose derivatives *Biopolymers I* (pp. 199-265): Springer.

Dominak, L. M., Omiatek, D. M., Gundermann, E. L., Heien, M. L., & Keating, C. D. (2010). Polymeric crowding agents improve passive biomacromolecule encapsulation in lipid vesicles. *Langmuir, 26*(16), 13195-13200.

Douglas, J. (1975). *Bacteriophages*. London: Chapman and Hall.

Downey, D. G., Brockbank, S., Martin, S. L., Ennis, M., & Elborn, J. S. (2007). The effect of treatment of cystic fibrosis pulmonary exacerbations on airways and systemic inflammation. *Pediatric Pulmonology, 42*(8), 729-735

Drenkard, E., & Ausubel, F. M. (2002). Pseudomonas biofilm formation and antibiotic resistance are linked to phenotypic variation. *Nature, 416*(6882), 740-743.

Dyer, A., Hinchcliffe, M., Watts, P., Castile, J., Jabbal-Gill, I., Nankervis, R., Illum, L. (2002). Nasal delivery of insulin using novel chitosan based formulations: a comparative study in two animal models between simple chitosan formulations and chitosan nanoparticles. *Pharmaceutical Research, 19*(7), 998-1008.

Eggers, D. K., & Valentine, J. S. (2001). Crowding and hydration effects on protein conformation: a study with sol-gel encapsulated proteins. *Journal of Molecular Biology, 314*(4), 911-922.

Evans, M. E., Feola, D. J., & Rapp, R. P. (1999). Polymyxin B sulfate and colistin: old antibiotics for emerging multiresistant gram-negative bacteria. *The Annals of Pharmacotherapy, 33*(9), 960-967.

Ewan, S. (2004). Viral treatment for MRSA. *Drug discovery today, 9*(6), 249.

Fischetti, V. A., Nelson, D., & Schuch, R. (2006). Reinventing phage therapy: are the parts greater than the sum? *Nature Biotechnology, 24*(12), 1508-1511.

Franz, M., Cohn, R., Wachnowskydiakiw, D., & Spohn, W. (1994). Management of children and adults with cystic-fibrosis-one centers approach. *Hospital Formulary, 29*(5), 364-&.

Frederiksen, B., Pressler, T., Hansen, A., Koch, C., & Høiby, N. (2006). Effect of aerosolized rhDNase (Pulmozyme®) on pulmonary colonization in patients with cystic fibrosis. *Acta Paediatrica, 95*(9), 1070-1074.

Fuchs, H. J., Borowitz, D. S., Christiansen, D. H., Morris, E. M., Nash, M. L., Ramsey, B. W., Wohl, M. E. (1994). Effect of aerosolized recombinant human DNase on exacerbations of respiratory symptoms and on pulmonary function in patients with cystic fibrosis. *New England Journal of Medicine,*

331(10), 637-642.

Fung, L. (2012). Continuous Infusion Vancomycin for Treatment of Methicillin-Resistant Staphylococcus aureus in Cystic Fibrosis Patients. *The Annals of Pharmacotherapy*, *46*(10), e26-e26.

Garcia-Contreras, L., & Hickey, A. J. (2002). Pharmaceutical and biotechnological aerosols for cystic fibrosis therapy. *Advanced Drug Delivery Reviews*, *54*(11), 1491-1504.

Geller DE, Konstan MW, Smith J, Noonberg SB, Conrad C. Novel tobramycin inhalation powder in cystic fibrosis: pharmacokinetics and safety. *Pediatric Pulmonology* 2007;42:307–13.

Geller, D. E., Konstan, M. W., Smith, J., Noonberg, S. B., & Conrad, C. (2007). Novel tobramycin inhalation powder in cystic fibrosis subjects: pharmacokinetics and safety. *Pediatric Pulmonology*, *42*(4), 307-313.

Gilliam, H., Ellin, A., & Strandvik, B. (1989). Increased bronchial chloride concentration in cystic fibrosis. *Scandinavian Journal of Clinical & Laboratory Investigation*, *49*(2), 121-124.

Gilligan, P. H. (1991). Microbiology of airway disease in patients with cystic fibrosis. *Clinical Microbiology Reviews*, *4*(1), 35-51.

Golec, P., Dąbrowski, K., Hejnowicz, M. S., Gozdek, A., Łoś, J. M., Węgrzyn, G., Łoś, M. (2011). A reliable method for storage of tailed phages. *Journal of Microbiological Methods*, *84*(3), 486-489.

Golshahi, L., Lynch, K., Dennis, J., & Finlay, W. (2010). In vitro Lung Delivery of Respirable Powders Containing Bacteriophages PhiKZ and KS4-M for Treatment of Burkholderia Cepacia Complex and Pseudomonas Aeruginosa Infections in Cystic Fibrosis. *Journal of Applied Microbiology,110*, 106–117.

Golshahi, L., Seed, K. D., Dennis, J. J., & Finlay, W. H. (2008). Toward modern inhalational bacteriophage therapy: nebulization of bacteriophages of Burkholderia cepacia complex. *Journal of Aerosol Medicine and Pulmonary Drug Delivery*, *21*(4), 351-360.

Gould, E. A. (1999). Methods for long-term virus preservation. *Molecular*

Biotechnology, 13(1), 57-66.

Gould, I. M. (2007). MRSA bacteraemia. *International Journal of Antimicrobial Agents, 30*, 66-70.

Govan, J. R., & Deretic, V. (1996). Microbial pathogenesis in cystic fibrosis: mucoid Pseudomonas aeruginosa and Burkholderia cepacia. *Microbiological Reviews, 60*(3), 539-574.

Grandgirard, D., Loeffler, J. M., Fischetti, V. A., & Leib, S. L. (2008). Phage lytic enzyme Cpl-1 for antibacterial therapy in experimental pneumococcal meningitis. *Journal of Infectious Diseases, 197*(11), 1519-1522.

Griebenow, K., & Klibanov, A. M. (1996). On protein denaturation in aqueous-organic mixtures but not in pure organic solvents. *Journal of the American Chemical Society, 118*(47), 11695-11700.

Griese, M. (1999). Pulmonary surfactant in health and human lung diseases: state of the art. *European Respiratory Journal, 13*(6), 1455-1476.

Griese, M., Duroux, A., Schams, A., Lenz, A., & Kleinsasser, N. (1997). Tracheobronchial surface active material in cystic fibrosis. *European Journal of Medical Research, 2*(3), 114-120.

Groneberg, D., Witt, C., Wagner, U., Chung, K., & Fischer, A. (2003). Fundamentals of pulmonary drug delivery. *Respiratory Medicine, 97*(4), 382-387.

Gu, J., Robinson, J., & Leung, S. (1988). Binding of acrylic polymers to mucin/epithelial surfaces: structure-property relationships. *Critical Reviews in Therapeutic Drug Carrier Systems, 5*(1), 21.

Hagens, S., Habel, A., Von Ahsen, U., Von Gabain, A., & Bläsi, U. (2004). Therapy of experimental pseudomonas infections with a nonreplicating genetically modified phage. *Antimicrobial Agents and Chemotherapy, 48*(10), 3817-3822.

Hagerman, J. K., Knechtel, S. A., & Klepser, M. E. (2007). Tobramycin solution for inhalation in cystic fibrosis patients: a review of the literature. *Expert Opinion on Pharmacotherapy, 8*(4), 467-75

Hanlon, G. W. (2007). Bacteriophages: an appraisal of their role in the treatment of

bacterial infections. *International Journal of Antimicrobial Agents, 30*(2), 118-128.

Harding, S. E. (2010). Some observations on the effects of bioprocessing on biopolymer stability. *Journal of Drug Targeting, 18*(10), 732-740.

Harding, S. E., Davis, S. B., Deacon, M. P., & Fiebrig, I. (1999). Biopolymer mucoadhesives. *Biotechnology and Genetic Engineering Reviews, 16*(1), 41-86.

Hardy, J., Lee, S., & Wilson, C. (1985). Intranasal drug delivery by spray and drops. *Journal of Pharmacy and Pharmacology, 37*(5), 294-297.

Harrison, F. (2007). Microbial ecology of the cystic fibrosis lung. *Microbiology, 153*(4), 917-923.

Hawe, A., & Frieß, W. (2006). Impact of freezing procedure and annealing on the physico-chemical properties and the formation of mannitol hydrate in mannitol–sucrose–NaCl formulations. *European Journal of Pharmaceutics and Biopharmaceutics, 64*(3), 316-325.

Henke, M. O., John, G., Germann, M., Lindemann, H., & Rubin, B. K. (2007). MUC5AC and MUC5B mucins increase in cystic fibrosis airway secretions during pulmonary exacerbation. *American Journal of Respiratory and Critical Care Medicine, 175*(8), 816-821.

Henriksen, I., Green, K. L., Smart, J. D., Smistad, G., & Karlsen, J. (1996). Bioadhesion of hydrated chitosans: an in vitro and in vivo study. *International Journal of Pharmaceutics, 145*(1), 231-240.

Henry, R. L., Gibson, P. G., Carty, K., Cai, Y., & Francis, J. L. (1998). Airway inflammation after treatment with aerosolized deoxyribonuclease in cystic fibrosis. *Pediatric Pulmonology, 26*(2), 97-100.

Heo, Y.-J., Lee, Y.-R., Jung, H.-H., Lee, J., Ko, G., & Cho, Y.-H. (2009). Antibacterial efficacy of phages against Pseudomonas aeruginosa infections in mice and Drosophila melanogaster. *Antimicrobial Agents and Chemotherapy, 53*(6), 2469-2474.

Hickey, A., & Thompson, D. (1992). Physiology of the airways. *Drugs and the*

Pharmaceutical Sciences, 54, 1-27.

Hodson, M., McKenzie, S., Harms, H., Koch, C., Mastella, G., Navarro, J., & Strandvik, B. (2003). Dornase alfa in the treatment of cystic fibrosis in Europe: a report from the Epidemiologic Registry of Cystic Fibrosis. *Pediatric Pulmonology, 36*(5), 427-432.

Høiby, N. (2002a). Understanding bacterial biofilms in patients with cystic fibrosis: current and innovative approaches to potential therapies. *Journal of Cystic Fibrosis, 1*(4), 249-254.

Hyman, P., & Abedon, S. (2009). Bacteriophage (overview). *Encyclopedia of Microbiology. Oxford: Elsevier*, 322-338.

Illum, L. (2002). Nasal drug delivery: new developments and strategies. *Drug Discovery Today, 7*(23), 1184-1189.

Illum, L. (2003). Nasal drug delivery: possibilities, problems and solutions. *Journal of Controlled Release, 87*(1), 187-198.

Illum, L., Fischer, A., Jabbal-Gill, I., & Davis, S. (2001). Bioadhesive starch microspheres and absorption enhancing agents act synergistically to enhance the nasal absorption of polypeptides. *International Journal of Pharmaceutics, 222*(1), 109-119.

Instruments, M. (2004). Zetasizer nano series user manual. *Worcestershire: Malvern Instruments Ltd*.

Karchmer, A. W. (2000). Nosocomial bloodstream infections: organisms, risk factors, and implications. *Clinical Infectious Diseases, 31*(Supplement 4), S139-S143.

Kayes, J. (1988). Disperse systems. *Pharmaceutics: the science of dosage form design. New York: Churchill Livingstone*, 81-118.

Kerem, B.-s., Rommens, J. M., Buchanan, J. A., Markiewicz, D., Cox, T. K., Chakravarti, A., Tsui, L.-C. (1989). Identification of the cystic fibrosis gene: genetic analysis. *Science, 245*(4922), 1073-1080.

Khanvilkar, K., Donovan, M. D., & Flanagan, D. R. (2001). Drug transfer through mucus. *Advanced Drug Delivery Reviews, 48*(2), 173-193.

Khmelnitsky, Y. L., Mozhaev, V. V., Belova, A. B., Sergeeva, M. V., & Martinek, K. (1991). Denaturation capacity: a new quantitative criterion for selection of organic solvents as reaction media in biocatalysis. *European Journal of Biochemistry, 198*(1), 31-41.

Kibbe, A. (2000). Handbook of Pharmaceutical Excipients American Pharmaceutical Association and Pharmaceutical Press. *Washington, DC*.

Kreiner, M., & Parker, M. C. (2004). High-activity biocatalysts in organic media: solid-state buffers as the immobilisation matrix for protein-coated microcrystals. *Biotechnology and Bioengineering, 87*(1), 24-33.

Kreiner, M., Fuglevand, G., Moore, B. D., & Parker, M.-C. (2005). DNA-coated microcrystals. *Chemical Communications*(21), 2675-2676.

Kreiner, M., Moore, B. D., & Parker, M. C. (2001). Enzyme-coated micro-crystals: a 1-step method for high activity biocatalyst preparation. *Chemical Communications*(12), 1096-1097.

Kuni, C., Regelmann, W., BOUDREAU, R., & BUDD, J. (1992). Aerosol scintigraphy in the assessment of therapy for cystic fibrosis. *Clinical Nuclear Medicine, 17*(2), 90-93.

Kunkelmann, H., Kleinbauer, D., Klink, F., & Oberheuser, F. (1988). Effects of intralipid and hydrocortisone upon human fetal lung cell cultures. *Research in Experimental Medicine, 188*(6), 411-423.

Lai, S. K., Wang, Y.-Y., & Hanes, J. (2009). Mucus-penetrating nanoparticles for drug and gene delivery to mucosal tissues. *Advanced Drug Delivery Reviews, 61*(2), 158-171.

Lansley, A.B. and Martin, G.P. (2000). Nasal Drug Delivery. In: Hillery, A.M. Lloyd, A.W. and Swarbrick, J. eds: Drug Delivery and Targeting for Pharmacists and Pharmaceutical Scientists, Harwood Academic Publishers, Amsterdam, p.p. 237-268.

Larson, J. E., Delcarpio, J. B., Farberman, M. M., Morrow, S. L., & Cohen, J. C. (2000). CFTR modulates lung secretory cell proliferation and differentiation. *American Journal of Physiology-Lung Cellular and Molecular Physiology,*

279(2), L333-L341.

Lee, J. C., & Timasheff, S. N. (1981). The stabilization of proteins by sucrose. *Journal of Biological Chemistry, 256*(14), 7193-7201.

Lenney, W., Edenborough, F., Kho, P., & Kovarik, J. M. (2011). Lung deposition of inhaled tobramycin with eFlow rapid/LC Plus jet nebuliser in healthy and cystic fibrosis subjects. *Journal of Cystic Fibrosis, 10*(1), 9-14.

Lenoir, G., Antypkin, Y. G., Miano, A., Moretti, P., Zanda, M., Varoli, G., Aryayev, N. L. (2007). Efficacy, safety, and local pharmacokinetics of highly concentrated nebulized tobramycin in patients with cystic fibrosis colonized with Pseudomonas aeruginosa. *Pediatric Drugs, 9*(1), 11-20.

Lenski, R. E. (1988). Dynamics of interactions between bacteria and virulent bacteriophage. *Advances in Microbial Ecology, 10*, 1-44.

Lerner, S. A., Schmitt, B. A., Seligsohn, R., & Matz, G. J. (1986). Comparative study of ototoxicity and nephrotoxicity in patients randomly assigned to treatment with amikacin or gentamicin. *The American Journal of Medicine, 80*(6), 98-104.

Lethem, M. I. (1993). The role of tracheobronchial mucus in drug administration to the airways. *Advanced Drug Delivery Reviews, 11*(3), 271-298.

Lethem, M. I., James, S. L., & Marriott, C. (1990). The Role of Mucous Glycoproteins in the Rheologic Properties of Cystic Fibrosis Sputum1-3. *American Review of Respiratory Disease, 142*, 1053-1058.

Levy, S. B. (2005). Antibiotic resistance—the problem intensifies. *Advanced Drug Delivery Reviews, 57*(10), 1446-1450.

Li, J., Nation, R. L., Milne, R. W., Turnidge, J. D., & Coulthard, K. (2005). Evaluation of colistin as an agent against multi-resistant Gram-negative bacteria. *International Journal of Antimicrobial Agents, 25*(1), 11-25.

Liu, Y., Johnson, M. R., Matida, E. A., Kherani, S., & Marsan, J. (2009). Creation of a standardized geometry of the human nasal cavity. *Journal of Applied Physiology, 106*(3), 784-795.

Livingstone, C. R., Andrews, M. A., Jenkins, S. M., & Marriott, C. (1990). Model

Systems for the Evaluation of Mucolytic Drugs: Acetylcysteine and S-Carboxymethylcysteine. *Journal of Pharmacy and Pharmacology, 42*(2), 73-78.

Lode, H. (1998). Tobramycin: a review of therapeutic uses and dosing schedules. *Current Therapeutic Research, 59*(7), 420-453.

Lu, Y., Harding, S. E., Rowe, A. J., Davis, K. G., Fish, B., Varley, P., Mulot, S. (2008a). The effect of a point mutation on the stability of IgG4 as monitored by analytical ultracentrifugation. *Journal of Pharmaceutical Sciences, 97*(2), 960-969.

Lu, Y., Harding, S. E., Rowe, A. J., Davis, K. G., Fish, B., Varley, P., Mulot, S. (2008b). The effect of a point mutation on the stability of IgG4 as monitored by analytical ultracentrifugation. *Journal of Pharmaceutical Sciences, 97*(2), 960-969.

Lyczak, J. B., Cannon, C. L., & Pier, G. B. (2002). Lung infections associated with cystic fibrosis. *Clinical Microbiology Reviews, 15*(2), 194-222.

Ma, Y., Pacan, J. C., Wang, Q., Xu, Y., Huang, X., Korenevsky, A., & Sabour, P. M. (2008). Microencapsulation of bacteriophage felix O1 into chitosan-alginate microspheres for oral delivery. *Applied and Environmental Microbiology, 74*(15), 4799-4805.

Marshall, K., Manolopoulos, V., Mancer, K., Staples, J., & Damyanovich, A. (2000). Amelioration of disease severity by intraarticular hylan therapy in bilateral canine osteoarthritis. *Journal of Orthopaedic Research, 18*(3), 416-425.

Martin, A., & Swarbrick, J. (1983). Cammarata. *Physical Pharmacy*, 496-501.

Martini, F., & Nath, J. (2009). Neural integration II: the autonomic nervous system and higher-order functions. *Fundamentals of Anatomy and Physiology*, 554-556.

Marza, J., Soothill, J., Boydell, P., & Collyns, T. (2006). Multiplication of therapeutically administered bacteriophages in *Pseudomonas aeruginosa* infected patients. *Burns, 32*(5), 644-646.

Massie, J., & Clements, B. (2005). Diagnosis of cystic fibrosis after newborn

screening: the Australasian experience—twenty years and five million babies later: a consensus statement from the Australasian Paediatric Respiratory Group. *Pediatric Pulmonology, 39*(5), 440-446.

Masuda, N., Sakagawa, E., Ohya, S., Gotoh, N., Tsujimoto, H., & Nishino, T. (2000). Contribution of the MexX-MexY-OprM efflux system to intrinsic resistance in Pseudomonas aeruginosa. *Antimicrobial Agents and Chemotherapy, 44*(9), 2242-2246.

Mathee, K., Ciofu, O., Sternberg, C., Lindum, P. W., Campbell, J. I., Jensen, P., Søren, M. (1999). Mucoid conversion of Pseudomonas aeruginos by hydrogen peroxide: a mechanism for virulence activation in the cystic fibrosis lung. *Microbiology, 145*(6), 1349-1357.

Matsubara, T., Emoto, W., & Kawashiro, K. (2007). A simple two-transition model for loss of infectivity of phages on exposure to organic solvent. *Biomolecular Engineering, 24*(2), 269-271.

Matsuzaki, S., Rashel, M., Uchiyama, J., Sakurai, S., Ujihara, T., Kuroda, M., Wakiguchi, H. (2005). Bacteriophage therapy: a revitalized therapy against bacterial infectious diseases. *Journal of Infection and Chemotherapy, 11*(5), 211-219.

Mattern, M., Winter, G., Kohnert, U., & Lee, G. (1999). Formulation of proteins in vacuum-dried glasses. II. Process and storage stability in sugar-free amino acid systems. *Pharmaceutical Development and Technology, 4*(2), 199-208.

McInnes, F. J., O'Mahony, B., Lindsay, B., Band, J., Wilson, C. G., Hodges, L. A., & Stevens, H. N. (2007). Nasal residence of insulin containing lyophilised nasal insert formulations, using gamma scintigraphy. *European Journal of Pharmaceutical Sciences, 31*(1), 25-31.

McInnes, F. J., Thapa, P., Baillie, A. J., Welling, P. G., Watson, D. G., Gibson, I., Stevens, H. N. (2005). In vivo evaluation of nicotine lyophilised nasal insert in sheep. *International Journal of Pharmaceutics, 304*(1), 72-82.

Meader, E., Mayer, M. J., Gasson, M. J., Steverding, D., Carding, S. R., & Narbad, A. (2010). Bacteriophage treatment significantly reduces viable *Clostridium*

difficile and prevents toxin production in an *in vitro* model system. *Anaerobe, 16*(6), 549-554.

Mogayzel Jr, P. J., Naureckas, E. T., Robinson, K. A., Mueller, G., Hadjiliadis, D., Hoag, J. B., Marshall, B. (2013). Cystic Fibrosis Pulmonary Guidelines: Chronic Medications for Maintenance of Lung Health. *American Journal of Respiratory and Critical Care Medicine, 187*(7), 680-689.

Mohamed, F., & van der Walle, C. F. (2006). PLGA microcapsules with novel dimpled surfaces for pulmonary delivery of DNA. *International Journal of Pharmaceutics, 311*(1), 97-107.

Moineau, S., Tremblay, D., & Labrie, S. (2002). Phages of lactic acid bacteria: from genomics to industrial applications. *American Society for Microbiology News, 68*(8), 388-393.

Moore, B. D., Deere, J., Edrada-Ebel, R., Ingram, A., & van der Walle, C. F. (2010). Isolation of recombinant proteins from culture broth by co-precipitation with an amino acid carrier to form stable dry powders. *Biotechnology and Bioengineering, 106*(5), 764-773.

Moore, B., Parker, M., Halling, P., & Partridge, J. (2000). RAPID DEHYDRATION OF PROTEINS: WO Patent 2,000,069,887.

Mortazavi, S. (1995). An in vitro assessment of mucus/mucoadhesive interactions. *International Journal of Pharmaceutics, 124*(2), 173-182.

Mukhopadhyay, S., Singh, M., Cater, J., Ogston, S., Franklin, M., & Olver, R. (1996). Nebulised antipseudomonal antibiotic therapy in cystic fibrosis: a meta-analysis of benefits and risks. *Thorax, 51*(4), 364-368.

Murdan, S., Somavarapu, S., Ross, A. C., Alpar, H., & Parker, M. (2005). Immobilisation of vaccines onto micro-crystals for enhanced thermal stability. *International Journal of Pharmaceutics, 296*(1), 117-121.

Murugesan, M., Cunningham, D., Martinez-Albertos, J.-L., Vrcelj, R. M., & Moore, B. D. (2005). Nanoparticle-coated microcrystals. *Chemical Communications* (21), 2677-2679.

Mygind, N., & Dahl, R. (1998). Anatomy, physiology and function of the nasal

cavities in health and disease. *Advanced Drug Delivery Reviews, 29*(1), 3-12.

Nakamura, K., Maitani, Y., Lowman, A. M., Takayama, K., Peppas, N. A., & Nagai, T. (1999). Uptake and release of budesonide from mucoadhesive, pH-sensitive copolymers and their application to nasal delivery. *Journal of Controlled Release, 61*(3), 329-335.

Newman, S. P. (1984). Therapeutic aerosols. *Aerosols and the lung. London: Butterworths*, 197-224.

Nishijima, S., Namura, S., Mitsuya, K., & Asada, Y. (1993). The incidence of isolation of methicillin-resistant Staphylococcus aureus (MRSA) strains from skin infections during the past three years (1989-1991). *The Journal of Dermatology, 20*(4), 193-197.

Nyamweya, N., & Hoag, S. W. (2000). Assessment of polymer-polymer interactions in blends of HPMC and film forming polymers by modulated temperature differential scanning calorimetry. *Pharmaceutical Research, 17*(5), 625-631.

Oberdörster, G. (1993). Lung dosimetry: pulmonary clearance of inhaled particles. *Aerosol Science and Technology, 18*(3), 279-289.

O'Flaherty, S., Ross, R., Flynn, J., Meaney, W., Fitzgerald, G., & Coffey, A. (2005). Isolation and characterization of two anti-staphylococcal bacteriophages specific for pathogenic Staphylococcus aureus associated with bovine infections. *Letters in Applied Microbiology, 41*(6), 482-486.

O'Neil, M. (2001). The Merck Index-an encyclopedia of chemicals, drugs and biologicals, New Jersy, Merk & Co. *Inc., P*.

Paisano, A., Spira, B., Cai, S., & Bombana, A. (2004). In vitro antimicrobial effect of bacteriophages on human dentin infected with Enterococcus faecalis ATCC 29212. *Oral Microbiology and Immunology, 19*(5), 327-330.

Pantucek, R., Rosypalova, A., Doskar, J., Kailerova, J., & Ruzickova, V. P. 761 Borecka, S. Snopkova, R. Horvath, F. Gotz, and S. Rosypal. (1998). The 762 polyvalent staphylococcal phage phi 812: its host-range mutants and related 763 phages. *Virology, 246*, 241-252.

Paschoal, I. A., de Oliveira Villalba, W., Bertuzzo, C. S., Cerqueira, E. M. F., &

Pereira, M. C. (2007). Cystic fibrosis in adults. *Lung, 185*(2), 81-87.

Payne, R. J., & Jansen, V. A. (2003). Pharmacokinetic principles of bacteriophage therapy. *Clinical Pharmacokinetics, 42*(4), 315-325.

Pereira, P., Kelly, S., Cooper, A., Mardon, H., Gellert, P., & Van der Walle, C. (2007). Solution formulation and lyophilisation of a recombinant fibronectin fragment. *European Journal of Pharmaceutics and Biopharmaceutics, 67*(2), 309-319.

Puapermpoonsiri, U., Ford, S., & van der Walle, C. (2010). Stabilization of bacteriophage during freeze drying. *International Journal of Pharmaceutics, 389*(1), 168-175.

Puapermpoonsiri, U., Spencer, J., & van der Walle, C. F. (2009). A freeze-dried formulation of bacteriophage encapsulated in biodegradable microspheres. *European Journal of Pharmaceutics and Biopharmaceutics, 72*(1), 26-33.

Puchelle, E., Bajolet, O., & Abély, M. (2002). Airway mucus in cystic fibrosis. *Paediatric Respiratory Reviews, 3*(2), 115-119.

Ramsey, B. W., Dorkin, H. L., Eisenberg, J. D., Gibson, R. L., Harwood, I. R., Kravitz, R. M., McBurnie, M. A. (1993). Efficacy of aerosolized tobramycin in patients with cystic fibrosis. *New England Journal of Medicine, 328*(24), 1740-1746.

Rathbone, M. J., & Hadgraft, J. (1991). Absorption of drugs from the human oral cavity. *International Journal of Pharmaceutics, 74*(1), 9-24.

Rees, P., & Fry, B. (1981). The morphology of staphylococcal bacteriophage K and DNA metabolism in infected Staphylococcus aureus. *Journal of General Virology, 53*, 293-307.

Ricevuti, G., Mazzone, A., Uccelli, E., Gazzani, G., & Fregnan, G. B. (1988). Influence of erdosteine, a mucolytic agent, on amoxycillin penetration into sputum in patients with an infective exacerbation of chronic bronchitis. *Thorax, 43*(8), 585-590.

Rommens, J. M., Iannuzzi, M. C., Kerem, B.-s., Drumm, M. L., Melmer, G., Dean, M., Hidaka, N. (1989). Identification of the cystic fibrosis gene: chromosome

walking and jumping. *Science, 245*(4922), 1059-1065.

Rosenstock, J., Cefalu, W. T., Hollander, P. A., Belanger, A., Eliaschewitz, F. G., Gross, J. L., Ogawa, M. (2008). Two-year pulmonary safety and efficacy of inhaled human insulin (Exubera) in adult patients with type 2 diabetes. *Diabetes Care, 31*(9), 1723-1728.

Rouse, J., Mohamed, F., & Van der Walle, C. (2007). Physical ageing and thermal analysis of PLGA microspheres encapsulating protein or DNA. *International Journal of Pharmaceutics, 339*(1), 112-120.

Rozov, T., de Oliveira, V. Z., Santana, M. A., Adde, F. V., Mendes, R. H., Paschoal, I. A., Pahl, M. (2010). Dornase alfa improves the health-related quality of life among Brazilian patients with cystic fibrosis—A one-year prospective study. *Pediatric Pulmonology, 45*(9), 874-882.

Ryan, K. J., Ray, C. G., & Sherris, J. C. (2004). Sherris medical microbiology: an introduction to infectious diseases.

Saadatian-Elahi, M., Teyssou, R., & Vanhems, P. (2008). Staphylococcus aureus, the major pathogen in orthopaedic and cardiac surgical site infections: A literature review. *International Journal of Surgery, 6*(3), 238-245.

Sabín, J., Prieto, G., & Sarmiento, F. (2010). Studying Colloidal Aggregation Using Liposomes *Liposomes* (pp. 189-198): Springer.

Salunkhe, P., Smart, C. H., Morgan, J. A. W., Panagea, S., Walshaw, M. J., Hart, C. A., Winstanley, C. (2005). A cystic fibrosis epidemic strain of Pseudomonas aeruginosa displays enhanced virulence and antimicrobial resistance. *Journal of Bacteriology, 187*(14), 4908-4920.

Sambrook, J., & Russell, D. W. (2001). Purification of Bacteriophage particles by isopuonic centrifugation through CsCl Gradients. Molecular cloning: a laboratory manual. Cold Spring Harbour Laboratory Press, New York: 2.47-2.51.

Schmitz, G., & Müller, G. (1991). Structure and function of lamellar bodies, lipid-protein complexes involved in storage and secretion of cellular lipids. *Journal of Lipid Research, 32*(10), 1539-1570.

Schreier, H., Gonzalez-Rothi, R. J., & Stecenko, A. A. (1993). Pulmonary delivery of liposomes. *Journal of Controlled Release, 24*(1), 209-223.

Schüle, S., Frieß, W., Bechtold-Peters, K., & Garidel, P. (2007). Conformational analysis of protein secondary structure during spray-drying of antibody/mannitol formulations. *European Journal of Pharmaceutics and Biopharmaceutics, 65*(1), 1-9.

Schüssele, A., & Bauer-Brandl, A. (2003). Note on the measurement of flowability according to the European Pharmacopoeia. *International Journal of Pharmaceutics, 257*(1), 301-304.

Schuster, A., Haliburn, C., Döring, G., & Goldman, M. H. (2013). Safety, efficacy and convenience of colistimethate sodium dry powder for inhalation (Colobreathe DPI) in patients with cystic fibrosis: a randomised study. *Thorax, 68*(4), 344-350.

Searles, J. A., Carpenter, J. F., & Randolph, T. W. (2001). The ice nucleation temperature determines the primary drying rate of lyophilization for samples frozen on a temperature-controlled shelf. *Journal of Pharmaceutical Sciences, 90*(7), 860-871.

Shao, Z., & Mitra, A. K. (1992). Nasal membrane and intracellular protein and enzyme release by bile salts and bile salt-fatty acid mixed micelles: correlation with facilitated drug transport. *Pharmaceutical Research, 9*(9), 1184-1189.

Siepmann, J., & Peppas, N. (2001). Modeling of drug release from delivery systems based on hydroxypropyl methylcellulose (HPMC). *Advanced Drug Delivery Reviews, 48*(2), 139-157.

Skurnik, M., Pajunen, M., & Kiljunen, S. (2007). Biotechnological challenges of phage therapy. *Biotechnology Letters, 29*(7), 995-1003.

Slopek, S., Weber-Dabrowska, B., Dabrowski, M., & Kucharewicz-Krukowska, A. (1987). Results of bacteriophage treatment of suppurative bacterial infections in the years 1981–1986. *Archivum Immunologiae et Therapiae Experimentalis, 35*, 569-583.

Smart, J. D. (2005). The basics and underlying mechanisms of mucoadhesion. *Advanced Drug Delivery Reviews, 57*(11), 1556-1568.

Smith, H. W., & Huggins, M. (1982). Successful treatment of experimental Escherichia coli infections in mice using phage: its general superiority over antibiotics. *Journal of General Microbiology, 128*(2), 307-318.

Smola, M., Vandamme, T., & Sokolowski, A. (2008). Nanocarriers as pulmonary drug delivery systems to treat and to diagnose respiratory and non respiratory diseases. *International Journal of Nanomedicine, 3*(1), 1.

Soane, R., Frier, M., Perkins, A., Jones, N., Davis, S., & Illum, L. (1999). Evaluation of the clearance characteristics of bioadhesive systems in humans. *International Journal of Pharmaceutics, 178*(1), 55-65.

Soothill, J. (1994). Bacteriophage prevents destruction of skin grafts by Pseudomonas aeruginosa. *Burns: Journal of the International Society for Burn Injuries, 20*(3), 209.

Sulakvelidze, A., & Kutter, E. (2005). Bacteriophage therapy in humans. *Bacteriophages: biology and applications*, 381-436.

Sulakvelidze, A., Alavidze, Z., & Morris, J. G. (2001). Bacteriophage therapy. *Antimicrobial Agents and Chemotherapy, 45*(3), 649-659.

Taylor, G. and Kellaway, I. (2001). Pulmonary drug delivery. In A. M. Hillery, A. W. Lloyd & J. Swarbrick (Eds.), *Drug Delivery and Targeting for Pharmacists and Pharmaceutical Scientists* (pp. 269-300). Boca Raton, Florida: CRC Press.

Taylor, R., Hodson, M. E., & Pitt, T. L. (1993). Adult cystic fibrosis: association of acute pulmonary exacerbations and increasing severity of lung disease with auxotrophic mutants of Pseudomonas aeruginosa. *Thorax, 48*(10), 1002-1005.

Thomas, A., Thomas, J., & Holloway, I. (1980). Microbiological and chemical analysis of polymyxin B and polymyxin E (colistin) sulphates. *Analyst, 105*(1256), 1068-1075.

Tian, F., Saville, D. J., Gordon, K. C., Strachan, C. J., Zeitler, J. A., Sandler, N., & Rades, T. (2007). The influence of various excipients on the conversion

kinetics of carbamazepine polymorphs in aqueous suspension. *Journal of Pharmacy and Pharmacology, 59*(2), 193-201.

Toro, H., Price, S., McKee, S., Hoerr, F., Krehling, J., Perdue, M., & Bauermeister, L. (2005). Use of bacteriophages in combination with competitive exclusion to reduce Salmonella from infected chickens. *Avian diseases, 49*(1), 118-124.

Torrado, S., & Torrado, S. (2002). Characterization of physical state of mannitol after freeze-drying: effect of acetylsalicylic acid as a second crystalline cosolute. *Chemical and Pharmaceutical Bulletin, 50*(5), 567-570.

Touw, D., Brimicombe, R., Hodson, M., Heijerman, H., & Bakker, W. (1995). Inhalation of antibiotics in cystic fibrosis. *European Respiratory Journal, 8*(9), 1594-1604.

Ugwoke, M. I., Verbeke, N., & Kinget, R. (2001). The biopharmaceutical aspects of nasal mucoadhesive drug delivery. *Journal of Pharmacy and Pharmacology, 53*(1), 3-22.

Villar, J., & Slutsky, A. S. (1989). The incidence of the adult respiratory distress syndrome. *American Review of Respiratory Disease, 140*(3), 814-816.

Voynow, J. A., & Rubin, B. K. (2009). Mucins, mucus, and sputum. *Chest Journal, 135*(2), 505-512.

Vybiral, D., Takáč, M., Loessner, M., Witte, A., Ahsen, U., & Bläsi, U. (2003). Complete nucleotide sequence and molecular characterization of two lytic Staphylococcus aureus phages: 44AHJD and P68. *FEMS Microbiology Letters, 219*(2), 275-283.

Wang, D., Haviland, D. L., Burns, A. R., Zsigmond, E., & Wetsel, R. A. (2007). A pure population of lung alveolar epithelial type II cells derived from human embryonic stem cells. *Proceedings of the National Academy of Sciences, 104*(11), 4449-4454.

Wang, W., Antonsen, K., & Nayar, R. (2002). A novel method for removing residual acetone from gelatin microspheres. *Pharmaceutical Development and Technology, 7*(2), 169-180.

Washington, N., Washington, C., & Wilson, C. G. (2001). Pulmonary drug delivery.

In N. Washington, C. Washington & C. G. Wilson (Eds.), *Physiological pharmaceutics: barriers to drug absorption* (2nd ed., pp. 221-248): CRC Press.

Weber-Dabrowska, B., Mulczyk, M., & Górski, A. (2003). *Bacteriophages as an efficient therapy for antibiotic-resistant septicemia in man.* Paper presented at the Transplantation proceedings.

Weber-Dąbrowska, B., Zimecki, M., Kruzel, M., Kochanowska, I., Łusiak-Szelachowska, M. (2006). Alternative therapies in antibiotic-resistant infection. *Advances in Medical Sciences, 51*, 242-244.

Welsh, M., M.P. Anderson, D.P. Rich, H.A. Berger, G.M. Denning, L.S. Ostedgaard, Sheppard, D.N. (1994). Abnormalities of Airway Epithelial Chloride Transport in Cystic Fibrosis. In: Airway Secretion: Physiological Bases for the Control of Mucus Hypersecretion. (T.Takishima, Ed.), Marcel Dekker, Inc., N.Y., 1994, pp. 513-526.

Welsh, M.J., Ramsey, B.W., Accurso, F., Cutting, G.R. (2001). Cystic fibrosis. The Metabolic and Molecular Basis of Inherited Disease. C.R. Scriver, A.L. Beaudet, W.S. Sly, and D. Valle, editors. McGraw-Hill Inc., New York. 5121–5188.

Widdicombe, J. G. (1997). Airway surface liquid: concepts and measurements *Airway mucus: basic mechanisms and clinical perspectives* (pp. 1-17): Springer.

Williams, O. W., Sharafkhaneh, A., Kim, V., Dickey, B. F., & Evans, C. M. (2006). Airway mucus: from production to secretion. *American Journal of Respiratory Cell and Molecular Biology, 34*(5), 527.

Witschi, C., & Mrsny, R. J. (1999). In vitro evaluation of microparticles and polymer gels for use as nasal platforms for protein delivery. *Pharmaceutical Research, 16*(3), 382-390.

Wright, A., Hawkins, C., Änggård, E., & Harper, D. (2009). A controlled clinical trial of a therapeutic bacteriophage preparation in chronic otitis due to antibiotic-resistant Pseudomonas aeruginosa; a preliminary report of efficacy.

Clinical Otolaryngology, *34*(4), 349-357.

Wright, J. R., & Dobbs, L. G. (1991). Regulation of pulmonary surfactant secretion and clearance. *Annual review of physiology, 53*(1), 395-414.

Yang, T., Hussain, A., Paulson, J., Abbruscato, T. J., & Ahsan, F. (2004). Cyclodextrins in nasal delivery of low-molecular-weight heparins: in vivo and in vitro studies. *Pharmaceutical Research, 21*(7), 1127-1136.

Yang, W., Peters, J. I., & Williams III, R. O. (2008). Inhaled nanoparticles—a current review. *International Journal of Pharmaceutics, 356*(1), 239-247.

Yang, Y., Tsifansky, M. D., Wu, C.-J., Yang, H. I., Schmidt, G., & Yeo, Y. (2010). Inhalable antibiotic delivery using a dry powder co-delivering recombinant deoxyribonuclease and ciprofloxacin for treatment of cystic fibrosis. *Pharmaceutical Research, 27*(1), 151-160.

Yuan, N.-Y., Lin, Y.-A., Ho, M.-H., Wang, D.-M., Lai, J.-Y., & Hsieh, H.-J. (2009). Effects of the cooling mode on the structure and strength of porous scaffolds made of chitosan, alginate, and carboxymethyl cellulose by the freeze-gelation method. *Carbohydrate polymers, 78*(2), 349-356.

APPENDIX I: Conference abstracts

The 3rd PharmSciFair Conference 2011

Formulation and Evaluation of A Novel Bacteriophage Delivery System for MRSA Nasal Colonisation

M. Alfadhel[1], C. Walle[1]

[1]University of Strathclyde, Glasgow, UK.

ABSTRACT

We describe a new solid state dosage form for bacteriophage therapy of nasal methicillin-resistant *Staphylococcus aureus* (MRSA) infections. Lyophilised nasal inserts carrying bacteriophage were formulated from 1-2% w/v hydroxypropyl methylcellulose (HPMC), chosen on account of its bioadhesive properties, and 1% mannitol.

The physical nature of the lyophilisate was characterised by scanning electron microscope (SEM) and differential scanning calorimetry (DSC). The localisation of fluorescein-labelled bacteriophage within the inserts was determined by confocal laser scanning microscopy (CLSM). The relationship between formulation parameters to bacteriophage stability was determined for residual water content, measured by Karl Fischer titration (KF), and water vapour sorption, assessed by dynamic vapour sorption (DVS).

Lytic activity determined by plaque assay showed only modest loss of the bacteriophage titre after lyophilisation and storage over 1 year. On comparison of the CLSM images and SEM micrographs, the bacteriophages seemed to be homogenously distributed throughout the matrix, without evidence of aggregation. The water content results obtained by Karl Fischer titration correlated well with the water vapour sorption results of the DVS.

We conclude that bacteriophage can be successfully formulated without significant loss of lytic activity in water soluble, bioadhesive matrices for nasal delivery, representing a potential treatment for MRSA colonisation.

REFERENCES

1. Puapermpoonsiri U., Ford S., Vander Walle C., Stabilization of bacteriophage during freeze drying, *Int J Pharm.*, 389 (2010) 168-175.
2. Puapermpoonsiri U., Spenser J., Vander Walle C., A freeze-dried formulation of bacteriophage encapsulated in biodegradable microspheres, *Eur J Pharm Biopharm.*, 72 (2009) 26-33.
3. McIness F. J., O'mahony B., Lindsay B., Band J., Wilson C.-G., Hodges L.-A., and Stevens H.-N., Nasal residence of insulin containing lyophilised nasal insert formulations, using gamma scintigraphy, *Eur J Pharm Sci.*, 31 (2007) 25-31.

The 5th Saudi International Conference 2012

Formulation and evaluation of a novel bacteriophage delivery system for MRSA nasal colonisation

M. Alfadhel[1], C. Walle[1]

[1]University of Strathclyde, Glasgow, UK.

ABSTRACT: Bacteriophage therapy is limited by a lack of understanding regarding their formulation as medicines that will efficiently deliver phage as therapeutics agents without deterioration. Since the oral route of administration minimizes the lytic activity of phages, nasal delivery system is proposed as an alternative. We hypothesize that using a nasal insert harbouring bacteriophage as the therapeutic agent will lead to more efficacious deliver locally. To this end, we formulated lyophilised nasal inserts carrying bacteriophage selective for *S. aureus*, and evaluated the effect of lyophilisation on phage viability. The evaluation of the formulations demonstrated that the bacteriophage were successfuly formulated without significant effect on the viability of bacteriophage to infect bacteria.

INTRODUCTION: Methicillin resistant *S. aureus* (MRSA) is considered the most important cause of antibiotic resistant infections. Recently, phage therapy has received more interest as alternative therapy for MRSA infections. The objective of our study was to formulate a new dosage form for bacteriophage therapy of MRSA infections. We formulated a lyophilised nasal insert using hydroxypropylmethylcellulose (HPMC) polymer due to its bioadhesion property. Mannitol was added to some of the formulations. It was selected because it is a non hygroscopic material that used extensively in the pharmaceutical formulations. We evaluated the effect of lyophilisation on the phage viability and the activity of phages during storage within a period of time. The effect of the selected polymer has also been studied.

METHODS: Formulations were prepared by various concentrations of HPMC and mannitol. The formulations were synthesized by lyophilisation using freeze drying technique. The lytic activity of bacteriophages before and after lyophilisation was evaluated by plaque assay method which was used for determination of the concentration of the phages in plaque forming unit per ml (pfu/ml). The physical nature of the lyophilisate was characterised by scanning electron microscope (SEM) technique. The localisation of fluorescein-labelled bacteriophage within the inserts was determined by confocal laser scanning microscopy (CLSM). The relation of formulation parameters to bacteriophage stability was studied. The residual water content was measured by performing karl Fischer titration (KF) and the water vapour sorption of the formulations was assessed by dynamic vapour sorption apparatus (DVS).

RESULTS AND CONCLUSION: It is known that lyophilisation may affect the activity of bacteriophages (Puapermpoonsiri et al., 2010). The plaque assay was performed to examine the lytic activity of the formulated bacteriophage. The phage titer loss during lyophilisation was reasonably low, suggesting that the phage was efficiently dispersed in the gel and lyophilised without significant detrimental effects on phage viability. The lytic activity of phage during storage was also studied. We found that the phage titer loss during storage for 60 day was very low. To examine possible aggregation of the bacteriophage during formulation fluorescein labelled bacteriophage were formulated and lyophilised. On comparing the CLSM and SEM micrographs, the bacteriophages appear to be homogenously distributed throughout the lyophilised nasal insert and no evidence of aggregation is apparent. The water content results obtained by Karl Fischer titration correlated well with the water sorption results of the DVS. Taking in considereation the processing parameters that need to be measured, we have presented a new successful formulation for bacteriophage therapy.

REFERENCES

1. Puapermpoonsiri U., Ford S., Vander Walle C., Stabilization of bacteriophage during freeze drying, *Int J Pharm.*, 389 (2010) 168-175.
2. McIness F. J., O'mahony B., Lindsay B., Band J., Wilson C.-G., Hodges L.-A., and Stevens H.-N., Nasal residence of insulin containing lyophilised nasal insert formulations, using gamma scintigraphy, *Eur J Pharm Sci.,* 31 (2007) 25-31.

American Association of Pharmaceutical Scientists 2012

Improved pulmonary delivery of antibiotics and bacteriophage using Lamellasomes™.

Munerah Alfadhel1*, Graham Park2, Christopher van der Walle1

1, University of Strathclyde, Glasgow, G4 0RE, UK. 2, Lamellar Biomedical Ltd, Caledonian House, Phoenix Crescent, Bellshill, ML4 3NJ, UK

Abstract

Background: LamellasomesTM (LMS) are multilamellar vesicles of phospholipids and cholesterol, representative of lamellar bodies in the lung. Their physico-chemical properties are suited to pulmonary delivery for the improvement of lung function. One area of therapeutic interest is cystic fibrosis (CF), since the CF lung may harbor antibiotic-resistant bacteria, such as mucoid strains of Pseudomonas aeruginosa.

Purpose: To improve the pulmonary delivery of nebulized solutions of antibiotics or bacteriophage by dilution into LMS.

Methods: Saline (control), bacteriophage or antibiotic (colistin, tobramyin) was diluted 1:6 into LMS and nebulized using either a Pari-boy or eFlow nebulizer (PARI GmbH). The aerosol mass median aerodynamic diameter (MMAD) was evaluated using a multi stage liquid impinger (MSLI) and compared to measurements of size by light scattering. Zeta potential was measured using a Zetasizer and structure imaged by transmission electron microscopy (TEM) and confocal laser scanning microscopy (CLSM). Following nebulization, the lytic activity of bacteriophage from each stage of the MSLI was examined by plaque assay, and antibiotic concentrations were determined indirectly by inhibition of P. aeruginosa growth.

Results: TEM micrographs showed that LMS is composed of multilamellar vesicles with various sizes from the sub-micron to several microns. CLSM of labeled LMS and phage showed that the phage did not partition into the vesicle or lipid lamellae. Small but significant differences between the MMAD of LMS aerosols generated by the Pari-boy and eFlow were found (3.3 and 4.1 µm respectively). The zeta potential of LMS suspended in 0.9% saline was between -60 to -70 mV. Bacteriophage remained stable in LMS since their lytic activity and deposition were the same as for resuspension in saline (control). Antibiotics diluted into LMS were predominantly deposited in stages 3-5 of the MLSI, compared to stages 1 and 2 when diluted in saline (control).

Conclusion: The dilution of antibiotic into LMS rather than saline increased the nebulized drug fraction deposited into the deep lung, with less drug lost by deposition in the 'throat'. This suggests that the surface activity of the LMS facilitates the generation of smaller aerosol droplets during nebulization, particularly for nebulization using the eFlow.

Academy of Pharmaceutical Sciences Conference 2013

Bioprocessing of Bacteriophages via Rapid Drying onto Micro-Crystals.

M. Al-fadhel[1], E. Alvarez-Gonzalez[1], C. Walle[1]

[1]Strathclyde Institute of Pharmacy and Biomedical Sciences, University of Strathclyde, Glasgow, UK.

Abstract - **Here we present an alternative phage bioprocess method involving co-precipitation of an aqueous mixture of phage and a crystallisable carrier (glutamine or glycine). Free-flowing dry powders generated have a phage titre high enough to permit subsequent formulation steps following bioprocessing. The phage-coated microcrystals remain stable under storage at room temperature for at least one month. We anticipate that this generic bioprocessing technique will have application to other phage families as required for the development of phage therapies.**

INTRODUCTION

Bacteriophage may provide alternative therapies for antibiotic resistant bacterial infection. Our goal is to investigate the utility of rapid co-precipitation, immobilization and drying of phage onto amino acid carriers. The approach draws from the process of generating protein coated microcrystals (PCMCs).

METHODS

Carrier (glutamine or glycine) and stabilizers (trehalose or albumin) were dissolved in aqueous phage stock solution. This solution was added drop-wise to excess organic solvent (isopropanol or isobutanol) while stirring.The immediately formed phage-coated microcrystals (phage-CMC) were harvested by vacuum filtration. Powders were dried at constant temperature and relative humidity until constant weight. The lytic activity of the phage was examined by plaque assay and powder morphology imaged by scanning electron microscopy (SEM). Residual water content was determined by Karl Fischer titration (KF).

RESULTS AND DISCUSSION

The activity of the phage powders was found to depend on the type of amino acid carrier, the presence or absence of stabilizer, the organic solvent and the storage conditions. The stability of the immobilized phage decreased over time. Nevertheless, the lytic activity of the phage-CMC following one month storage at room temperature was comparable to doses of phage reported in the literature regarding therapeutic application in man. A relatively high residual water content was shown to arise from the hygroscopic nature of the phage.

SEM micrographs showed that the phage-CMC morphology was dependent on the amino acid carrier: glutamine generating a thin layer morphology, with glycine generating well-defined, discrete spherical aggregates.

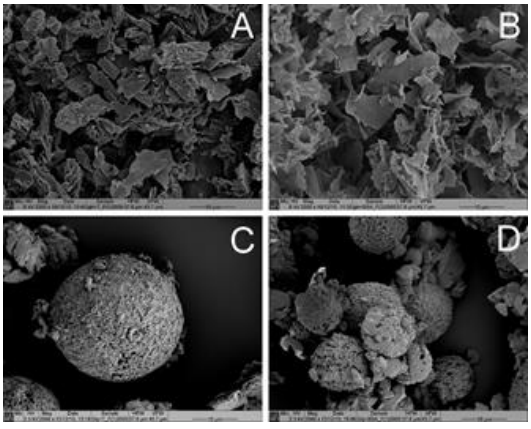

Fig.1. SEM micrographs of dried phage-CMC generated from mixing with isopropanol. (A) Gln and 5 % w/w trehalose, (B) Gln and 5 % w/w BSA, (C) Gly and 5 % w/w trehalose, (D) Gly and 5 % w/w BSA.

CONCLUSION

These results demonstrate a feasible and novel approach for the storage and transport of phage in the solid state. The method would also allow rapid concentration of phage from dilute solutions.

ACKNOWLEDGMENTS

The author thanks the Saudi Government for the funding towards this work. The project was also supported by the Bioprocessing Research Industry Club (BRIC)-UK. Electron micrographs were prepared with technical support from Margaret Mullin, Electron Microscopy Unit, University of Glasgow, UK.

REFERENCES

[1] M. Kreiner and M.C Parker, "High-activity biocatalysts in organic media: solid-state as the immobilisation matrix for protein-coated microcrystals" *Biotechnol Bioeng*., **87**(2004) 24-33.

[2] U. Puapermpoonsiri, S.J. Ford and C.F. Walle, "Stabilization of phage during freeze drying" *Int J Pharm.*, **389** (2010) 168-175.

[3] E. Alvarez-Gonzalez, M. Alfadhel, P. Mane, S.J. Ford, B.D. Moore and C.F. Walle, "Bioprocessing of bacteriophages via rapid drying onto microcrystals". *Biotechnol. Prog*., **28** (2012) 540-548.

International Journal of Pharmaceutics 416 (2011) 280–287

Contents lists available at ScienceDirect

International Journal of Pharmaceutics

journal homepage: www.elsevier.com/locate/ijpharm

Lyophilized inserts for nasal administration harboring bacteriophage selective for *Staphylococcus aureus*: In vitro evaluation

Munerah Alfadhel[a], Utsana Puapermpoonsiri[a,1], Steven J. Ford[b], Fiona J. McInnes[a], Christopher F. van der Walle[a,*]

[a] Strathclyde Institute of Pharmacy and Biomedical Sciences, University of Strathclyde, 161 Cathedral St., Glasgow G4 0RE, UK
[b] Cancer Research UK Formulation Unit, University of Strathclyde, 161 Cathedral St., Glasgow G4 0RE, UK

ARTICLE INFO

Article history:
Received 30 April 2011
Received in revised form 1 July 2011
Accepted 4 July 2011
Available online 13 July 2011

Keywords:
Bacteriophage
Staphylococcus aureus
Nasal insert
Lyophilization
Hydroxypropyl methylcellulose

ABSTRACT

Nasal carriage of methicillin-resistant *Staphylococcus aureus* (MRSA) poses an infection risk and eradication during hospitalization is recommended. Bacteriophage therapy may be effective in this scenario but suitable nasal formulations have yet to be developed. Here we show that lyophilization of bacteriophages in 1 ml of a viscous solution of 1–2% (w/v) hydroxypropyl methylcellulose (HPMC) with/without the addition of 1% (w/v) mannitol, contained in Eppendorf tubes, yields nasal inserts composed of a highly porous leaflet-like matrix. Fluorescently labeled bacteriophage were observed to be homogenously distributed throughout the wafers of the dried matrix. The bacteriophage titer fell 10-fold following lyophilization to 10^8 pfu per insert, then falling a further 100- to 1000-fold over 6 to 12 months storage at 4 °C. This compares well with a total dose of 6×10^5 pfu in 0.2 ml liquid applied into the ear during a recent clinical trial in humans. The residual water content of the lyophilized inserts was reduced upon the addition of mannitol to HPMC, but this did not have any correlation to the lytic activity. Mannitol underwent a transition from its amorphous to crystalline state during exposure of the inserts to increasing relative humidities (as would be experienced in the nose), although this transition was suppressed by higher HPMC concentrations and the presence of buffer containing gelatin and bacteriophages. Our results therefore suggest that lyophilized inserts harboring bacteriophage selective for *S. aureus* may be a novel means for the eradication of MRSA resident in the nose.

1. Introduction

Bacteriophages have long been known to be clinically effective and safe to use in animals and humans (Weber-Dabrowska et al., 2000). Their administration commonly involves only simple solutions for oral or topical administration (Soothill et al., 2004). For example, concurrent bacterial infection including septicemia in patients was reportedly treated after oral administration of bacteriophages three times a day (Weber-Dabrowska et al., 2001, 2003). Controlled release formulations of bacteriophages have included the development of microencapsulated bacteriophage Felix O1 for oral delivery using chitosan-alginate-$CaCl_2$ systems (Ma et al., 2008), and polyester microspheres as dry powders for pulmonary delivery (Puapermpoonsiri et al., 2009). Pulmonary delivery of a *Burkholderia capacia* complex (BCC) bacteriophage by nebulization has demonstrated that bacteriophages can successfully reduce bacterial lung infection (Golshahi et al., 2008). However, it is only recently that a controlled clinical trial has been reported, investigating the efficacy and safety of bacteriophages in ear drop preparations for the treatment of antibiotic resistant *Pseudomonas aeruginosa* in chronic otitis (Wright et al., 2009).

The current emergence and spread of profoundly antibiotic resistant pathogens is well documented. Methicillin-resistant *Staphylococcus aureus* (MRSA) is a major source of antibiotic resistant infections in hospitals and the community, though nasal decolonization offers an effective treatment strategy (Critchley, 2006). The nasal cavity is a common route for local and systemic drug delivery, including poorly bioavailable polar drugs such as peptides, since the 'first pass' hepatic metabolism is avoided (Illum, 2003). The nose is highly vascularized and the tight junctions of the nasal epithelium may be transiently loosened during dehydration to delivery vehicles (Arora et al., 2002). However, mucociliary transport is rapid, which decreases the residence time to short periods of less than 30 min (Mygind and Dahl, 1998). It is for this reason that oligosaccharide bioadhesive polymers are attractive (Henriksen et al., 1996; Soane et al., 1999), since their hydration at the mucosa

* Corresponding author. Tel.: +44 0141 548 5755; fax: +44 0141 552 6443.
E-mail address: chris.walle@strath.ac.uk (C.F. van der Walle).
[1] Current address: Faculty of Pharmaceutical Sciences, Ubon Ratchathani University, Ubon Ratchathani 34190, Thailand.

0378-5173/$ – see front matter © 2011 Elsevier B.V. All rights reserved.
doi:10.1016/j.ijpharm.2011.07.006

promotes extensive hydrogen bonding and physical entanglement with mucin chains in the mucus layer (Mortazavi, 1995).

In this study, hydroxypropyl methylcellulose (HPMC) was selected because of its high viscosity on rehydration *in situ* which may explain why, in animal models, HPMC formulations have been observed to result in longer drug residence times in the nasal cavity (McInnes et al., 2005). HPMC nasal inserts lyophilized from HPMC solutions between 1 and 3% are tolerated in humans; with the 1 and 2% HPMC formulations showing good hydration and spreading properties and, for the 2% HPMC formulation, extending nasal residence times to over 4 h (McInnes et al., 2007b). It is hypothesized that, upon application of the HPMC nasal insert, water sorption from the nasal mucosa results in a higher HPMC gel concentration than that prepared prior to lyophilization; the highly viscous gel then attenuates mucociliary clearance.

Although lyophilization is one of several methods for long term bacteriophage storage (Ackermann et al., 2004; Fortier and Moineau, 2009), the process may cause protein denaturation (Ma et al., 2008). This is of concern given the complex nature of the head and tail structure of bacteriophages of the Siphoviridae family used in this study (Puapermpoonsiri et al., 2010). For this reason, mannitol was investigated as a stabilizer since it is a non hygroscopic material used extensively as an excipient (Rowe et al., 2009) and as a lyoprotectant during lyophilization of complex biopharmaceuticals including plasma (Bakaltcheva et al., 2007) and immunoglobulin-G (Schule et al., 2007). However, characterization of the amorphous/crystalline forms of mannitol following lyophilization is required since this can affect solid state stability (Torrado and Torrado, 2002). The present study evaluates the viability and stability of bacteriophages in lyophilized HPMC/mannitol formulations, characterizing the residual water, water sorption and solid state of the lyophilizates.

2. Materials and methods

2.1. Materials

Hydroxypropyl methylcellulose (HPMC) powder K4MP grade was obtained from Dow Chemicals, Michigan, IL, USA. D-mannitol powder was purchased from VWR International, Lutterworth, UK. Granulated agar, tryptone, yeast extract and sodium chloride were all purchased from Melford Laboratories, Ipswich, UK. Trizma base, magnesium sulphate heptahydrate, gelatin, fluorescein isothiocyanate (FITC) and methanol were purchased from Sigma–Aldrich, Dorset, UK. Dichloromethane (DCM) and methanol were purchased from Fisher Scientific, Leicestershire, UK. All chemicals were at analytical grade or equivalent.

2.2. Bacterial and bacteriophage strains

The bacterial strain used as a model for MRSA was *S. aureus* FDA209 P variant, acquired from the NCIMB, Aberdeen, UK (strain 8588; ATCC ref: 11522). The bacteriophage selective for this *S. aureus* strain is of the family Siphoviridae and was acquired from the NCIMB, Aberdeen, UK (cat. no. 9563; ATCC ref: 6538-B).

2.3. Culture conditions

S. aureus bacterial cultures were grown in Luria Bertani (LB) medium (1% tryptone, 1% yeast extract, 0.5% NaCl). Frozen stocks were initially streaked and grown on LB medium containing 1.5% agar, to select for individual colonies. Cells were cultured by inoculating 5 ml of LB medium with a single colony of *S. aureus* bacteria and incubating overnight at 37 °C with vigorous shaking. These overnight cultures were then used for bacteriophage preparation.

2.4. Bacteriophage preparation

A mixture of 300 μl bacterial culture and 450 μl bacteriophage stock solution (10^9–10^{10} plaque forming units per ml (pfu/ml) was incubated for 20 min at 37 °C, and 200 μl was then added to 4 ml of partially cooled LB agar (LB broth containing 1.5% agar). This partially cooled LB agar containing bacteriophage was poured onto a LB agar plate which was then incubated at 37 °C overnight. Bacteriophages were collected by adding 5 ml of storage medium (SM) buffer (1 M Tris–HCl; 2 g/l $MgSO_4 \cdot 7H_2O$; 0.1 M NaCl; 0.1 g/L gelatin, pH 7.5) to flood the plates which were kept at 4 °C for 3–4 h and swirled gently every 0.5 h. Bacteriophages were then collected by decanting the storage medium from the plates which then filtered by using 0.22 μm pore size filter (Millipore Ltd., Watford, UK), and stored at 4 °C.

2.5. Bacteriophage titration (plaque assay)

The lytic activity of the bacteriophage (the phage titer) was determined by plaque assay. To determine the phage titer, a bacteriophage stock solution was titrated by 10-fold serial dilutions in SM buffer and 100 μl of each dilution was mixed with 100 μl of overnight bacterial culture. The mixture was added to 4 ml of partially cooled LB agar and poured onto LB agar plates. Plates were then incubated overnight at 37 °C. The number of plaques was counted the following day and used to calculate the concentration of bacteriophage (pfu/ml). A negative control (bacterial culture without bacteriophage) and positive control (bacterial culture with a known concentration of bacteriophage) were also prepared for comparison. To determine the residual lytic activity of the lyophilized bacteriophage in the nasal inserts, each lyophilizate was reconstituted in 1 ml sterile water and the plaque assay was performed from the serial dilutions as above. Phage titers were calculated from the dilutions giving a countable number of plaques (<300) per plate, this was generally around a dilution of 10^6. Bacteriophage formulations before lyophilization were also tested for lytic activity, in order to evaluate the effect of lyophilization and storage on phage integrity.

2.6. Bacteriophage purification

Purified bacteriophages were prepared using a modified method (Sambrook and Russell, 2001). Briefly, 0.5 g caesium chloride (CsCl) was added to each ml of bacteriophage solution and allowed to dissolve. A step gradient was prepared by pouring 2 ml of CsCl solutions of decreasing density (1.7, 1.5, and 1.4 g/ml) on top of one another in a thick-walled 38 ml polycarbonate centrifugation tube (Beckman–Coulter, High Wycombe, UK). The aqueous solution of bacteriophage in CsCl was then carefully poured on top of these layers, and the interface between the layers was marked on the outside of the tube. After centrifugation at 22,000 rpm in a Beckman SW 28 rotor (64,000 × *g*) at 4 °C for 2 h a visible bluish band was formed at the interface between the CsCl solutions of 1.4 and 1.5 g/ml densities. This band was carefully collected using a syringe with small bore needle (21G) and stored at 4 °C to use for labeling or formulation. The lytic activity (titer) of the purified bacteriophage solution was tested by plaque assay as above.

2.7. Fluorescein labeling

Fluorescein isothiocyanate powder (FITC), 0.5 g, was added to 1 ml of purified bacteriophage solution and diluted in 10 ml of 46 mM $NaHCO_3$ (pH 9) and shaken gently for 2 h. The resulting suspension was centrifuged briefly and dialyzed extensively in phosphate buffered saline (PBS), pH 7.4, by 3× exchange over

24 h, using a cellulose dialysis bag with a MW cut-off of 12,400 Da (D9777, Sigma–Aldrich, UK).

2.8. Preparation of formulations

Control samples (labeled C) were prepared by dissolving the required amount of HPMC powder in one third of the final volume of sterile distilled water (at 80–90 °C), by slow addition of HPMC with stirring until a consistent dispersion was obtained. The remaining amount of sterile water was then added (using water at room temperature) and stirring was continued until a uniform gel of 1% and 2% (w/v) HPMC was obtained. The required mass of mannitol powder was also added, where appropriate, to produce a concentration of 1%. The gel was stored at 4 °C overnight to partially degas the gel and allow complete hydration of the polymer chains. Blank samples (labeled B) were prepared as above but using sterile storage media (SM) instead of sterile distilled water. Formulated samples (labeled F), for inserts harboring bacteriophages, were prepared as for the blank samples, but adding the required amount of stock phage solution to the aqueous HPMC dispersion with gentle stirring.

2.9. Lyophilization of formulations

Nasal inserts were prepared by lyophilizing 1 ml of formulation solution (Table 1) in a 1.5 ml Eppendorf tube using a VirTis AdVantage freeze-dryer (VirTis, USA). The freeze-drying protocol was carried out following a method previously devised for bacteriophage (Puapermpoonsiri et al., 2010): freezing was initiated by cooling to 5 °C for 30 min, followed by cooling to −5 °C at a rate of 1 °C/min, held for 30 min, and then to −30 °C at 1 °C/min, held for 1 h; primary drying was started at −30 °C with a chamber pressure of 100 mTorr for 1000 min, with secondary drying following heating to 25 °C at 1 °C/min, maintained for 6 h under vacuum. After lyophilization, the samples were collected and stored in a container with silica gel at 4 °C. The lytic activity of the bacteriophage from the lyophilizate was tested at day 1, 4, 7, 14, 30, 60, 180, 240 and 360.

To investigate the effect of the freezing and drying protocol on lyophilizate morphology, a simple rapid freeze/dry protocol was also used, involving freezing of gels to −80 °C over 30 min and subsequent drying at 10 °C for 24 h under vacuum (MicroModulyo, Thermo Scientific Ltd., UK).

2.10. Scanning electron microscopy (SEM)

Lyophilized samples were prepared by cutting a section of the sample with a sharp scalpel blade, fixed onto metal stubs using double-sided adhesive copper tape and coated with gold under vacuum. Samples were imaged using a Jeol JSM-6400 scanning electron microscope at 10 kV intensity, at the electron microscopy facility at the University of Glasgow, UK.

2.11. Confocal laser scanning microscopy (CLSM)

Lyophilizates for CLSM were prepared as above but using fluorescein labeled bacteriophage during formulation. A small section of the lyophilizate for each formulation was placed on a glass slide and covered with a cover slip. Samples were analyzed and imaged on a Leica DM 6000B microscope at the Centre for Biophotonics, University of Strathclyde, using an Argon laser line at 488 nm with emission bandwidth of 521–616 nm. Scans were performed using 10× and 20× objectives and images were converted with Volocity® software (Improvision, PerkinElmer, Cambridge, UK).

2.12. Residual water content

Gel samples of 1 g were formulated as above but lyophilized in 10 ml, tared glass vials. The mass of the dried cakes was obtained by difference and the vials were then stored in an air-tight box at 4 °C. For residual water determination, the dried cakes were reconstituted with 4 ml solvent mixture (dichloromethane and methanol 50:50). The mass of the solvent for each sample was obtained and a blank sample containing a known solvent mass was also prepared. The water content of each cake was determined by the Karl Fischer (KF) titration method (Mettler Toledo DL 37, Leicester, UK). After calibration with a Karl Fischer water content standard (Hydranal, Sigma–Aldrich, Gillingham, UK), the apparatus was used to determine the water content of the blank solvent mixture. The water content for each formulation was determined twice from four independent samples and the result of the titration was expressed as a percentage.

2.13. Dynamic vapor sorption (DVS)

The isothermal sorption behavior was studied using a DVS 1000, Surface Measurement Systems, Cheshire, UK, consisting of a highly sensitive Cahn microbalance to measure any changes in the mass of the sample as a result of sorption or desorption of water vapor. The method of McInnes et al. (2007a) was followed. Briefly, samples were subjected to a controlled cycle of relative humidity (RH) ranging from 0 to 95% in stepwise increments of 10%. RH was then decreased through the same steps. Changes in the mass of the sample due to sorption or desorption of moisture were expressed as a percentage of its dry mass.

2.14. Differential scanning calorimetry (DSC)

Samples of 4–6 mg were accurately weighed into 40 μl aluminium pans, hermetically sealed with pin-hole lids, and heated under a nitrogen purge in a Mettler Toledo DSC822e (Mettler–Toledo, Leicester, UK). Thermal transitions for the blank and test lyophilized samples were analyzed using a modulated DSC method for determination of the glass transition (T_g) of HPMC, and a standard linear DSC method to determine the crystallization and melting events of mannitol. The T_g of HPMC was represented in the reversing signal and the mid-point of the T_g determined at a heating rate of 2 °C/min from 25 to 240 °C. A quench-cool method was used for determination of the enthalpy of crystallization (ΔH_c) for mannitol from 25 to 200 °C at a heating rate of 10 °C/min. The data analysis was performed using Mettler STARe software.

3. Results and discussion

3.1. Bacteriophages remain relatively stable over one year storage in the lyophilized inserts

There is no current guidance on the bacteriophage titer that may be clinically effective against MRSA resident in the (human) nose, though some indications can be obtained from previous related studies of bacteriophage therapy. For example, the bacteriophage titers for respirable powders developed by Golshahi et al. (2010), were *ca.* 10^8–10^9 pfu per 100 mg of powder, with a single dose capsule load for inhalation of *ca.* 10^7–10^8 pfu. Furthermore, in a clinical trial testing the efficacy and safety of bacteriophages targeting *Pseudomonas aeruginosa* in otitis in humans, 10^5 pfu of each of six bacteriophages in 0.2 ml liquid was applied into the ear (Wright et al., 2009). On consideration of these two studies, we aimed for a bacteriophage titer of 10^9 pfu per nasal insert, pre-lyophilization, with the expectation that the titer would fall following lyophilization. Loss of titer has been previously reported (Puapermpoonsiri

Table 1
Notation and composition of the test and control formulations described in this study.

Notation/formulation	C1	C2	C3	C4	B1	B2	B3	B4	F1	F2	F3	F4
HPMC	1%	1%	2%	2%	1%	1%	2%	2%	1%	1%	2%	2%
Mannitol	–	1%	–	1%	–	1%	–	1%	–	1%	–	1%
Phage stock 10^{10} pfu/ml	–	–	–	–	–	–	–	–	10%	10%	10%	10%
	Diluent = sterile water				Diluent = storage media				Diluent = storage media			

et al., 2010) and is most likely associated with conformational changes to the bacteriophage protein coat, since proteins are well known to experience stress during freezing and drying. The plaque assay was used to determine the lytic activity of the bacteriophages in the formulations by enumeration of observable plaques, wherein each observed plaque represents a single phage.

The results presented in Table 2 show the lytic activity of the bacteriophages before and after lyophilization of the formulations. Enumerating the plaques for a given dilution enabled calculation of the bacteriophage titer that would have been present in each undiluted sample tested. A titer of 10^9 pfu/ml was calculated for the HPMC/mannitol gel formulations prior to lyophilization, indicating that there was no loss of lytic activity during mixing of the bacteriophages into the gels (since the titers added to the gel were consistently 10^{10} pfu/ml and a 10-fold dilution of the bacteriophage stock was made). In contrast, lyophilization of formulations resulted in a titer of 10^8 pfu/ml, which implied that 90% of the original lytic activity had been lost. Although this may seem high, this loss was less than or equivalent to previous losses following encapsulation (Puapermpoonsiri et al., 2009), or lyophilization with high concentrations of sucrose (Puapermpoonsiri et al., 2010). A titer of 10^8 pfu/ml is still considerable, comparable with bacteriophage doses of *ca.* 10^7–10^8 pfu for inhalation (Golshahi et al., 2010) and 6×10^5 pfu for dosing of the ear (Wright et al., 2009); this warranted long term stability testing of the lyophilized inserts.

From Table 2, the lytic activity was seen to decrease around 10- to 1000-fold over 1–12 months storage at 4 °C: lytic activity decreased from 10^8 pfu/ml on day 1 to around 10^7, 10^6 and 10^5 pfu/ml after 1, 2 and 12 months, respectively. The stability of the bacteriophage in the lyophilized nasal inserts was therefore far greater than for encapsulated phage in polyester matrices, wherein no lytic activity was observed after 1 week (Puapermpoonsiri et al., 2009). This was encouraging, particularly since the bacteriophage titer in the inserts after 12 months may still represent a therapeutic dose (Wright et al., 2009). No particular correlation could be observed between the formulations and the bacteriophage titers; *i.e.* neither the addition of mannitol nor the higher HPMC concentration conferred any additional benefit as regards long-term stabilization of the bacteriophages. The addition of HPMC at either 1 or 2% brings about 'molecular crowding' through excluded volume effects experienced by the bacteriophage, a phenomenon well understood through studies using macromolecules such as polyethylene glycol (PEG), dextran and Ficoll, or sol–gels (Eggers and Valentine, 2001). The concentrations required to bring about molecular crowding using PEG or dextran are equivalent to the HPMC concentrations used here (Dominak et al., 2010). While the excluded volume experienced by the bacteriophage increases for further addition of HPMC and/or mannitol, this does not necessary imply further change to the lytic activity since the effect of a concomitant increase in viscosity in these systems remains unknown. A 1% HPMC concentration would therefore appear to be sufficient as regards cryo- and lyoprotection of the bacteriophages. The stabilizing effect of HPMC is greater than the stabilization of bacteriophage by PEG 6000 (Puapermpoonsiri et al., 2010), and would suggest that high molecular weight, polyol polymers are useful formulation excipients for bacteriophages.

However, a simple explanation involving stabilization of protein (bacteriophage coat) structure via polyols, is not complete. This is because sucrose conferred no additional stability to lyophilized bacteriophages tested over 30 days (Puapermpoonsiri et al., 2010). Similarly, the lytic activity of the bacteriophages lyophilized from 1% solutions of mannitol, *i.e.* without the addition of HPMC, showed a large loss of around 6 log cycles by day 1 (Supplementary Data, Table S1). A further consideration involves the possible adsorption of the bacteriophages to crystalline domains of mannitol within the lyophilizate. This method of surface stabilization would reflect that proposed for protein coated microcrystals which have been shown to stabilize both enzymes and DNA through surface adsorption to the crystalline carriers during dehydration (Kreiner et al., 2005; Moore et al., 2010). However, given that mannitol conferred no additional stabilizing effect, this mechanism is unlikely to play a significant role in these studies. The addition of mannitol is therefore only justified in order to improve the strength of nasal inserts, as previously described (McInnes et al., 2007a). Stabilization conferred through immobilization of the bacteriophages onto the HPMC matrix is also unlikely since immobilization onto polyester matrices retained lytic activity for only 7 days (Puapermpoonsiri et al., 2009). Molecular crowding is well known to increase the conformational stability of

Table 2
Calculated phage titer for each phage formulation during storage at 4 °C.

	F1 (titer ± SD)[a], pfu/ml	F2 (titer ± SD)[a], pfu/ml	F3 (titer ± SD)[a], pfu/ml	F4 (titer ± SD)[a], pfu/ml
Before lyophilization	$(8.90 \pm 7.5) \times 10^9$	$(5.53 \pm 8.5) \times 10^9$	$(2.90 \pm 8.4) \times 10^9$	$(4.00 \pm 4.5) \times 10^9$
Day(s) after lyophilization				
1	$(4.40 \pm 5.2) \times 10^8$	$(8.53 \pm 1.4) \times 10^8$	nd	$(8.70 \pm 1.2) \times 10^8$
4	$(4.27 \pm 2.2) \times 10^8$	$(1.47 \pm 4.7) \times 10^8$	$(3.93 \pm 2.6) \times 10^8$	$(7.37 \pm 4.0) \times 10^8$
7	$(3.53 \pm 1.7) \times 10^8$	$(3.20 \pm 1.2) \times 10^8$	$(3.90 \pm 1.1) \times 10^8$	$(4.20 \pm 7.9) \times 10^8$
14	$(5.00 \pm 2.0) \times 10^7$	$(1.03 \pm 1.0) \times 10^8$	$(5.77 \pm 1.5) \times 10^8$	$(1.21 \pm 8.8) \times 10^9$
21	$(8.00 \pm 1.4) \times 10^7$	$(1.33 \pm 7.5) \times 10^8$	$(1.53 \pm 1.0) \times 10^8$	$(6.60 \pm 7.0) \times 10^8$
30	$(2.60 \pm 2.7) \times 10^7$	$(6.00 \pm 4.3) \times 10^7$	$(4.33 \pm 2.5) \times 10^7$	$(4.00 \pm 1.4) \times 10^8$
60	$(7.33 \pm 1.1) \times 10^6$	$(9.00 \pm 5.5) \times 10^6$	$(8.67 \pm 5.1) \times 10^6$	$(3.47 \pm 8.5) \times 10^7$
180	$(8.07 \pm 9.5) \times 10^6$	$(4.13 \pm 2.3) \times 10^6$	$(3.25 \pm 3.5) \times 10^6$	$(8.87 \pm 1.0) \times 10^6$
240	$(5.33 \pm 8.5) \times 10^6$	$(5.67 \pm 8.9) \times 10^6$	$(6.00 \pm 1.9) \times 10^6$	$(1.32 \pm 3.1) \times 10^7$
360	$(2.23 \pm 1.2) \times 10^6$	$(4.67 \pm 1.5) \times 10^5$	$(8.00 \pm 4.5) \times 10^5$	$(2.30 \pm 7.9) \times 10^6$

[a] Each value represents an average from three independent experiments; nd, not determined.

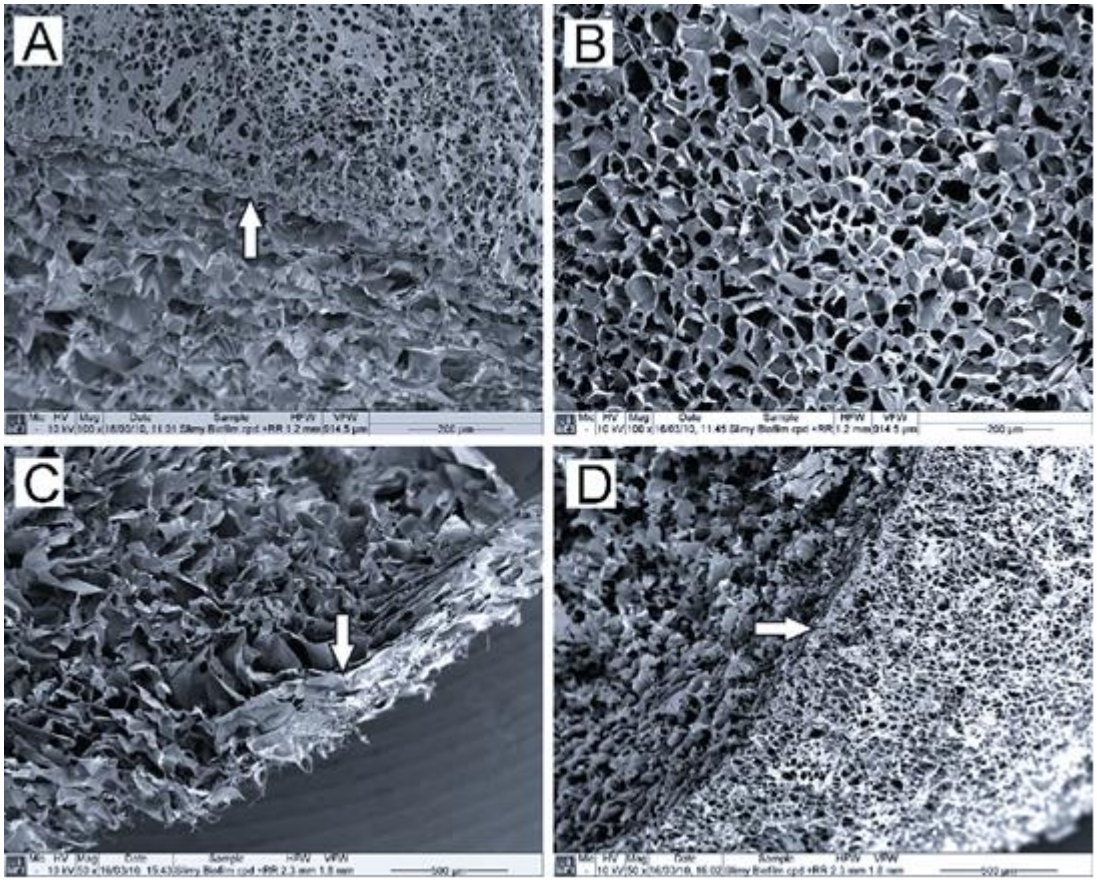

Fig. 1. Representative scanning electron micrographs for lyophilized nasal inserts, comparing the controls against formulations containing bacteriophage. (A) 1% HPMC; (B) 1% HPMC/1% mannitol; (C) 1% HPMC containing bacteriophage; (D) 1% HPMC/1% mannitol containing bacteriophage. The white arrows point from the internal matrix to the boundary with the surface of the insert. The scale bar is shown in bottom right of each pane.

proteins (Eggers and Valentine, 2001) and this effect may have contributed to the observed stabilization of the bacteriophage by HPMC.

Another explanation for the observed lytic activities is to compare the T_g of the amorphous materials: the T_g of the polyester used was ~45 °C (Rouse et al., 2007), while the T_g for sucrose is ~72 °C (Puapermpoonsiri et al., 2010). Differential scanning calorimetry (DSC) is widely used for the determination of the T_g of amorphous materials and modulated temperature DSC (MTDSC) has been shown to be applicable to the study of HPMC blends (Nyamweya and Hoag, 2000). We also chose MTDSC since the T_g of HPMC can be obscured by an associated enthalpic relaxation peak, which for some amorphous materials can be considerable (Rouse et al., 2007). The midpoint of the T_g of HPMC for formulations without mannitol was consistent, varying around 186 ± 7 °C (Table 3). The T_g values are also in agreement with previous data, reporting the T_g of HPMC K4M powder to be 184 °C (Doelker, 1993). The range in the T_g values reported is reasonable given that the change in the heat capacity of HPMC during the transition event was small, making the extrapolation of the baseline less certain. The difference in the values may also reflect the difference in the water content of the samples, since water is well known plasticizer of amorphous materials, with a general tendency to decrease the T_g (Hagens et al., 2004; Bouissou et al., 2005). It was not possible to observe the small T_g for HPMC when mannitol was added to the formulations. The T_g of the excipient may therefore relate to the resultant stability of the formulated bacteriophage in the solid state; i.e., the more stable the excipient's amorphous state, the more stable the lyophilized bacteriophages remain.

Table 3
Glass transition temperature (T_g) of HPMC polymer for different formulations.

Formulation	HPMC powder[a]	C1	C3	B1	B3	F1	F3
T_g (°C)	187	190	188	192	188	179	186

[a] As received.

further distinction. To investigate the effect of the lyophilization protocol on lyophilizate morphology, a rapid freezing/rapid drying protocol was used. The structure of the lyophilizate remained composed of individual leaflets but the porous structure had been changed to a structure better described as lamellar (Supplementary Data, Fig. S1). This presumably represents the formation of large sheet-like ice crystals during the rapid freezing step, since similar structures have been described as a consequence of changes in ice nucleation (Searles et al., 2001). Thus, the morphology of the nasal insert would appear to be reproducible so long as careful control over freezing and drying steps can be maintained throughout the lyophilization process.

To examine possible aggregation and/or localization of the bacteriophages during the freeze-dry steps, the distribution of fluorescein-labeled bacteriophages was visualized by CLSM. Confocal micrographs show the bacteriophages to be distributed in a homogenous manner throughout the lyophilizate (Fig. 2), which reflects the overlapping of the leaflets and pore structure observed by SEM (cf. Fig. 1). Although it is not possible to resolve nanometer-sized aggregates of small numbers of bacteriophages in these images, there is no evidence of gross aggregation or localization of the bacteriophages, *i.e.* the freezing step would appear to have avoided slow formation of ice crystals and supersaturated regions of liquid.

3.3. Residual water content and water sorption of the lyophilizates

Residual moisture content is an important consideration for both the stability of the bacteriophage and amorphous polymeric materials. Fig. 3 shows that the addition of mannitol to the HPMC gels appeared to promote the drying of the lyophilizate, particularly

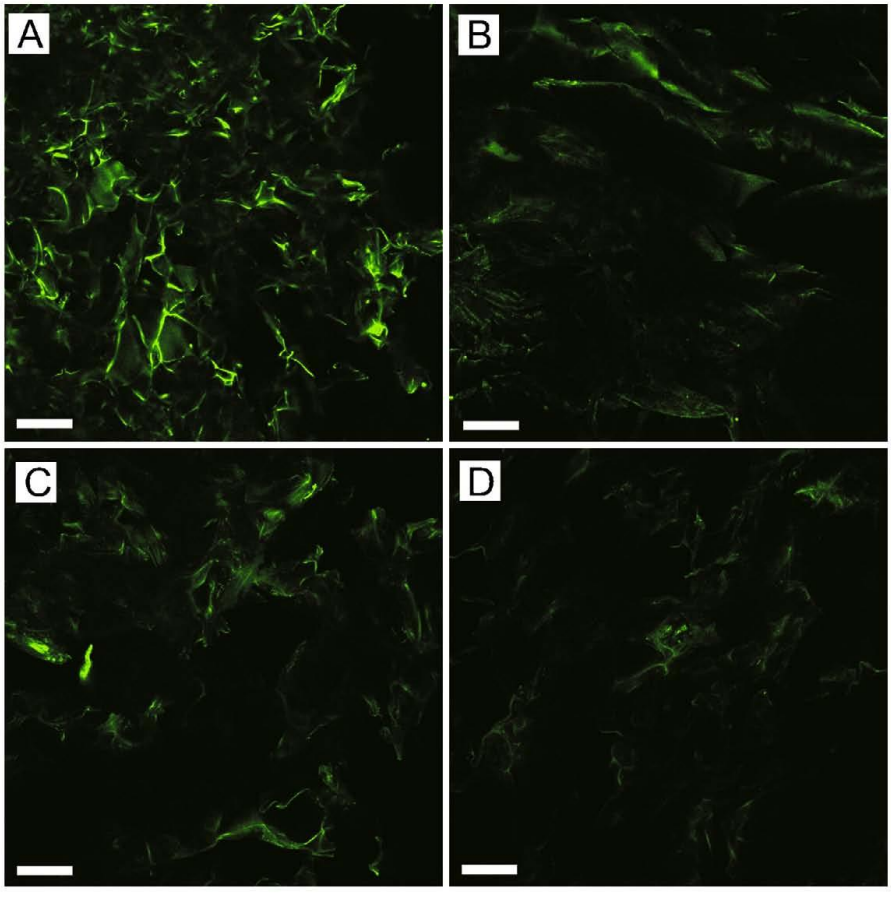

Fig. 2. CLSM images of fluorescein-labeled bacteriophage distributed through the lyophilized formulations. (A) 1% HPMC; (B) 1% HPMC/1% mannitol; (C) 2% HPMC; (D) 2% HPMC/1% mannitol. Bar = 250 μm.

for the 1% HPMC formulations, maybe due to its non-hygroscopic nature; although the difference between formulations F3 and F4 was not statistically significant ($P > 0.01$). Previous studies with lyophilized bacteriophages suggested that a more porous cake resulted in better mass transfer and lower residual moisture, with a value of 4–6% correlating to maximum retention of bacteriophage titer (Puapermpoonsiri et al., 2010). Except for the 1% HPMC/1% mannitol lyophilizate, the residual moisture content in these formulations was comparatively high. The resultant stability of the formulations over 12 months storage would therefore not have been predicted, and corroborates the suggestion above that the high T_g of the HPMC is more important in maintaining the stability of the bacteriophages. These HPMC/mannitol formulations are therefore not comparable to lyophilized formulations designed for reconstitution to yield non-viscous fluids for injection or nebulization, for example.

DVS was used to mimic the water sorption that may be experienced by the lyophilized inserts in the nose. The water sorption profiles showed an increase in mass as a result of exposure to increasing relative humidities (RH) to 95%, and corresponding drying as RH returned to zero (Fig. 4). For lyophilizates containing mannitol, a small but noticeable mass loss was observed during the water sorption phase between 5 and 10% RH. This was due to the transformation of amorphous mannitol to the crystalline form, with concomitant loss of water from the lyophilizate. Mannitol itself adsorbed very little water vapor during the same cycle: showing only a 0.3 and 1% mass increase for the powder as received and lyophilized, respectively. In contrast, HPMC powder (as received) displayed a 30% increase in mass for the same cycle. The addition of mannitol reduced water sorption only for the control samples and, to a lesser extent, the blank and bacteriophage formulations containing 1% HPMC (Fig. 4). However, the water sorption profile was not determined only by HPMC since a marked difference was observed between inserts formulated with water (28–52% mass increase), storage media (67–102% mass increase) and bacteriophage (101–143% mass increase). Since the storage medium contained buffer salts and gelatin, the gelatin component is most likely responsible for the difference between the control and blank samples, since proteins are well known to retain 'bound' water and gelatin powder is deliquescent. This was confirmed by DVS analysis for gelatin powder alone, which demonstrated a 41% mass increase over the same cycle. The difference between the blank and bacteriophage samples is therefore due to the bacteriophage themselves, presumably for the same reason of bound water associated with the protein capsule coat. Our results agree well with those for comparable lyophilized formulations in the study by McInnes et al. (2005), who showed that HPMC absorbs more than 50% of its dry mass while mannitol demonstrated very low water vapor sorption.

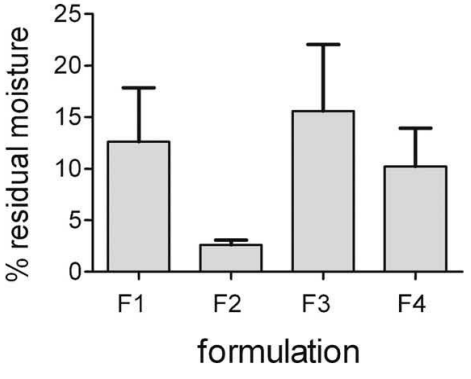

Fig. 3. Residual moisture content of the lyophilized bacteriophage formulations.

Table 4
Heat of crystallization (ΔH_c) values for mannitol in different formulations.

Formulation	ΔH_c (mJ)[a]
Mannitol powder[b]	1120
Mannitol lyophilizate	798
HPMC/mannitol physical mixture 1:1	488
HPMC/mannitol physical mixture 2:1	251
C2	360
C4	99
B2	231
B4	44
F2	58
F4	9

[a] Calculated from the integral of the exothermic ΔH_c peak for thermograms normalized by the mass of sample analyzed.
[b] As received.

Since it has been reported that polymeric excipients inhibit crystal transformation by slowing crystal growth or by removing excess water by absorption (Tian et al., 2007), we investigated if this was also true for the lyophilizates. Following a quench-cool cycle in order to transfer the mannitol into its amorphous state, DSC thermograms showed an exothermic re-crystallization peak followed by an endothermic melting peak at 166 °C, corresponding to previous data (Torrado and Torrado, 2002). The heat of crystallization (ΔH_c) was determined for each formulation after normalization of the thermograms (Table 4). A clear decrease in the ΔH_c for mannitol was observed upon the addition of HPMC in simple powder blends, dependent on the relative amount of HPMC added. ΔH_c values for the corresponding lyophilized mixtures (C2 and C4) also indicated that re-crystallization of mannitol was directly inhibited by HPMC.

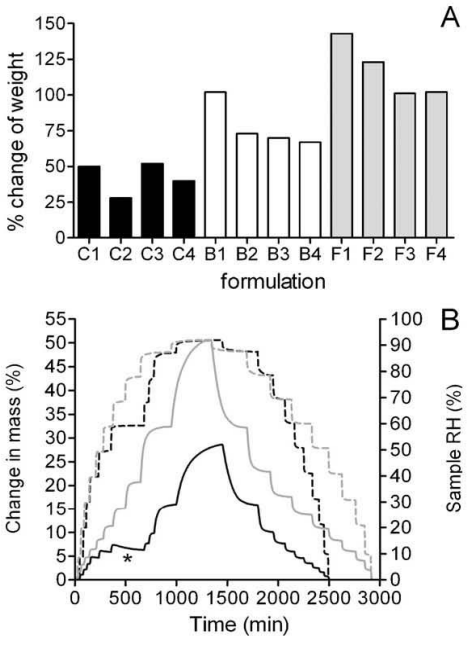

Fig. 4. (A) Percentage change in mass obtained during dynamic vapor sorption for the lyophilized formulations (at 95% RH). (B) Example profiles of the percentage change in sample mass (solid lines) versus RH (dashed lines) for formulations C1 (grey lines) and C2 (black lines); the * indicates the loss of mass as a consequence of the change from amorphous to crystalline mannitol.

The addition of storage media containing gelatin further decreased the ΔH_c (B2 and B4), with the presence of bacteriophage in the 2% HPMC formulation (F4) almost completely attenuating mannitol re-crystallization. The inhibition of mannitol re-crystallization by proteinaceous material has been previously reported (Hawe and Friess, 2006), consistent with the respective changes to ΔH_c seen between the control and blank/bacteriophage formulations. Given these data, it is reasonable to assume that the amorphous form of mannitol is stabilized to varying extents in the lyophilizates, dependent on the original percentage of HPMC in the gel and the presence of gelatin and bacteriophages.

4. Conclusions

Lyophilized nasal inserts harboring doses of bacteriophage corresponding to doses used in previous clinical trials of bacteriophage therapy can be formulated and remain stable in the fridge for up to 1 year. The addition of mannitol to the lyophilizate does not confer added stability to the bacteriophages and may be omitted if this was the sole consideration. However, given that lyophilization can be a costly step, formulations which dry to a defined percentage more rapidly may be preferred on these grounds, in which case the 1% HPMC/1% mannitol formulation would be preferred. Increasing the relative amount of HPMC in the blend with mannitol would appear to stabilize the amorphous form of mannitol in the lyophilizate, though transition of mannitol from its amorphous to crystalline form does not affect bacteriophage stability, the structure of the internal matrix, or the distribution of the bacteriophages with the matrix.

Appendix A. Supplementary data

Supplementary data associated with this article can be found, in the online version, at doi:10.1016/j.ijpharm.2011.07.006.

References

Ackermann, H.W., Tremblay, D., Moineau, S., 2004. Long-term bacteriophage preservation. World Federation Cult. Collections Newsl. 38, 35–40.

Arora, P., Sharma, S., Garg, S., 2002. Permeability issues in nasal drug delivery. Drug Discov. Today 7, 967–975.

Bakaltcheva, I., O'Sullivan, A.M., Hmel, P., Ogbu, H., 2007. Freeze-dried whole plasma: evaluating sucrose, trehalose, sorbitol, mannitol and glycine as stabilizers. Thromb. Res. 120, 105–116.

Bouissou, C., Begat, P., van der Walle, C., Price, R., 2005. Study of the surface mobility of PLGA microspheres using high-resolution topography measurements with the atomic force microscope. J. Control. Release 101, 290–292.

Critchley, I.A., 2006. Eradication of MRSA nasal colonization as a strategy for infection prevention. Drug Discov. Today: Ther. Strateg 3, 189–195.

Doelker, E., 1993. Cellulose derivatives. Adv. Polym. Sci. 107, 199–265.

Dominak, L.M., Omiatek, D.M., Gundermann, E.L., Heien, M.L., Keating, C.D., 2010. Polymeric crowding agents improve passive biomacromolecule encapsulation in lipid vesicles. Langmuir 26, 13195–13200.

Eggers, D.K., Valentine, J.S., 2001. Crowding and hydration effects on protein conformation: a study with sol–gel encapsulated proteins. J. Mol. Biol. 314, 911–922.

Fortier, L.C., Moineau, S., 2009. Phage production and maintenance of stocks, including expected stock lifetimes. Methods Mol. Biol. 501, 203–219.

Golshahi, L., Seed, K.D., Dennis, J.J., Finlay, W.H., 2008. Toward modern inhalational bacteriophage therapy: nebulization of bacteriophages of burkholderia cepacia complex. J. Aerosol Med. Pulm. Drug Deliv. 21, 1–9.

Golshahi, L., Lynch, K.H., Dennis, J.J., Finlay, W.H., 2010. In vitro lung delivery of bacteriophages KS4-M and PhiKZ using dry powder inhalers for treatment of Burkholderia cepacia complex and *Pseudomonas aeruginosa* infections in cystic fibrosis. J. Appl. Microbiol. 110, 106–117.

Hagens, S., Habel, A., von Ahsen, U., von Gabain, A., Blasi, U., 2004. Therapy of experimental pseudomonas infections with a nonreplicating genetically modified phage. Antimicrob. Agents Chemother. 48, 3817–3822.

Hawe, A., Friess, W., 2006. Impact of freezing procedure and annealing on the physico-chemical properties and the formation of mannitol hydrate in mannitol-sucrose-NaCl formulations. Eur. J. Pharm. Biopharm. 64, 316–325.

Henriksen, I., Green, K.L., Smart, J.D., Smistad, G., Karlsen, J., 1996. Bioadhesion of hydrated chitosans: an in vitro and in vivo study. Int. J. Pharm. 145, 231–240.

Illum, L., 2003. Nasal drug delivery – possibilities, problems and solutions. J. Control. Release 87, 187–198.

Kreiner, M., Fuglevand, G., Moore, B.D., Parker, M.C., 2005. DNA-coated microcrystals. Chem. Commun. (Camb.), 2675–2676.

Ma, Y., Pacan, J.C., Wang, Q., Xu, Y., Huang, X., Korenevsky, A., Sabour, P.M., 2008. Microencapsulation of bacteriophage felix O1 into chitosan-alginate microspheres for oral delivery. Appl. Environ. Microbiol. 74, 4799–4805.

McInnes, F., Baillie, A.J., Stevens, H.N., 2007a. The use of simple dynamic mucosal models and confocal microscopy for the evaluation of lyophilised nasal formulations. J. Pharm. Pharmacol. 59, 759–767.

McInnes, F.J., O'Mahony, B., Lindsay, B., Band, J., Wilson, C.G., Hodges, L.A., Stevens, H.N.E., 2007b. Nasal residence of insulin containing lyophilised nasal insert formulations, using gamma scintigraphy. Eur. J. Pharm. Sci. 31, 25–31.

McInnes, F.J., Thapa, P., Baillie, A.J., Welling, P.G., Watson, D.G., Gibson, I., Nolan, A., Stevens, H.N., 2005. In vivo evaluation of nicotine lyophilised nasal insert in sheep. Int. J. Pharm. 304, 72–82.

Moore, B.D., Deere, J., Edrada-Ebel, R., Ingram, A., van der Walle, C.F., 2010. Isolation of recombinant proteins from culture broth by co-precipitation with an amino acid carrier to form stable dry powders. Biotechnol. Bioeng. 106, 764–773.

Mortazavi, S.A., 1995. An in-vitro assessment of mucus mucoadhesive interactions. Int. J. Pharm. 124, 173–182.

Mygind, N., Dahl, R., 1998. Anatomy, physiology and function of the nasal cavities in health and disease. Adv. Drug Deliv. Rev. 29, 3–12.

Nyamweya, N., Hoag, S.W., 2000. Assessment of polymer-polymer interactions in blends of HPMC and film forming polymers by modulated temperature differential scanning calorimetry. Pharm. Res. 17, 625–631.

Puapermpoonsiri, U., Spencer, J., van der Walle, C.F., 2009. A freeze-dried formulation of bacteriophage encapsulated in biodegradable microspheres. Eur. J. Pharm. Biopharm. 72, 26–33.

Puapermpoonsiri, U., Ford, S.J., van der Walle, C.F., 2010. Stabilization of bacteriophage during freeze drying. Int. J. Pharm. 389, 168–175.

Rouse, J.J., Mohamed, F., van der Walle, C.F., 2007. Physical ageing and thermal analysis of PLGA microspheres encapsulating protein or DNA. Int. J. Pharm. 339, 112–120.

Rowe, R.C., Sheskey, P.J., Quinn, M.E., 2009. Handbook of Pharmaceutical Excipients, 6th ed. Pharmaceutical Press, London, p. 928.

Sambrook, J., Russell, D.W., 2001. Bacteriophage Lambda and its Vectors Molecular Cloning: A Laboratory Manual. Cold Spring Harbour Laboratory Press, New York, pp. 2.47–2.51.

Schule, S., Friess, W., Bechtold-Peters, K., Garidel, P., 2007. Conformational analysis of protein secondary structure during spray-drying of antibody/mannitol formulations. Eur. J. Pharm. Biopharm. 65, 1–9.

Searles, J.A., Carpenter, J.F., Randolph, T.W., 2001. The ice nucleation temperature determines the primary drying rate of lyophilization for samples frozen on a temperature-controlled shelf. J. Pharm. Sci. 90, 860–871.

Soane, R.J., Frier, M., Perkins, A.C., Jones, N.S., Davis, S.S., Illum, L., 1999. Evaluation of the clearance characteristics of bioadhesive systems in humans. Int. J. Pharm. 178, 55–65.

Soothill, J., Hawkins, C., Anggard, E., Harper, D., 2004. Therapeutic use of bacteriophages. Lancet Infect Dis 4, 544–545.

Tian, F., Saville, D.J., Gordon, K.C., Strachan, C.J., Zeitler, J.A., Sandler, N., Rades, T., 2007. The influence of various excipients on the conversion kinetics of carbamazepine polymorphs in aqueous suspension. J. Pharma. Pharmacol. 59, 193–201.

Torrado, S., Torrado, S., 2002. Characterization of physical state of mannitol after freeze-drying: Effect of acetylsalicylic acid as a second crystalline cosolute. Chem. Pharm. Bull. 50, 567–570.

Weber-Dabrowska, B., Mulczyk, M., Gorski, A., 2000. Bacteriophage therapy of bacterial infections: an update of our institute's experience. Arch. Immunol. Ther. Exp. (Warsz.) 48, 547–551.

Weber-Dabrowska, B., Mulczyk, M., Górski, A., 2001. Bacteriophage therapy for infections in cancer patients. Clin. Appl. Immunol. Rev. 1, 131–134.

Weber-Dabrowska, B., Mulczyk, M., Gorski, A., 2003. Bacteriophages as an efficient therapy for antibiotic-resistant septicemia in man. Transplant. Proc. 35, 1385–1386.

Wright, A., Hawkins, C.H., Anggard, E.E., Harper, D.R., 2009. A controlled clinical trial of a therapeutic bacteriophage perparation in chronic otitis due to antibiotic-resistant *Pseudomonas aeruginosa*; a preliminary report of efficacy. Clin. Otolaryngol. 34, 349–357.

Yuan, N.Y., Lin, Y.A., Ho, M.H., Wang, D.M., Lai, J.Y., Hsieh, H.J., 2009. Effects of the cooling mode on the structure and strength of porous scaffolds made of chitosan, alginate, and carboxymethyl cellulose by the freeze-gelation method. Carbohyd. Polym. 78, 349–356.

AIChE

Bioprocessing of Bacteriophages via Rapid Drying onto Microcrystals

Eva Alvarez-Gonzalez, Munerah Alfadhel, and Parag Mane
Strathclyde Institute of Pharmacy and Biomedical Sciences, University of Strathclyde, Glasgow G4 0RE, U.K.

Steven J. Ford
Cancer Research UK Formulation Unit, University of Strathclyde, Glasgow G4 0RE, U.K.

Barry D. Moore
Department of Pure and Applied Chemistry, University of Strathclyde, Glasgow G1 1XL, U.K.

Christopher F. van der Walle
Strathclyde Institute of Pharmacy and Biomedical Sciences, University of Strathclyde, Glasgow G4 0RE, U.K.

DOI 10.1002/btpr.740
Published online November 2, 2011 in Wiley Online Library (wileyonlinelibrary.com).

*We present an alternative bioprocess for bacteriophages involving room temperature coprecipitation of an aqueous mixture of phage (*Siphoviridae*) and a crystallizable carrier (glutamine or glycine) in excess of water miscible organic solvent (isopropanol or isobutanol). The resultant suspension of phage-coated microcrystals can be harvested by filtration and the residual solvent removed rapidly by air-drying at a relative humidity of 75%. Albumin or trehalose added at 5% w/w of the crystalline carrier provide for better stabilization of the phage during co-precipitation. Free-flowing dry powders generated from an aqueous solution of phage (~13 $\log_{10}$ pfu/mL) can be reconstituted in the same aqueous volume to a phage titer of almost 10 $\log_{10}$ pfu/mL; high enough to permit subsequent formulation steps following bioprocessing. The phage-coated microcrystals remain partially stable at room temperature for at least one month, which compares favorably with phage immobilized into polyester microcarriers or lyophilized with excipient (1–5% polyethylene glycol 6000 or 0.1–0.5 M sucrose). We anticipate that this bioprocessing technique will have application to other phage families as required for the development of phage therapies.* © 2011 American Institute of Chemical Engineers *Biotechnol. Prog.*, 28: 540–548, 2012
Keywords: bacteriophages, immobilization, Staphylococcus aureus*, bioprocessing, protein-coated microcrystals*

Introduction

Bacteriophage (or phage) therapy has emerged as a potential treatment of bacterial infections in plants,[1] animals,[2] humans,[3] and foodstuffs.[4] Indeed, the use of phages as an alternative to antibiotics is reported to have several advantages: (i) a high affinity for specific pathogenic bacteria without targeting "beneficial bacteria" such as the normal gut microflora; (ii) a restricted distribution following local administration, e.g., to skin wounds; (iii) an activity against bacteria with multiple resistance to antibiotics such as methicillin; (iv) an absence of systemic side effects in clinical studies reported to date; (v) self-replication at the site of infection, potentially reducing the frequency of administration; and (vi) a relatively rapid selection and characterization against a particular bacterium and subsequent scale-up, compared to the development of new antibiotics.[5-7] However, regulatory bodies may ask that each newly identified phage intended for therapeutic use be characterized in detail, such as genomic analysis to screen for potential toxins, and proof of therapeutic activity.[8,9] To suppress the emergence of bacterial resistance, mixtures of phages have been used in the first reported double-blind clinical trial, for treatment of chronic otitis in humans.[10]

If phages are to become more widely established in medicine, then issues relating to processing and formulation must be addressed. As for any biomacromolecule, key steps in the bioprocess are concentration and storage,[11] particularly with respect to possible aggregation of proteins.[12] Phages, as individual strains, have a wide range of stabilities; thus, some strains do not require special conditions for storage, but others do.[8] Comparison of various methods of preservation such as freezing and lyophilization, indicate that phages become inactivated over a period of 6 weeks to 2 years, dependent on the method and strain.[13] Nevertheless, long-term stability (i.e., retention of high phage titers) is desirable in terms of practicality. This would depend on the type of phage, the method of formulation and the choice of excipients for chemical compatibility with the phage.[14] Bacteriophages may be stable for up to several years if kept at 4°C in filter-sterilized broth, and one of the most common media used is Trypticase Soy Agar and Brain Heart Infusion

Correspondence concerning this article should be addressed to B. D. Moore at b.d.moore@strath.ac.uk or C. F. van der Walle at chris.walle@strath.ac.uk.

broth.[15] Some additives can be used to assure sterility of the media, such as chloroform in the case on non-lipid enveloped phages.[16] Phage-lysates are then kept at 4°C or at ultra-low temperatures (below −60°C) or in liquid nitrogen without further treatment; glycerol and DMSO may be used as cryoprotectants.[8]

Lyophilization (freeze-drying) has been reported as a feasible technique for the preservation of phages,[17] which may retain their viability up to 20 years when a vacuum is present in the storage ampoule.[15] Additives reported to retain the stability of lyophilized phages include bovine serum albumin,[15,16] carbohydrates such as lactose and sucrose,[8,18] glycerol,[15] skimmed milk, and peptone.[13] As a general conclusion, it can be said that the lower the storage temperature, the longer the phage will survive.[16] However, studies reveal a wide variability in the storage requirements for individual phages, without there being a universal method for long-term preservation. One recently reported, novel method for the long-preservation of tailed phages, involved their storage in frozen infected cells at −80°C.[19] Their results suggested that the viability of the tailed phages using this method was generally improved upon, compared to the aforementioned storage methods.

In this study, we present a new approach for the rapid drying of phage from solution and subsequent storage at room temperature (or below) in the form of dry powders, with the phage bound onto the surface of an inert excipient. The approach draws from the process of generating protein-coated microcrystals (PCMCs); a rapid, cost-efficient technique to immobilize biomolecules on the surface of a crystalline carrier. An aqueous solution containing the target biomolecule and the carrier (generally an amino acid) is rapidly mixed with an excess of water-miscible organic solvent. In this process, very rapid dehydration takes places, as the water surrounding the biomolecule dissolves into the water miscible solvent and co-precipitation of the carrier and the biomolecule occurs.[20] The particles can be isolated from the solvent by filtration or simple isothermal vacuum drying and so costly processes such as lyophilization can be avoided. The biomolecule retains its stability without further treatment and PCMC techniques have been successfully applied to biomolecules such as proteins,[20] enzymes,[21] DNA,[22] and nanoparticles.[23] Bacteriophages present unique challenges for the PCMC process on account of their complex self-assembled structure and resultant lability. Key variables in the PCMC process have been screened to try to maintain maximal lytic activity during storage, and the results present a protocol that will have application to phage bioprocessing and support the drive towards the formulation of phages as medicinal products/devices for "phage therapy."[24]

Materials and Methods

Materials

Glutamine, trehalose, bovine serum albumin (BSA), gelatine, magnesium nitrate hexahydrate and sodium chloride, and organic solvents: methanol, isopropanol and isobutanol (2-methyl-1-propanol), were purchased from Sigma-Aldrich Chemical Company (Dorset, UK). Water was purified to >16 MΩ cm. Granulated agar, yeast extract, tryptone, and glycine were supplied by Melford Laboratories (UK). Trizma base and magnesium sulfate heptahydrate were purchased from Fluka (UK). All chemical and solvents were of analytical grade or equivalent.

Bacterial and bacteriophage strains

Staphylococcus aureus FD209 P variant (strain 8588) was acquired from NCIMB, Aberdeen (UK; ATCC ref. 11522). The bacteriophage specific for this strain of *S. aureus* was also obtained from NCIMB, Aberdeen (UK; Cat. No: 9563; ATCC ref. 6538-B) and belongs to the *Siphoviridae* family, having a ~80 nm isometrically hexagonal head and a ~200 nm noncontractile tail with a knoblike structure at its distal end.[17]

Bacteriophage preparation and harvest

Individual colonies of *Staphylococcus aureus* were grown in Luria Bertani (LB) medium (% tryptone, 1% yeast extract, 0.5% NaCl) containing 1.5% of granulated agar by streaking frozen stocks in a Petri dish. Cells were then cultured by inoculating 5 mL of LB broth with a single colony. This bacteria culture was incubated overnight at 37°C with vigorous shaking and then a 300 μL aliquot was mixed with 450 μL of bacteriophage stock solution. This mixture was incubated at 37°C for 20 min and then a 200 μL aliquot was mixed with 4 mL of partially cooled LB agar (LB broth containing 1% agar), pored onto a cooled LB agar plate (1.5% agar), and incubated at 37°C overnight. Phages were collected by flooding the agar plates with "storage media" (SM; 1 M Tris-HCl, 0.1 M NaCl, 8 mM $MgSO_4$, 0.1 g/L gelatin, pH 7.5) and gently swirling every 30 min over 4 h, while storing at 4°C. SM containing bacteriophage was then decanted and filtered through a 0.22 μm syringe filter (Millipore, Ireland). The phage stock solution was then stored at 4°C without further treatment, and the lytic activity of this solution was determined by plaque assay. A high-titer bacteriophage stock solution (10^{13}–10^{14} pfu/mL) was harvested with the aim of having a wider phage-activity range for analysis of results.

Plaque assay

A serial ten-fold dilution of the bacteriophage stock was made in triplicate. A 100 μL aliquot of each dilution and an equal volume of overnight-incubated bacterial culture were added to 4 mL of partially cooled 0.75% LB agar, and pored onto a 1.5% LB agar plate, kept at 37°C for 18 h. Positive and negative controls were prepared in the same way by adding bacterial culture and a known concentration of bacteriophage and solely bacterial culture, respectively. Following overnight incubation, the number of plaques was counted for each dilution and the phage titer given in units of plaque forming units (pfu) per mL (pfu/mL). The titer of the phage was calculated from the last dilution containing between 30 and 300 plaques: less than 30 plaques per plate are considered to be too few to count (TFTC) and more than 300 plaques are considered to be too many to count (TMTC).[25] For each formulation, the plaque assay was performed in triplicate (three serial dilutions), therefore the final titer results are presented as the mean of the three values obtained for each formulation together with the standard deviation thereof.

Phage-coated microcrystals

Glutamine and glycine were diluted into the corresponding volume of bacteriophage stock to sub-saturation concentrations of 15 mg/mL and 112.5 mg/mL, respectively. (Where

Table 1. Phage Titer Following Initial Immobilization of Phage to Amino Acid Carriers Without Additives

Formulation	Titer of the Neat Phage (pfu/mL)	Titer of the Reconstituted Powder (pfu/mL)
Gln (15 mg/mL)	$(1.7 \pm 0.9) \times 10^{13}$	$(1.4 \pm 0.4) \times 10^{4}$
Gly (112.5 mg/mL)	$(1.7 \pm 0.9) \times 10^{13}$	$(7.1 \pm 2.2) \times 10^{2}$

comparisons in process parameters were required, the same phage stock was used, with lytic activities reported in the results.) Stabilizing additives, where used, were also added to the bacteriophage stock at a concentration yielding 5% w/w relative to the mass of amino acid. This aqueous phase was added drop-wise into the organic solvent whereas stirring with a magnetic bar at 1100 rpm for 1 min (magnetic stirrer KMO2 basic from IKA® Werke GmbH & Co. KG). Isopropanol and/or isobutanol were used as the organic phase. The aqueous phase to organic solvent ratio by volume was found to be optimum at 1:9 (10% aq. sol.) for isopropanol and 1:19 (5% aq. sol.) for isobutanol, based on their full and partial miscibility with water, respectively. The crystalline precipitate formed immediately on mixing and was harvested by vacuum filtration across a hydrophobic membrane filter with 0.45 μm pore-size (Millipore, Ireland). The harvested phage-coated microcrystals (Φ-CMC) were then dried and stored at a constant temperature of 25°C and constant relative humidity (RH) of 52% and 75% RH obtained using saturated solutions of $Mg(NO_3)_2 \cdot 6H_2O$ and NaCl in sealed containers, respectively. Φ-CMC were dried until constant weight and, for plaque assay, reconstituted in distilled water to amino acid concentrations originally used in their preparation. The titer of the phage in the reconstituted Φ-CMC was compared to the titer of the neat phage used in their preparation, to determine the preservation of integrity of the phage after processing. The yield of the dry powders was calculated as: (Mass of dried powder recovered)/(Mass dissolved in aqueous phase) × 100; where "mass" included additives (BSA or trehalose) but not phage since the latter was considered to be negligible.

Endotoxin detection: Limulus ameobocyte lysate assay

The possible removal of endotoxins from the phage solution prepared as described above, using the PCMC technology, was tested by end-point method with chromogenic limulus ameobocyte lysate (LAL) reagent [the pyrochrome kit, control standard endotoxins (CSE) and endotoxins-free LAL reagent water were purchased from Associates of Cape Cod Inc., USA]. The assay was performed, as directed by the supplier, in endotoxin-free borosilicate test tubes (0.75 × 75 mm). Serial two-fold dilutions of standard-endotoxins (from *E. coli* O113:H10) for the calibration curve, negative control (LAL reagent water), positive control (CSE and LAL reagent water), and serial dilutions of neat phage and reconstituted powder were incubated at 37°C for 70 min after addition of pyrochrome, according to the manufacture's specifications. The reaction was stopped with 50% glacial acetic acid and the optical density (OD) was measured at 405 nm with a UV-visible Varian Cary 50 BIO spectrophotometer.

Physical characterization of dried powders

The residual water content of the dry powders was determined by Karl Fisher titration (Mettler Toledo DL 37, Leicester, UK). Fifty milligrams of dried powders was suspended in 500 μL of anhydrous methanol. Samples were centrifuged with the aim of obtaining a clear supernatant. The apparatus was calibrated with Karl Fisher water standard (2-methoxy ethanol) and blanked with the addition of anhydrous methanol. The water content was determined for each formulation in duplicate for each independently prepared sample and expressed as the percentage.

The morphology of the powders was imaged by scanning electron microscopy (SEM), using a JEOL 6400 scanning electron microscope, scandium imaging platform (University of Glasgow, UK) at either 2.5 kV or 6 kV and at different magnifications. Dry powders were fixed onto metal stubs using double-sided adhesive copper tape. Stubs were coated with gold under vacuum for 30 min using a sputter coater (Polaron SC515) before imaging.

Sizing of the powders was performed by laser diffractometry using Mie scattering theory (Mastersizer 2000, Malvern Instruments, UK), dispersing the powders in isopropanol (non-solvent) until a laser obscurity around 10% was reached. The zeta potential of the powders was measured by photon correlation spectroscopy using a Malvern Zetasizer Nano-ZS (Malvern Instruments, Malvern, United Kingdom) at 25°C, using methanol (non-solvent) as the dispersant.

Results and Discussion

Phage lytic activity is attenuated during the PCMC process without the addition of excipients

Phage-coated microcrystals (Φ-CMC) were first produced by immobilization of phages onto an amino acid carrier, precipitated by mixing with isopropanol. This simple method was found to be inadequate since the phage titers following reconstitution of the Φ-CMC had fallen ~9 $\log_{10}$ and ~11 $\log_{10}$ for the glutamine and glycine carriers, respectively (Table 1). At this stage, it was not appropriate to screen all 20 natural amino acids since the efficiency of the various carriers has been previously investigated.[20-22] Phage inactivation is known to occur upon exposure to water miscible organic solvents[26] and is also likely to occur during adsorption induced unfolding of the phage protein coat at the carrier surface, discussed further below. Such a large loss of lytic activity would clearly be unacceptable for phage bioprocessing and additives were therefore sought which would stabilize the phage. The additives chosen included trehalose, since non-reducing sugars are widely accepted to be protein stabilizers,[27] and BSA, since this is an exceptionally stable and surface active protein.[28] (BSA is itself amenable to bioprocessing since it shares 75% identity with human serum albumin which is prepared clinically as a plasma substitute.) Thus, two mechanisms were investigated for the stabilization of the phage during the PCMC process: first, thermodynamically favoring the folded state by preferential exclusion of non-reducing sugars from the protein domains of the phage;[29] second, minimization of adsorption to the water/organic solvent interface through competition with BSA and subsequent attenuation of adsorption-induced unfolding.[28] We also investigated the effect of drying/storage conditions on lytic activity, since storage of medicines at varying humidities is a commonly used technique to determine the stability of a drug in a particular formulation.

An important measure of the PCMC process is the overall yield of dry powder. For the process to be commercially

Table 2. Yield Calculation for the Φ-CMC Precipitated from Isopropanol after Drying at 25°C

Formulation	RH for Drying (%)	Yield (%)
Gln[a]	n.a	90.33
Gly[b]	n.a	96.54
Gln + Trh[c]	52	101.35
Gln + Trh	75	–
Gly + Trh	52	–
Gly + Trh	75	94.60
Gln + BSA[c]	52	96.53
Gln + BSA	75	94.33
Gly + BSA	52	97.68
Gly + BSA	75	103.16

–, not determined; Trh, trehalose; BSA, bovine serum albumin.
[a] Concentration in aqueous phase = 15 mg/mL. [b] Concentration in aqueous phase = 112.5 mg/mL. [c] Concentration in aqueous phase = 5% w/w.

viable, the yield would be expected to be near 100%. Table 2 shows that the yield was above 90% for all measured powders, with most powders having around 95–100% yield. This indicates that the mixing of the aqueous and solvent phases, and subsequent precipitation of the carrier (and additive where used), was very efficient. In those cases where the yield was slightly above 100%, this may have been due to errors in weighing at the microscale or incomplete drying of the powder. Scale-up of the process would be expected to reduce the effect of small variations in weighing measurements on the calculation of yield. Scale-up of the process could be envisaged using in-line pump mixing and would be expected to at least match, or better, the yields obtained here.

Using isopropanol as the water miscible organic solvent, Figure 1 summarizes the results obtained for Φ-CMC formulations containing stabilizers dried at 25°C and relative humidities (RH) of 52 and 75%. The most noticeable difference arises from the humidity at which the Φ-CMC were dried: at 52% RH a fall in the lytic activity of ~11 $\log_{10}$ was observed despite the addition of trehalose to the amino acid carriers, while for the same formulations dried at 75% RH, a fall of ~7 $\log_{10}$ was observed. The intention of drying at different humidities was not to specifically generate Φ-CMC with low/high residual moisture content, but rather to accelerate the rate and extent of removal and/or exchange of residual organic solvent from the phage on the carrier surface.[30] In this respect, it is clear that a rapid removal of residual organic solvent from the Φ-CMC by exchange with water vapor present at 75% RH prevented further loss of lytic activity; i.e., minimizing the exposure of the phages to residual organic solvent better maintained their integrity. This result is in agreement with previous work showing that inactivation of filamentous phages is accelerated on exposure to water-miscible organic solvents in a concentration dependent manner.[26]

The addition of BSA to the amino acid carriers improved the lytic activity of the reconstituted Φ-CMC compared to carriers including trehalose, particularly when dried at 52% RH. However, the extent of BSA-mediated stabilization of phage immobilized to the two amino acid carriers was more variable than that afforded by trehalose (Figure 1). This may reflect the more complex, macromolecular nature of BSA, whose chemical and physical structure will be expected to change during exposure to solvent and also to increasing RH. Examples of detrimental and advantageous effects on proteins exposed to differing RH can be found in the literature. For example, the physical (conformational) stabilization

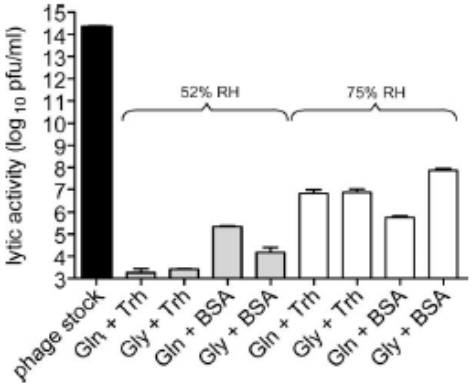

Figure 1. Lytic activities of the Φ-CMC generated from mixing with isopropanol and reconstituted in water.

The core substrate of the Φ-CMC were composed of Gln, glutamine; Gly, glycine; Trh, trehalose; and BSA, bovine serum albumin. Gray and white bars represent drying at 52 and 75% RH, respectively. The black bar indicates the titer of the phage stock from which the Φ-CMC were generated. Data show Mean ± SD for $n = 3$.

of dried lactate dehydrogenase and granulocyte colony-stimulating factor by amino acids was compromised by uptake of residual moisture.[31] In contrast, the enhancement of physical stability has been observed for antibodies in the presence of high residual moisture.[32] The same enhancement of physical stability would therefore appear to be true for phage, with respect to their proteinaceous head group and tail. Given these considerations, trehalose may be preferable over BSA for the stabilization of phage during the Φ-CMC process, since the outcome with regard to lytic activity is less variable.

Production of Φ-CMC harboring high titers of phage

Although the effect of additives and increasing RH on Φ-CMC lytic activity was encouraging, the phage titers remained below what could be considered practically useful. That is, after reconstitution of Φ-CMC, it would be expected that the resultant phage titers remain sufficiently high for further formulation for a particular phage therapy. One such example would be the recent clinical trial testing the efficacy and safety of bacteriophages targeting *Pseudomonas aeruginosa* in chronic otitis in humans.[10] In that clinical trial, 10^5 pfu of each of six bacteriophages in 0.2 mL liquid were applied into the ear. Taking this titer as a guide leads to the conclusion that reconstitution of Φ-CMC should yield a titer in the order of at least 6 $\log_{10}$ pfu/mL. While the Φ-CMC process allows for concentration of the phage by reconstituting the dried powder into a smaller aqueous volume than that originally containing the phage, there is a limit to this due to the solubility of the amino acid carrier. For Φ-CMC precipitated from isopropanol, containing trehalose or BSA and dried at 75% RH, phage titers from reconstituted powders were around 7 $\log_{10}$ pfu/mL. These titers may be at the lower limit for subsequent formulation, at least with respect to the clinical trial by Wright et al.[10] Higher titers following Φ-CMC reconstitution would therefore be desirable.

To this aim, the same Φ-CMC process was used but with the substitution of isobutanol for isopropanol during the mixing step. The logic behind this decision was that the nature

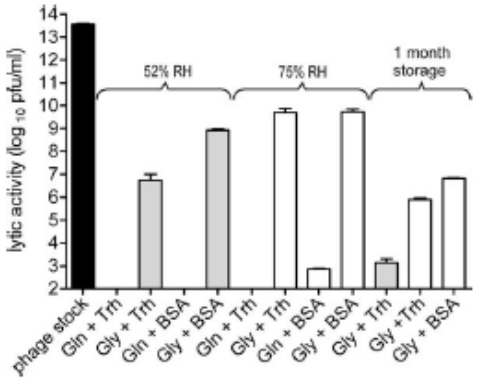

Figure 2. Lytic activities of the Φ-CMC generated from mixing with isobutanol and reconstituted in water.

The core substrate of the Φ-CMC were composed of Gln, glutamine; Gly, glycine; Trh, trehalose; BSA, bovine serum albumin. Gray and white bars represent drying at 52 and 75% RH, respectively. The black bar indicates the titer of the phage stock from which the Φ-CMC were generated. Data show Mean ± SD for $n = 3$.

Table 3. Yield Calculation for the Φ-CMC Precipitated from Isobutanol After Drying at 25°C

Formulation	RH in Storage (%)	Yield (%)
Gln[a] + Trh[b]	52	89.98
Gln + Trh	75	84.93
Gly[c] + Trh	52	98.65
Gly + Trh	75	90.14
Gln + BSA[b]	52	98.59
Gln + BSA	75	95.31
Gly + BSA	52	96.80
Gly + BSA	75	96.81

[a] Concentration in aqueous phase = 15 mg/mL. [b] Concentration in aqueous phase = 5% w/w. [c] Concentration in aqueous phase = 112.5 mg/mL.

of the solvent in aqueous-organic mixtures is known to effect the extent of protein denaturation.[33] However, due to the low miscibility of isobutanol in water, the aqueous:organic solvent ratio (by volume) was changed to 1:19 during the mixing step, compared to 1:9 for isopropanol. In this case, the results showed that the lytic activity of the phage was very much dependent on the amino acid carrier (Figure 2). For powders dried at 52% RH, the reconstituted glutamine Φ-CMC showed a complete loss of lytic activity, irrespective of the addition of trehalose or BSA. In contrast, reconstituted glycine Φ-CMC retained high lytic activity, with the titer remaining at between 6 $\log_{10}$ and 8 $\log_{10}$. The reason for this large discrepancy in the titer between glycine and glutamine Φ-CMC formed with isobutanol can be related in part to the efficiency of the process and yield. Table 3 shows that the yield of glutamine/trehalose powders was below 90%, distinct from glutamine/BSA and all glycine powders which retained the high yields also observed for precipitation in isopropanol. The relatively poor efficiency of glutamine/trehalose precipitation would be expected to attenuate the immobilization of phage on the carrier surface and thereby bring about a perceived loss of lytic activity. Process efficiency is not sufficient however to explain the loss of lytic activity for glutamine/BSA powders. Here, consideration of the "solid-state buffering capacity" may be relevant. When proteins (and therefore phage) are immobilized onto a crystal carrier through mixing with non-solvent, their ionization state will change according to the nature of the carrier and its buffering capacity. Previous studies of PCMCs using various crystal carriers have demonstrated this in situ control of ionization-state for an immobilized enzyme, showing large differences in enzyme activity dependent on the nature of the carrier.[34] Thus, the combination of the low glutamine concentration (15 mg/mL, cf. 112.5 mg/mL glycine) and reduced aqueous: organic solvent ratio in isobutanol, may not only have reduced process efficiency but also been insufficient for in situ control of the phage ionization-state.

When the Φ-CMC produced from isobutanol were dried at 75% RH, the same discrepancy between glutamine and glycine carriers was observed, but of particular interest was that the reconstituted glycine Φ-CMC showed a fall in titer of only <4 $\log_{10}$. This was encouraging, since the resultant titer of the powders was almost 10 $\log_{10}$ pfu/mL, well within the range which could be considered practically useful for formulation, as described above. Given that all other parameters except the choice of solvent remained the same, this result also demonstrates that a key driver of phage inactivation in this bioprocess is exposure to organic solvent. A suitable bioprocess method was therefore identified in this study, wherein Φ-CMC were generated from glycine as the core substrate following mixing with isobutanol and drying at 75% RH. There did not appear to be a preferred mechanism for stabilization of the phage during this bioprocess since there was no statistical difference between titers for glycine Φ-CMC incorporating trehalose or BSA, at least at 75% RH (Figure 2). At 52% RH, BSA would appear to have some advantage over trehalose as regards phage stabilization, but this is a secondary effect compared to the importance of RH.

Stability testing of the Φ-CMC generated from glycine with trehalose/BSA as stabilizer and drying at 25°C and 52/75% RH, showed that the phage partially lost their lytic activity over a 1-month-period (Figure 2). The fall in titer was between 3 and 4 $\log_{10}$ for all Φ-CMC tested, irrespective of the initial titer, stabilizer and RH. This rate of loss of titer for phage immobilized to crystal carriers was however much less than that observed for phage immobilized to amorphous polyesters, also in the solid state following lyophilization.[18] This would suggest that the mobility of the carrier plays a role in the inactivation of immobilized phage during storage, with crystalline materials being preferred over amorphous materials. With comparison to the stability of freeze dried phage, our previous data for phage lyophilized from solutions containing 1–5% polyethylene glycol 6000 or 0.1–0.5 M sucrose and stored under standard temperatures and pressures also showed a drop in phage activity over a 30-day-period.[17] However, as discussed in the introduction, some freeze dried phage preparations subsequently stored under vacuum at ultra-low temperatures may remain stable for up to 20 years. Although "shelf life" is more accurately associated with a final formulated product, it could be said that the Φ-CMC, optimized as far as possible in this work, have a useful shelf life of up to 1 month when stored "dry" at room temperature. This compares well to a maximum of 1 week for polyester-encapsulated phage[18] under similar conditions.

Surface characteristics and morphology of the Φ-CMC

LAL testing indicated that endotoxins were not removed from the phage solution following co-precipitation onto

crystal carriers, i.e., the measured levels of endotoxin before and after bioprocessing were almost the same (null data not shown). This is not surprising since it has been repeatedly shown that the PCMC process is not an alternative purification step in bioprocessing, although the removal of selected metabolites from yeast culture has been demonstrated.[35] Endotoxins must therefore have been immobilized and concentrated onto the surface of the Φ-CMC along with the phage. This is not a problem with respect to bioprocessing since downstream removal of endotoxins can be carried out following reconstitution of the Φ-CMC.[14] However, this does mean that the Φ-CMC cannot be used directly as drug delivery vehicles for phage therapy without prior removal of endotoxins.

Karl Fisher analysis of residual moisture was used to indirectly demonstrate that the phages were immobilized onto the surface of the Φ-CMC (and not within the crystal carriers). When using the same phage stock solution for all Φ-CMC formulations, high and low phage loadings per unit mass of glutamine and glycine will result, since the concentration of glutamine and glycine in the aqueous phase was 15 and 112.5 mg/mL, respectively. Comparing the residual moisture content of Φ-CMC incorporating trehalose or BSA for high and low phage loadings (Table 4), it can be seen that the glutamine Φ-CMC had a significantly higher residual moisture content than the equivalent glycine Φ-CMC, irrespective of whether the Φ-CMC were dried at 52 or 75% RH. The probable explanation for this is that phage are proteinaceous and will therefore be associated with hydrogen-bonded water after drying (the bulk water evaporating off the surface). The same reasoning can be used to explain why the residual moisture content for Φ-CMC incorporating BSA were higher than Φ-CMC incorporating trehalose. The residual water measured must be associated with the surface of the Φ-CMC since the amino acid carriers are practically insoluble in the methanol used for Karl Fisher analysis. When the number of phages loaded onto the Φ-CMC was such that the ratio of phage (pfu): amino acid (mass) was equivalent for glycine and glutamine formulations, the residual moisture levels also approached equivalence (Table 4). Thus, for the Φ-CMC precipitated in isopropanol, the residual moisture content was largely determined by the relative phage loading.

For Φ-CMC with the same phage loadings but precipitated in isobutanol, the residual water content was observed to be strongly dependent on the % RH during drying (Table 5). At 75% RH, the residual moisture content was between ca. 13 and 17% (barring the Gly/trehalose formulation), whereas at 52% RH the residual moisture content was between ca. 1.9 and 3.3%. This is in contrast to Φ-CMC with the same phage loadings precipitated from isopropanol, where the effect of RH on moisture content was much weaker (Table 4). This difference most probably reflects the miscibility of the two solvents with water condensing at the carrier surface from high (75%) RH and the effect this has on the vapor pressure. Isobutanol is only 8.5% miscible with water, whereas isopropanol is entirely miscible. Isopropanol therefore results in greater disruption and weakening of the transient H-bonding networks in water, thus generating a solvent mixture with a higher vapor pressure than the pure components (i.e., positive deviation from Raoult's law) and therefore a drier surface as measured by the Karl Fisher technique. In principle, it would be interesting to use a wider range of solvents, but there are constraints with respect to scale-up and introduction to the biopharmaceutical industry. Currently, isopropanol and isobutanol are known to be the most promising candidates for the PCMC process.

Table 4. Residual Moisture of the Φ-CMC Precipitated from Isopropanol After Drying at 25°C

Formulation	% RH for Drying	% Water Content: High (Gln) and Low (Gly) Phage-Loading[a]	% Water Content: Same Phage-Loading[a]
Gln[b] + Trh[c]	52	5.27 ± 0.67	1.02 ± 0.05
Gln + Trh	75	14.65 ± 0.81	1.93 ± 0.07
Gly[d] + Trh	52	2.02 ± 0.28	1.64 ± 0.08
Gly + Trh	75	4.15 ± 0.22	3.19 ± 0.98
Gln + BSA[c]	52	6.29 ± 0.22	1.51 ± 0.07
Gln + BSA	75	17.60 ± 0.68	2.62 ± 0.68
Gly + BSA	52	1.62 ± 0.26	1.92 ± 0.09
Gly + BSA	75	4.07 ± 0.07	3.77 ± 0.16

[a] Defined as pfu per mg of carrier. [b] Concentration in aqueous phase = 15 mg/mL. [c] Concentration in aqueous phase = 5% w/w. [d] Concentration in aqueous phase = 112.5 mg/mL.

Table 5. Residual Moisture of the Φ-CMC Precipitated from Isobutanol After Drying at 25°C

Formulation	% RH for Drying	% Water Content for Φ-CMC with the Same Phage-Loading[a]
Gln[b] + Trh[c]	52	3.29 ± 0.19
Gln + Trh	75	17.1 ± 0.73
Gly[d] + Trh	52	1.26 ± 0.02
Gly + Trh	75	3.71 ± 0.03
Gln + BSA[c]	52	3.12 ± 0.11
Gln + BSA	75	13.0 ± 0.22
Gly + BSA	52	1.88 ± 0.06
Gly + BSA	75	13.8 ± 0.19

[a] Defined as pfu per mg of carrier. [b] Concentration in aqueous phase = 15 mg/mL. [c] Concentration in aqueous phase = 5% w/w. [d] Concentration in aqueous phase = 112.5 mg/mL.

Physical characterization of the powders by SEM indicated that the Φ-CMC morphology was highly dependent on the amino acid carrier. With glutamine as the carrier, in the presence of both trehalose and BSA, Φ-CMC presented a thin-layer morphology, with overlap of different layers and sizes, arranged apparently randomly (Figures 3A,B). For Φ-CMC made with glycine as the carrier, well-defined, discrete spherical aggregates were observed, among other sections of the material which formed random clusters and aggregates of particles (Figures 3C,D). The tendency of the glycine Φ-CMC to aggregate can be associated with the smaller zeta potential of the particles (-11.1 ± 1.2 mV) compared to glutamine Φ-CMC (-47.4 ± 1.2 mV). As the zeta-potential decreases we can expect less electrostatic repulsion which, according to the DLVO theory, will then favor aggregation of the particles. Although the amide side chain of glutamine does not carry a charge, delocalization of the lone electron pairs gives a strong dipole moment, and hence the greater zeta potential of glutamine Φ-CMC over glycine Φ-CMC.

Micrographs of the Φ-CMC generated from mixing in isobutanol indicated that the nature of the organic solvent did not have a major influence on particle morphology (Figure 4, cf. Figure 3). As for precipitation from isopropanol, the glycine Φ-CMC tended to aggregate into spheres with diameters ≈10 μm (Figures 4C,D), although the use of isobutanol appeared to be cause a slight tendency of the glutamine Φ-CMC to aggregate as well (Figures 4A,B). It is possible that

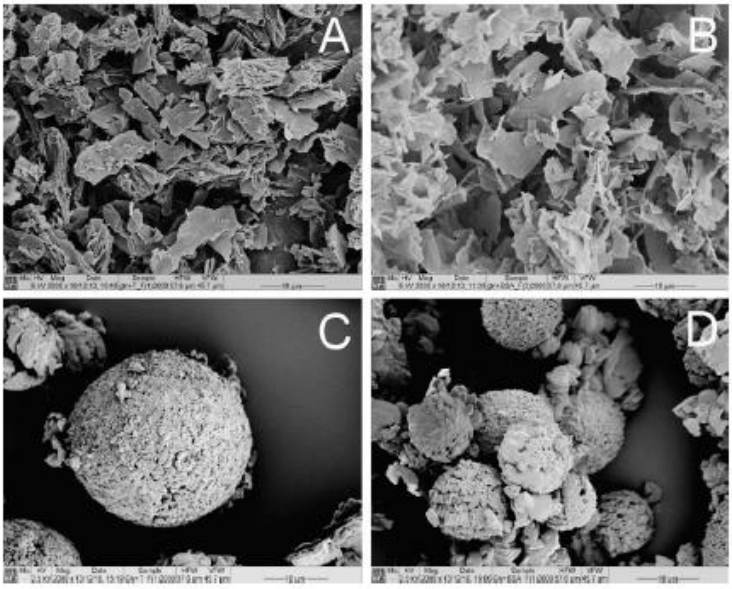

Figure 3. SEM micrographs of dried Φ-CMC generated from mixing with isopropanol.

The core substrate of the Φ-CMC being composed of Gln and 5% w/w trehalose (A), Gln and 5% w/w BSA (B), Gly and 5% w/w trehalose (C), Gly and 5% w/w BSA (D). Magnification, ×2000; scale bar = 10 μm.

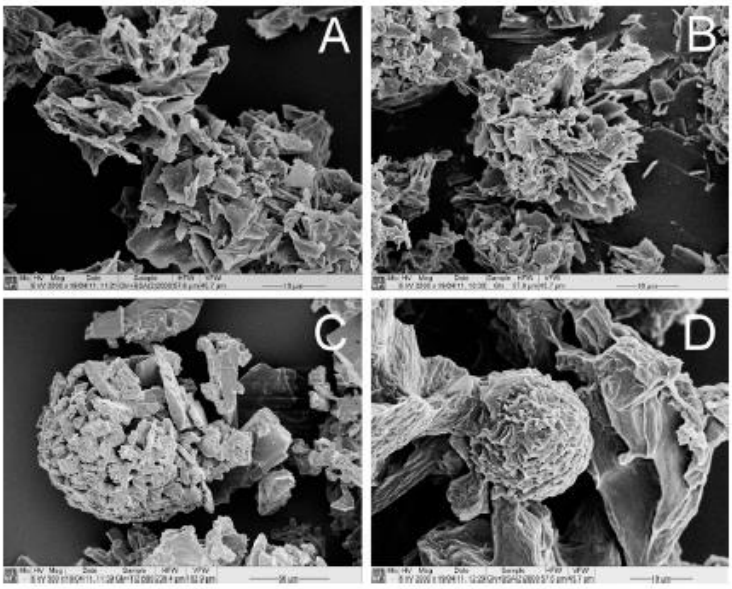

Figure 4. SEM micrographs of dried Φ-CMC generated from mixing with isobutanol.

The core substrate of the Φ-CMC being composed of Gln and 5% w/w trehalose (A), Gln and 5% w/w BSA (B), Gly and 5% w/w trehalose (C), Gly and 5% w/w BSA (D). For A, B, and D, magnification = ×2000; scale bar = 10 μm. For C, magnification = ×500; scale bar = 50 μm.

the aggregation observed was an artifact of the sample preparation for SEM. However, sizing of the Φ-CMC suspended in isopropanol by light scattering showed bimodal profiles corresponding to dispersed and aggregated crystal particles (ca. 8 and 130 μm diameter) for all samples tested, irrespective of the solvent. For the purposes of bioprocessing, the aggregation of the particles is not expected to be problematic since this does not have any affect on reconstitution into aqueous buffer. As regards powder handling, a bimodal distribution of particle sizes in a powder is often beneficial. For example, in pharmaceutical processes such as tableting, Emcompress® (calcium hydrogen phosphate dihydrate and dibasic calcium phosphate) is used because of good flowability on account of its agglomeration and resultant bimodal size distribution (ca. 30 and 180 μm diameter),[36] approximating that for the Φ-CMC powders.

Conclusions

We have shown that the use of organic solvents for bioprocessing of phages is not necessarily harmful if the process is controlled, with careful selection of solvents, stabilizing additives and drying conditions. Although there are safety issues when handling large volumes of organic solvent, the practice is well established and controled in many small molecule processes; one notable example being continuous process crystallization in the pharmaceutical industry.[37] The Φ-CMC process requires the addition of trehalose or BSA as stabilizer and drying under elevated humidities to accelerate the removal of organic solvent. Core carriers with high aqueous solubilities are required when isobutanol is used as the solvent, and other carriers such as inositol and potassium phosphate could be usefully compared against glycine. It is expected that other groups aiming to bring phage therapies into mainstream Western medicine will be able utilize the method reported here for various applications; such as rapid concentration and drying of phage stock solutions, and storage/shipment of phages at room temperature. Further testing of the process with other phage families would be useful since phage therapies are likely to require the use of multiple phage strains.

Acknowledgments

This project was supported by the BBSRC Bioprocessing Research Industry Club, grant ref. BB/F004664/1. Electron micrographs were prepared with technical support from Margaret Mullin, Electron Microscopy Unit, University of Glasgow, UK.

Literature Cited

1. Jackson RE. Bacteriophage prevention and control of harmful plant bacteria. Patent number CA-1306671,1992.
2. Smith HW, Huggins MB. Effectiveness of phages in treating experimental *Escherichia coli* diarrhoea in calves, piglets and lambs. *J Gen Microbiol*. 1983;129:2659–2675.
3. Soothill J, Hawkins C, Anggard E, Harper D. Therapeutic use of bacteriophages. *Lancet Infect Dis*. 2004;4:544–545.
4. Hagens S, Loessner MJ. Application of bacteriophages for detection and control of foodborne pathogens. *Appl Microbiol Biotechnol*. 2007;76:513–519.
5. Barrow PA, Soothill JS. Bacteriophage therapy and prophylaxis: rediscovery and renewed assessment of potential. *Trends Microbiol*. 1997;5:268–271.
6. Sulakvelidze A, Alavidze Z, Morris JG Jr. Bacteriophage therapy. *Antimicrob Agents Chemother*. 2001;45:649–659.
7. Hanlon GW. Bacteriophages: an appraisal of their role in the treatment of bacterial infections. *Int J Antimicrob Agents*. 2007;30:118–128.
8. Skurnik M, Pajunen M, Kiljunen S. Biotechnological challenges of phage therapy. *Biotechnol Lett*. 2007;29:995–1003.
9. Carlton RM, Noordman WH, Biswas B, de Meester ED, Loessner MJ. Bacteriophage P100 for control of Listeria monocytogenes in foods: genome sequence, bioinformatic analyses, oral toxicity study, and application. *Regul Toxicol Pharmacol*. 2005;43:301–312.
10. Wright A, Hawkins CH, Anggard EE, Harper DR. A controled clinical trial of a therapeutic bacteriophage perparation in chronic otitis due to antibiotic-resistant *Pseudomonas aeruginosa*: a preliminary report of efficacy. *Clin Otolaryngol*. 2009;34:349–357.
11. Harding SE. Some observations on the effects of bioprocessing on biopolymer stability. *J Drug Target*. 2010;18:732–740.
12. Cromwell MEM, Hilario E, Jacobson F. Protein aggregation and bioprocessing. *AAPS J*. 2006;8:E572–E579.
13. Clark WA, Geary D. Proceedings: preservation of bacteriophages by freezing and freeze-drying. *Cryobiology*. 1973;10:351–360.
14. Golshahi L, Lynch KH, Dennis JJ, Finlay WH. In vitro lung delivery of bacteriophages KS4-M and PhiKZ using dry powder inhalers for treatment of Burkholderia cepacia complex and *Pseudomonas aeruginosa* infections in cystic fibrosis. *J Appl Microbiol*. 2010;110:106–117.
15. Ackermann H-W, Tremblay D, Moineau S. Long-term bacteriophage preservation. *World Federation Cult Collections Newsl*. 2004;38:35–40.
16. Gould EA. Methods for long-term virus preservation. *Mol Biotechnol*. 1999;13:57–66.
17. Puapermpoonsiri U, Ford SJ, van der Walle CF. Stabilization of bacteriophage during freeze drying. *Int J Pharm*. 2010;389:168–175.
18. Puapermpoonsiri U, Spencer J, van der Walle CF. A freeze-dried formulation of bacteriophage encapsulated in biodegradable microspheres. *Eur J Pharm Biopharm*. 2009;72:26–33.
19. Golec P, Dabrowski K, Hejnowicz MS, Gozdek A, Los JM, Wegrzyn G, Lobocka MB, Los M. A reliable method for storage of tailed phages. *J Microbiol Methods*2011;84:486–489.
20. Moore BD, Parker MC, Halling PJ, Partridge J, Stevens HNE. Rapid dehydration of proteins. Patent number WO-0069887, 2000.
21. Kreiner M, Moore BD, Parker MC. Enzyme-coated micro-crystals: a 1-step method for high activity biocatalyst preparation. *Chem Commun. (Camb.)*2001:1096–1097.
22. Kreiner M, Fuglevand G, Moore BD, Parker MC. DNA-coated microcrystals. *Chem Commun. (Camb.)*2005:2675–2676.
23. Murugesan M, Cunningham D, Martinez-Albertos JL, Vrcelj RM, Moore BD. Nanoparticle-coated microcrystals. *Chem Commun. (Camb.)*2005:2677–2679.
24. Alfadhel M, Puapermpoonsiri U, Ford SJ, McInnes FJ, van der Walle CF. Lyophilized inserts for nasal administration harboring bacteriophage selective for *Staphylococcus aureus*: in vitro evaluation. *Int J Pharm*. 2011;416:280–287.
25. Cappuccino JG, Sherman N. Microbiology: A Laboratory Manual. Benjamin Cummings (9th Ed.), 2011.
26. Matsubara T, Emoto W, Kawashiro K. A simple two-transition model for loss of infectivity of phages on exposure to organic solvent. *Biomol Eng*. 2007;24:269–271.
27. Pereira P, Kelly SM, Cooper A, Mardon HJ, Gellert PR, van der Walle CF. Solution formulation and lyophilization of a recombinant fibronectin fragment. *Eur J Pharm Biopharm*. 2007;67:309–319.
28. Annan WS, Fairhead M, Pereira P, van der Walle CF. Emulsifying performance of modular beta-sandwich proteins: the hydrophobic moment and conformational stability. *Protein Eng Des Sel*. 2006;19:537–545.
29. Lee JC, Timasheff SN. The stabilization of proteins by sucrose. *J Biol Chem*. 1981;256:7193–7201.
30. Wang W, Antonsen K, Nayar R. A novel method for removing residual acetone from gelatin microspheres. *Pharm Dev Technol*. 2002;7:169–180.
31. Mattern M, Winter G, Kohnert U, Lee G. Formulation of proteins in vacuum-dried glasses. II. Process and storage stability in sugar-free amino acid systems. *Pharm Dev Technol*. 1999;4:199–208.

32. Breen ED, Curley JG, Overcashier DE, Hsu CC, Shire SJ. Effect of moisture on the stability of a lyophilized humanized monoclonal antibody formulation. *Pharm Res*. 2001;18:1345–1353.
33. Griebenow K, Klibanov AM. On protein denaturation in aqueous-organic mixtures but not in pure organic solvents. *J Am Chem Soc*. 1996;118:11695–11700.
34. Kreiner M, Parker MC. High-activity biocatalysts in organic media: solid-state buffers as the immobilization matrix for protein-coated microcrystals. *Biotechnol Bioeng*. 2004;87:24–33.
35. Moore BD, Deere J, Edrada-Ebel R, Ingram A, van der Walle CF. Isolation of recombinant proteins from culture broth by co-precipitation with an amino acid carrier to form stable dry powders. *Biotechnol Bioeng*. 2010;106:764–773.
36. Schussele A, Bauer-Brandl A. Note on the measurement of flowability according to the European Pharmacopoeia. *Int J Pharm*. 2003;257:301–304.
37. Lawton S, Steele G, Shering P, Zhao LH, Laird I, Ni XW. Continuous crystallization of pharmaceuticals using a continuous oscillatory baffled crystallizer. *Org Process Res Dev*. 2009;13:1357–1363.

Manuscript received Aug. 10, 2011, and revision received Sept. 13, 2011.